Department of Chemical Engineering
Clean Gas Technologies Australia

Sonochemical Reduction of Carbon Dioxide

Alexander Koblov

This thesis is presented for the Degree of
Doctor of Philosophy
of
Curtin University

May 2011

To the best of my knowledge and belief this thesis contains no material previously published by any other person except where due acknowledgement has been made. This thesis contains no material which has been accepted for the award of any other degree or diploma at any university.

Acknowledgements

I would like to show my deepest gratitude to my supervisor, Professor Robert Amin, for his instructions, guidance and great assistance throughout the every step of my research. Without his encouragement, patience and enormous support, it is certain none of this would have been possible.

I gratefully acknowledge Professor Rolf Gubner, Associate Professor Ahmed Barifcani and Associate Professor David Pack for fruitful discussions and helpful advice.

I wish to thank Ms. Sabine Isbarn for her kind-heartedness and help in many aspects of academic life.

I would also like to thank Mr. Saif Ghadhban for his supervision and assistance in the laboratory.

I would like to thank a great team of fellow students at Clean Gas Technologies Australia for the rich learning and working environment created by the combination of their personalities.

I wish also to thank Doctor Alf Larcher, Doctor John Bromly, Doctor Gia Pham and Ms. Faye Chong for their invaluable help with GC and GC-MS analyses.

I gratefully acknowledge the financial support to this work from Woodside Energy Ltd.

I would like to express my great appreciations to my family and friends for their inspiration and support.

Abstract

Emissions from the combustion of fossil fuels and cement production are responsible for approximately 75% of the increase of carbon dioxide (CO_2) concentration in the atmosphere. 80% of the generated world energy is produced by burning fossil fuels (IPCC 2007) and such tendency is likely to remain unchanged in the nearest future. These number look more intimidating if consider the fact that in 2030, global energy demand was estimated to increase by 57% in comparison to 2004 (from 14.9 terrawatts (TW) in 2004 to 23.4 TW in 2030; International Energy Outlook 2007). Moreover, only 45% of CO_2, released due to human activity since 1959, is absorbed by the nature (plants and the ocean) (IPCC 2007). Thus, the other 55% of CO_2 from human activity remains in the atmosphere undeniably causing serious changes in the Earth‟s climate.

With the potential impact of climate changes there is a considerable motivation to find solutions for reducing greenhouse gas emissions, particularly CO_2. Moreover, the development of alternative energy sources is a commercially important task considering the fact that fossil fuels are non-renewable resources and will eventually deplete. It is well known that CO_2 is a cheap and abundant source of carbon. Thus, the conversion of CO_2 into fuels can be considered as a prospective method providing the possibility of CO_2 recycling and as a result the decrease of CO_2 concentrations in the atmosphere. Thus, over the past decades an increasing amount of global research efforts has focused on developing a CO_2 utilization system. However, because CO_2 is a very stable molecule, a large amount of energy is required to initiate its reduction. So the invention of an economically feasible method is the primary task in development of a CO_2 reduction technology. The vast majority of work in this direction devoted to:

- the application of new catalysts for CO_2 reduction processes,
- the use of various semiconductor technologies to harness solar energy as the energy input to the reaction of CO_2 reduction, and
- the development of bio-inspired processes in order to amplify the photosynthesis process in living organisms or create the artificial photosynthesis

An area of investigation that has received less attention is that of sonochemical reduction of CO_2, or the use of ultrasound irradiation to reduce CO_2 to basic fuel stock components. The chemical effect of ultrasound comes from acoustic cavitation phenomena – the formation, growth and collapse of cavitation bubbles. The collapse of cavitation bubbles results in generation of micro-zones of extremely high temperature (over 5000 K) and pressures (300 bar) (Nolting, and Nepparis 1950) which is the driving force for sonochemical reactions. Molecules trapped in cavitation bubbles undergo processes of radicalization and recombination due to the great amount of energy generated during the cavitation collapse.

This thesis is devoted to experimental investigation of chemical utilization of CO_2 using ultrasound as a source of energy. Sonochemical reduction of CO_2 in various sonicating media is carried out in a wide range of experimental conditions. The main idea behind the experimental work performed is to investigate the ways of CO_2 utilization into useable chemicals by its direct sonolysis or recombination of it with H_2 while using the ultrasound (vibrational) energy, provided by the 20 kHz ultrasonic probe system. The study on sonochemical fixation of dense-phase and supercritical CO_2 is also conducted. The efficiency and prospective usage of ultrasonic energy in the process of CO_2 reduction is estimated based on the experimental results obtained. Additional study of the ultrasound-assisted oxidative desulfurization process of sulphur containing compounds by potassium permanganate ($KMnO_4$) is conducted in order to investigate the effect of ultrasound on oxidation processes.

Nomenclature

Acronyms and Abbreviations

ADEME	Agence de l'Environnement et de la Maîtrise de l'Energie (French Environment and Energy Management Agency)
CRIEPE	Central Research Institute for the Electric Power Industry (Japan)
DMC	Dimethyl Carbonate
EGR	Enhanced Gas Recovery
EOR	Enhanced Oil Recovery
EOS	Equation of State
ERCBM	Enhanced Recovery of Coal Bed Methane
FID	Flame Ionization Detector
GC	Gas Chromatography
GC-MS	Gas Chromatography-Mass Spectrometry
GHC	Greenhouse Gases
HDS	Hydrodesulfurization
ODS	Oxidative Desulfurization
REDOX	Reduction-Oxidation
SY	Sonochemical Yield
TCD	Thermal Conductivity Detector
UAODS	Ultrasound-Assisted Oxidative Desulfurization
UK	United Kingdom
UK SDC	United Kingdom Sustainable Development Commission
US	United States

Parameters

μ	Viscocity
A	Area
a, b, A, B	Constants of fluid in the Peng-Robinson EOS
c	Speed of sound
C_p	Heat capacity at constant pressure
C_v	Heat capacity at constant volume
D	Distance

dx	Thickness
E	Energy
E_k	Kinetic energy
f	Frequency
G	Gibb‟s free energy
H	Enthalpy
I	Intensity
k	Thermal conductivity
M	Molecular weight
m	Mass
$mol\%$	Molar percent
n	Amount of substance, stoichiometric number
P	Pressure
P_0	Constant ambient pressure
P_a	Acoustic pressure
P_g	Gas pressure
P_h	Hydrostatic pressure
P_m	Hydrostatic pressure during the cavitation bubble collapse
P_v	Vapour pressure
R	Universal gas constant, radius
R_m	Radius of a cavitation bubble at its collapse
S	Entropy
T	Temperature
t, τ	Time
T_0	Temperature of a sonicating medium
v	Velocity
V_m	Molar volume
w/w	Mass fraction
w_a	Equal applied circular frequency
Z	Compressibility factor
γ	Ratio of specific heats
π	pi number
ρ	Density
σ	Surface tension

α	Function of temperature
ω	Acentric factor

Subscripts

1, 2 ... i	Numbers
av	Average
c	Critical
cyl	Cylinder
cyl-p	Cylinders-pump tubing
l	Loaded
max	Maximum
p	Pump
p-r	Pump-reactor tubing
r	Reactor
t	Total

Table of Contents

List of Figures

List of Tables

Chapter 1. Introduction to the Research

1.1. The CO_2 Problem

Since 1750 the concentration of carbon dioxide (CO_2) in the atmosphere has increased by approximately 30% and the Earth‟s average temperature has risen by 0.5˚C over the last three decades of the 20th century. Moreover, keeping the same trends in the emissions of greenhouse gases (GHG) during the next 100 years will raise the Earth‟s average temperature between 1.4 and 5.8˚C (De P. R. Silva et al. 2010). Such changes in temperature on the earth can lead to serious climate changes and cause dire consequences for the planet and the people, animals and plants inhabiting it. Moreover, the responsibility for such a sharp increase in GHG concentration, which has risen since the industrial revolution from 280 to 377 ppm by 2004 (Cnossen et al. 2009), lies with human activity. The idea of finding a technology that will allow significant reduction of GHG remains a research focus since the Kyoto Protocol was adopted in 1997. This protocol commits those countries, which accepted it, to cut GHGs emissions by 5.2% against 1990 levels during the five year period from 2008 to 2012. The contribution of greenhouse gases produced by mankind is depicted in Figure 1.1. From this data it can be seen that CO_2 is the largest source of total greenhouse gases emissions. The main anthropogenic sources of CO_2 emission are based on the production and combustion of fossil fuels and industrial processes where CO_2 is a byproduct (production of cement, limestone, ammonia, hydrogen and ethylene oxide, Figure 1.1) (Song, Gaffney, and Fujimoto 2002; Aresta 2003). Even though other GHG such as methane, nitrous oxide and chlorofluorocarbons have a stronger effect than CO_2 due to their high global warming potentials, the amount of CO_2 emitted annually in the atmosphere is much larger than that of those gases (see global warming potentials of anthropogenic greenhouse gases, Table 1.1).

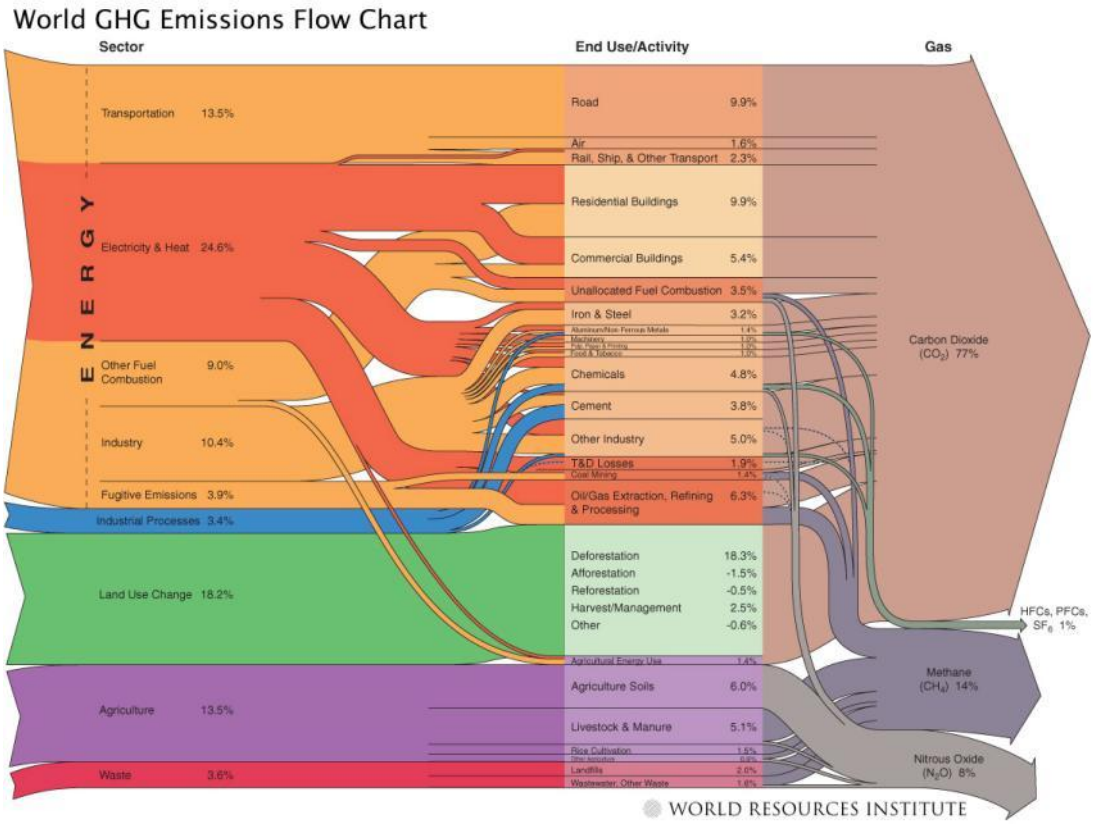

Figure 1.1. World GHG emissions flow chart (Source: http://cait.wri.org/figures/World-FlowChart.jpg)

Thus, developing an efficient technology of CO_2 utilization remains the major task for science as long as CO_2 has the biggest effect on the climate changes in comparison to other GHG.

1.2. Existing and Emerging Applications for CO_2 Utilization

1.2.1. Physical Utilization of CO_2

Today, market utilization of CO_2 includes many applications such as food processing, carbonated beverages, the chemical industry, agriculture, metal fabrication, rubber and plastic processing, water treatment, nuclear, oil and gas well re-injection, dry ice production. However, despite this, the market for CO_2 utilization represents less than 0.1% of the total amount of CO_2 released into the atmosphere (Aresta 2003). Moreover, almost all CO_2 used in the applications named above (except for some applications in the wastewater treatment and chemical industries) is eventually released into the atmosphere.

Table 1.1. Global warming potentials of anthropogenic greenhouse gases (Source: IPCC Second assessment report: climate change 1995 (SAR) 1996)

Species	Chemical formula	Lifetime (years)	Global Warming Potential		
			20 years	100 years	500 years
CO_2	CO_2	*variable**	1	1	1
Methane	CH_4	12±3	56	21	6.5
Nitrous oxide	N_2O	120	280	310	170
HFC-23	CHF_3	264	9100	11700	9800
HFC-32	CH_2F_2	5.6	2100	650	200
HFC-41	CH_3F	3.7	490	150	45
HFC-43-10mee	$C_5H_2F_{10}$	17.1	3000	1300	400
HFC-125	C_2HF_5	32.6	4600	2800	920
HFC-134	$C_2H_2F_4$	10.6	2900	1000	310
HFC-134a	CH_2FCF_3	14.6	3400	1300	420
HFC-152a	$C_2H_4F_2$	1.5	460	140	42
HFC-143	$C_2H_3F_3$	3.8	1000	300	94
HFC-143a	$C_2H_3F_3$	48.3	5000	3800	1400
HFC-227ea	C_3HF_7	36.5	4300	2900	950
HFC-236fa	$C_3H_2F_6$	209	5100	6300	4700
HFC-245ca	$C_3H_3F_5$	6.6	1800	560	170
Sulphur hexafluoride	SF_6	3200	16300	23900	34900
Perfluoromethane	CF_4	50000	4400	6500	10000
Perfluoroethane	C_2F_6	10000	6200	9200	14000
Perfluoropropane	C_3F_8	2600	4800	7000	10100
Perfluorobutane	C_4F_{10}	2600	4800	7000	10100
Perfluorocyclobutane	c-C_4F_8	3200	6000	8700	12700
Perfluoropentane	C_5F_{12}	4100	5100	7500	11000
Perfluorohexane	C_6F_{14}	3200	5000	7400	10700

* *Derived from the Bern carbon cycle model*

Thus, the applications for CO_2 recovery can be divided into two groups (Aresta 2003):

- Applications which temporarily use CO_2 and eventually release it into to the atmosphere, and
- Applications which permanently utilize CO_2 reducing its concentration in the atmosphere.

Another way to reduce the atmospheric concentration of CO_2 is through storage. Today, there are several CO_2 storage applications such as

- CO_2 storage in depleted oil and gas reservoirs,
- CO_2 storage in unminable coal seams,
- CO_2 storage in aquifers, and
- CO_2 storage in deep oceans.

In the first two technologies the injected CO_2 allows performing enhanced oil recovery (EOR), enhanced gas recovery (EGR) and enhanced recovery of coal bed methane (ERCBM), so recovered quantities of oil or methane make it possible to partly offset the cost of CO_2 storage.

Based upon the information above, it can be fairly stated that the chemical conversion of CO_2 into useable compounds is the only way to permanently utilize CO_2.

1.2.2. Chemical Utilization of CO_2

As is well known, CO_2 is potentially a cheap source of carbon for chemical transformations. Moreover, its benignity, natural abundance, non-toxicity and non-flammability make CO_2 a very attractive source for many chemical syntheses (Beckman 2004; Zhou et al. 2008; Dai, W. L. et al. 2009). So, as is stated above, CO_2 can be considered as both a GHG emission and as an abundant source of carbon for chemical transformations. From where, it can be reasonably suggested that the chemical conversion of CO_2 to organic chemicals is the best solution for CO_2 utilization.

Today, a number of various processes for chemical utilization of CO_2 are being studied in the laboratory, and many ways to fix CO_2 into organic compounds such as formic, acetic and oxalic acids, long chain aliphatic carboxylic acids, esters, carbamates and isocyanates can be found in literature (Sakakura, Choi, and Yasuda 2007; Aresta 2003), but only a few of them have reached large-scale production and

exist as technologies in the chemical industry. The synthesis of urea, methanol and salicylic acid are the representatives of industrial processes of CO_2 chemical conversion (Sakakura, Choi, and Yasuda 2007). However, such technologies face market limitations on produced chemicals (Song, Gaffney, and Fujimoto 2002). So, considering existing applications of CO_2 utilization and technologies of CO_2 conversion to organic compounds, it can be seen that only a very small part of the annually produced amount of CO_2 is utilized permanently.

1.3. Concepts for Creation of Successful Technology of CO_2 Utilization

Searching for a technology enabling a significant reduction in CO_2 emissions is one of the priority aims for the science today. However, every technology being developed has barriers and strategies which have to be overcome in order to be reasonable and competitive. Any such new technology for CO_2 utilization should fulfill economic, engineering, market and ecological requirements (Song, Gaffney, and Fujimoto 2002, p. 20). Moreover, to be successful and applicable the new technology has to be more advantageous than existing ones in every aspect. So, considering the barriers and strategies for the chemical utilization of CO_2 there are some major criteria which the technology should meet. Those criteria include:

a) transportation cost:

Utilization of CO_2 directly at its source significantly diminishes its transportation expenses. Moreover, applying the CO_2 utilization unit on-site makes it possible to include this unit in the existing production scheme.

b) CO_2 feed preparation:

The possibility of using CO_2 along with H_2O, O_2 and other impurities for chemical conversion without CO_2 pre-separation dramatically cuts the cost of separation.

c) co-reactants availability and low cost:

Co-reactants for chemical reactions with CO_2 have to be cheap and widely available. Also, co-reactants production must not be accompanied by CO_2 formation. For example, in the case of hydrogenation of CO_2 by H_2 to synthesize methanol, the H_2 is produced by reforming of hydrocarbons which consumes a lot of energy and where CO_2 is its byproduct.

d) products of technology and market limitations:

The technology should be able to produce valuable chemicals such as fuel or a carbon source for its further transformations to other chemicals (for example, CO as

a syngas component). Moreover, produced chemicals by such technology should have minimal market limitations or should not have them at all.

e) efficiency and cost of technology:

The technology should enable a considerable decrease in the CO_2 concentration in the atmosphere. Also, technology must be financially feasible.

1.4. The Objectives of the Research

The main objective of this thesis is to investigate a new technology of CO_2 permanent utilization using ultrasound energy to synthesize industry valuable compounds. The investigation includes the following stages:

Development and design of experimental apparatus: This requirement consists of the construction of low-pressure and high-pressure experimental setups in order to be capable to investigate the sonochemical reduction of CO_2 dissolved in liquid mediums such as water, hydrocarbons and methanol as well as the sonochemical utilization of liquified and supercritical CO_2. The design of the low-pressure apparatus must provide an option of uninterrupted sonication during a test in view of using an ultrasonic probe system as a source of ultrasound. So, the major requirement for this apparatus is to provide an excellent temperature control.

Investigation of the sonochemical utilization of CO_2 dissolved in a liquid medium at low pressure conditions: The major aim of this objective is to investigate the ultrasonic technique of the chemical reduction of CO_2 in various liquid media. The research implies the chemical conversion of CO_2 into industrially valuable compounds such as CO and CH_4. Moreover, H_2 is also considered as a product of the sonochemical reduction of CO_2 as long as it is suggested to be generated in the process of sonodecomposition of a liquid medium during sonolysis. Thus, chosen sonicating media must satisfy several requirements. They must be widely available in significant amounts, be relatively cheap and be a source of H_2 during sonolysis.

Investigation of sonochemical utilization of CO_2 in both liquid and supercritical states: The objective of this work is the sonochemical reduction of liquid and supercritical CO_2. Dense-phase CO_2 alone and its recombination with various gases such as CH_4 and H_2 (considered as a source of H*) subjected to ultrasound in order to initiate the sonochemical reactions is the main idea behind investigation.

Analysis of efficiency of ultrasound usage in CO_2 chemical utilization: The main purpose of this part of research is to estimate the perspective and efficiency of

ultrasound in the chemical fixation of CO_2 based on the experimental results obtained.

1.5. Significance of the Research

- The development of a novel pilot-plant sonochemical reactor based on using a low-frequency, high-power ultrasound probe system as a source of ultrasound.
- The idea to use ultrasound energy for CO_2 utilization has been thoroughly investigated, both theoretically and experimentally in this research. Water, methanol and liquid hydrocarbons are suggested both as sonicating media and a source of H_2 for the sonochemical reduction of CO_2 were studied in this research in order to fix CO_2 chemically using ultrasonic energy. It was found that an aqueous medium provides the best rates of the CO_2 sonochemical reduction.
- The possibility to initiate reactions of CO_2 reduction into useable compounds such as CO and CH_4 by ultrasonic energy is shown. The research includes a vast range of experimental conditions. For the first time, sonolysis of CO_2 in a hydrocarbon sonicating medium is experimentally demonstrated.
- The sonolysis of heptane in an aqueous medium was studied. It is shown that the rate of sonochemical decomposition of n-heptane in an aqueous medium is larger than the rate of sonodegradation of pure n-heptane. The mechanism of sonodegradation of heptane in an aqueous medium is proposed according to the products obtained. The products of sonolytic decomposition of heptane are shown to be similar to the products obtained in the low temperature pyrolysis.
- The option of ultrasound-assisted chemical fixation of CO_2 by its conversion into dimethyl carbonate (DMC) in a methanol sonicating medium is investigated.
- The decomposition of iodomethane (CH_3I) in the synthesis of DMC is revealed. Due to the physical properties of CH_3I, the products obtained, conditions of the experimental work and the design of experimental apparatus, it is proposed that sonolysis of CH_3I takes place in a methanol medium. The mechanism of CH_3I decomposition is proposed and compared to the processes of decomposition of iodomethane at pyrolysis and photolysis.
- Investigation on sonolysis of dense-phase and supercritical CO_2 alone and in a mixture with other gases was performed.

- Ultrasound-assisted oxidative desulfurization of condensate containing thiols and disulfides by potassium permanganate is carried out in order to investigate the effect of ultrasound on oxidation processes.
- The perspective and efficiency of the ultrasonic technique in the process of CO_2 chemical fixation was estimated based on the results obtained during the research.

1.6. Thesis Chapter Outline

This thesis is divided into nine chapters. Chapter 1 states the problem and introduces the main idea of the research. It includes the current state of the art as well as the objectives of the actual research as well as its significance. Chapter 2 presents a literature review which reflects some general information on ultrasound energy and sonochemistry as a science. Also, the review sheds light on the choice of conditions of the following experimental work as well as the choice of equipment in terms of its technical characteristics. Chapter 3 contains a detailed description of equipment which is employed during the study. This chapter presents advantages of two experimental apparatus constructed in our laboratory. Chapter 4 contains the experimental work conducted in this research. All results divided into separate sections according to different types of liquid media such as water, hydrocarbons and alcohols. For each liquid medium there are theoretical information, procedures for choosing a sonicating medium and atmospheric gas which provides a base for the experimental work. Moreover, all experimental investigations have linking connections between them through brief conclusions what allows to present the whole experimental work as a logical sequence of experiments. All results obtained in Chapter 4 are brought together in Chapter 5 where discussion and conclusions are presented according to the obtained experimental data. This chapter summarizes the findings and provides the mechanisms of the chemical transformations obtained during the experimental research. Chapter 6 of the thesis presents the experimental work on sonochemical reduction of CO_2 at liquefied state. Also, sonolysis of CO_2 at supercritical conditions was investigated. Chapter 7 contains the experimental work on ultrasonic-assisted oxidative desulfurization of sulfur compounds by potassium permanganate. This study is performed in order to find out the influence of ultrasound on oxidation processes. Chapter 8 contains the analysis of the prospective to use sonochemical reduction of carbon dioxide as a technique for CO_2 chemical

utilization. Research finding and conclusions are summarized and presented in Chapter 9. The relevant information not included in chapters is given in Appendixes A and B.

Chapter 2. Literature Review

2.1. Definition of Ultrasound and its Industrial Applications

Ultrasound is sound waves of high frequency which is beyond the human upper frequency limit (> 20 kHz). The upper limit of ultrasound is usually taken to be 5 MHz for gases and 500 MHz for liquids and solids. In terms of energy, ultrasound can be understood as a form of energy, different from heat, light or pressure, which can be used for the modification of chemical reactivity in many chemical applications (Mason and Lorimer; Kuijpers 2004). Generally, ultrasound is divided into two groups:

- High frequency and low intensity ultrasound (2-500 MHz and 0.1-0.5 W/cm^2)
- Low frequency and high intensity ultrasound (20-100 kHz and >10 W/cm^2) which is also known as "high power ultrasound". In fact, lately the range of frequencies of "high power ultrasound" has been extended up to 2 MHz with the development of appropriate equipment.

Today, ultrasound is used in many areas of the chemical, medicine and food processing industries. Table 2.1 presents some of major applications where ultrasound is used (Kuijpers 2004; Mason and Lorimer 2002).

Table 2.1. Ultrasonic applications in different areas

Field	Application	Type of ultrasound
Biology, Biochemistry	Cell disruption in order to realise its content	High power ultrasound
Food industry	Emulsification of sauces, mayonnaise; tenderization of meat; improving aging of wine	High power ultrasound
Sonochemistry	Acceleration and initiation of reactions; reduction of steps/time in synthesis; initiation of alternative pathways of reactions	High power ultrasound
Engineering	Ultrasonic welding; ultrasonic cutting (both metal and plastic); assistance to drilling	High power ultrasound
Dentistry	Cleaning and drilling of teeth	High power ultrasound
Medicine	Kidney stone disruption; the treatment of muscle strains, blood clots; cancer treatment	High power ultrasound
Medicine	Ultrasonic imaging	High frequency/low power ultrasound
Industry	Flaw detection	High frequency/low power ultrasound

In chemistry, ultrasound is proven to help increase the conversion, change the selectivity of produced compounds, improve the rate of chemical reactions and/or initiate reactions, which require severe conditions or long induction time periods, at milder conditions and during a shorter time (Ondrey et al., 1996).

On the one hand, the wide use of ultrasound in industry is limited because of its low-energy efficiency and, consequently, high operating cost (huge consumption of energy to generate ultrasound) (Gogate and Pandit 2007). However, on the other hand, the use of ultrasound becomes more attractive in cases where applying ultrasonic energy reduces or eliminates other processes costs. For example, when the number of synthesis steps is lowered, when a process can be performed at milder conditions (lower temperature and pressures) or when reaction yields and/or activity of applied catalysts are increased due to using ultrasonic energy.

2.2. Sonochemistry

2.2.1. The Origin of Sonochemistry

Ultrasound has its effect through the phenomenon called cavitation. Interest in cavitation appeared much earlier than sonochemistry was developed. In 1895 Thornycroft and Barnaby (1895) published the first work on cavitation in which it was suggested that cavitation is responsible for damaging the propeller of a submarine. Lord Rayleigh, in 1917, was the first who theoretically described the collapse of a cavitation bubble. However, until the late 1940s all articles were considering hydrodynamically-generated cavitation bubbles (Plesset 1949). The first theoretical works on the dynamics of acoustically-formed cavities (by means of ultrasonic waves) were published at the late 1940s-early 1950s (Noltingk and Neppiras 1950; Neppiras and Noltingk 1951).

Meantime, 1927 became the important year for sonochemistry. In this year Richards and Loomis (1927) were the first to publish an article devoted to "*The chemical effect of high frequency sound*". They studied the hydrolysis of dimethyl sulphate and the oxidation of sulphite under ultrasound irradiation. In their work, the authors noted that under applied ultrasound the studied reactions were accelerated in comparison to conventional conditions. Thus, Richards and Loomis (1927) derived two types of sonochemical reactions based on their work: the acceleration of conventional reactions and the reduction processes in aqueous solution. So, it is thought that this work laid the foundations of sonochemistry as a science (Henglein

1987), even though the term "sonochemistry" was introduced for the first time by Neppiras (1980) in his article on acoustic cavitation. Also in 1927, Wood and Loomis (1927) also presented an article where the physical and biological effects of ultrasound were revealed. A decade later Brohult (1937) discovered the process of biological polymer degradation under the effects of high frequency sound.

As can be seen, sonochemistry is far from being a new subject – it was under study from the beginning of the last century. However, the renaissance is the sonochemistry has developed only in the last few decades (from the 1980s) due to the development and increased availability of ultrasonic equipment (Berlan and Mason 1992).

Mainly, there is an interest in high power ultrasound among chemists studying or working with sonochemistry as long as ultrasound is considered as a new form of energy which can be applied for the enhancement of chemical reactivity. After, Richards and Loomis (1927) made their discovery, a lot of experimental works involving ultrasound on different types of chemical reactions and using various liquid media were conducted. Today, all sonochemical reactions can be divided into four types in accordance with their mechanisms (Henglein 1987):

1. The acceleration of conventional reactions
2. Reduction processes in aqueous solution
3. The degradation of polymers
4. The decomposition of and reactions in organic solvents

To make it clear how ultrasound works, it has to be understood that it has its effect due to the cavitation phenomena. When a high frequency sound wave passes through a medium, during the rarefaction cycle it generates micro-bubbles or voids called cavitation bubbles. These bubbles can be filled with gases dissolved in the medium or with evaporated medium itself (vapour). Cavitation bubbles are generated during a rarefaction half-cycle of the ultrasonic wave when an applied negative pressure is large enough to overcome the cohesive forces of the medium and tear molecules of medium apart to form cavitation. Further, these cavitation bubbles undergo a compression half-cycle of the ultrasonic wave collapsing violently and generating temperatures of several thousand Kelvin and pressures of several thousand atmospheres (Flint and Suslick 1991; David and Boldo 2008; McNamara III, Didenko, and Suslick 1999; Flannigan and Suslick 2005; Yasui et al. 2005). So, the

collapse of cavitation bubbles causing chemical transformations is the main event by which ultrasound has its effect.

2.2.2. Cavitational collapse theories

There are four theories of the process of generating energy through the collapse of cavitation bubbles: the "hot-spot" theory of Nolting and Nepparis (1950), the new theory of the local electrification of cavitation bubbles (the new electrical theory) proposed by Margulis (Margulis 1985; Margulis 1992), the plasma theory by Lepoint and Mullie (1994) and the supercritical theory proposed by Hoffmann and colleagues (1995). Also, there are some other theories such as old electric theories (Frenkel 1940; Harvey 1939; Degrois, and Baldo 1974) but they were shown to be inappropriate (Margulis 1981).

The "hot-spot" theory is the most popular among scientists. So, in general, most studies involving sonochemical transformations refer to the "hot-spot" concepts in order to explain experimental results. The "hot-spot" theory implies the adiabatic collapse of transient cavitation bubbles during the compression cycle (Figure 2.1). Nolting and Neparris (1950) suggest that the cavitation bubble collapse occurs extremely rapidly, consequently the heat transfer between the cavity and the surrounding medium can be neglected. Thus, the adiabatic compression and collapse of the cavitation bubble generates micro-zones of extremely high temperatures and pressures (Nolting, and Nepparis 1950; David and Boldo 2008) which is a driving force for sonochemical reactions.

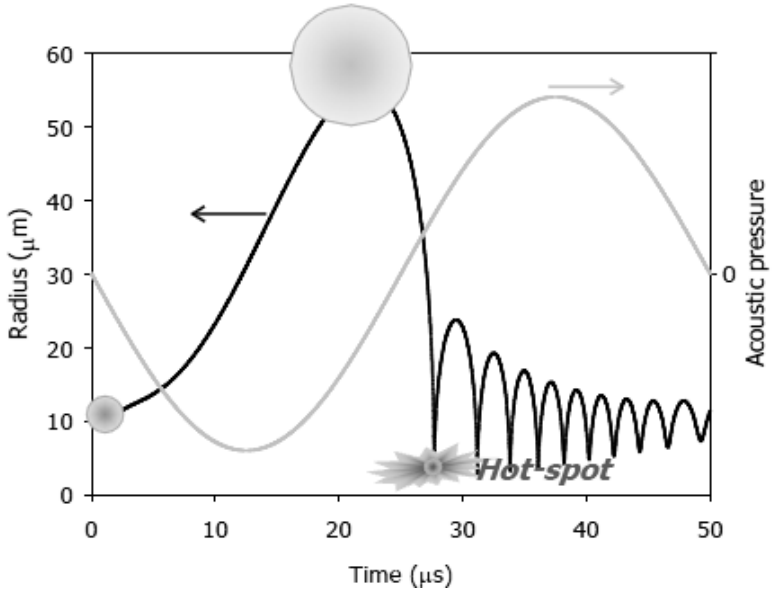

Figure 2.1. Diagram of the collapse of a transient cavitation bubble leading to a "hot-spot"

The first approaches of the new theory of the local electrification appeared comparatively recently (Margulis 1985). Margulis stated that the hot-spot theory of cavitation collapse is not able to explain the wide range of conditions at which sonochemical reactions and sonolumiescence are detected (Figure 2.2) and which can be explained by the electrical theory (Margulis 1992, 1994). As it can be seen from the Figure 2.2, the experimental region of sonoluminescence and sonochemuluminescene for which the hot-spot theory can be applied is significantly smaller than the actual region where sonoluminescence and sonochemuluminescene phenomena occur.

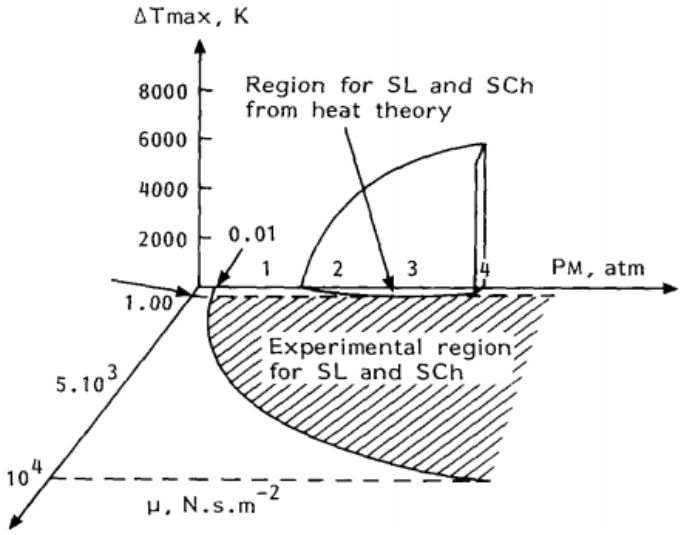

Figure 2.2. Dependence of maximum increase in temperature in the cavitation bubble on the sound pressure amplitude and viscocity of liquid and the range of experimental conditions where sonoluminescence and sonochemical reactions can be registered (hatched area)

The theory of the local electrification implies that a large number of cavitation bubbles oscillating in a liquid medium can interact and coalesce with one another. This leads cavitation bubbles to deformation and splitting into fragment bubbles. An electrical double layer adjacent to the neck of a fragment bubble is generated during the separation. As the charge of electricity is transferred by the liquid stream to the fragment bubble, an electrical discharge through the fragment bubble occurs (Figure 2.3). Thus Margulis (1992, 1994) proposed that splitting of cavitation bubbles during an electrical breakdown into small spherical bubbles leads to luminescence and chemical reactions.

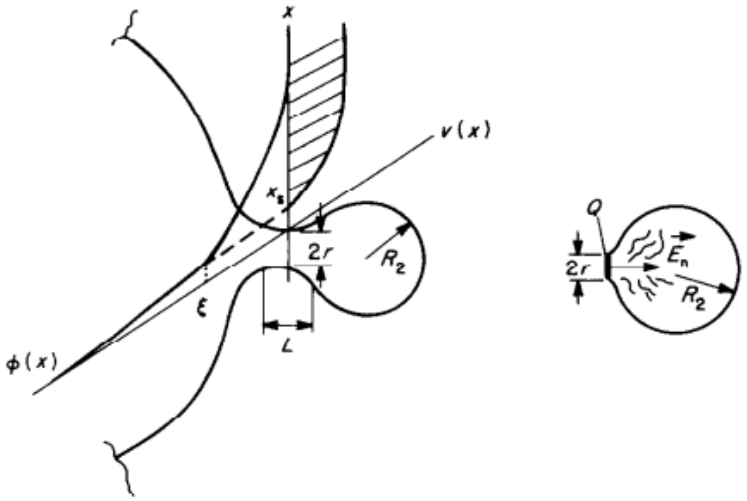

Figure 2.3. Separation of a fragmentation bubble from a primary cavitation bubble according to the theory of the local electrification, where φ(x) and υ(x) are potential and liquid speed-space distribution near collapsing neck, and E_n is electrical field intensity at the instance of separation of a fragmentation bubble from a primary cavitation bubble.

Sometime later, Lepoint-Mullie et al. (Lepoint-Mullie, de Pauw, and Lepoint 1996) in their article "*Analysis of the 'new electrical model' of sonoluminiscence*" proved that the electrical theory by Margulis (1985) is not satisfactory from a physico-chemical point of view and cannot be responsible for sonoluminescence and any process occurring in sonochemistry. However, in 1999 Margulis (Margulis M. A., and Margulis I. M., 1999) published an article where new approaches to the theory of local electrification of cavitation bubbles solving the problem of uncompensated charge on the surface of the deformed cavitation bubbles was reconsidered and resolved.

The plasma theory presented by Lepoint and Mullie suggests that the origin of sonochemical effects lie in corona-like discharges produced in a fragmentation bubble and the formation of microplasmas in the ionization region inside a bubble The main difference from the previous theories is that during a corona-like discharge, the produced extreme conditions (temperatures and pressures) are not limited to the gas phase but include a liquid part opposite the zone of accumulated charge (Figure 2.4).

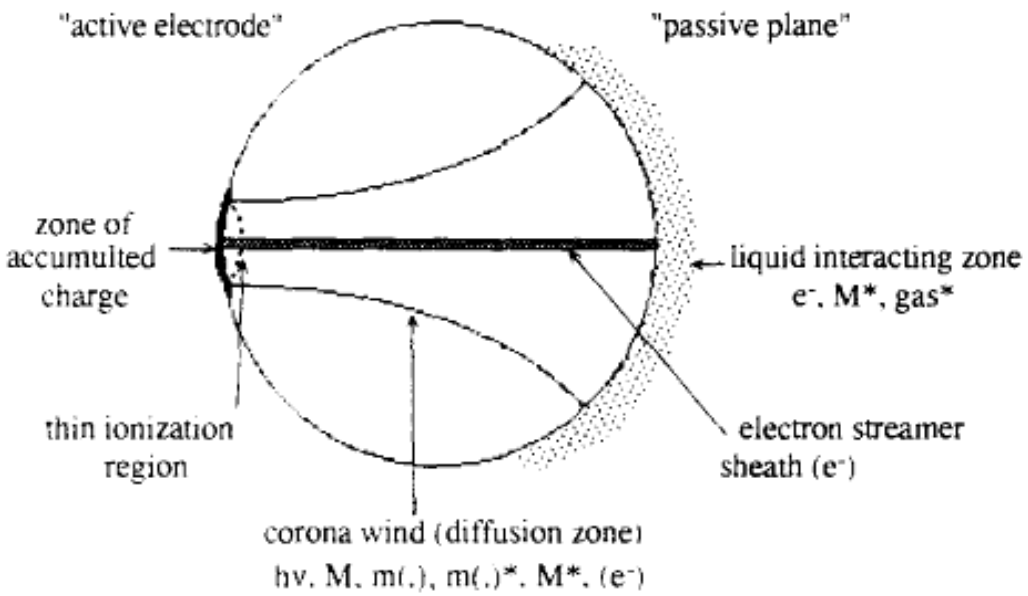

Figure 2.4. Corona-like discharge produced in a fragmented bubble according to the plasma theory

The supercritical theory suggested by Hoffmann and colleagues (1995) was based on the experimental results on sonolysis of p-nitrophenyl acetate in an aqueous phase. This model assumes that the temperature inside the cavitation bubble just after its collapse is uniform (at about 5000 K for considered conditions) while the temperature of surrounding water is 300 K. Then, having considered the heat-transfer and calculated the reduced temperature as a function of the distance from the center of the bubble (Figure 2.5), the authors (Hoffmann, Hua, and Hochemer 1995) assumed that there is a thin layer of water surrounding the cavitation bubble after the collapse where temperatures and pressure exceed 647 K and 221 bar, respectively. So, supercritical water is generated at these experimental conditions, and as it was suggested by Hoffmann and colleagues namely supercritical water accelerates chemical reactions and provides reaction rates enhancement.

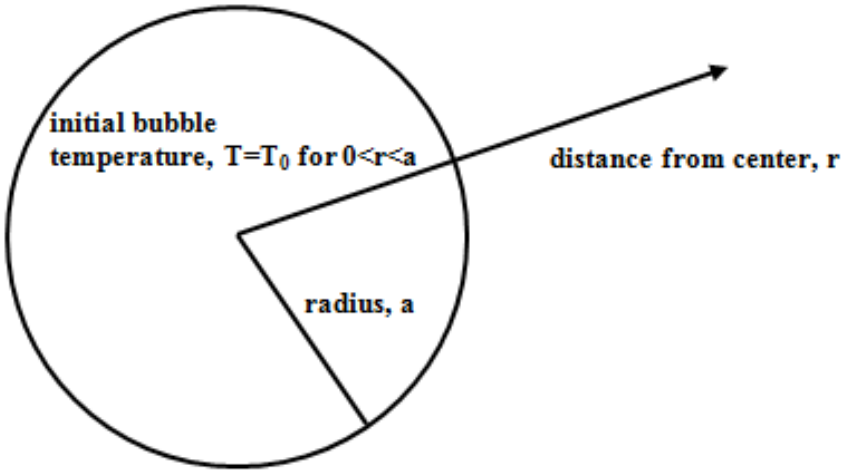

Figure 2.5. The heat-transfer model with initial conditions (for the supercritical theory)

2.2.3. Types of Reaction Zones of Sonochemical Reactions

Despite the nature of the cavitation bubble collapse, huge temperatures and pressures evolve (5000 K and 500 bar). High temperatures and pressures create radicals and excited state particles from the compounds trapped in the micro-bubble. Then, these radicals and excited state particles react immediately because of their very high reaction activity.

So, as the "hot-spot" theory of cavitation collapse is generally more accepted in the scientific community, three different regions, which are responsible for the occurrence of chemical reactions, according to the "hot-spot" theory are presented below. It has been stated that the sonochemical reactions occur directly in the micro-bubble and reactions in the solution as free radicals generated in the cavitation bubble attack the liquid phase (Hart et al. 1989). However, more detailed, three regions where sonochemical reactions occur have been identified (Henglein, 1987, Riesz et al. 1990, David and Boldo 2008). As an example, Figure 2.6 presents a model of the cavitational microbubble during the collapse consisting of the heart or core of the microbubble, the surrounding shell zone (gas-liquid interfacial region) and bulk solution region. So, it was distinguished that all sonochemical transformations can be divided into three groups according to the region where these reactions occur:

- Reactions taking place in the microbubble core (heart). In this case, the cavitation bubble can be considered as a microreactor. In this region, high

temperatures and pressures (5000 K and 500 bar, respectively) generated during the cavitational collapse provide the activation energy required for the bond cleavage and the formation of free radicals and excited states from molecules of atmospheric gases and vapour of a sonicating medium.

- Reactions occurring in the vicinity of the microbubble heart (interfacial region) where temperatures and pressure are not as high as in the core of the cavitation bubble. Mainly, pyrolysis and free-radical reactions take place in this gas-liquid shell surrounding the collapsing bubble. It was found that majority of degradation reactions occur particularly in this area (Hoffmann, Hua, and Hochemer 1995)

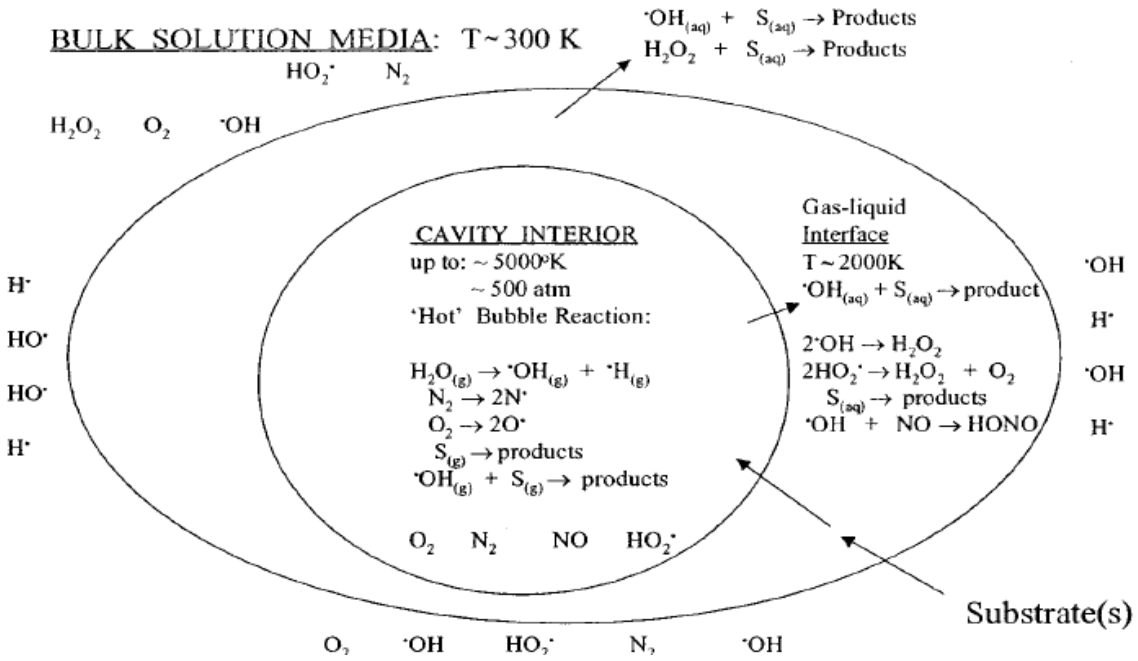

Figure 2.6. Three reaction regions in the cavitation process

- Reactions occurring in the bulk liquid. In this region, no primary sonochemical reactions take place. In general, the formation of products from reactions of a bulk liquid with a small number of free radicals produced in the microbubble core or surrounding shell, occurs here.

It has been postulated that every reaction is favored to occur in a certain region of the micro-bubble according to its thermodynamic properties.

2.2.4. Types of Cavitation

When a liquid medium is subjected to ultrasound, numerous microbubbles appear. This phenomenon is called cavitation (Neppiras 1980; Yasui et al. 2010). Cavitation

can be divided into two types called *stable* and *transient*. These commonly used today terms were first introduced by Flynn (1964).

2.2.4.1. Stable Cavitation

Usually the term "stable" cavities refers to bubbles which have a stable shape and exist during a number of cycles, oscillating around some equilibrium size without collapsing (Flynn 1964; Apfel 1972; Riesz and Kondo, 1992). So, those stable cavities can be visible due to their long lifetime.

2.2.4.2. Transient Cavitation

Transient cavities exist for less than one or at most a few cycles increasing in size to double or more of their original size during a rarefaction half-cycle and, eventually, violently collapsing during a compression half-cycle (Flynn 1964; Apfel 1972; Riesz and Kondo, 1992). So, transient cavities cannot be seen by the naked eye, because they exist during a very short period of time (microseconds) and transient cavities produce high temperatures and pressures during the collapse. The existence of this cavitation can be proven by such disruptive effects as erosion, emulsion, molecular degradation and sonolumiescence. For example, Balanchandran et al. (2006) in their experimental work used aluminium foil strips placed in the sonication reactor to prove the existence of transient cavitation during sonolysis due to damage caused to aluminium foil by collapse of transient cavitation bubbles.

Due to the short life period of transient cavities no mass diffusion of gas in or out of the bubble occurs. However, it is suggested that evaporation and condensation processes in such cavities take place (Neppiras 1980). In the case of stable cavitation, such processes as mass diffusion of gas, thermal diffusion along with evaporation and condensation can occur freely. So, during these processes stable cavitation bubbles grow and there is a possibility that stable cavities can evolve into transient ones in the course of time or during changes in ultrasound or environmental conditions (such as temperature, pressure, frequency and intensity). It is thought that the intensity of ultrasound is related directly to the type of cavitation produced. So at atmospehic pressure conditions, stable cavitation usually occurs at lower intensities of 1-3 W/cm^2, whereas transient microbubbles are generated by applying high ultrasound intensities (over 10 W/cm^2; Henglein 1987).

It can be summarized that application of ultrasound for chemical transformations is conditioned by the generation of transient cavitation during a sonolysis. Thus, it is very important to subject a liquid medium to ultrasonic irradiation of intensity at which transient cavitation bubbles are produced.

2.2.5. The Main Characteristics of Ultrasound

Frequency, intensity and acoustic pressure of ultrasound are the most important charachteristics of ultrasonic waves. By frequency of ultrasonic wave it it understood a time of one cavitation cycle. The unit of frequency is the Hertz (Hz). Frequency is inversly related to time expressed in seconds. For example, at a frequency of 20 kHz, one cavitation cycle lasts 0.00005 seconds (50 μs).

Intensity of an ultrasonic wave represents the amount of sound energy carried by the wave per second per unit area (Watt/cm^2, where Joule/s = Watt).

Acoustic pressure is the pressure caused by a sound (ultrasound) wave passing through the medium.

There is a relationship between the intensity and the acoustic pressure of ultrasound (Berlan and Mason 2002). Intensity is the amount of energy passing per unit area per unit time. Consider a layer of a meduim of an area *A* and a thickness *dx* (Figure 2.7). As long as medium particles subjected to ultrasonic wave are in vibrational motion, they have a kinetic energy (E_k):

$$E_k = \frac{1}{2}\, m\, v^2 \qquad \text{[Eqn. 2.1]},$$

where

v – Velocity of particles of a medium

m – Mass of a layer, given by

$m = \rho\, A\, dx$, where

ρ – Density of a medium

A dx – Volume of a medium subjected to sound wave

Thus, the kinetic energy of the layer is presented by Equation 2.2:

$$E_k = \frac{1}{2}\, (\rho\, A\, dx)\, v^2 \qquad \text{[Eqn. 2.2]}$$

where

x – thinckness of the layer

Then by integrating the previous equation, we find a new equation for energy for the whole wave:

$$E_t = \frac{1}{2}\,(\rho\, A\, x)\, v^2 \qquad \text{[Eqn. 2.3]},$$

where

E_t – Energy of the whole wave (the wave passing through the layer of thickness x)

So, energy per unit volume will be as follows:

$$E = \frac{1}{2}\,\rho\, v^2 \qquad \text{[Eqn. 2.4]},$$

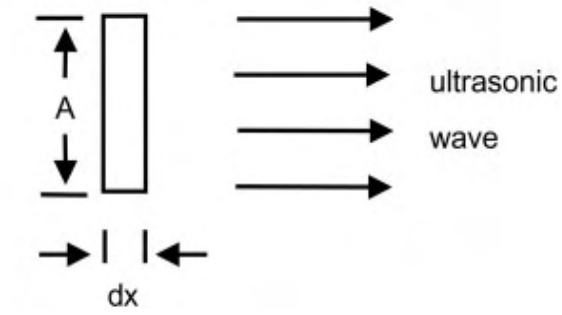

Figure 2.7. Ultrasonic wave passing through a layer of a medium of an area *A* and a thickness *dx*

As is stated, the intensity is the amount of energy passing per unit area per unit time:

$$I = \frac{E}{(A\, t)} \qquad \text{[Eqn. 2.5]},$$

where

I – Intensity of ultrasonic wave

t – Time

The speed of the sound in a medium is referred to c. Thus, distance which the sound travels through a medium during time that can be given by:

$$D = c\, t \Leftrightarrow t = \frac{D}{c} \qquad \text{[Eqn. 2.6]},$$

where

D – Distance

c – Speed of sound in a medium

So, ultrasound, passing trough the layer per unit volume ($A\, D = 1$) per unit time ($t = 1$), has the intensity which can be defined as follows:

$$I = E\ c \qquad \text{[Eqn. 2.7]}$$

In this way, Equation 2.8 can be found by combining Equations 2.4 and 2.7 we obtain:

$$I = \frac{1}{2}\ \rho\ v^2\ c \qquad \text{[Eqn. 2.8]}$$

It is shown that when the layer of the medium is subjected to an ultrasonic wave, the velocity of particles in that layer (v) is related to the acoustic pressure (P_a):

$$P_a = v\ c\ \rho \qquad \text{[Eqn. 2.9],}$$

So, the relationship between the intensity of ultrasound and the acoustic pressure can be expressed using Equations 2.8 and 2.9 as:

$$I = \frac{P_a^2}{2\ \rho\ c} \Leftrightarrow P_a = \sqrt{2\ \rho\ c\ I} \qquad \text{[Eqn. 2.10]}$$

Equation 2.10 is used in experimental work to estimate the maximum acoustic pressure at any known intesity, density and speed of sound in a medium.

2.3. Parameters, Physical Properties and Ultrasound Characteristics that Determine the Cavitation Threshold

2.3.1. Effect of an Atmospheric Gas

Cavitation threshold or Blake threshold pressure is the pressure required to create cavitation bubbles in the medium. The degassed liquid has an increased cavitation threshold in comparison to liquids which have gas dissolved in them. Gas molecules serve as nuclei for initiating cavitation. Cavitation only becomes possible when the negative acoustic pressure applied to the medium exceeds hydrostatic liquid pressure. This negative acoustic pressure must overcome the cohesive forces of a liquid for cavitation to be generated. So removing all gas nuclei from a liquid will increase threshold values significantly. Further, solid micro-particles are able to reduce the cavitation threshold pressure. Although, solid particles cannot affect the Blake's threshold pressure themselves such particulate matter has crevices where gas nuclei are trapped (Figure 2.8). Greenspan (1967) found one of the largest water threshold pressures to have an approximate value of 200 atm using ultrafiltration of the water

(removing all particulate matter), although the theoretical value of it is calculated to be as high as 1500 atm.

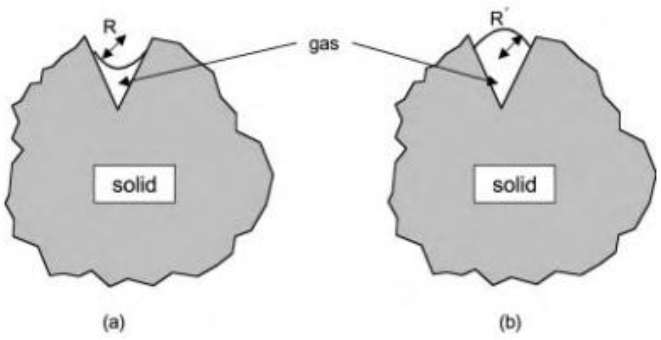

Figure 2.8. Gas nuclei trapped in the crevices of particulate matter; a) for applied external positive pressure; b) for applied external negative pressure.

The choice of an atmospheric gas (gas which is dissolved in a sonication medium) is a very important task. Monoatomic gases usually are used in sonochemistry in preference to diatomic or triatomic ones. It can be explained by the fact that usually monoatomic gases have a lower thermal conductivity in comparison to diatomic (such as O_2, N_2) or triatomic (such as CO_2, N_2O) gases. Thus, the lower the thermal conductivity of the atmospheric gas, the less heat (from the bubble collapse) will be dissipated to the surrounding medium (Hoffmann, Hua, and Hochemer 1995).

As can be seen from the discussion above, increasing the gas content in a medium leads to an increase in the number of cavitation nuclei and lowers the cavitation threshold (Van Iersel, Cornel, Benes, and Keurentjes 2007). However, it lowers the intensity of bubble collapse. In other words, an increase in a gas dissolved in a liquid phase results in a decrease in both P_{max} and T_{max} during the cavitation bubbles‟ collapse (Eqn. 2.12 and 2.13). Such a fact can be explained by the presence of a large number of cavitational bubbles in a unit of volume of the sonicating medium which causes the so-called „cushioning effect‟ (Behrend and Schubert 2001). That is why when choosing the atmospheric gas it is also important to consider gases with low thermal conductivities and solubilities to reduce maximally any possible negative consequences of gas dissolution.

It was suggested that four different types of cavities may be formed during a sonication depending on the properties of the liquid medium and the atmospheric gas (Mason and Lorimer 2002). The first type is the empty cavity and it is formed when a degassed liquid medium undergoes sonolysis. This cavity does not contain any gas or

vapour inside. The second type is the vapour filled cavity. Such cavities can be generated if a liquid which has a high vapour pressure is subjected to sonication. Moreover, if the formed cavity is stable and exists for many cycles without implosion then more vapour penetrates inside the cavity. The third type of cavity is one filled with an atmospheric gas. Formation of these cavities is possible when sonication is performed in a liquid medium of low vapour pressure (a liquid which has a high boiling point) under the atmospheric gas. As discussed above the presence of gas molecules in a liquid lowers the liquid‟s tensile strength and these gas molecules serve as centres of nucleation for cavitation bubbles. So, such cavitation bubbles contain the atmospheric gas inside when formed.

The last type of cavity represents a combination of the second and third types. The fourth type cavity is filled with a vapour and a gas. The generation of such cavities is probable when a liquid with a low boiling point undergoes a sonication under an atmospheric gas. So, both the vapour and the gas appear to be inside these cavities.

It is also important to add that chemical effects caused by ultrasound were not found to happen when there are no dissolved atmospheric gases in the liquid medium. However, in some cases, high intensity ultrasound and very volatile sonication mediums (Fitzgerald, Griffing, and Sullivan 1956) allow cavitation to occur without an atmospheric gas dissolved.

2.3.2. Effect of Viscosity and Surface Tension on Cavitation

An increase in viscosity increases cohesive forces in a liquid and, consequently, raises the threshold pressure of cavitation and fewer cavitation bubbles are produced. However, having formed, these bubbles collapse more violently which means higher temperatures and pressures are generated during the collapse (Berlan and Mason 1992). So, greater intensities of ultrasound are needed to be applied for more viscous liquids in order to produce cavitation (Raso et al. 1999). These larger ultrasound amplitudes overcome the cohesive forces between the molecules of the liquid and create the cavitation bubbles. However, an increase in the viscosity of a liquid does not affect significantly the pressure amplitude.

Table 2.2 presents the effect of the viscosity increase on the acoustic pressure (Mason and Lorimer 2002, p. 40).

Table 2.2. The effect of medium viscocity on the acoustic pressure

Liquid	μ, poise	ρ, g/cm^3	c, m/s	P_a, atm
Castrol oil	6.30	0.969	1477	3.90
Olive oil	0.84	0.912	1431	3.61
Corn oil	0.63	0.914	1463	3.05
Linseed oil	0.38	0.921	1468	2.36
CCl_4	0.01	1.600	926	1.75

From the data in Table 2.2 it can be seen that the tenfold increase in viscosity between corn and castrol oil corresponds to a 30% increase in the acoustic pressure.

Raso et al. (1999) have shown in their work that the increase in viscosity firstly led to greater T_{max} and P_{max} during cavitation collapse. However, at some point of increased viscosity it is not possible to create cavitation.

Surface tension is also an important parameter for determination of the Blake threshold (Hilgenfeldt et al. 1998). It is stated that the lower the surface tension of a liquid the stronger the cavitation bubble collapse. Thus, the small surface tension of a liquid allows the cavitation to occur at lower pressure amplitude (Kuijpers et al. 2002).

2.3.3. Effect of Frequency of Ultrasound on Cavitation

The frequency of ultrasound is inversely proportional to ultrasound intensity. On the one hand, low-intensity and high-frequency ultrasound does not generate cavitation in the liquid medium and, consequently, does not trigger any physical or chemical changes. Such applications of ultrasound are used for non-destructive evaluation and medical needs. On the other hand, it is possible to create cavitation when a liquid medium is subjected to ultrasound, thus physical and chemical transformations can occur. Such types of ultrasonic devices are typically used for sonochemical application (see Table 2.1). Low frequency ultrasound 20-50 kHz are usually (Mason and Lorimer 2002) used in sonochemical applications where there is a need to create violent cavitation. It has a simple logical explanation. With an increase in ultrasound frequency it is more difficult to create cavitation. For example, one cycle at 20 kHz lasts for 50 ms, where 25 ms is taken by compression and 25 ms by rarefaction half-cycles (Entezari, Kruus, and Otson 1997). The same values for rarefaction and compression half-cycles at an applied frequency of 20 MHz equals 0.025 ms.

However, this time is not enough to overcome the cohesive forces of the liquid and generates cavitation during the rarefaction, or the bubble collapse requires more compression half-cycle time to occur than at 20 MHz. Moreover, at such high frequencies the greater intensities of sound have to be applied for those short periods of rarefaction to initiate cavitation. More power is required to make liquid cavitate at, for example, 1 MHz than at 20 kHz (Figure 2.9). Frequencies below 16 kHz also can be employed in sonochemistry, but a lot of noise is produced by applications at such low frequencies. So, in this way, frequencies of 20 kHz and higher are usually used in sonochemical applications.

However, it was recently observed (Entezari and Kruus 1994) that ultrasound of higher frequencies can lead to higher reaction rates in comparison to low frequency one in oxidation reactions.

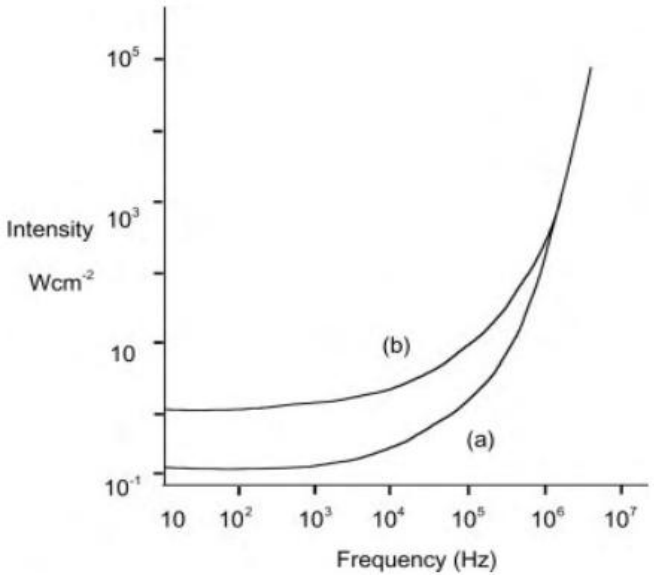

Figure 2.9. The relation between an ultrasound frequency and its intensity in a) aerated water and b) air free water

Frequency of ultrasound also defines whether the physical or chemical effect domintates when the liquid medium is subjected to ultrasound. Low frequency ultrasound (20 – 100 kHz) provides more violent agitation, higher temperatures and pressures during the cavitation collapse. In case of high frequency ultrasound (over 100 kHz), the chemical effect dominates: the radical production is very high. However, power of high frequency ultrasound unit is low in comparison to the low frequency ultrasound unit (Thompson and Doraiswamy, 1999).

2.3.4. Effect of Intensity of Ultrasound on Cavitation

Sonochemical transformations occur when ultrasound of specific intensity is applied (depending on experimental conditions and the properties of the sonicating medium). Then, generally, a larger number of cavitation bubbles are generated with increasing ultrasound intensity. In other words, there is some range of intensities where rates of sonochemcal reactions change proportional to intensity (Margulis 1984, p. 63). However, intensity of ultrasound cannot be increased infinitely. Rates of sonochemical reactions may also reduce at high intensities of ultrasound. This effect can be explained differently. On the one hand, as known, an increase in intensity of ultrasound leads to increasing the negative acoustic amplitude. It can be seen from Equation 2.11 that a cavitation bubble radius also depends on the negative pressure amplitude, i.e. a value of amplitude of a sound wave during the compression cycle (Mason and Lorimer 2002, p. 59):

$$R_{max} = \frac{4}{3\,w_a}\,(P_a - P_h)\left(\frac{2}{\rho\,P_a}\right)^{1/2}\left[1 + \frac{2\,(P_a - P_h)}{3\,P_h}\right]^{1/3} \qquad \text{[Eqn. 2.11]},$$

where

R_{max} – Maximum radius of cavitational bubble

P_a – Acoustic pressure

P_h – Applied hydrostatic pressure

ρ – Density of a medium

w_a – Equal applied circular frequency given by

$w_a = 2\pi f$, where

f – Frequency of ultrasound

π – pi number (3.141592)

Thus, the cavitation bubble may grow so large from its initial size during a rarefaction cycle that the time which is left for collapse is not enough**.** So, at some point of the intensity increase, depending on other conditions (such as pressure, temperature, surface tension), there is no further enhancement in rates of sonochemical reactions and, moreover, the further increase in the ultrasonic intensity will reduce the number of collapsed cavities which would lead to lower yields of the products of sonolysis. On the other hand, some authors (Suslick 1988) explain it by the fact that at high intensities the density of cavitation bubbles near the radiating surface (the tip of ultrasonic transducer) is increased. In such situation the absorbtion

of ultrasonic waves by cavitation bubbles prevent them (ultrasonic waves) from transmission further into the liquid medium.

2.3.5. Effect of Hydrostatic Pressure on the Cavitation

Generally, an increase in the hydrostatic pressure results in decreasing the vapour pressure of a liquid medium and, consequently, in an increase in the strength of cavitation bubbles collapse and sonochemical effect (Behrend and Schubert 2001). Several authors (Whillock and Harvey 1998; Dahnke and Keil 1999), assuming the adiabatic nature of the cavitation bubble collapse, derived Equations 2.12 and 2.13 to calculate maximum temperatures and pressures occurring during the cavitation bubble implosion:

$$T_{max} = T_0 \left\{\frac{P_m(\gamma-1)}{P}\right\} \quad \text{[Eqn. 2.12]}$$

$$P_{max} = P \left\{\frac{P_m(\gamma-1)}{P}\right\}^{\gamma(\gamma-1)} \quad \text{[Eqn. 2.13],}$$

where

T_{max} – Maximum temperature of the cavitation bubble collapse, K

P_{max} – Maximum pressure of the cavitation bubble collapse, Pa

T_o – Experimental temperature or temperature of a sonicating medium, K

P – Pressure in the bubble at its maximum size, m

P_m – Hydrostatic pressure during the cavitation bubble collapse, Pa

γ – Ratio of specific heats given by

$\gamma = \frac{C_p}{C_v}$, where

C_v – Heat capacity at constant volume, J/(mol·K)

C_p – Heat capacity at constant pressure, J/(mol·K)

Thus, from these equations can be seen that increasing the hydrostatic pressure of a liquid medium allows greater values of maximum temperatures and pressures during the cavitation bubbles implosion to be achieved. Moreover, changes in the hydrostatic pressure of a liquid medium have an effect on the cavitation collapse time (τ). Rayleigh (1917) deduced Equation 2.14 describing the collapse time (τ) of a cavitation bubble:

$$\tau = 0.915\, R_m \left(\frac{\rho}{P_0}\right)^{1/2} \quad \text{[Eqn. 2.14],}$$

where

τ – Time, second

R_m – Radius of a cavitation bubble at its collapse, m

ρ – The density of a liquid medium, kg/m^3

P_0 – Constant ambient pressure, Pa

However, Khoroshev (1963) stated that it is unlikely that a cavitation bubble feels a constant pressure (P_0) during sonication as long as the acoustic pressure is a time dependent value. It was assumed (Khoroshev 1963) that the cavitation bubbles filled with gas and/or vapour at the time of implosion, so such values as the hydrostatic pressure of a medium and the pressure in the bubble at its collapse should not be neglected. Thus, Khoroshev (1963) suggested that Equation 2.14 must be modified to (Eqn. 2.15):

$$\tau = 0.915\, R_m \left(\frac{\rho}{P_m}\right)^{\frac{1}{2}} \left(1 + \frac{P}{P_m}\right) \qquad \text{[Eqn. 2.15]},$$

where

P – Pressure inside a cavitation bubble at the time of its collapse, Pa

However, it is known that in order for the bubble to stay in equilibrium, the forces inside the bubble (P_v and P_g) should be equal to counteracting ones (P_h and $2\sigma/R_0$) which try to crush the bubble (Eqn. 2.16).

$$P_v + P_g = P_h + 2\left(\frac{\sigma}{R_0}\right) \qquad \text{[Eqn. 2.16]},$$

where

P_v – Vapour pressure inside a cavitation bubble, Pa

P_g – Gas pressure inside a cavitation bubble, Pa

P_h – Hydrostatic pressure of a liquid medium, Pa

R_0 – Radius of a cavitation bubble, m

σ – Surface tension of a liquid medium, N/m

This means that if the liquid medium, for example water, is at ambient conditions and is not subjected to ultrasound, bubbles cannot be generated in the system. Moreover, gaseous bubbles which already exist in the system do not collapse. Thus, in order to initiate the cavitation process, the effect of P_v and P_g forces must overcome the effect of P_h and $2\sigma/R_0$. When the liquid medium becomes subjected to ultrasound and an ultrasonic wave goes through the system, the formation of cavities

becomes highly improbable due to a positive value of the acoustic pressure created by ultrasound as given in (Eqn. 2.17):

$$P_v + P_g < P_h + 2\left(\frac{\sigma}{R_0}\right) + P_a \qquad \text{[Eqn. 2.17]},$$

where

P_a – Acoustic pressure, Pa

However, during the rarefaction cycle of the ultrasonic wave, the acoustic pressure becomes negative as shown in Equation 2.18. So at this moment cavitation bubbles are formed, because the forces *(P_v* and P_g) trying to disrupt the liquid overcome the ones (P_h and $2\sigma/R_0$) which hold the liquid medium together:

$$P_v + P_g > P_h + 2\left(\frac{\sigma}{R_0}\right) - P_a \qquad \text{[Eqn. 2.18]}$$

After that, depending on the characteristics of the ultrasound, transient cavitation bubbles will collapse when the ultrasonic wave again goes through its compression cycle, whereas stable cavities will oscillate during a number of acoustic cycles. Also, it should be understood that increasing the hydrostatic pressure will lead to an increase in the Blake‟s threshold which will result in a suppression of cavitation. In this case, the higher the static pressure of a liquid the less cavitation bubbles can be generated at fixed ultrasound intensity as long as a rise in intensity of ultrasound leads to higher acoustic pressure values. Consequently, applying the more intense ultrasound (higher acoustic pressure) will allow the cavitation threshold to be decreased. With further increase in the intensity, there is a point when the hydrostatic pressure of the medium is large enough, so that the maximum power of ultrasound provided by the ultrasonic device is not enough to initiate cavitation at all (Suslick 1988). So there is an optimum operating pressure for any sonication system and ultrasound generating device which depends on the properties of the system and the characteristics of the ultrasonic device (Moulton, Koritala, and Frankel 1983; Berlan et al. 1994).

2.3.6. Effect of Temperature on the Cavitation

The temperature is also one of the main parameters determining the cavitation threshold. Theoretically, it resembles boiling, but there is a significant difference between boiling and cavitation phenomena. Boiling occurs when the vapour pressure

exceeds a hydrostatic pressure of a liquid. Mainly, it happens due to an increase in temperature. Contrariwise cavitation is produced when the hydrostatic pressure of a liquid falls below the vapour pressure of the liquid, i.e. when negative pressure is applied to a liquid. It occurs with almost no significant changes in temperature of a liquid medium. Even though boiling and cavitation have different mechanisms, increases in temperature will lower the cavitation threshold, so more cavitation bubbles can be produced. In other words, the vapour pressure of liquid rises with an increase in temperature, so ultrasound of less intensity has to be applied to the same liquid at 60^0C than to that at 30^0C to make hydrostatic pressure lower than the vapour pressure and, consequently, to cause cavitation. However, at higher temperatures, the vapour pressure of a liquid medium is increased and, consequently, more vapour penetrates inside the cavitation bubble increasing its vapour pressure. So, due to a high value of the thermal conductivity of liquid mediums, such increase in the vapour pressure of the cavitation bubble cushions the collapse of the bubble and the lower temperatures and pressures are generated during the implosion (Kirpalani and McQuinn 2006).

Another fact is that the surface tension of a liquid medium decreases with a temperature rise. Thus, as it was discussed in Section 2.3.2, less intense ultrasound is needed to generate cavitation bubbles. Also, the viscosity of a liquid medium decreases with a temperature increase which lowers the cavitation threshold. So from this discussion it can be seen that the temperature is a very important parameter determining the cavitation threshold and the power of the bubble collapse. Changes in the temperature of a medium have an effect on parameters inherent to this medium. So, the temperature does not affect the cavitation collapse itself but act through such parameters as viscosity, the liquid‟s vapour pressure and surface tension.

It can be concluded that cavitation bubbles at higher temperatures occur more readily during sonication. However, at some point in the temperature increase the sonochemical effects of such bubbles may be reduced, mainly due to the effect of the bubble collapse „cushioning". For example, Weissler in his work showed that the rate of a reaction decreases with the experimental temperature increase (Weissler 1953). This relation was also observed in other later works (Entezari and Kruus 1995; Merouani et al. 2010; Segebarth et al. 2002). On the contrary, some ultrasound initiated reactions have a greater rate with an increase in the ambient temperature up

to some point, then the rate of reaction decreases again (Mizukoshi et al. 1999; Ibisi and Brown 1967).

2.3.7. Liquid Medium for Sonication

From all information of physical properties discussed above it can be stated that the choice of a better medium for sonication, in order to generate higher temperatures and pressures during the cavitation collapse, should be based on three parameters of a liquid medium. The viscosity and surface tension are important parameters in the choice of a medium for sonication. As discussed previously in Section 2.3.2, the higher the values of viscosity and surface tension the higher the intensity of the ultrasound must be applied to create cavitation bubbles, and consequently the more energy that must be spent. The third parameter, the vapour pressure, is also a very important property of a liquid medium. The higher the vapour pressure of a liquid subjected to sonication the larger the amount of vapour inside the cavitation bubbles formed, and consequently, the lower the maximum pressures and temperatures generated during the cavitation collapse of these bubbles. However, when the liquid medium is not volatile enough and its vapour does not enter cavities during sonication, there is no sonochemical effect observed at all (Griffing 1952). Although these properties of a liquid medium should not be neglected, it is important to remember that such parameters are extremely dependent on the chosen conditions of the sonication process such as the temperature and hydrostatic pressure of a sonicating medium.

2.4. Ultrasonic Equipment Used in Sonochemistry

2.4.1 Types of Transducers

Rapid improvement and development in ultrasonic equipment and its better availability in the market is one of the reasons why sonochemistry has drawn such an enormous attention over the last 30 years (Berlan and Mason 1992). Ultrasonic equipment consists of a device which converts mechanical and electrical types of energies into sound energy (vibrational energy). The piece of equipment which is directly responsible for providing this energy conversion is called a transducer. Generally, all ultrasonic transducers can be divided into four categories (Mason and Lorimer 2002):

- Gas driven transducers

- Liquid driven transducer
- Electromechanical transducers
- Magnetically driven transducers

Today, the electromechanical type of transducer is the most popular among the scientists involved with sonochemistry. All electromechanical transducers can be divided into piezoelectric and magnetostrictive ones depending on which effect they are based on. Figure 2.10 depicts examples of both types of electromechanical transducers. Although, a magnetostrictive transducer seems to have a simple and durable construction, it has two significant disadvantages which reduce its range of applications. First, the available working frequency is limited to 100 kHz, and second it has got low conversion efficiency of only about 40% of the consumed electrical energy is converted to heat (Mason and Lorimer 2002).

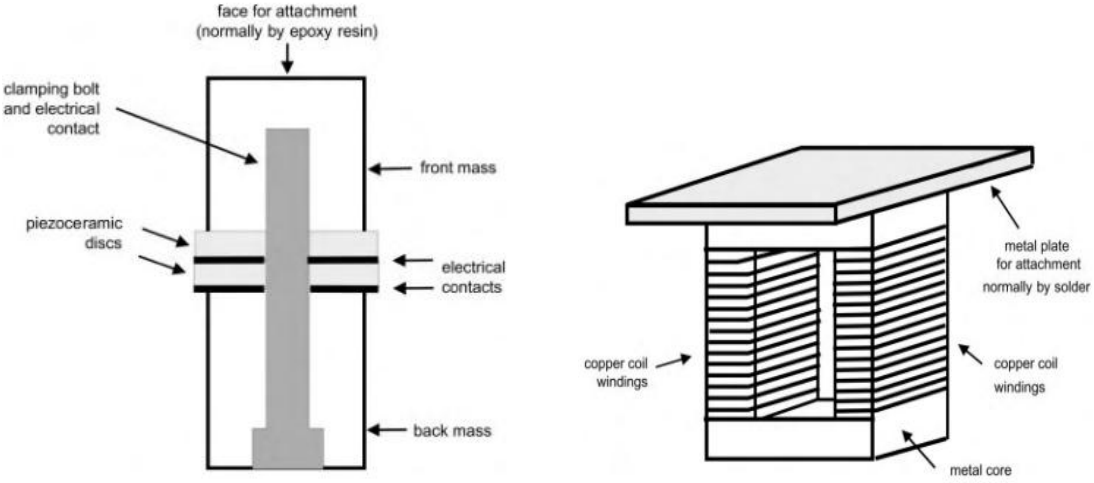

Figure 2.10. Piezoelectric (left) and magnetostrictive (right) types of electromechanical transducers

However, magnetostrictive transducers are used in a range of industrial applications which require heavy duty usage. So, piezoelectric transducers due to the wide frequency range and higher electrical efficiency are the better choice for sonochemistry, especially at laboratory studies (Hunicke 1990).

2.4.2 Types of Ultrasonic Apparatuses

Today, based on piezoelectric property there are three types of apparatuses widely used in sonochemical research: the ultrasonic bath, the ultrasonic probe and the cup-horn systems. All three have both advantages and disadvantages as described below.

2.4.2.1 Ultrasonic Bath System

The ultrasonic bath (Figure 2.11) is the most widely available and cheapest ultrasonic apparatus on the market, and today it is widely used by sonochemists, though originally ultrasonic baths were produced for cleaning purposes. An advantage of the ultrasonic bath is that it has a simple construction of a stainless steel tank with piezoelectric transducers coupled to its base. However, the bath‟s intensity is usually lower than that of the probe system and the ultrasonic energy for the reaction mixture must be delivered through the walls of the reaction vessel and the liquid with which the bath is filled (Mason 1992). So, the process of sonication when an ultrasonic bath is used is called 'indirect sonication'. Also, the temperature control in the ultrasonic bath system is problematic, so ultrasonic bathes which are used in sonochemistry should preferably be equipped with cooling coils. However, such coils may reduce the amount of ultrasonic power transferred to the reaction vessel.

Figure 2.11. Simple ultrasonic bath with transducer attached to its base

2.4.2.2 Ultrasonic Probe System

The ultrasonic probe is a more powerful system than the ultrasonic bath. Originally, ultrasonic probe systems were used mainly for cell disruption in order to extract a cell‟s content. The simple ultrasonic probe (Figure 2.12) system consists of a transducer which converts the electrical energy to the vibrational and a probe (or horn) which acts as an amplifier for the vibration. Such system is very simple in operation. As a rule, all ultrasonic probe systems have a fix frequency at which they operate. However, the power control is adjustable what is one of the most important advantages of such systems. The power control can be performed in two ways. First,

all ultrasonic probe types of apparatus have an option to setup the needed power input to the transducer by increasing or decreasing the amplitude of ultrasound (see Figure 2.12). Second, the ultrasound amplitude can be controlled by design of the probe used or by using additional amplifiers (boosters). However, despite of all advantages the poor temperature control remains the main disadvantage of such types of ultrasonic system. Therefore, additional adjustments providing better temperature monitoring should be implemented when the ultrasonic probe system is used in sonochemistry. Moreover, the "cushioning effect" caused by the large number of generated cavitation bubbles reduces the sonication efficiency. Erosion and pitting of the probe tip during sonication is another significant disadvantage, because it may lead to contamination of the reaction solution.

Figure 2.12. Simple ultrasonic probe system

Design of ultrasonic probes is a very important aspect of ultrasonic engineering. Firstly, because the intensity of ultrasound produced directly by the transducer is not enough to generate cavitation, and secondly, because the ultrasonic power delivered to a sonication medium significantly depends on the probe design (shape).

2.4.2.2.1. Ultrasonic Probe Design

First of all, it has to be emphasized that ultrasonic probes have to be made of a material that has high tensile strength, low acoustic loss, chemical inertness and resistance to cavitation erosion. Today, a high grade titanium alloy is the most appropriate material for this purpose, although for some applications probes can be made of such materials as aluminium and steel alloys (Berlan and Mason 1992).

There are two main parameters considered for designing an ultrasonic probe: its length and its shape. The length of an ultrasonic probe depends on the frequency used in the sonication and the material from which the horn is fabricated. There are many different types of horns used in ultrasonic applications such as cylindrical, bar, block and many others (Perkins 1990). However, there are four basic shapes of the cylindrical type of ultrasonic probes employed in sonochemistry: uniform, linear taper, exponential taper and stepped. The advantage of using the last three shaped probes is that these horns enchance significantly the amplitude of the vibration energy produced by the transducer. For example, linear taper probes provide about a 4-fold increase in amplitude, whereas exponential taper probes increase amplitude approximately by 6 - to 8 – fold. The largest magnification to amplitude is provided by stepped probes up to 16-fold (Mason and Lorimer 2002).

2.4.2.3 Ultrasonic Cup-horn System

The main benefit of ultrasonic cup-horn systems (Figure 2.13) is that they have a much better temperature control than an ultrasonic bath and probe systems (Mason and Lorimer 2002). Figure 2.13 presents a simple ultrasonic cup-horn system where a sonotrode is fitted into a glass cup. This glass cup serves as a thermostat, circulating water and maintaining a temperature of sonication. The actual sample for sonication should be placed into a vessel, such as a test-tube or vial, and immerged into water. Nevertheless, it should be borne in mind that the limited volume of a reaction cell and reduced power in comparison to the probe system are the noted as the shortcomings of the cup-horn system.

Figure 2.13. Simple ultrasonic cup-horn system

Chapter 3. Apparatus Design and Methodology of Experimental Work

3.1. Introduction

The chapter provides information about the experimental equipment used throughout the research. Each piece of equipment used in the experimental work is thoroughly described. Photographs and technological schemes are presented in this chapter for better understanding. Methodologies of experimental work at low-pressure and at high-pressure are presented in great detail from gas composition preparation to the sample's analysing techniques. Moreover, this chapter contains information about the chemicals used during the experimental work. Two experimental apparatus have been constructed and employed during this research. The first apparatus was designed to be used for tests requiring a low hydrostatic pressure (up to 1 MPa), whereas another apparatus was designed for experimental work under high pressure conditions (up to 14 MPa).

3.2. Low Pressure Experimental Apparatus

This section present the description of the low pressure apparatus used for experimental work on sonochemical reduction of CO_2. The apparatus was constructed in the Clean Gas Technology Australia laboratory. The following sections present descriptions of all part of the experimental apparatus.

3.2.1. Ultrasonic probe system

20 kHz ultrasonic system UIP1000hd (maximum power of 1000 Watts) was purchased from Hielscher Ultrasonics GmbH (Figure 3.1). The system consists of a 22 millimetres titanium alloy sonotrode, ultrasonic transducer and ultrasonic generator. All the frequency and power characteristics of the system were selected in order to generate “high power ultrasound” (see Section 2.1, Chapter 2).

3.2.2. Reactor

A reactor (cell) (FC100L1K-1S) was also purchased from Hielscher Ultrasonics GmbH. It is a 1 litre flow cell made of stainless steel. The cell is equipped with a cooling jacket for temperature control. The reactor is able to withstand pressures up

to 1 MPa. The reactor is coupled with a sonotrode by means of an O-ring-flange connection (Figure 3.2).

Figure 3.1. Ultrasonic probe system

Figure 3.2. Ultrasonic reactor (cell)

3.2.3. Micro-Gear Pump

A pulse micro-gear pump (Figure 3.3) was purchased from Dynapumps Australia. The technical characteristics of the pump were selected in such way that the pump could be used in experimental work at slightly elevated pressures (up to 1 MPa). So, the discharge capacities range of the pump and a range of pressures for which the pump can be applied were 0-10 litres and 0.1 - 1 MPa, respectively.

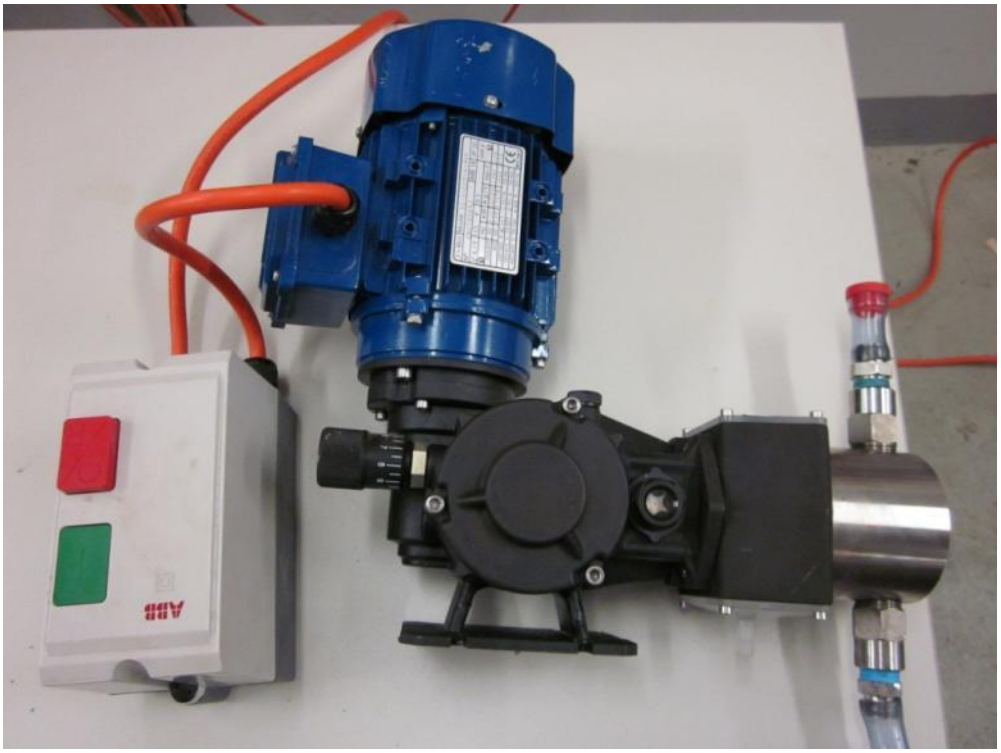

Figure 3.3. Micro-gear pump

3.2.4. External Cooling System

The external cooling system (Figure 3.4) was constructed in our laboratory and was used for the regulation of experimental temperatures. This system consists of two 2 inch diameter coreless plastic pipes secured over the tubing connection between the ultrasonic reactor and the micro-gear pump, a plastic tank of approximately 40 litres filled with iced water and an aquarium submersible pump (Weipro WH-1000) purchased from Guppy‟s Aquarium Products (maximum of 20 lpm water discharge). Briefly, the aquarium pump immersed in the tank runs the iced water through the 2 in. plastic tubes and the cooling jacket of the reactor providing the required cooling rate of a reacting mixture inside the reactor. The cooling rate can be regulated by the discharge value of the pump. Moreover, this system is enclosed, so recycled cooling water is used.

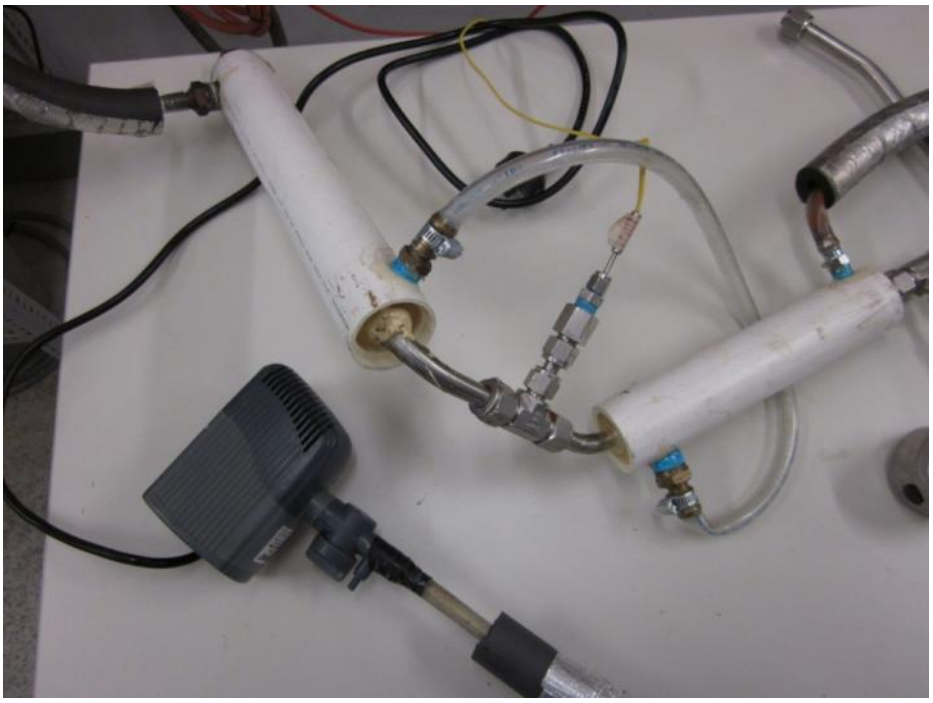

Figure 3.4. External cooling system

3.2.5. Two Stage Rotary Vane Pump

A two stage rotary vane pump was purchased from Edwards Vacuum Ltd. The vacuum pump served to eliminate air or any other gases from the reactor system in each experiment (Figure 3.5). It was also used for evacuating stainless steel cylinders before loading any composition of gases in them.

Figure 3.5. Two stage rotary vane pump

3.2.6. Pressure Gauges and Temperature Sensor

A temperature sensor was purchased from Swagelok Australia (Figure 3.6). Two pressure gauges (Figure 3.7) with ranges of up to 2.5 MPa were also obtained from Swagelok Australia.

Figure 3.6. Temperature sensor

Figure 3.7. Pressure gauges

3.2.7. 500 cm^3 Stainless Steel Cylinders

500 cm^3 stainless steel cylinders which withstand pressures up to 12 MPa (Figure 3.8) were obtained from Swagelok Australia. The cylinders were utilized in order to prepare various compositions of gases.

Figure 3.8. 500 cm3 stainless steel cylinders

3.2.8. Other Equipment

Other equipment included ½ and ¼ inch diameter tubes, valves and other fittings used in building the setup were purchased from Swagelok Australia.

3.3. Experimental Apparatus Description

The setup was assembled using the ultrasonic equipment, stainless steel reactor, micro-gear pump, cooling system and other pieces of equipment described in detail above and shown in Figure 3.9. The scheme of the setup is presented in Figure 3.10. The ultrasonic transducer system is linked to the reactor by means of an O-ring-flange connection. The reactor cell has two openings. The first and second openings are connected with the micro-pump‟s inlet and outlet respectively by means of ½ inch tubing. The total volume of the reactor and its circulating tubes minus the space taken by the sonotrode is estimated to 1000±2 cm^3. Also, two plastic 2 inch pipes are secured on the tubing connection between the first cell‟s opening and the micro-gear pump in order to provide a better temperature control of the reacting mixture and opportunity of the interrupted use of ultrasound. The temperature control of the

reaction medium is provided by means of the circulation of iced water from the tank. Moreover, a temperature could be also regulated by adjusting the amplitude of the generated ultrasound. So, the lower the amplitude of ultrasound is set the lower the experimental temperature reached. However, decreasing the ultrasound amplitude leads to a decrease in intensity of produced ultrasound. Thus, the variable amplitude option is not used as the main tool of the temperature control. Pressures and temperatures during experimental work are monitored by using pressure gauges and the temperature sensor. The loading-sampling valve serves for both transferring the sonication medium and atmospheric gases into the reactor, and taking gaseous samples.

Figure 3.9. Low pressure experimental apparatus

3.4.Test Preparation and Experimental Procedures Description

3.4.1. Preparation of Experiment

The reactor, ultrasonic horn and tubing connections were washed with tap water and dried with compressed air every time before test preparation.

After that, all parts of the experimental apparatus were connected to each other as is depicted on Figures 3.8 and 3.9. A strip of aluminum foil is placed inside the reactor

in every test so the phenomenon of transient cavitation could be detected. Then the system was evacuated with the vacuum pump to approximately minus 1 bar (Figure 3.5) and left for 30 minutes in order to detect any possible leaks. Additional pressure sensor (Figure 3.18) was used in order to monitor negative pressures.

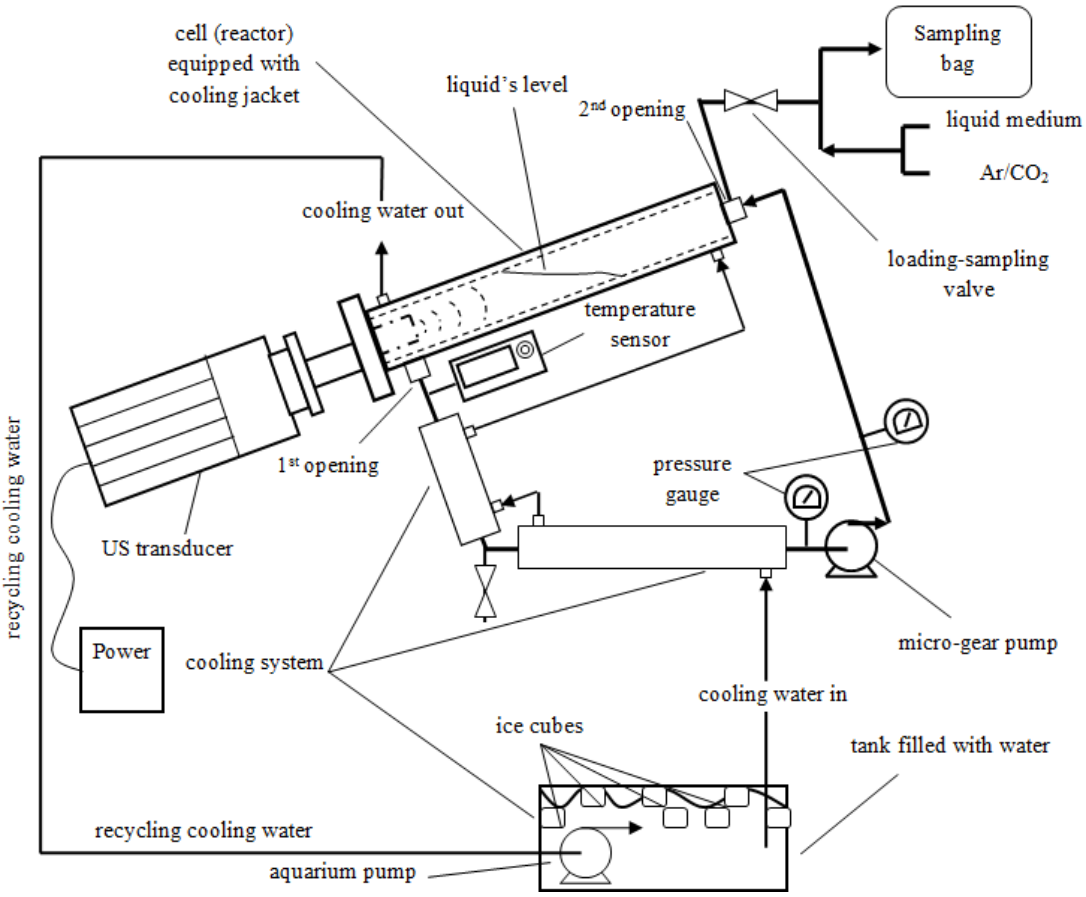

Figure 3.10. The schematic prepresentation of the apparatus used for experimental work at low pressures

3.4.2. Liquid Medium Loading

At the next step all liquid reagents (and if needed solid reagents mixed within a liquid medium) are transferred into the reactor through a loading-sampling valve by means of the difference in the ambient pressure and a negative pressure inside the system. A total load of liquid reagent in the reactor was equal 500-550 cm^3 for all experiments performed. After that, the reactor system was pressurized with Argon to 0.3 – 0.4 MPa and kept for 10 minutes. Then, the gas was released to the atmosphere and the reactor evacuated over 30 minutes in order to maximize the elimination of any gases dissolved in the liquid medium.

3.4.3. Preparation of Atmospheric Gas

A mixture of atmospheric gases with the required percentages is prepared according to predetermined molar percentages of gases (*mol%(A)* and *mol%(B)*) using Equations 3.1 and 3.2. The 500 cm^3 stainless steel cylinders (Figure 3.8), withstanding pressures up to 12 MPa, were used for mixture preparation.

$$mol\%(A) = \frac{n_A}{n_t} * 100 \quad \text{[Eqn. 3.1]}$$

$$mol\%(B) = \frac{n_B}{n_t} * 100 \quad \text{[Eqn. 3.2],}$$

where

mol%(A) – Molar percent of gas A, %

mol%(B) – Molar percent of gas B, %

n_A – Amount of gas A, mol

n_B – Amount of gas B, mol

The relation between n_A and n_B is given by

$n_t = n_A + n_B$, where

n_t – Total amount of gas composition, mol

Then, the atmospheric gas composition was transferred into the reactor system through the loading-sampling valve until the desired hydrostatic pressure was reached. At this point all preparations for an experiment are completed.

3.5. High-pressure Experimental Apparatus

3.5.1. Ultrasonic Probe System

The ultrasonic probe system was purchased from Sonics & Materials Inc., USA (Figure 3.11). The system consisted of the ultrasonic generator, ultrasonic transducer and 1/3 in. titanium alloy sonotrode. The ultrasonic generator was able to produce 20 kHz ultrasound and its maximum power capacity amounted to 1500 Watts.

3.5.2. The High-pressure Vessel

The high-pressure reactor was designed by Parr Instruments Inc., USA (Figure 3.12). The working range of pressures and temperatures for the high-pressure vessel are up to 15 MPa and 473.15 K, respectively. The reactor consists of two main parts, such as the vessel and the head of reactor held together by means of a split ring with

12 cap screws (Figure 3.13). The construction of the high-pressure vessel provided a rupture disk assembly in case of an emergency (unexpected pressure increase). According to Parr Instruments Inc, the provided rupture disks‟ burst pressure varied in a range of 15.16 – 16.7 MPa at ambient temperature (288.15 – 303.15 K) and in a range of 14.25 – 15.75 MPa at 473.15 K. The approximate capacity of the vessel, excluding the volumes taken by the immersed sonotrode and fittings from the head of the reactor, was estimated to be approximately 800 cm^3.

Figure 3.11. Ultrasonic probe system

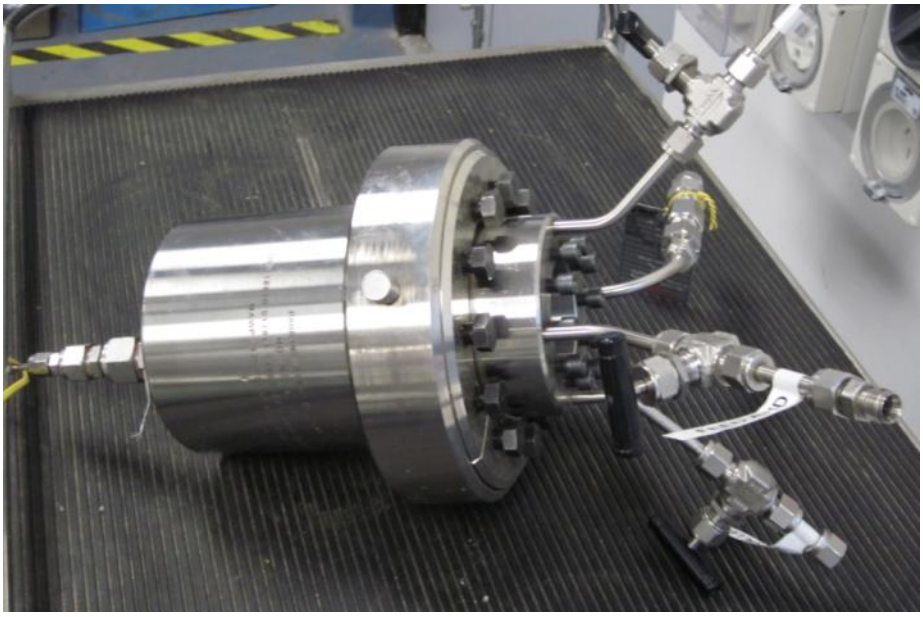

Figure 3.12. High pressure vessel (reactor)

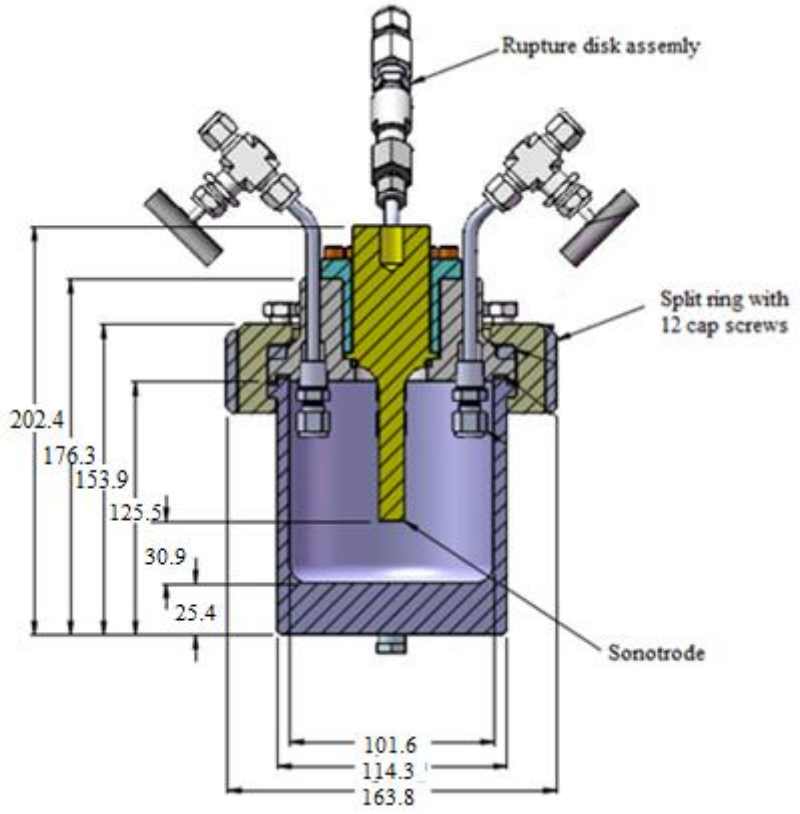

Figure 3.13. The scheme of the high pressure vessel with the sonotrode coupled (NOTE: all dimensions are presented in millimeters; drawing is not to the scale)

3.5.3. Air Driven Gas Booster

An air driven gas booster (Figure 3.14) purchased from Haskel was used to transfer a gas composition from a 500 cm^3 stainless steel cylinder to a high-pressure pump (see below).

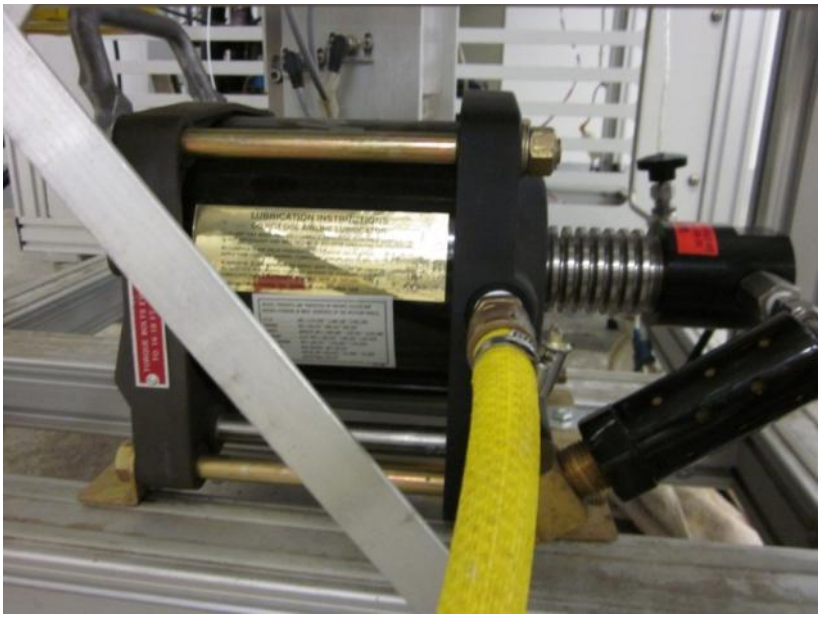

Figure 3.14. Air driven gas booster

3.5.4. High Pressure Pump

The high-pressure pump was constructed by Sanchez Technologies (France), (Figure 3.15). The pump was used to transfer the composition of gases into the reactor and compress it to required pressures.

3.5.5. Two Stage Rotary Vane Pump

A two stage rotary vane pump was purchased from Edwards Vacuum Ltd. The vacuum pump serves to eliminate air or any other gases from the reactor system in each experiment (Figure 3.5). Also, it is used for evacuating stainless steel cylinders before preparing a composition of gases.

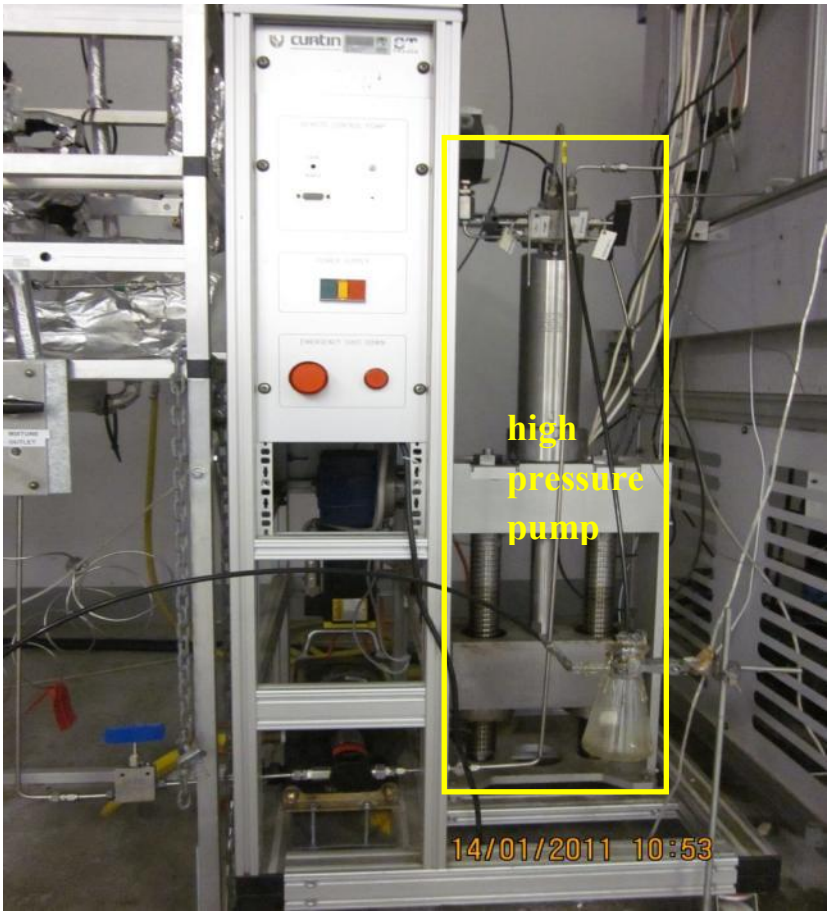

Figure 3.15. High pressure pump

3.5.6. Drying Oven

The drying oven (Figure 3.16 (a, b)) is employed to bring a reacting mixture of gases at supercritical conditions by changing a temperature.

Figure 3.16 (a and b). Drying oven

3.5.7. Cooling Chamber

A cooling chamber available at the CGTA laboratory is used to adjust temperature requirements for the composition of gases (Figure 3.17). The chamber can be set to a temperature of down to minus 223 K.

Figure 3.17. Cooling chamber

3.5.8. Temperature and Pressure Sensors

Temperature and pressure (Figure 3.18) sensors were obtained from Swagelok Australia.

Figure 3.18. Pressure (left) and temperature (right) sensors

3.5.9. Other Equipment

Other equipment included ½ and ¼ inch tubes, flexible tubing connections, valves and other fittings which were obtained from Swagelok Australia.

3.6. Experimental Apparatus Description

A photograph of the complete high-pressure experimental apparatus is presented in Figure 3.19 and a simple schematic representation of the experimental setup is shown in Figure 3.20.

Figure 3.19. High pressure experimental apparatus

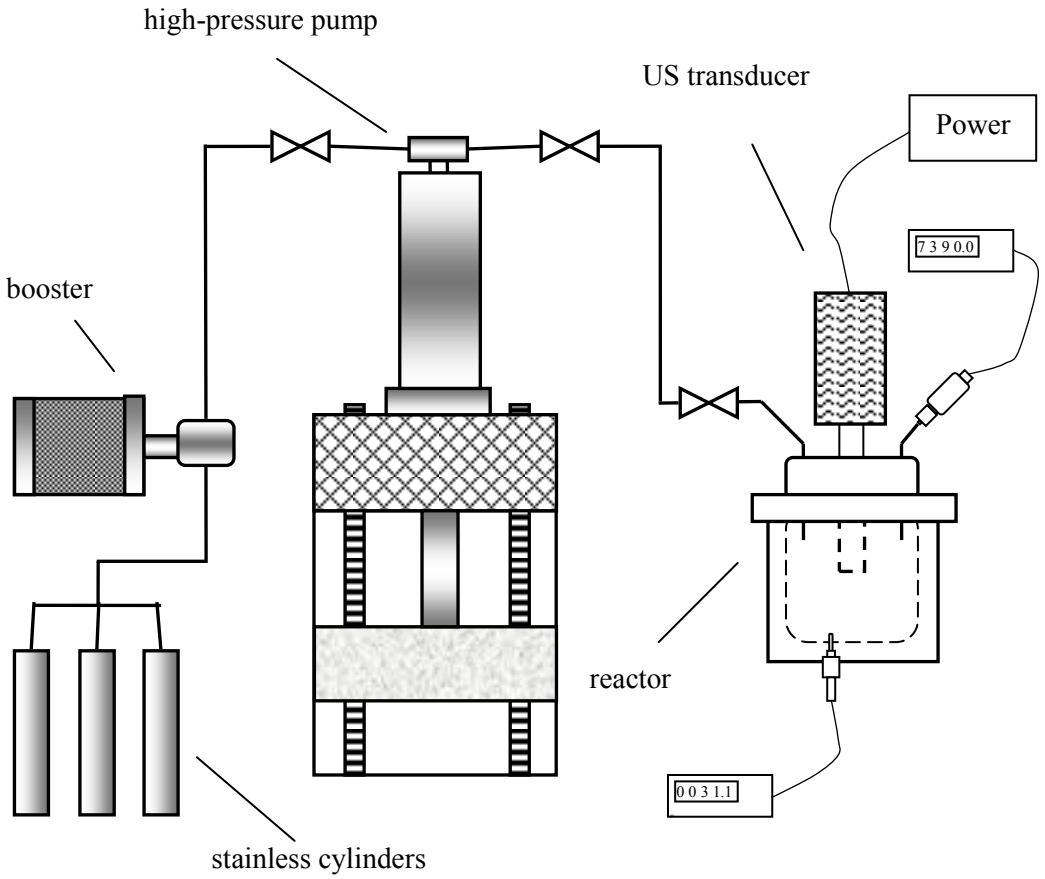

Figure 3.20. Simple schematic representation of the high pressure experimental apparatus

3.7. Test Preparation and Experimental Procedures

The methodology of test preparation can be divided into three parts: calculations, gas mixture preparation and gas composition loading. The inner volume of the high-pressure reactor was set to 500±1 cm^3 by placing stainless steel disks at the bottom of the reactor. This was done in order to reduce the usage of gases during preparation of the required gas compositions. After the adjustment of the reactor‟s inner volume the distance between the sonotrode and the bottom of the reactor was 2±0.2 cm and at least 230-250 cm^3 of the liquid phase is needed in order to perform a sonication test.

3.7.1. Estimation of Gas Amount for Experiment

Calculation of gas amount required for experiment was performed using the Aspen HYSIS 2006.5 computer software. The Peng-Robinson equation of state (EOS) (Peng and Robinson 1976) was selected because this method is widely used in chemical engineering for phase envelops prediction give by Equation 3.3:

$$P = \frac{R\,T}{V_m - b} - \frac{a}{V_m^2 + 2V_m\,b - b^2} \qquad \text{[Eqn. 3.3],}$$

where

P – Pressure, Pa

T – Temperature, K

V_m – Molar volume, m^3/mol

R – Universal gas constant, $m^3 \cdot Pa \cdot K^{-1} \cdot mol^{-1}$

a – Gas constant dependent on temperature given by

$$a = \frac{0.457236 R^2\,\alpha\,T_c^2}{P_c}\text{, where}$$

P_c – Critical pressure, Pa

T_c – Critical temperature, K

α – Function of temperature described by

$$\alpha = \left(1 + (0.37464 + 1.54226\omega - 0.26992\omega^2)\left(1 - \sqrt{\frac{T}{T_c}}\right)\right)^2\text{, where}$$

ω – Acentric factor

b – Volumetric constant given by

$$b = \frac{0.0777961 R\,T_c}{P_c}$$

In polynomial form the Peng-Robinson EOS is given by:

$$Z^3 - (1 - B)\,Z^3 + (A - 3B^3 - 2B) - (A\,B - B^2 - B^3) = 0\text{, where}$$

$$A = \frac{a\,P}{(R\,T)^2}$$

$$B = \frac{b\,P}{R\,T}$$

Z – Compressibility factor which can be express by

$$Z = \frac{P\,V_m}{R\,T}$$

Molar volume (V_m) is the starting point in a calculation of the amount of gases which has to be prepared. When an approximate value of molar percentage (*mol%*) of every component of a gas mixture is decided, the required value of molar volume (V_m) can be easily found using the HYSYS computer software. The P-V diagram depicted in Figure 3.21 shows various pressures as a function of molar volumes (V_m) for an Ar/CO_2 gas mixture containing 10 mol% of Ar. The red and blue lines are

bubble point and dew point lines, respectively, and the green line corresponds to an isotherm at 288.15 K (selected randomly as an example). It can be noted from the diagram that 100% of a gas mixture is in liquid state at the point (Point 1 see Figure 3.21) where the isotherm crosses the bubble point line, whereas 100% of the mixture is in gaseous state at the point (Point 2 see Figure 3.21) where the isotherm crosses the dew-point line. Thus, the amount of gas phase between those two points (the isotherm) varies from 0 to 100 %. Moreover, every point on the isotherm corresponds to a particular molar volume (V_m) of the gas composition which can be estimated by the HYSYS computer software.

Once the desired molar volume (V_m), at which a required percentage of the gas mixture is at the liquid state was determined, then the total amount (n_t) of the gas composition, which had to be prepared, was estimated.

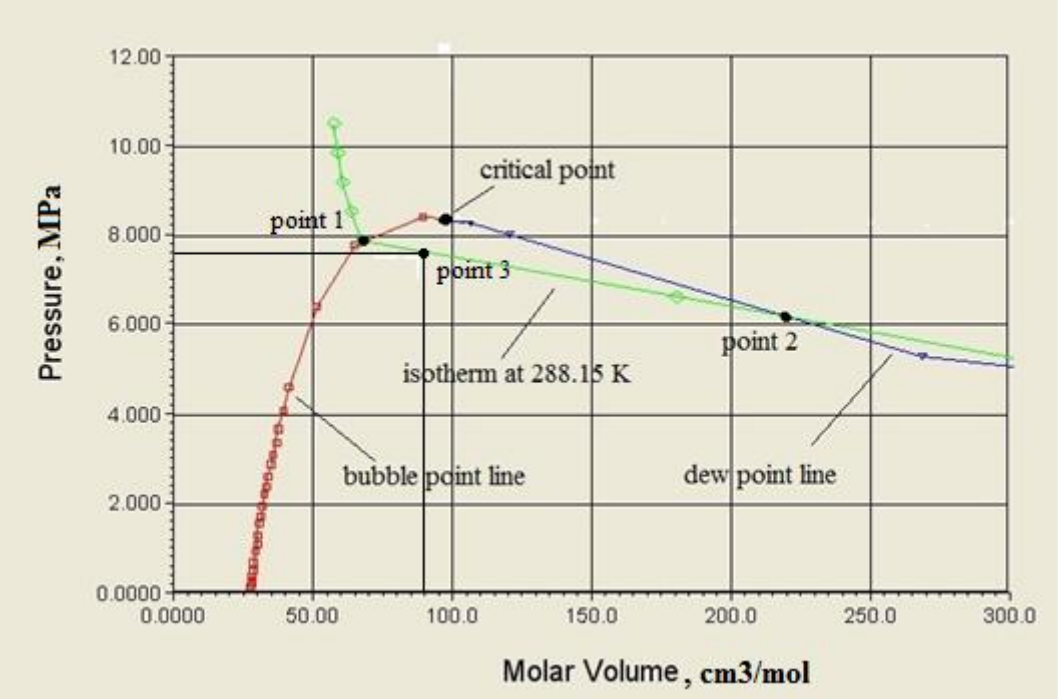

Figure 3.21. P-V diagram for 90% CO_2 – 10% Ar mixture

For example, a mixture of Ar and CO_2 gases (see graph on Figure 3.21) containing 10 mol% of Ar should be liquefied so that there is at least 230-250 cm^3 of the liquid phase in the reactor. The inner volume of the reactor (V_r) is set to 500 cm^3. So, according to calculations made by using the HYSYS computer software, at the point where a temperature and pressure are 288.15 K and 7.6 MPa, respectively, there is 93% of the gas composition is at the liquid state and a molar volume of 90 cm^3/mol corresponds to this point (see point 3). The volume of the liquid phase at such

experimental conditions could is to be approx. 330 cm^3 using data provided by the HYSYS and Equations 3.4 or 3.5.

$$V = \frac{Z\,n\,R\,T}{P} \qquad \text{[Eqn. 3.4],}$$

where

V – Volume, m^3

Z – Compressibility factor

n – Amount of substance, mol

R – Universal gas constant, $m^3 \cdot Pa \cdot K^{-1} \cdot mol^{-1}$

T – Temperature, K

P – pressure, Pa

$$V = \frac{m}{\rho} \qquad \text{[Eqn. 3.5],}$$

where

V – Volume, m^3

ρ – Density, kg/m3

m – Mass, g, given by $m = n \cdot M_{av}$, where

M_{av} – Average molecular weight, kg/kmol

n – Amount of substance, mol

Thus, at selected experimental conditions, there is sufficient amount of the liquid phase present to conduct a sonolysis test. The total amount of the gas mixture which should be prepared can be found by Equation 3.6 as follows:

$$n_t = \frac{V_r}{V_m} \qquad \text{[Eqn. 3.6],}$$

where

n_t – Total amount of gas composition, mol

V_r – Volume of the reactor, m^3

V_m – Molar volume, m^3/mol

This gives the total amount of approximately 5.56 mol of CO_2/Ar mixture that should be prepared in order to obtain over 93% of gas composition at the liquid phase.

This raises a question why the total amount of gases cannot be compressed to the point where 100% of the mixture is at liquid phase?

The answer is very simple. Practically, it is possible to convert 100% of a gas mixture to the liquid state, however, when this point is reached, any slight decrease in a molar volume will cause a very steep increase in temperature or pressure.

3.7.2. Gas Mixtures Preparation

When the total amount of the composition is determined, the amount of each component (n_A and n_B) of the mixture can be calculated using Equations 3.1 and 3.2, which give:

$$mol\%(A) = \frac{n_A}{n_t}\ 100 \Leftrightarrow n_A = \frac{mol\%(A)\ n_t}{100}$$

$$mol\%(B) = \frac{n_B}{n_t}\ 100 \Leftrightarrow n_B = \frac{mol\%(B)\ n_t}{100}$$

It is crucial not to use any volume dependant quantity when the amounts of gases are calculated in order to avoid mistakes due to a compressibility factor.

3.7.3. Technique of Loading a Gas Mixture into the Reactor

In this section the technique of loading a gas composition into the reactor is described. For example, the required amount of composition of gases was prepared using three stainless steel cylinders. The prepared gas mixture was then transferred into the reactor (Figure 3.22a).

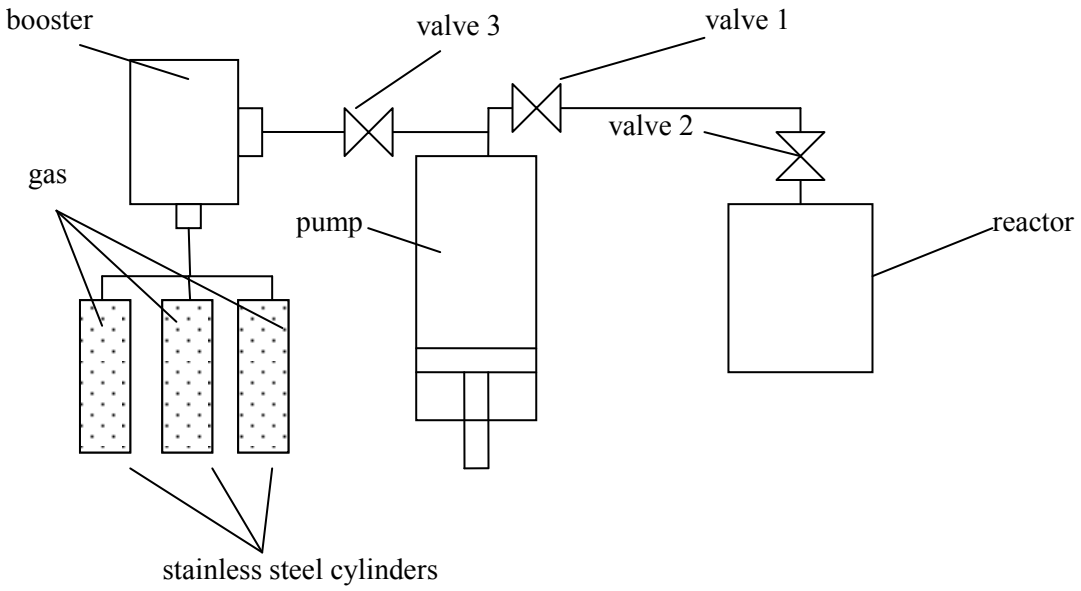

Figure 3.22a. Schematic process of loading a gas mixture into the reactor (Step 1)

First, the pump and reactor were filled with the gas composition by using the booster, so that the content of two cylinders was transferred to the reactor (Figure 3.22b). As long as the booster cannot be used for compression of gas mixtures, compositions from only two cylinders was pumped over to the pump-reactor system.

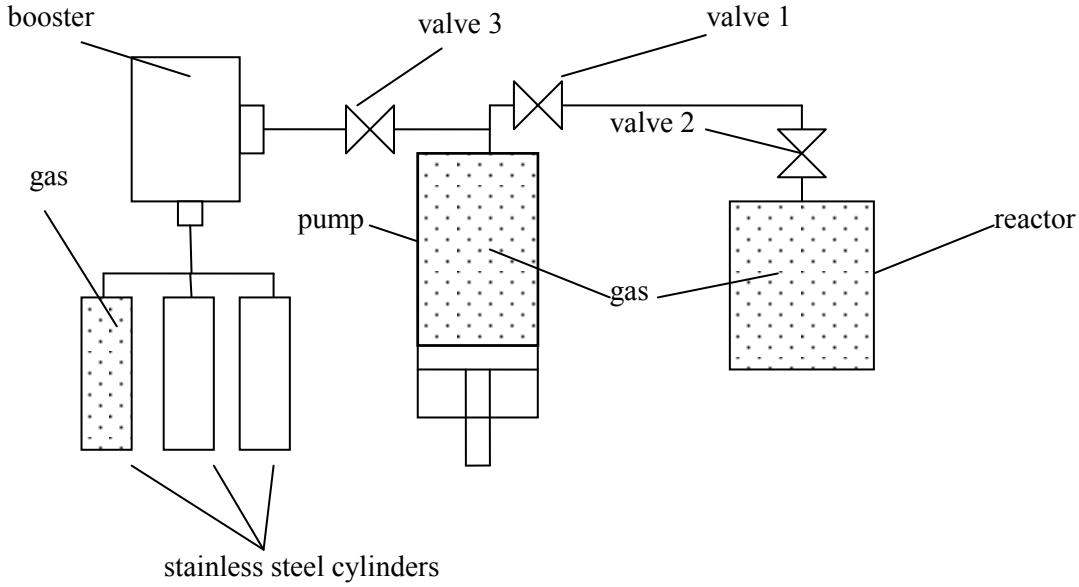

Figure 3.22b. Schematic process of loading a gas mixture into the reactor (Step 2)

At the next step, Valve 3 was closed while Valves 1 and 2 were kept open. Then, the gas mixture from the pump was transferred to the reactor by compression with Valves 1 and 2 closed. Here, some percentage of the gas composition in the reactor is liquefied (Figure 3.22c).

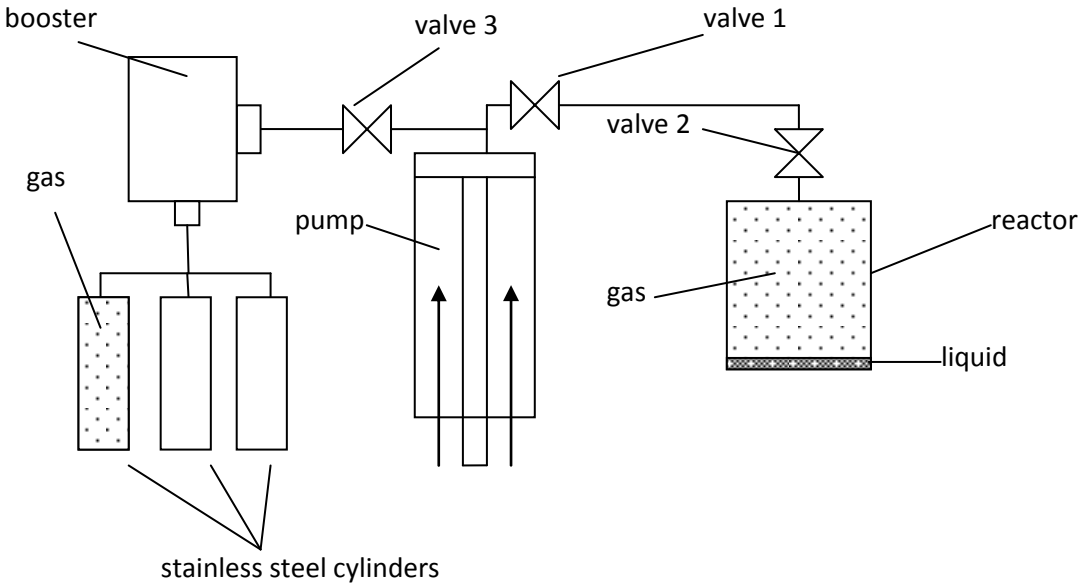

Figure 3.22c. Schematic process of loading a gas mixture into the reactor (Step 3)

During the next step, Valve 3 was opened and the pump returned to the initial position and filled with the remaining gas composition, whereupon Valve 3 was closed. Valves 1 and 2 remained closed (Figure 3.22d).

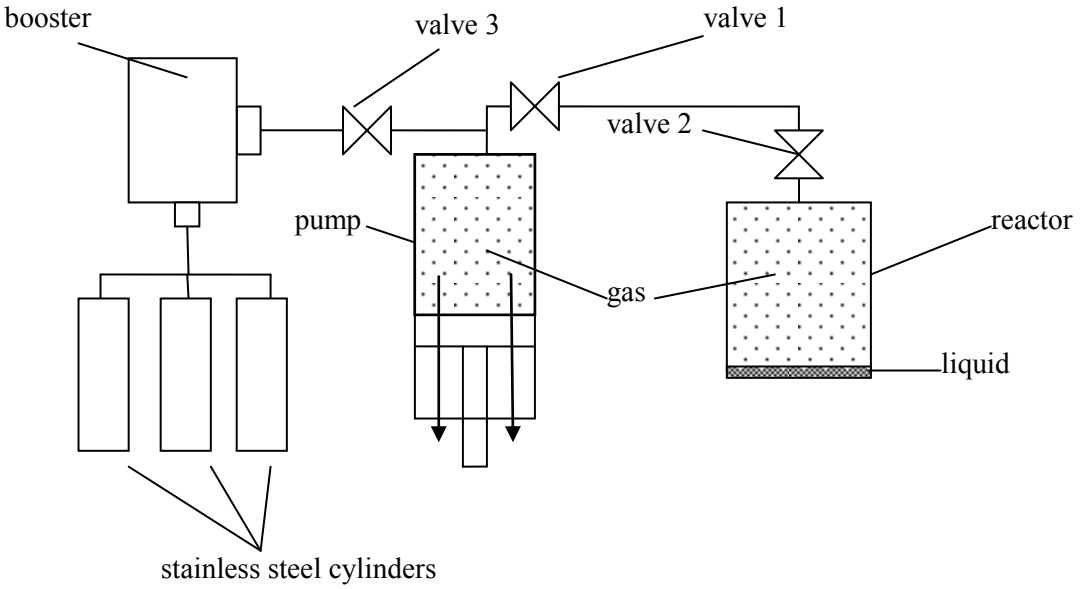

Figure 3.22d. Schematic process of loading a gas mixture into the reactor (Step 4)

Then, at the final stage of loading, Valves 1 and 2 were opened and the gas mixture from the pump transferred to the reactor (Figure 3.22e).

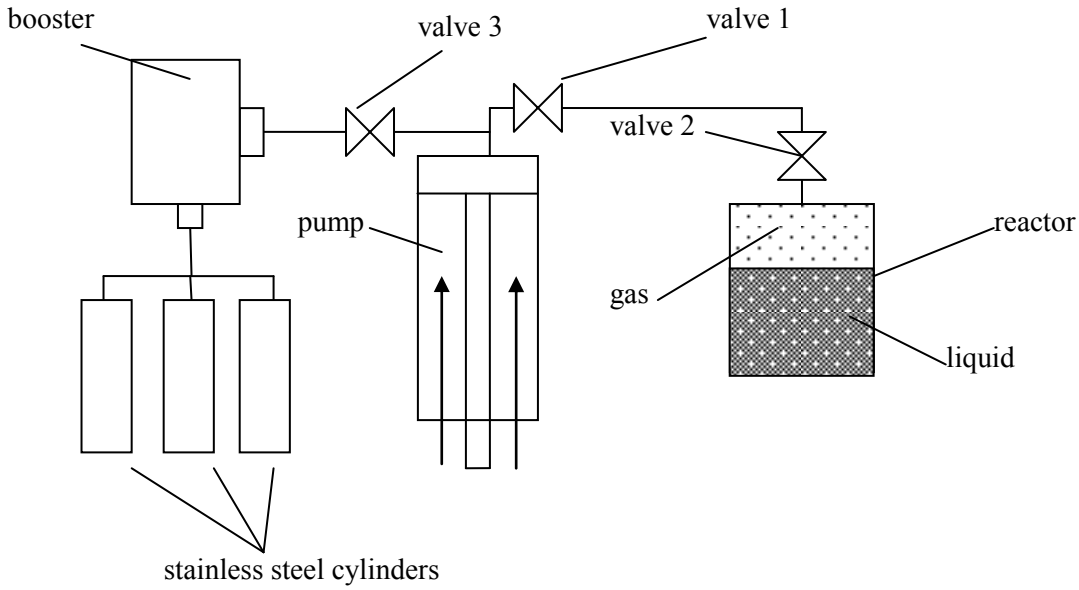

Figure 3.22e. Schematic process of loading a gas mixture into the reactor (Step 5)

So, if the required amount of gases is compressed in the reactor at assumed experimental conditions, the desired percentage of gas mixture will be liquefied.

NOTE: Losses of gas in the tubing connection between the cylinders and the pump and between the pump and the reactor during the loading stage must be taken into account when the total amount of composition is calculated. Also, the amount of gas mixture trapped in the pump should be considered.

3.8. Method of Sample Analysis

The analysing equipment was kindly provided by the Curtin Centre for Advanced Energy Science and Engineering (CCAESE). The presence of products in gaseous and liquid samples was determined by using a gas chromatograph GC-2014 Simadzu, equipped with TCD (Molecular Sieves 5A) and FID (Plot U) detectors. The GC-2014 was equipped with a methanizer (packed with Ni catalyst powder) which provided a better detection of small quantities of CO and CO_2 by a FID detector. An Agilent 5973 GC-MS fitted with a capillary column (0.25µm HP-5MS phase) was also determined for liquid samples analysis. Also, some experimental samples were analyzed at CoreLab Australia using the equipment available there.

Plastic gas sampling bags and glass vials used for collecting samples were purchased from Grace Davison Discovery Sciences (Australia). 500 cm^3 stainless steel cylinders (Figure 3.8) obtained from Swagelok (Australia) were also used to store samples.

3.9. Chemicals description

Industrial pure grade Ar, H_2, CH_4 and CO_2 gases used in experimental work were supplied by BOC Australia. Activated Raney Ni and carbon supported ruthenium (Ru-C) catalysts; methyl iodide (CH_3I) (≥ 99 %), ethyl iodide (C_2H_5I) (≥ 99 %) and methylene iodide (CH_2I_2) (≥ 99 %) were purchased from Sigma-Aldrich (Australia). Other chemicals such as glycerol (≥ 99 %), ethylene glycol (≥ 99 %), n-heptane (C_7H_{16}) (≥ 99 %), methanol (CH_3OH) (≥ 99 %), n-pentane (C_5H_{12}) (≥ 99 %), sodium hydroxide (NaOH) (≥ 98 %), potassium carbonate (K_2CO_3) (≥ 99 %) and potassium hydroxide (assay ≥85 % KOH basis) were obtained from Sigma Chemicals Pty Ltd (Australia).

3.10. Conclusion

Two experimental setups were constructed in order to investigate the effect of pressure and ultrasound power on the sonochemical reduction of carbon dioxide.

First, a novel high-power, low-frequency, pilot-scale sonochemical reactor for studying the process of ultrasonic reduction of CO_2 at low hydrostatic pressure conditions (up to 1 MPa) was designed. A 20 kHz ultrasonic probe system of maximum power of 1000 Watt was used as a source of ultrasound. Due to the great difficulty of the temperature control in the ultrasonic applications, a novel system combining the circulation of sonicating medium along with comprehensive cooling was (proposed) incorporated in this design. Such construction enables one to keep a uniform temperature of a sonicating medium during an experiment.

Second, a high-pressure sonochemical setup was developed in order to examine the possibility of sonochemical reduction of CO_2 at both liquefied and supercritical states. The design of the setup permits the application of hydrostatic pressures as high as 15 MPa during investigations. Another important feature of this design is that the tip of the ultrasonic transducer is imbedded into the high-pressure vessel which enables the direct distribution of ultrasound from the ultrasonic transducer into a sonicating medium. Also, a technique for liquefying of any specified amount of gases by using an air driven gas booster and high-pressure pump was exploited. Furthermore, a methodology for calculation of the specified amount of gases based on Peng-Robinson EOS using the HYSYS computer software was generated.

Chapter 4. Sonochemical Reduction of Carbon Dioxide in Various Sonicating Media under Low Hydrostatic Pressure Conditions

4.1. Introduction

This chapter describes the experimental work which was devoted to the sonochemical utilization of carbon dioxide at low pressure conditions (0.2 – 0.3 MPa) using various liquid media. The proposed method of CO_2 reduction was based on using ultrasound as a source of energy for CO_2 reduction. The basic principles of sonochemistry and the effects of different parameters on the phenomenon of cavitation are not explained in detail in this chapter as this has been discussed thoroughly in Chapter 2. Instead, the chapter contains more specific background information on effects of ultrasound on media and atmospheric gases which were chosen for the investigation. Moreover, choosing appropriate liquids for sonication was a very important task of this theoretical review as long as it is only possible to generate cavitation when a liquid medium is subjected to the ultrasound wave. So, this specific literature review is considered as a theory relevant to experimental work and helps in the chose of the right sonication media, atmospheric gases and conditions for experiments that were conducted. The experimental work, which is presented in this chapter, is divided into subsections. Each subsection represents experiments on CO_2 reduction performed in a different liquid chosen to be the sonicating medium. After a thorough theoretical examination of different types of liquid media, water, hydrocarbons and alcohols were chosen. However, apart from being just a medium for cavitation, all these liquids act as chemical reagents and take part in the CO_2 chemical transformation by means of providing hydrogen for the CO_2 reduction process. The main idea behind the experimental work performed was to investigate the ways of CO_2 chemical fixation into useable chemicals by its direct sonolysis or recombination with H_2, while using the ultrasound (vibrational) energy provided by the 20 kHz ultrasonic probe system.

4.2. Theoretical Approach

4.2.1. The Proposition of Carbon Dioxide Reduction Mechanisms

Two methods of CO_2 reduction, namely direct sonolysis of CO_2 and sonochemical reduction of CO_2 by hydrogen are investigated in this research. There are only a few articles (Henglein 1985; Harada 1998, 2003) devoted to sonochemical reduction of CO_2 which can be found in the literature. First, it was found by Henglein (1985) that the direct sonolysis of CO_2 can occur when water with dissolved CO_2, is subjected to ultrasonic irradiation. The first step of CO_2 sonolysis is described as a reaction of carbon dioxide splitting into oxygen and carbon monoxide (CO) (Reaction 4.1):

$$CO_2 \rightarrow CO + \frac{1}{2}O_2 \qquad \text{[R. 4.1]}$$

According to thermodynamics the reaction of direct dissociation of a CO_2 molecule is favorable at temperatures above 3200 K (see calculation below) and since Reaction 4.1 is reversible there is a reverse reaction to CO_2 formation (Reaction 4.2).

$$CO + \frac{1}{2}O_2 \rightarrow CO_2 \qquad \text{[R. 4.2]}$$

In addition, thermoreduction of carbon dioxide by dissolving it in water decreases the rate of the reverse reaction of CO_2 formation (Lyman and Jensen 2001). To evaluate a favorable range of temperatures for Reaction 4.1, some calculations based on estimation of the Gibbs free energy were performed. All data on standard enthalpies and entropies of formation for CO_2, CO and O_2 were obtained from Knovel Critical Tables (2003) and presented in Table 4.1.

Table 4.1. Standard enthalpies and entropies of formation for CO_2, CO and O_2

	CO_2	CO	O_2
$\Delta H^{298}, kJ/mol$	-393.522	-110.527	0
ΔS^{298}, *J/(mol K)*	3.019	89.522	0

Enthalpy of reaction

$\Delta H^{298}{}_{reaction} = \sum(n\,\Delta H^{298})_{products} - \sum(n\,\Delta H^{298})_{reagents}$,

where

ΔH^{298} – standard enthalpy, kJ/mol

n – stoichiometric number

$$\Delta H^{298}{}_{reaction} = (1 * (-110.527) + \frac{1}{2} * 0) - (1 * (-393.522))$$

$$\Delta H^{298}{}_{reaction} = 282.595\ kJ/mol,$$

Such value of $\Delta H^{298}{}_{reaction}$ means that the reaction is endothermic and it requires a lot of energy from outside.

Entropy of reaction

$$\Delta S^{298}{}_{reaction} = \sum(n\ \Delta S^{298})_{products} - \sum(n\ \Delta S^{298})_{reagents},$$

where

ΔS^{298} – standard entropy, J/mol K

$$\Delta S^{298}{}_{reaction} = (1 * 89.522 + \frac{1}{2} * 0) - (1 * 3.019)$$

$$\Delta S^{298}{}_{reaction} = 86.503 \frac{J}{mol\ K}$$

Gibbs free energy

$$\Delta G^{298}{}_{reaction} = \sum(n * \Delta G)_{products} - \sum(n * \Delta G)_{reagents},$$

where

ΔG^{298} – Standard Gibbs free energy, kJ/mol

If $\Delta G^{298} < 0$ – reaction is spontaneous (favored at standard conditions (298.15 K and 1 bar)),

$\Delta G^{298} = 0$ – reaction is at equilibrium (neither the forward not the reverse reaction prevails at statndard conditions),

$\Delta G^{298} > 0$ – reaction is nonspontaneous (unflavored at standard conditions).

$$\Delta G^{298}{}_{reaction} = (-137.163 + \frac{1}{2} * 0) - (-394.389)$$

$$\Delta G^{298}{}_{reaction} = 257.226\ kJ/mol,$$

The value of $\Delta G^{298}{}_{reaction}$ shows that the reaction is unfavorable at 298.15 K and 1 bar. So an increase in the temperature of the reaction will make it favorable. Thus order to estimate a temperature at which this reaction will occur spontaneously, the Gibbs free energy was estimated as follows:

$$\Delta G = \Delta H - T\ \Delta S \qquad \text{[Eq. 4.1]}$$

where

T – Reaction temperature, K

So,

$$\Delta G^{3270} = 282595 \frac{J}{mol} - 3270\ K * 86.503 \frac{J}{mol\ K}$$

$\Delta G^{3270} = -0.269\ kJ/mol < 0$ => This reaction is favorable at temperatures of 3270 K and higher.

The second method used was the reduction of CO_2 by hydrogen (H_2) where cavitation bubbles, which are generated during sonication of a liquid, serve as micro-reactors where a CO_2 reduction process occurs. It is proposed by Harada 1998 that there are reactions between CO_2 and H_2 which can take place in a liquid medium subjected to ultrasonic irradiation. However, Mead, Sutherland, and Verrall (1976) found that usage of an atmospheric gas with a high thermal conductivity reduces maximum temperatures and pressures significantly during the cavitation collapse. H_2 has a high thermal conductivity of 0.168 W/m·K which is 10.5 – 11.5 times larger than that of CO_2 (0.0146 W/m·K (even though a molecule of CO_2 is triatomic) and argon (Ar) (0.016 W/m·K). So, if H_2 is used as an atmospheric gas in sonolysis then lower temperatures and pressures are formed during the cavitation collapse of bubbles in comparison to temperatures and pressures generated during sonication under, for instance, an Ar atmosphere. Moreover, it should be noted that the usage of H_2 as an atmospheric gas assumes its purchase or generation in a different process which can be costly. Thus, according to considered method, H_2 for CO_2 reduction should be generated from the liquid medium during sonication. This approach suggests that H_2 generated during sonication will immediately reacts with CO_2 and no excess of H_2 will remain in the system. This option was considered to be optimal for the actual research in this project.

It has been suggested by Harada (1998) and Harada, Hosoki, and Ishikane (2003) that CO and methane (CH_4) are possible products formed during CO_2 reduction by H_2 during sonolysis (proposed products, see Reactions 4.3 and 4.4).

$$CO_2 + H_2 \rightarrow CO + H_2O \qquad \text{[R. 4.3]}$$

$$CO_2 + 4H_2 \rightarrow CH_4 + 2H_2O \qquad \text{[R. 4.4]}$$

It is also assumed that reduction of CO_2 can take place when it reacts with $H^{\bullet}$ radicals rather than with H_2 (see Reactions 4.5 and 4.6) as follows:

$$CO_2 + H^{\cdot} \rightarrow CO + OH^{\cdot} \quad \text{[R. 4.5]}$$

$$CO_2 + 6H^{\cdot} \rightarrow CH_4 + 2\,OH^{\cdot} \quad \text{[R. 4.6]}$$

Moreover, in a pioneering work on CO_2 sonolysis Henglein (1985) experimentally showed traces of formic acid as another product of CO_2 sonolysis in water (Reactions 4.7 and 4.8). However, the rate of formic acid formation is more than 30 times lower than that of CO.

$$CO_2 + H^{\cdot} \rightarrow HCOO^{\cdot} \quad \text{[R. 4.7]}$$

$$HCOO^{\cdot} + H^{\cdot} \rightarrow HCHO + O^{\cdot} \quad \text{[R. 4.8]}$$

So, an idea of performing a sonication in a medium such as water where H_2 is produced and consumed during a sonication process (see Section 4.3.2) seems to be preferable, because a sonication medium does not contain H_2 in large amounts, consequently there are insignificant alterations in temperatures and pressures of the cavitation explosion. Also, it can be considered more beneficial from an economic point of view (no H_2 need to be purchased).

4.3. Selection of Sonicating Medium, Atmospheric Gas and Choice of Hydrostatic Pressure

4.3.1. Selection of Atmospheric Gas

The choice of the atmospheric gas is very important. The dissolved gas bubbles serve as nucleation sites for initiating cavitation. It was stated that cavitation does not occur in a completely degassed liquid, because its threshold pressure is very large. According to the literature (Suslick, Doktycz, and Flint 1990; Segebarth et al. 2002) monoatomic gases provide larger sonochemical effects than diatomic or triatomic ones. This phenomenon can be explained by differences in physical properties of various gases. Thus, based on the adiabatic model of cavitational collapse (Neppiras 1980; Flynn 1964; Noltingk and Neppiras 1950; Equations 2.12 and 2.13 from Chapter 2, Section 2.3.5), it is stated that gases which possess a large γ (ratio of specific heats) values ($\gamma = C_v/C_p$) provide higher temperatures and pressure during collapse of cavities. The thermal conductivity of gases also plays an important role in determination of sonochemical effects. It was found (Margulis 1984) that heat transfer during the cavitation collapse is an important factor which affects maximal parameters of cavitation collapse (T_{max} and P_{max}) by decreasing them. Even though a

strong relation between the thermal conductivity and sonochemical effects has not be observed (see Table 4.1), it is generally considered that the lower the thermal conductivity of the gas, the less heat (energy) generated during the collapse of bubbles will be transferred to the surrounding liquid (Mason 2002). Mead and colleagues (Mead, Sutherland, and Verrall 1976) showed in their work that O_2 and air atmospheres provide a better rate of water decomposition than an Ar atmosphere does. Furthermore, in the case of dissociation of carbon disulphide, the rate of reaction increased in the order He > H_2 > Air > Ar > O_2 > CO_2 (Entezari, Kruus, and Otson 1997). However, Ar gas was found to give larger yields of CO_2 reduction in water, while no products of CO_2 decomposition were found when Air or pure CO_2 was used as an atmospheric gas during sonolysis (Harada 1998). So, low reaction rates under CO_2 atmosphere can be explained by its relatively small value of γ (1.289). Therefore, based on information on atmospheric gases‟ properties obtained from the literature, Ar was chosen to be the atmospheric gas for experimental work.

Table 4.2. Rate of formation of free chlorine by irradiation of water containing CCl_4 in relation to the nature of the atmospheric gas

Gas	Reaction rate, (mM/min^{-1})	Ration of specific heats (γ)	Thermal conductivity (k), (10^{-2}·W/m·K)
Ar	0.074	1.66	1.73
Ne	0.058	1.66	4.72
He	0.049	1.66	14.30
O_2	0.047	1.39	1.64
N_2	0.045	1.40	2.52
CO	0.028	1.43	2.72

4.3.2. Aqueous Medium for Sonication

Selection of a medium for investigation of CO_2 sonolysis implied that transient cavitation and their consequent collapse occur freely in the chosen liquid under ultrasonic irradiation. However, apart from being just media for cavitation, a liquid is considered as a chemical reagent which also takes part in the CO_2 chemical transformation by means of providing hydrogen for the CO_2 reduction process.

Water was the first liquid, containing hydrogen in its chemical structure, which was considered to be a sonication medium in the CO_2 sonochemical reduction process (Fig. 2.6).

Until the 1980s (Suslick et al. 1984) water was the only medium used in sonochemical experiments. Some authors (Anbar and Pecht 1964; Weissler 1959; Mead, Sutherland, and Verrall 1976; Henglein 1987) showed that under ultrasound irradiation water can be sonolyzed, and H_2 and H_2O_2 are generated during water irradiation by ultrasound. So, it was stated that splitting of water molecules into $H^{\cdot}$ and $OH^{\cdot}$ radicals is the first step of sonolysis of water (Reaction 4.9). Moreover, also the reverse reaction (Reaction 4.10) is possible to occur (Henglein 1987):

$$H_2O \rightarrow H^{\cdot} + OH^{\cdot} \quad \text{[R. 4.9]}$$

$$H^{\cdot} + {}^{\cdot}OH \rightarrow H_2O \quad \text{[R. 4.10]}$$

It is also thought that both active types of formed radicals react with each other. So, the final products H_2, O_2, H_2O_2 can be generated during recombination (R. 4.11, 4.12, 4.14, 4.16, 4.17, 4.21 and 4.24). Moreover, such Reactions as 4.13, 4.15, 4.18-4.20, 4.22 and 4.23 also occur at ultrasonic dissociation of water.

$$H^{\cdot} + H^{\cdot} \rightarrow H_2 \quad \text{[R. 4.11]}$$

$${}^{\cdot}OH + {}^{\cdot}OH \rightarrow H_2O_2 \quad \text{[R. 4.12]}$$

$${}^{\cdot}OH + {}^{\cdot}OH \rightarrow O^{\cdot} + H_2O \quad \text{[R. 4.13]}$$

$$O^{\cdot} + O^{\cdot} \rightarrow O_2 \quad \text{[R. 4.14]}$$

$$H^{\cdot} + O_2 \rightarrow HO_2{}^{\cdot} \quad \text{[R. 4.15]}$$

$$HO_2{}^{\cdot} + HO_2{}^{\cdot} \rightarrow H_2O + \frac{3}{2}O_2 \quad \text{[R. 4.16]}$$

$$H^{\cdot} + HO_2{}^{\cdot} \rightarrow H_2O_2 \quad \text{[R. 4.17]}$$

$$OH^{\cdot} + HO_2{}^{\cdot} \rightarrow H_2O + O_2 \quad \text{[R. 4.18]}$$

$$\frac{1}{2}O_2 + 2H^{\cdot} \rightarrow H_2O \quad \text{[R. 4.19]}$$

$$H^{\cdot} + H_2O_2 \rightarrow OH^{\cdot} + H_2O \quad \text{[R. 4.20]}$$

$$H^{\cdot} + H_2O_2 \rightarrow H_2 + HO_2{}^{\cdot} \quad \text{[R. 4.21]}$$

$$OH^{\cdot} + H_2O_2 \rightarrow H_2O + HO_2{}^{\cdot} \quad \text{[R. 4.22]}$$

$$OH^{\cdot} + H_2 \rightarrow H_2O + H^{\cdot} \quad \text{[R. 4.23]}$$

$$H_2O + OH^{\cdot} \rightarrow H_2O_2 + H^{\cdot} \quad \text{[R. 4.24]}$$

In the case of using an atmospheric gas, some specific reactions due to the presence of the atmosphere occur. In our work, Ar, CO_2 and H_2 generated from a sonicating medium are found to be present in the reacting system during sonolysis. So, in the

case where Ar is the atmospheric gas Reactions 4.25-4.38 also occur in the system (where M is a collision partner):

$$OH^{\cdot} + H^{\cdot} + M \rightarrow H_2O + M \quad \text{[R. 4.25]}$$

$$2OH^{\cdot} + M \rightarrow O^{\cdot} + H_2O + M \quad \text{[R. 4.26]}$$

$$2OH^{\cdot} + M \rightarrow H_2O_2 + M \quad \text{[R. 4.27]}$$

$$2H^{\cdot} + M \rightarrow H_2 + M \quad \text{[R. 4.28]}$$

$$2O^{\cdot} + M \rightarrow O_2 + M \quad \text{[R. 4.29]}$$

$$O^{\cdot} + H_2O + M \rightarrow H_2O_2 + M \quad \text{[R. 4.30]}$$

$$O_2 + H^{\cdot} + M \rightarrow HO_2^{\cdot} + M \quad \text{[R. 4.31]}$$

$$OH^{\cdot} + H_2O_2 + M \rightarrow HO_2^{\cdot} + H_2O + M \quad \text{[R. 4.32]}$$

$$2OH_2^{\cdot} + M \rightarrow H_2O_2 + O_2 + M \quad \text{[R. 4.33]}$$

$$HO_2^{\cdot} + H^{\cdot} + M \rightarrow H_2O + O^{\cdot} + M \quad \text{[R. 4.34]}$$

$$O^{\cdot} + H_2O + M \rightarrow 2OH^{\cdot} + M \quad \text{[R. 4.35]}$$

$$Ar \rightarrow Ar^{\cdot} \quad \text{[R. 4.36]}$$

$$Ar^{\cdot} + H_2O \rightarrow H_2O^{\cdot} + Ar \quad \text{[R. 4.37]}$$

$$H_2O^{\cdot} \rightarrow H^{\cdot} + OH^{\cdot} \quad \text{[R. 4.38]}$$

When CO_2 presents in the system the next specific reactions which were discussed in Section 4.1.1 occur (Reactions 4.1- 4.8). The presence of H_2 gas in the reacting system implies the occurance of Reactions 4.39 and 4.40 involving the dissociation of molecular H_2.

$$H_2 \rightarrow H^{\cdot} + H^{\cdot} \quad \text{[R. 4.39]}$$

$$H_2 + OH^{\cdot} \rightarrow H_2O + H^{\cdot} \quad \text{[R. 4.40]}$$

More detailed information on sonochemical decomposition of water under other atmospheres and all specific reactions proceeding in the case of each atmospheric gas can be found in the review of sonochemistry by Adewuyi (2001). So based on obtained information, it was decided to consider water as a sonicating medium due to the formation of H_2 during water sonolysis.

4.3.3. Hydrocarbon Medium for Sonication

The next proposed type of sonication medium was hydrocarbons. Even through the first observation of sonochemistry took place in the 1920-30s (Richards and Loomis

1927; Wood and Loomis 1927; Brohult 1937) up to the beginning of 1980s non-aqueous (organic) compounds did not receive enough attention among sonochemists and only a few reports exist on this matter, and those mainly on sonolysis of water-organic liquid mixtures (Weissler, Pecht, and Anbar 1965; Donaldson, Farrington, and Kruus 1979). The reason for this is very simple. In those days, it was thought that organic components do not support cavitation bubbles formation, and consequently, do not represent any interest for sonochemistry. Later this mistaken point of view was reconsidered in favour of organic solvents as numerous sonochemical investigations using non-aqueous liquids appeared after 1980 (Suslick et al. 1983; Suslick et al. 1984; Mizukoshi et al. 1999). Also, there were reports on sonolysis of water under various gaseous hydrocarbon atmospheres where the possibility of decomposition of hydrocarbon was shown (Hart, Fischer, and Henglein 1990a; Hart, Fischer, and Henglein 1990b). It was stated by many authors (Suslick et al. 1983; Hart, Fischer, and Henglein 1990b) that the products which were formed during the decomposition of hydrocarbons during sonolysis are very similar to those at pyrolysis of hydrocarbons. K. Suslick et al. (1983) and later Muzukoshi et al. (1999) in their works proposed a mechanism of decomposition of hydrocarbons under ultrasonic irradiation. This mechanism is presented below on example of decane and includes three stages: initiation of radicals, their propagation and termination (where $R_x^{\cdot}$ represents various hydrocarbon radicals, where ***x*** represents the number of carbons (C) in a radical).

1) Initiation stage. During the initiation stage, molecules of hydrocarbon break down into various radicals with smaller amount of carbon atoms:

$$C_{10}H_{22} \rightarrow R_1^{\cdot} + R_2^{\cdot} + \ldots + R_9^{\cdot} \quad \text{[R. 4.41]}$$

$$R_{2n}^{\cdot} \rightarrow C_2H_4, H^{\cdot}, C_2H_5^{\cdot} \quad \text{[R. 4.42]}$$

$$R_{2n} + 1 \rightarrow C_2H_4, CH_3^{\cdot} \quad \text{[R. 4.43]}$$

2) Propagation stage. Radicals formed at the initiation stage undergo further degradation into smaller radicals or react with non-radical species producing different radicals. Also, final products can be formed at this stage.

$$C_{10}H_{22} + R^{\cdot} \rightarrow C_{10}H_{21}^{\cdot} + RH \quad \text{[R. 4.44]}$$

$$C_{10}H_{21}^{\cdot} \rightarrow C_2H_4 + R^{\cdot} \quad \text{[R. 4.45]}$$

$$C_{10}H_{22} + H^{\cdot} \rightarrow H_2 + C_{10}H_{21}^{\cdot} \quad \text{[R. 4.46]}$$

3) Termination stage. At the termination stage there are reactions between radicals which end in the formation of products.

$$R^{\cdot} + R^{\cdot} \rightarrow R - R \quad \text{[R. 4.47]}$$

$$R^{\cdot} + H^{\cdot} \rightarrow R - H \quad \text{[R. 4.48]}$$

$$H^{\cdot} + H^{\cdot} \rightarrow H_2 \quad \text{[R. 4.49]}$$

It was also suggested, that during sonication of hydrocarbons, the primary produced big radicals undergo further radicalization into smaller radicals such as $CH_3^{\cdot}$, $C_2H_5^{\cdot}$ and $H^{\cdot}$. So it is worth noting that hydrogen radicals/hydrogen is formed during sonication of hydrocarbons which makes liquid hydrocarbons a theoretically prospective sonication medium for CO_2 sonochemical reduction.

4.3.4. Alcohol's Medium for Sonication

Alcohols were the last type of liquids chosen to be considered as a sonicating medium. Methanol was selected for the current experimental work. The investigation of sonochemical reduction of CO_2 in the methanol medium was examined. This experimental work was divided into two parts. In the first part, methanol was used as a sonicating medium for sonochemical utilization of CO_2. Whereas, in the second part of experiment, methanol was used as one of reagents for dimethyl carbonate synthesis (DMC).

4.3.4.1. Sonochemical Reduction of Carbon Dioxide in Methanol Medium

It is known that alcohol undergo degradation when subjected to ultrasonic irradiation. As it was reported, the sonication of methanol proceeds in the same way as its pyrolysis (Buttner, Gutierrez, and Henglein 1991; Reaction 4.50-4.67) where the primary step is the cleavage of the C–O bond (Aronowitz, Naegeli, and Glassman, 1977). Also, it was shown that the process of the dissociation of the methanol molecule is favourable through the heterolytic cleavage of the C–O bond (Calatayud, Andres, and Beltran 1999).

$$CH_3OH \rightarrow CH_3^{\cdot} + {}^{\cdot}OH \quad \text{[R. 4.50]}$$

$${}^{\cdot}OH + CH_3OH \rightarrow H_2O + CH_2OH^{\cdot} \quad \text{[R. 4.51]}$$

$$CH_3^{\cdot} + CH_3OH \rightarrow CH_4 + CH_2OH^{\cdot} \quad \text{[R. 4.52]}$$

$$CH_2OH^{\cdot} + M \rightarrow CH_2O + H^{\cdot} + M \quad \text{[R. 4.53]}$$

$$CH_2O + M \rightarrow H^{\cdot} + HCO^{\cdot} + M \quad \text{[R. 4.54]}$$

$$HCO^{\cdot} + M \rightarrow CO + H^{\cdot} + M \quad \text{[R. 4.55]}$$

$$H^{\cdot} + CH_3OH \rightarrow CH_3^{\cdot} + H_2O \quad \text{[R. 4.56]}$$

$$CH_3^{\cdot} + CH_2O \rightarrow CH_4 + HCO^{\cdot} \quad \text{[R. 4.57]}$$

The formation of hydrogen in the sonolysis as well as pyrolysis of methanol occurs according to Reactions 4.58-4.60, 4.62, 4.65:

$$H^{\cdot} + CH_3OH \rightarrow H_2 + CH_2OH^{\cdot} \quad \text{[R. 4.58]}$$

$$H^{\cdot} + CH_2O \rightarrow HCO^{\cdot} + H_2 \quad \text{[R. 4.59]}$$

$$H^{\cdot} + CH_4 \rightarrow CH_3^{\cdot} + H_2 \quad \text{[R. 4.60]}$$

Moreover, low hydrocarbons such as acetylene, ethylene and ethane are proposed to be the products the pyrolysis of methanol (Aronowitz, Naegeli, and Glassman, 1977; Reactions 4.61-4.67):

$$CH_3^{\cdot} + CH_3^{\cdot} + M \rightarrow C_2H_6 + M \quad \text{[R. 4.61]}$$

$$H^{\cdot} + C_2H_6 \rightarrow C_2H_5^{\cdot} + H_2 \quad \text{[R. 4.62]}$$

$$CH_3^{\cdot} + C_2H_6 \rightarrow C_2H_5^{\cdot} + CH_4 \quad \text{[R. 4.63]}$$

$$C_2H_5^{\cdot} + M \rightarrow C_2H_4 + H^{\cdot} + M \quad \text{[R. 4.64]}$$

$$C_2H_4 + H^{\cdot} \rightarrow C_2H_3^{\cdot} + H_2 \quad \text{[R. 4.65]}$$

$$C_2H_4 + CH_3^{\cdot} \rightarrow C_2H_3^{\cdot} + CH_4 \quad \text{[R. 4.66]}$$

$$C_2H_3^{\cdot} + M \rightarrow C_2H_2 + H^{\cdot} + M \quad \text{[R. 4.67]}$$

Buttner, Gutierrez, and Henglein (1991) in their study on sonolysis of methanol-water mixtures under an argon atmosphere found traces of C_2H_4 and C_2H_6 in products of sonolysis. However, later in a study devoted to sonolysis of pure CH_3OH, the formation of C2 hydrocarbons (C_2H_6, C_2H_4 and C_2H_2) as products of CH_3OH degradation was not detected (Mizukoshi et. al 1999).

It can be noted that CO and CH_4, the main products of the CH_3OH sonolysis, are also the proposed products of CO_2 sonochemical reduction. Thus, certain difficulties can be encountered by the nature of generated CO and CH_4 during sonochemical reduction of CO_2 in a CH_3OH medium.

4.3.4.2. Dimethyl Carbonate Synthesis from Methanol and Carbon Dioxide under Ultrasonic Irradiation

CH_3OH can be also considered as a co-reactant in the reaction of the direct synthesis of dimethyl carbonate (DMC) from CH_3OH and CO_2. This is another prospective method of CO_2 chemical utilization. Therefore, the possibility of applying ultrasonic energy in order to synthesize DMC directly from CH_3OH and CO_2 needs be investigated. The direct synthesis of the DMC from CH_3OH and CO_2 is a very prospective route, because it implies the chemical utilization of CO_2 as a carbon source. Furthermore, in this route the usage of such poisonous reagents as phosgene, hydrogen chloride and nitric oxide are avoided (Fujita et al. 2001). DMC is a valuable chemical compound which can be used for a number of different applications such as a polar solvent, fuel additive, carbonylation and methylation reagents (Fujita et al. 2001; Guo et al. 2008). The equation of the direct synthesis of DCM can be expressed as follows:

$$CH_3OH + CO_2 \xrightarrow{base\ catalyst+CH_3I} DMC + H_2O \qquad \text{[R. 4.68]}$$

However, the process of the DMC formation from CH_3OH and CO_2 (as well as any process of methyl carbonates (such as ethyl carbonate)) requires the usage of base catalysts such as KOH, Na_2CO_3, K_2CO_3. (Hou et al. 2002; Wang et al. 2005; Chun, He, and Zhu 2001; Gasc, Thiebaud-Roux, and Mouloungui 2009; Fang and Fujimoto 1996). Moreover, iodomethane (CH_3I) is a crucial reagent in this synthesis and it is used as $CH_3^{\cdot}$ radicals' provider (Chun, He, and Zhu 2001; Fujito et al. 2001; Fang and Fujimoto 1996). The mechanism of DMC formation can be represented by the reactions 4.69-4.73:

$$CH_3OH + K_2CO_3 \rightarrow CH_3OK + KHCO_3 \qquad \text{[R. 4.69]}$$

$$CH_3OK + CO_2 \rightarrow CH_3O(C=O)OK \qquad \text{[R. 4.70]}$$

$$CH_3I + CH_3O(C=O)OK \rightarrow CH_3O(C=O)OCH_3 + KI \qquad \text{[R. 4.71]}$$

Iodomethane consumed during the process can be reproduced (Reactions 4.61 and 4.62):

$$KI + CH_3OH \rightarrow HI + CH_3OK \qquad \text{[R. 4.72]}$$

$$HI + CH_3OH \rightarrow CH_3I + H_2O \qquad \text{[R. 4.73]}$$

It should also be noted that the synthesis of DMC requires high pressure in the process (over 10 MPa). Moreover, high reaction temperatures (353 – 393 K) are essential (Hou et al. 2002; Fang and Fujimoto 1996). Thus, usage of the energy of the cavitation bubble collapse in order to generate conditions at which the proposed synthesis of DMC can be performed is another possible method of CO_2 sonochemical reduction in the methanol medium.

4.3.5. Choice of Hydrostatic Pressure

The hydrostatic pressure conditions for the experimental work were selected based on a thorough analysis. On the one hand, high hydrostatic pressure provides the more intense collapse of bubbles (Chapter 2, Equations 4.7 and 4.8) and a better solubility of atmospheric gases which leads to a larger number of nuclei for cavitation. On the other hand, the increase in the external pressure is limited by characteristics of ultrasonic equipment (Chapter 2, Equation 4.13) and properties of the liquid medium (such as viscosity, surface tension, etc.) (Mason and Lorimer, 2002). Van Iersel (2007) in his investigation on sonolysis of an aqueous solution of KI at elevated pressure (0.1-0.8 MPa) showed that with an increase in the hydrostatic pressure up to 0.5 MPa, the slight increase in liberation of iodide was observed but at pressures higher than 0.5 MPa there was a significant drop in the sonochemical yield. In order to estimate the effect of elevated hydrostatic pressure, the series of experiments on sonolysis of various liquid mediums under an Ar/CO_2 atmosphere at elevated pressures were performed (see Appendix A). On the basis of results of these experiments, it was decided to work with low hydrostatic pressure in a range of 0.2-0.3 MPa.

4.4. Experimental Research on Sonochemical Reduction of Carbon Dioxide

The current section of experimental work is devoted to sonolysis of water in an Ar/CO_2 atmosphere. All experiments were carried out in a liquid medium at low hydrostatic pressure of 0.2-0.3 MPa. Moreover, all experiments were divided into two parts. In the first part, the influence of CO_2 concentration in an atmospheric gas, effects of intensity of ultrasound are studied. Also, the effect of the experimental temperature was confirmed. In the second part of investigation the effect of H_2 on the sonolysis of CO_2 in water was investigated. At least two parallel tests were carried out for every investigation at different experimental conditions. The difference in

results between two tests at similar conditions did exceeded 10%. Average result for each experimental point was used.

4.4.1. Sonochemical Reduction of Carbon Dioxide in Aqueous Medium

The aim of the first part of experiments was to find out dependences between the effectiveness of CO_2 sonolysis and such factors as Ar/CO_2 gases ratio and ultrasonic power. As pointed out in Chapter 3, a small piece of aluminium foil was placed into the reactor in every experiment to detect the presence of a transient cavitation phenomenon, and consequently, to make sure that the cavitation collapse of bubbles takes place during the process of sonication. Ar is selected as the atmospheric gas for the experimental work because of its properties (see Section 4.3.1). The experimental apparatus used for this investigation and methodology of the test preparation are described in Chapter 3 in detail.

4.4.1.1. Effect of Ar/CO_2 Atmospheric Gas Ratio on Rates of Carbon Dioxide Reduction

A series of experiments on water sonolysis under different Ar/CO_2 atmospheres were carried out. Effect of Ar/CO_2 atmospheres containing 75, 45, 30, 20, 13 and 5 mol% of CO_2 on efficiency of CO_2 sonolysis in a water medium was investigated.

a) First, sonolysis of water under the Ar/CO_2 atmosphere containing 75 mol% of CO_2 was conducted. The liquid medium is pressured to 0.2 MPa by the atmospheric gas. The ultrasonic power applied during the test was set to approximately 60 W/cm^2 (410 W/l). The experimental temperature was kept in the range of 278.15±1 K by circulating iced water through the cooling system (see Chapter 3, Figure 3.10). Sonication was carried out for 60 minutes, then a final gas mixture was collected in a sampling bag and analysed by the gas chromatography (GC). No products of CO_2 sonolysis was detected by the GC analysis. However, some negligible traces of H_2 were spotted in the final gas mixture.

b) At the next step, the molar concentration of CO_2 in the gas atmosphere was reduced to 50%. Sonication of water subjected to 0.2 MPa atmosphere of Ar and CO_2 gases was carried out for 1 hour. The other experimental parameters such as temperature and applied ultrasound power were same as those in the previous run. The analysis of a gas mixture taken after the experiment did not detect products of

CO_2 sonochemical reduction but the presence of H_2 in trace amounts (0.129 µmol/l) is observed as shown in (Figure 4.1).

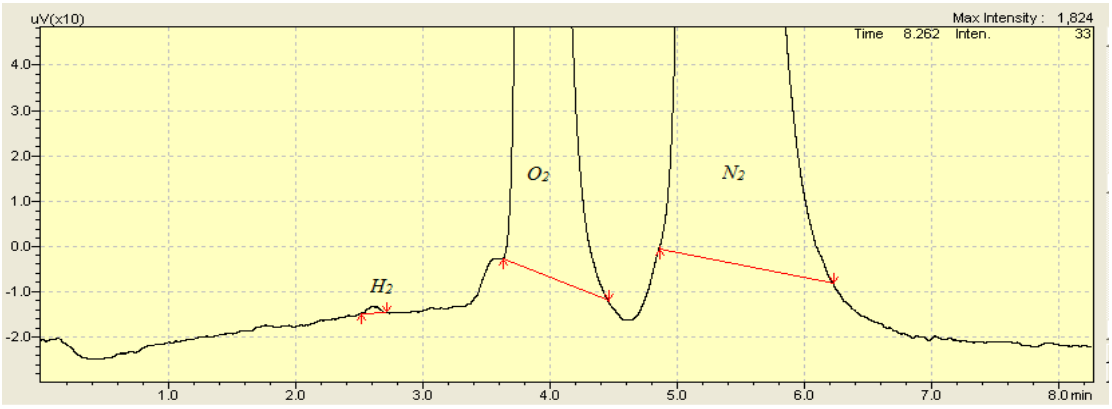

Figure 4.1. TCD chromatogram for H_2 formation in sonolysis of water under an Ar/CO_2 atmosphere containing 50 mol% of CO_2

The presence in the sample of small amount O_2 and N_2 was determined by air atmosphere contaminations in the sample due to the process of sample transfer to a sampling bag. Figure 4.2 presents a TCD chromatogram of the blank sample taken from the reactor subjected to Ar/CO_2 atmosphere without sonolysis.

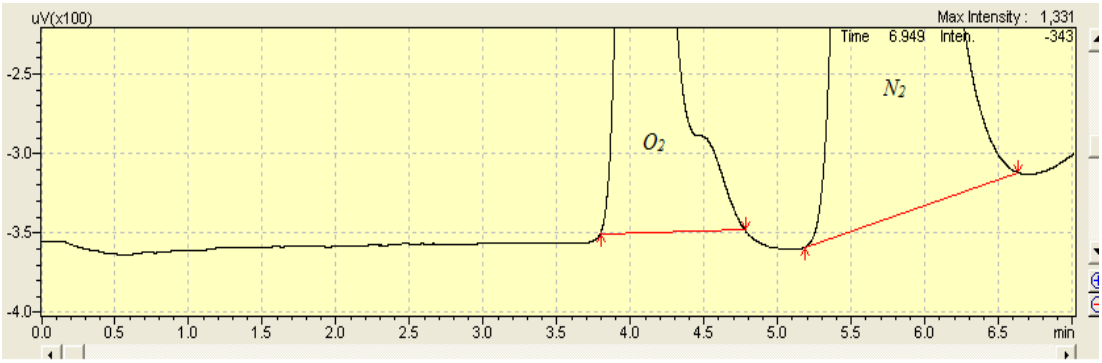

Figure 4.2. TCD chromatogram of the blank Ar/CO_2 atmosphere transferred from the reactor system to a sampling bag

c) For the next test, the molar concentration of CO_2 in the atmosphere of gases amounted to 30%. So, 550 cm^3 of distilled water was pressured with the CO_2/Ar atmosphere (0.3 molar fraction of CO_2) to the pressure of 0.2 MPa. Then, the gas-liquid system was irradiated by ultrasound with power of approx. 60 W/cm^2 (410 W/l) for 60 minutes. The temperature of the liquid medium was kept in a range of 287.15±1 K by using the heat-exchanging system. After the test was conducted, the gas sample was transferred into a sampling bag and forwarded for the GC analysis. Results of the analysis showed that 2.07 µmol/l of CO and 0.51 µmol/l of H_2 from CO_2 and water, respectively, were produced during the sonication as shown in Figures 4.3 and 4.4.

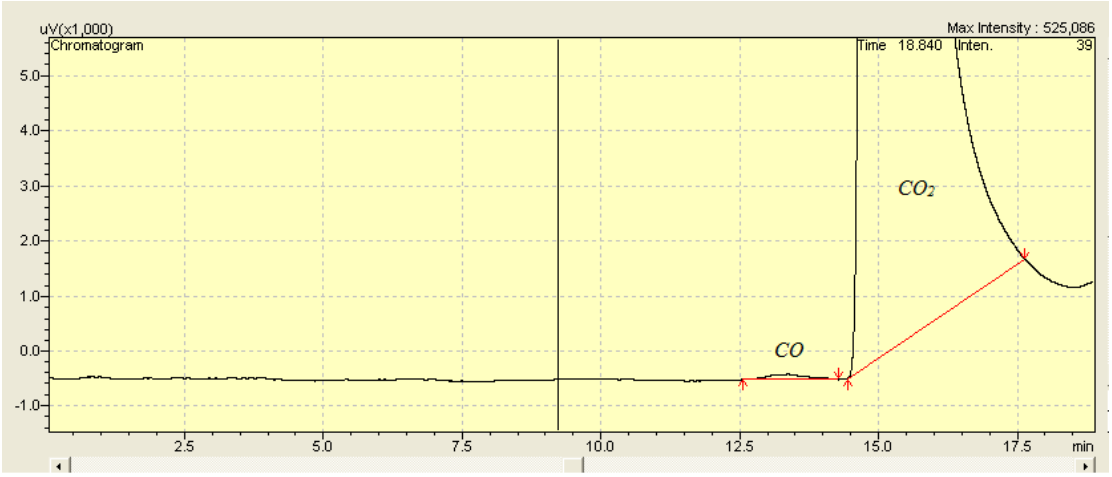

Figure 4.3. FID chromatogram for CO formation in sonolysis of water under an Ar/CO_2 atmosphere containing 30 mol% of CO_2

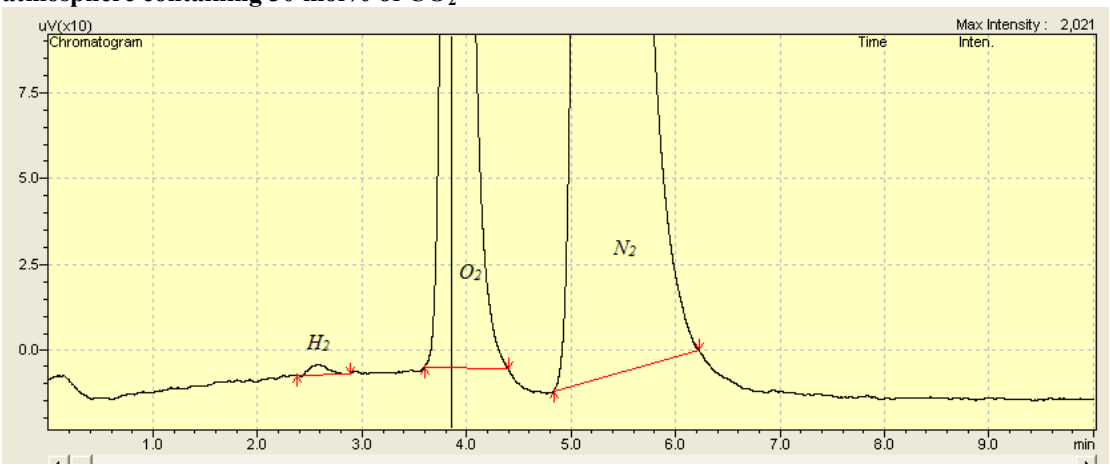

Figure 4.4. TCD chromatogram for H_2 formation in sonolysis of water under an Ar/CO_2 atmosphere containing 30 mol% of CO_2

d) After obtaining CO and H_2 from CO_2 sonolysis in water medium it was decided to conduct some more tests to investigate the effect of a further decrease in the CO_2 molar fraction in the atmospheric gas on the efficiency of the product's formation. The Ar/CO_2 atmospheric gas containing 20 mol% of CO_2 was prepared for the next run. The hydrostatic pressure of the liquid medium was set to 0.2 MPa by introducing the atmospheric gas into the reactor. The test was conducted over one hour while the power of the ultrasound irradiation amounted to 60 W/cm^2. The experimental temperature of the medium was maintained at the same values as in the previous experiments. 3.95 µmol/l of CO and 0.56 µmol/l of H_2 were found in the final gas mixture by the GC analysis (Figures 4.5 and 4.6).

Figure 4.5. FID chromatogram for CO formation in sonolysis of water under an Ar/CO_2 atmosphere containing 20 mol% of CO_2

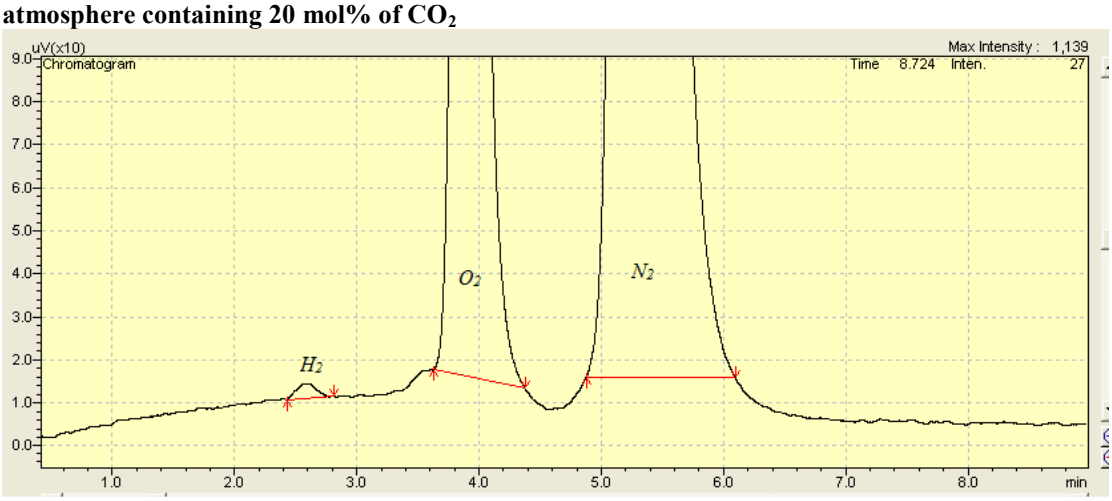

Figure 4.6. TCD chromatogram for H_2 formation in sonolysis of water under an Ar/CO_2 atmosphere containing 20 mol% of CO_2

e) For a further investigation, two more tests on sonochemical reduction of CO_2 in a water media subjected to Ar/CO_2 atmospheres containing 0.13 and 0.05 molar fraction of CO_2 are conducted. The hydrostatic pressure of the liquid medium was set up to 0.2 MPa by the mixture of atmospheric gases and the power of the applied ultrasound set to 60 W/cm^2 (410 W/l). Ultrasonic irradiation was applied to the system for 60 minutes in both cases. When CO_2 concentration in the atmospheric gas was 13 mol%, 5.13 µmol/l of CO and 0.78 µmol/l of H_2 was detected in the gas sample by the GC analysis (Figures 4.7 and 4.8).

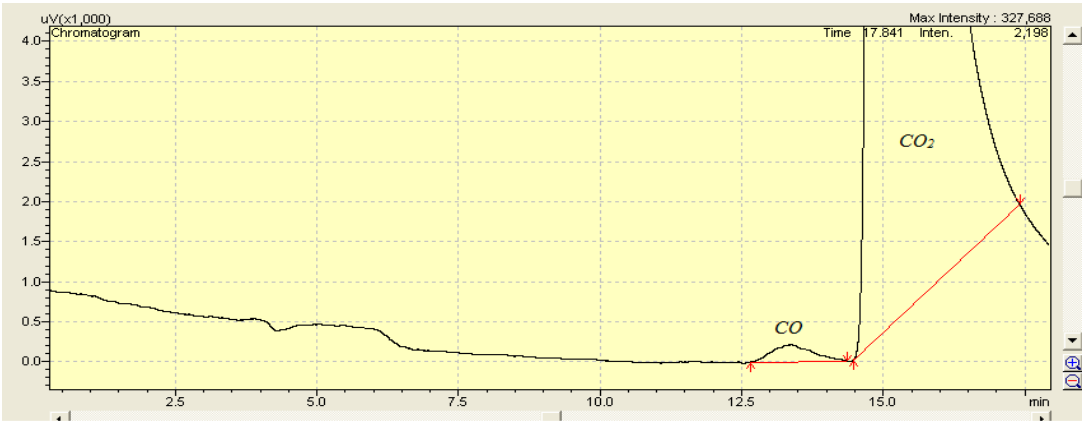

Figure 4.7. FID chromatogram for CO formation in sonolysis of water under an Ar/CO_2 atmosphere containing 13 mol% of CO_2

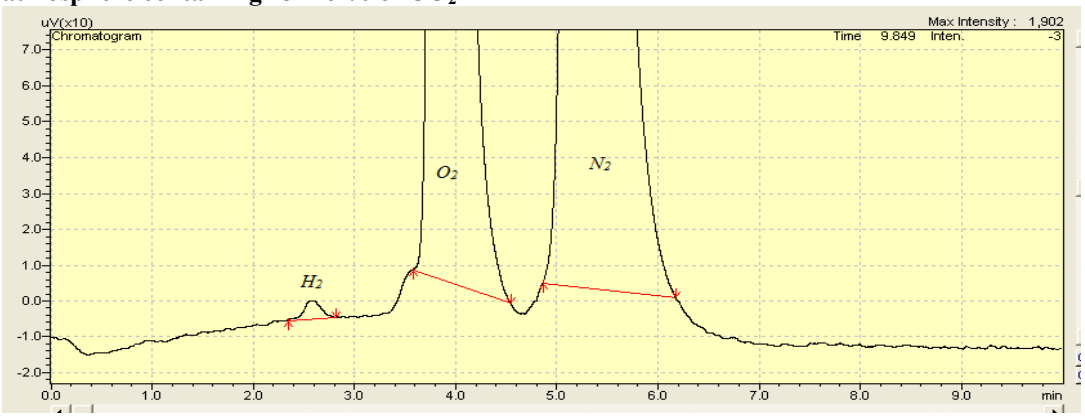

Figure 4.8. TCD chromatogram for H_2 formation in sonolysis of water under an Ar/CO_2 atmosphere containing 13 mol% of CO_2

When the atmospheric gas contained approximately 5% of CO_2, the yields of CO and H_2 were larger, namely 5.54 μmol/l and 1.07 μmol/l for CO and H_2, respectively (Figures 4.9 and 4.10).

Figure 4.9. FID chromatogram for CO formation in sonolysis of water under an Ar/CO_2 atmosphere containing 5 mol% of CO_2

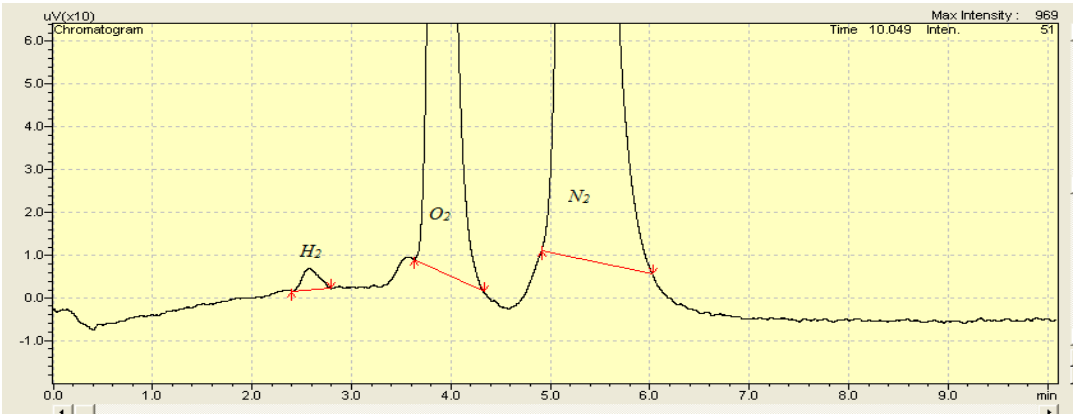

Figure 4.10. TCD chromatogram for H_2 formation in sonolysis of water under an Ar/CO_2 atmosphere containing 5 mol% of CO_2

4.4.1.2. Effect of Ultrasound Power on Rates of Carbon Dioxide Reduction

An investigation of the influence of ultrasound power on rates of CO_2 sonolysis was also carried out. A mixture of atmospheric gases containing 0.3 molar fraction of CO_2 was prepared. The hydrostatic pressure of a liquid medium was set to 0.2 MPa by the atmospheric gas and sonication is performed for 60 minutes at ultrasound power of 40 and 95 W/cm^2 (275 and 650 W/l). The temperature in a range of 287.15±1 K was maintained during the experiment at lower ultrasonic power and the experimental temperature in a range of 291.15±1 K was kept while ultrasonic irradiation of 95 W/cm^2 (650 W/l) was applied. The analyses performed after the experiments showed a negligible amount of H_2 (0.04 µmol/l) and no CO were produced during sonication at 40 W/cm^2 (275 W/l; Figure 4.11).

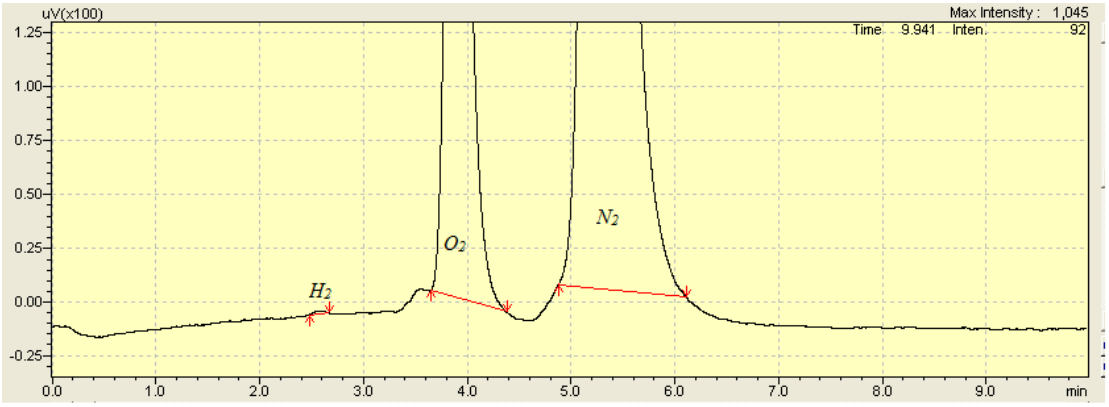

Figure 4.11. TCD chromatogram for H_2 formation in sonolysis of water at 40 W/cm^2 (275 W/l) under an Ar/CO_2 atmosphere containing 30 mol% of CO_2

However, when the test was carried out at 95 W/cm^2 (650 W/l) ultrasound power, 0.84 µmol/l of H_2 and 3.95 µmol/l of CO were generated (see Figures 4.12 and 4.13).

Thus the obtained results were compared to those which were achieved in the previous investigation using the atmospheric gas at the same concentration of CO_2 but at different applied ultrasonic power as shown in Figures 4.3 and 4.4. It can be seen that an increase in the intensity leads to larger amounts of generated products.

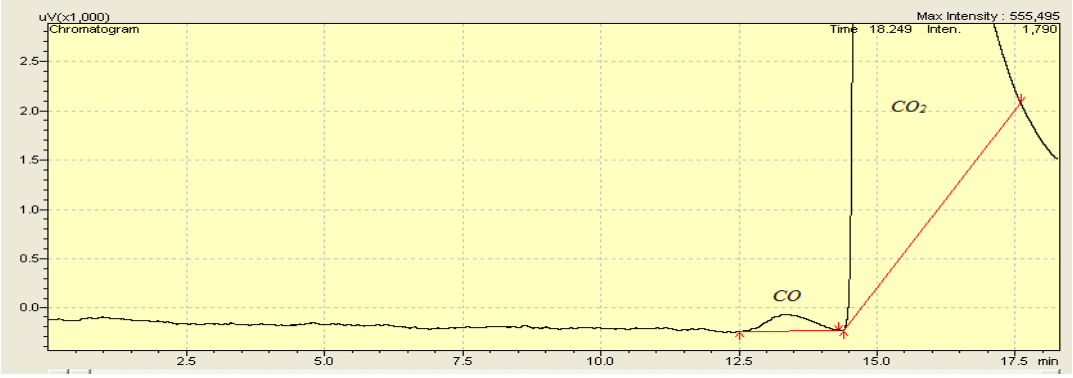

Figure 4.12. FID chromatogram for CO formation in sonolysis of water at 95 W/cm^2 (650 W/l) under an Ar/CO_2 atmosphere containing 30 mol% of CO_2

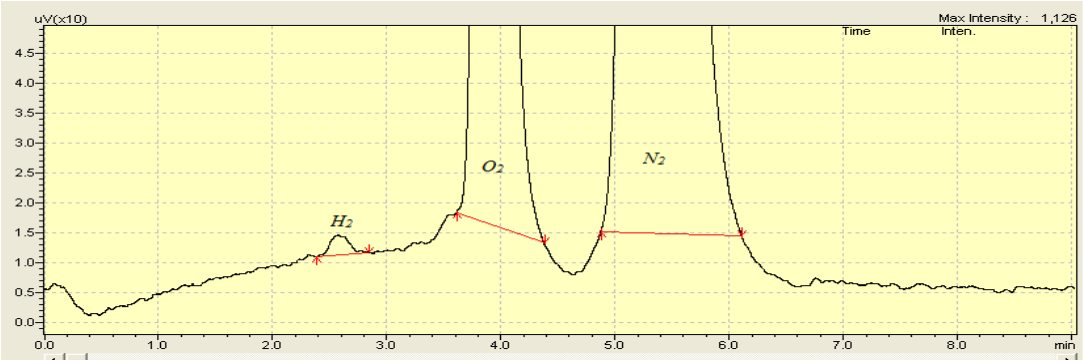

Figure 4.13. TCD chromatogram for H_2 formation in sonolysis of water at 95 W/cm^2 (650 W/l) under an Ar/CO_2 atmosphere containing 30 mol% of CO_2

Table 4.3. Influence of Ar/CO_2 ratio and ultrasonic intensity on the effectiveness of the sonochemical reduction of CO_2 under an Ar atmosphere

Test #	CO_2 molar fraction	Average hydrostatic Pressure, MPa	Average experimental temperature, K	Average ultrasonic power, W/cm^2	Duration of run, min	Products
1	0.75	0.2	287.15	60	60	-
2	0.5	0.2	287.15	60	60	H_2 traces
3	0.3	0.2	287.15	60	60	H_2, CO
4	0.2	0.2	287.15	60	60	H_2, CO
5	0.13	0.2	287.15	60	60	H_2, CO
6	0.05	0.2	287.15	60	60	H_2, CO
7	0.3	0.2	287.15	40	60	H_2
8	0.3	0.2	291.15	95	60	H_2, CO

The experimental results obtained are summarized in Table 4.2. The detailed discussion of the results obtained on the effect of CO_2 concentration in an atmospheric gas on the rates of CO_2 reduction is presented in Chapter 5.

4.4.2. Sonochemical Catalytic Reduction of Carbon Dioxide in Aqueous Medium

The previous experimental work shows that sonolysis of CO_2 in a water medium leads to CO and H_2 formation from CO_2 and water, respectively. However, it is assumed that the formation of CO as well as CH_4 could also go through the reaction of CO_2 with H_2 or $H^{\cdot}$ radicals (Reactions 4.3-4.6). After analysing the results, it was decided to move to the next set of experiments, the main purpose of which was to initiate CH_4 formation by means of applied catalytic systems and to enhance H_2 generation in the reaction system during CO_2 sonolysis in an aqueous medium.

Activated Raney Ni is the first catalyst which is considered to be applied for sonochemical CO_2 reduction. On the one hand, due to its large surface area, activated Raney Ni catalyst contains adsorbed hydrogen and can be considered as an excellent provider of hydrogen for CO_2 reduction (Fouilloux 1983). Aluminium, which remains in a catalyst structure after the catalyst activation process, along with water solution of NaOH can also be considered as a hydrogen provider (Kudo and Komatsu 1999).

$$2\,Al + 2\,NaOH + 6\,H_2O \rightarrow 2\,Na[Al(OH)_4] + 3\,H_2 \qquad \text{[R. 4.74]}$$

On the other hand, Raney Ni is widely used for hydrogenation and reduction processes such as benzene reduction to cyclohexane (Li and Xu 2001; Fouilloux 1983). Also, Raney Ni is known to accelerate the reaction of CO_2 conversion to methane (Lee et al. 2005; Hochard-Poncet et al. 1995). So it is thought that cavities which are formed on the surface of the catalyst contain the generated H_2 and molecules of CO_2 and the following cavitation collapse will provide necessary conditions for CO_2 reduction. Moreover, particles of catalyst can be used as nuclei helping to generate more cavitational bubbles (see Chapter 2, Figure 2.5). The results of experimental work are presented in Table 4.3.

Table 4.4. Sonocatalytic reduction of CO_2 using different catalytic systems

Test #	CO_2 molar fraction	Average hydrostatic pressure, MPa	Average experimental temperature, K	Average ultrasonic power, W/cm^2	Catalytic system/Co-reactant	Products
1	0.15	0.25	287.15±1	60	Raney Ni	H_2; CO
2	0.15	0.34	~353.15	60	Raney Ni	H_2
3	0.15	0.25	~353.15	60	-	-
4	0.15	0.25	287.15±1	60	Raney Ni – Ru/C – NaOH	H_2; CO
5	0.15	0.2	287.15±1	60	7 mol% of H_2	CH_4, CO, H_2

4.4.2.1. Sonochemical Catalytic Reduction of Carbon Dioxide with Activated Raney Ni Catalyst

In the first experiment, 2 grams of Raney Ni catalyst was applied. The average temperature and average hydrostatic pressure of the medium during experiments were 287.15 K and 0.25 MPa, respectively. Ultrasonic irradiation of approximately 60 W/cm^2 was applied and the test was performed under an Ar/CO_2 atmosphere containing approximately 15 mol% of CO_2. The duration of the test was 60 minutes. The GC analysis detected the presence of 4.47 µmol/l of CO and 3.95 µmol/l of H_2 in the final gas mixture (Figures 4.14 and 4.15). The presence of a relatively large amount of H_2 can be explained by the adsorption of the gas from the catalytic surface. Therefore, no obvious increases in the CO formation rate as well as the predicted formation of CH_4 were observed.

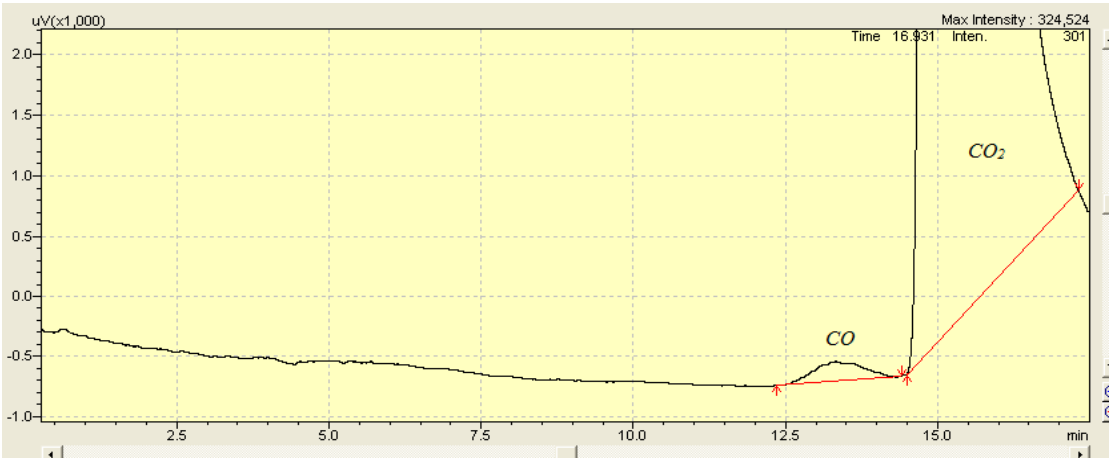

Figure 4.14. FID chromatogram for CO formation in catalytic sonolysis of water under an Ar/CO_2 atmosphere containing 15 mol% of CO_2

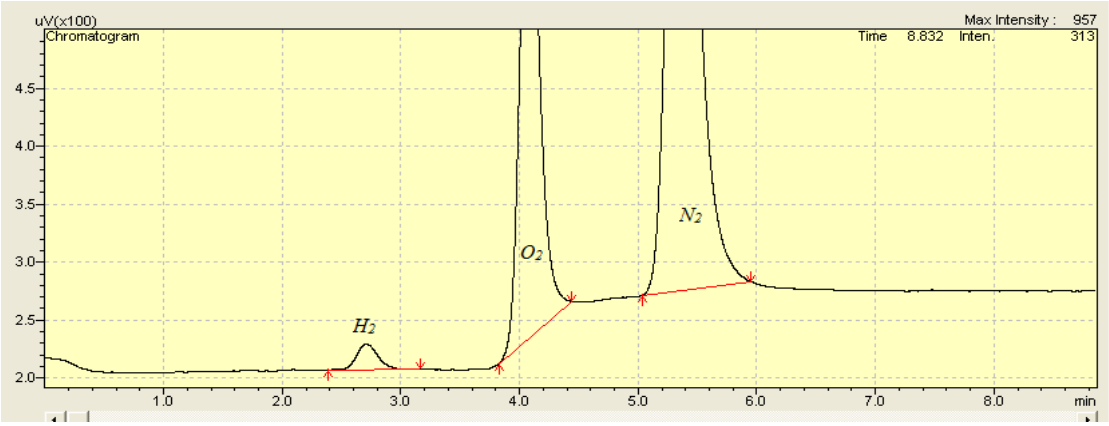

Figure 4.15. TCD chromatogram for H_2 formation in high-temperature catalytic sonolysis of water under an Ar/CO_2 atmosphere containing 15 mol% of CO_2

4.4.2.2. Sonochemical Catalytic Reduction of Carbon Dioxide on Activated Raney Ni Catalyst at High Temperature Conditions

a) In the next step it was decided to investigate the effect of a temperature increase. The sonication medium was pressurized with an Ar/CO_2 atmosphere containing 15 mol% of CO_2 to 0.25 MPa and subjected to ultrasound. The standard 2 gram of Raney Ni catalyst was used for the CO_2 sonochemical reduction. The temperature of the process is not controlled by means of the external cooling system, so the temperature increased to ~353.15 K over 15 minutes. The time of the experiment, after the system reaches a necessary temperature, is one hour. It is important to note that the hydrostatic pressure in the reactor system increased by almost 0.1 MPa from the initial value when the temperature increased to ~353.15 K. The GC analysis detected a larger amount of released H_2 (45.76 μmol/l) (Figure 4.16) than in the previous tests, which can be explained by the effect of the high experimental temperature (desorption of H_2 from the surface of the catalyst increases with a temperature rise). Also, a negligible amount of CO was detected which presumably was generated at the very beginning of the test. So the increase in the experimental temperature led to a greater amount of H_2 evolving from the surface of a catalyst. Furthermore, the absence of CO as a product was the result of the high temperature, because the vapour pressure of the medium increased which made the cavitation reactions unfavourable to proceed at such conditions. In other words, high vapour pressure of water at elevated temperature significantly lowers temperatures and pressures of the cavitational collapse so that the sonochemical reactions of CO_2 reduction can hardly occur. Moreover, it was also suggested that sonolysis of water

does not proceed at such conditions and, consequently, all detected H_2 is the result of H_2 desorption from the catalytic surface.

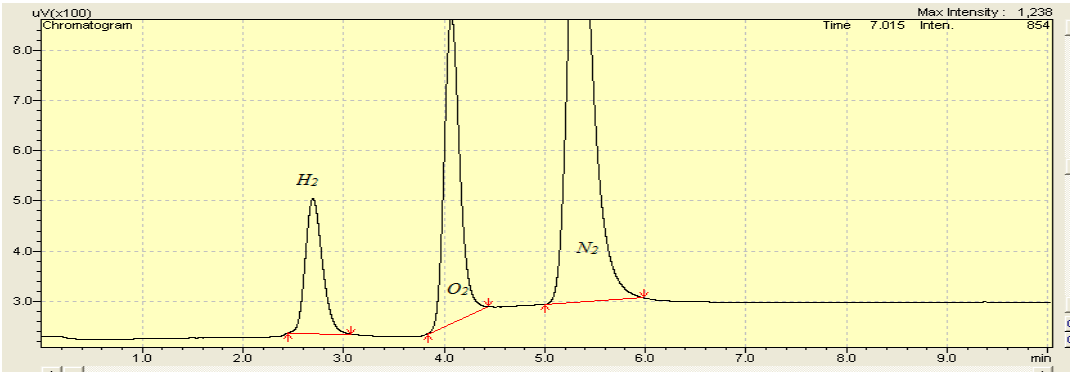

Figure 4.16. TCD chromatogram for H_2 formation in high-temperature catalytic sonolysis of water under an Ar/CO_2 atmosphere containing 15 mol% of CO_2

b) In order to prove or disprove the statement that the desorption of H_2 from the surface of the catalyst is the only source of H_2 in the previous test, an additional experiment on sonolysis of CO_2 in a water medium at high temperature (~ 353.15 K) without addition of any catalytic system was performed. In this experiment, a 550 cm^3 of distilled water was preliminary heated approximately to 348.15 K by placing it into the drying oven (see Chapter 3, Section 3.3.1.6) in order to maximally exclude sonolysis at low temperature conditions. Then, the aqueous medium was quickly transferred into the reactor and subjected to a 0.3 MPa Ar/CO_2 atmosphere with a molar percentage of CO_2 equal 15%. After that, the reaction system was subjected to ultrasonic irradiation of 60 W/cm^2 while the cooling system was disabled. The test was carried out for one hour after the experimental temperature reached the required 353.15 K. The GC analysis of gaseous mixture did not reveal the presence of H_2 (except for only indistinguishable traces, see Figure 4.17). Moreover, it was worth noting that the CO formation during this experiment was not detected (Figure 4.18).

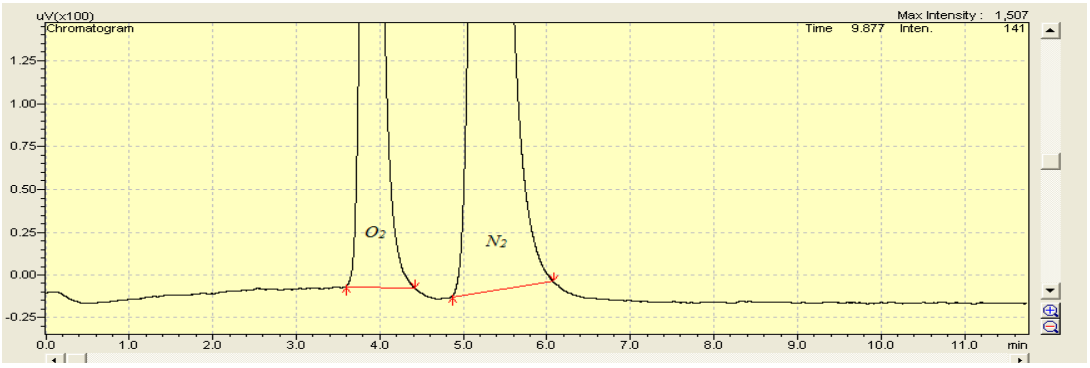

Figure 4.17. TCD chromatogram for gaseous product in high temperature sonolysis of water under an Ar/CO_2 atmosphere containing 15 mol% of CO_2

Figure 4.18. FID chromatogram for gaseous products in high temperature sonolysis of water under an Ar/CO_2 atmosphere containing 15 mol% of CO_2

4.4.2.3. Sonochemical Catalytic Reduction of Carbon Dioxide with Raney Ni – Ru/C Catalytic System

The idea for the next experiment consisted in applying the Raney Ni – Ru/C catalytic system for sonochemical reduction of CO_2. Kudo and Komatsu (1999) applied this system to the thermo-catalytic conversion of CO_2 to CH_4. The mechanism for the CO_2 thermo-catalytic conversion, proposed by them, is represented in Figure 4.19.

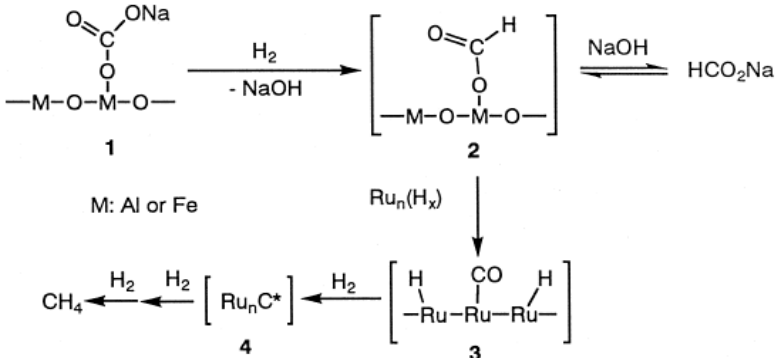

Figure 4.19. Thermo-catalytic conversion of CO_2 to CH_4 using the Raney Ni – Ru/C catalytic system

For the next stage of investigation, a catalytic system containing 2 grams of Raney Ni, 0.5 gram of supported Ru on activated carbon and 3.9 grams of sodium hydroxide (NaOH) was prepared. The sonochemical-catalytic reduction of CO_2 was conducted under an Ar/CO_2 atmosphere during 60 minutes. The molar fraction of CO_2 in the atmospheric gas amounted to 0.15. The average hydrostatic pressure and temperature for the experiment were 0.25 MPa and 287.15 K, respectively. 17.06 µmol/l of H_2 and 3.93 µmol/l of CO are detected in the final gas mixture by the chromatographic analysis (Figures 4.20 and 4.21). The greater amount of H_2, in comparison with the test (section 4.4.2.1) where only Raney Ni was used, can be

explained by the reaction of sodium hydroxide dissolved in water with Al-cites remained in the catalyst after its activation (Reaction 4.74).

Figure 4.20. FID chromatogram for CO formation in catalytic sonolysis of water under an Ar/CO_2 atmosphere containing 15 mol% of CO_2

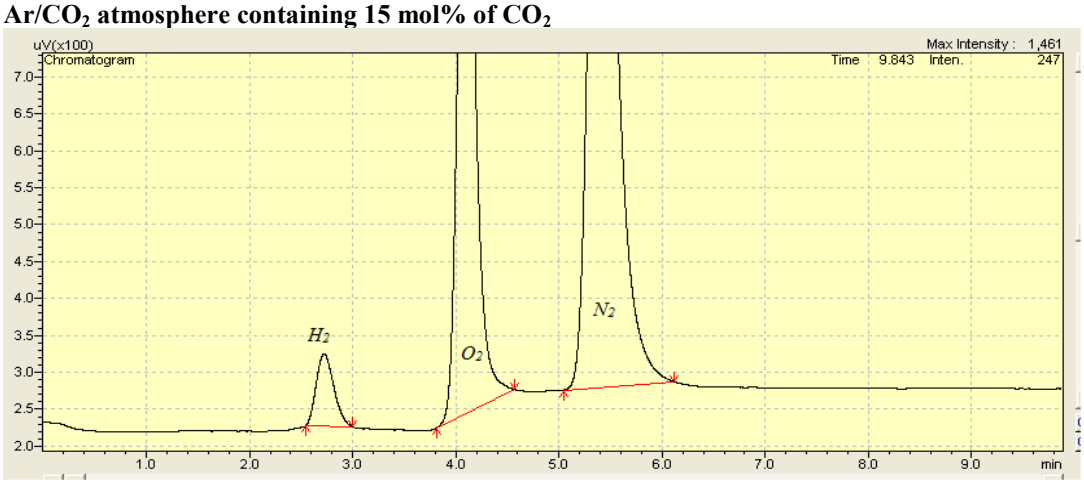

Figure 4.21. TCD chromatogram for H_2 formation in catalytic sonolysis of water under an Ar/CO_2 atmosphere containing 15 mol% of CO_2

4.4.2.4. Sonochemical Reduction of Carbon Dioxide under an Ar/CO_2/H_2 Atmosphere

The performed experimental work shows that the introduction of the Raney Ni – Ru/C catalytic system and greater amount of H_2 in the sonicating system did not lead to the CO_2 reduction by H_2 into CH_4. Also, the amount of produced CO was almost equal to that when additional H_2 was not added to the system (see Section 4.4.1).

At this point, it was decided to artificially introduce H_2 into an atmospheric gas mixture in order to see the effect of it on the sonochemical reduction of CO_2. Thus, an atmospheric gases mixture of 15 mol% of CO_2, 7 mol% of H_2 and 77 mol% of Ar was prepared. An aqueous medium was subjected to a 0.2 MPa atmospheric gas containing 7 mol% of H_2 and sonolysis was carried out for 60 minutes. After the

experiment was completed, the final gas was analysed by the GC. Results showed that 2.32 µmol/l of CH_4 and 1.25 µmol/l of CO were formed during the test (Figure 4.22). The amount of H_2 in the final mixture did not undergo any distinguishable changes during the experiment and remained at 3161.2 µmol/l which makes approximately 7 mol% of the initial gas mixture (Figure 2.23).

Thus, it can be seen that the introduction into an atmospheric gas a significant amount of H_2 lead to the reaction of CO_2 reduction to CH_4. However, it also must be noted that the rate of CO_2 reduction according to the amounts of the products obtained did not significantly increase or decrease in comparison to that obtained in sonolysis of water under an Ar/CO_2 atmosphere only (see Section 4.4.1.1).

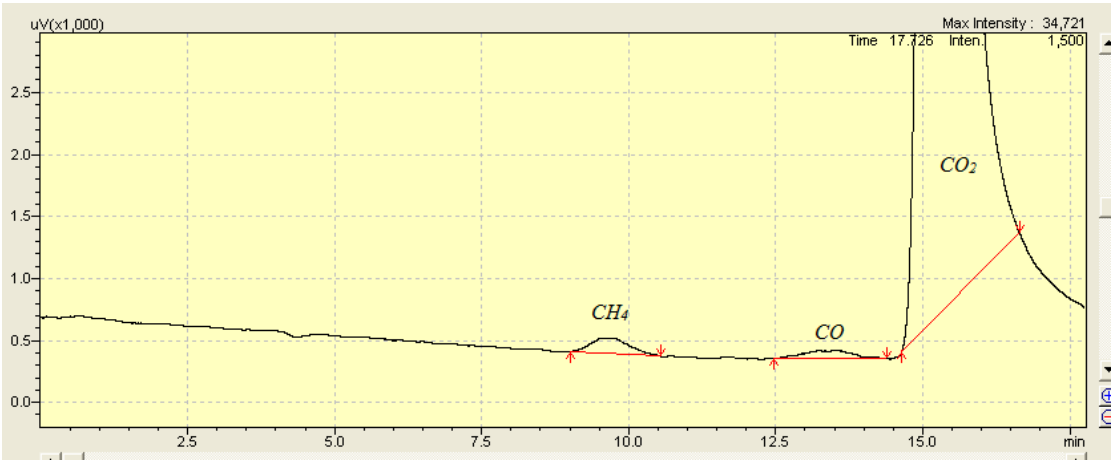

Figure 4.22. FID chromatogram for formation of CH_4 and CO in sonolysis of water under an $Ar/H_2/CO_2$ atmosphere containing 7 mol% of H_2 and 15 mol% of CO_2

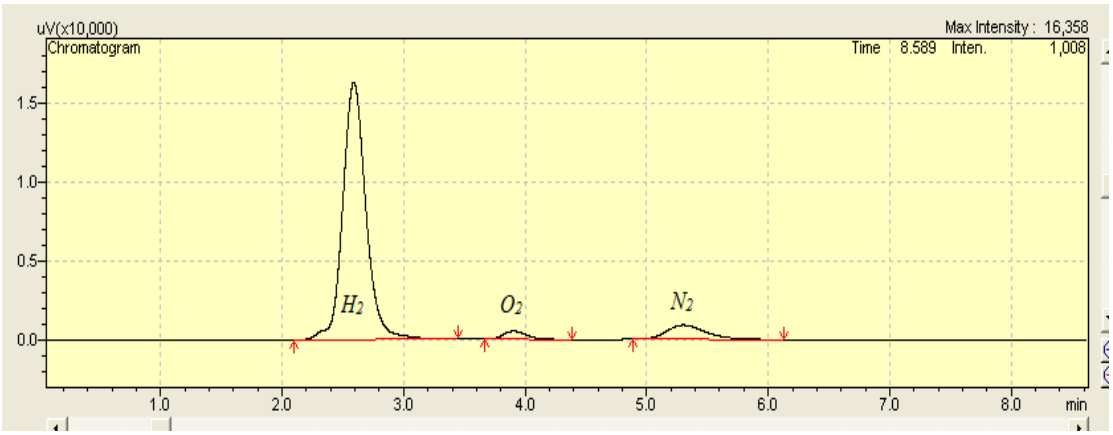

Figure 4.23. TCD chromatogram of the presence of 7 mol% of H_2 in the final gas mixture after sonolysis of water under an $Ar/H_2/CO_2$ atmosphere containing 7 mol% of H_2 and 15 mol% of CO_2

More detailed discussion of the results on sonoreduction of carbon dioxide in a water media is presented in Chapter 5.

4.4.3. Sonochemical Reduction of Carbon Dioxide in Hydrocarbon Medium

The purpose of this experimental work is to perform the sonochemical reduction of CO_2 using hydrocarbons as sonicating media. The influence of such parameters as the duration of a test and power of ultrasonic irradiation were studied.

As it was described in the theoretical part of this chapter on sonolysis of hydrocarbons, H_2 is one of the products which are formed during the pyrolysis of hydrocarbons. So, the mechanism of the proposed sonochemical reduction assumed that CO_2 dissolved in hydrocarbons can be reduced by hydrogen generated from a liquid medium under applied ultrasonic irradiation. Pentane (C_5H_{12}) and heptane (C_7H_{16}) were chosen for this experimental work. It is also worth noticing that these two chemicals have vapour pressures which differ more than 10 times, so the effect of vapour pressure on the sonication process can also be studied. For studying the effect of the concentrations of atmospheric gases on the effectiveness of sonoreduction of CO_2, it was decided to conduct the following experiments under atmospheres with the low concentration of CO_2. At least two parallel tests were carried out for every investigation at different experimental conditions. The difference in results between two tests at similar conditions did exceeded 10%. Average result for each experimental point was used. The obtained results were submitted in Table 4.4.

Table 4.5. Effects of various parameters on the effectiveness of the sonochemical reduction of CO_2 in hydrocarbon sonicating media

Series of tests # (medium)	CO_2 molar fraction	Average hydrostatic pressure, MPa	Average experimental temperature, K	Average ultrasonic power, W/cm^2	Duration of test, min	Products
1 (pentane)	0.15	0.2	284.15	35	60	-
2 (pentane)	0	0.2	284.15	35	60	-
3 (pentane)	0.11	0.2	284.15	60	60	-
4 (pentane)	0.10	0.2	284.15	60	240	-
5 (heptane)	0	0.2	284.15	35	60	-
6 (heptane)	0.10	0.2	284.15	35	60	-
7 (heptane)	0.10	0.2	284.15	60	300	CO; H_2
8 (heptane - water)	0.10	0.2	287.15	60	60	products of heptane degradation

4.4.3.1. Sonochemical Reduction of Carbon Dioxide in Pentane Medium

a) First, an experiment on sonochemical reduction of CO_2 in pentane (C_5H_{12}) under an Ar/CO_2 atmosphere was performed. The concentration of CO_2 in the atmospheric gas was equal to 15% mol. The hydrocarbon medium was pressurized to 0.2 MPa with the mixture of Ar and CO_2 and 65% of ultrasonic power which the generator was able to produce was applied for the test. The sonolysis was conducted for 60 minutes at ultrasonic power of 35 W/cm^2 (240 W/l). The lower intensity of ultrasound at the similar settings of the ultrasound generator and condition of experiments was determined by the density value of the sonicating medium. The experiment was carried out at a temperature 284.15±1 K. The GC analysis of the sample taken after the run did not show the presence of any products of either C_5H_{12} decomposition or CO_2 sonolysis (Figures 4.24 and 4.25).

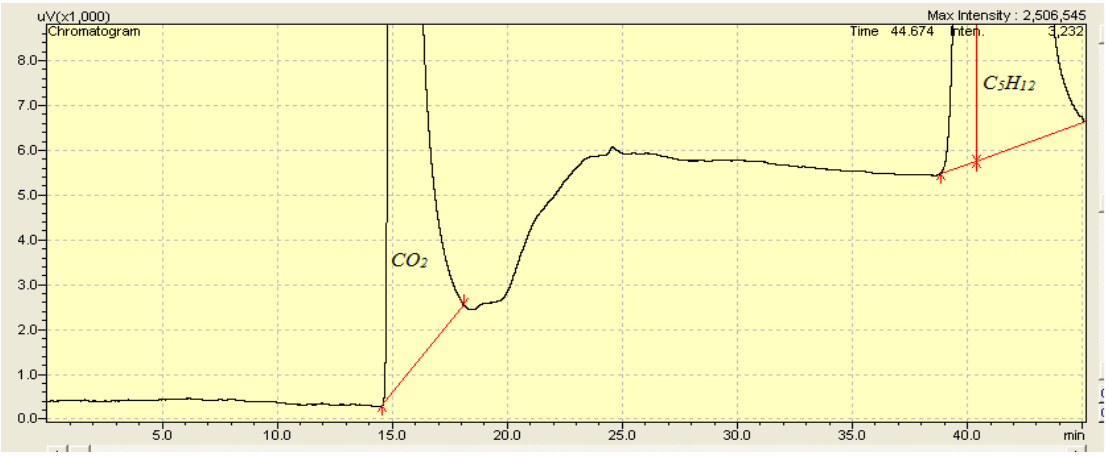

Figure 4.24. FID chromatogram for gaseous product in sonolysis of pentane under an Ar/CO_2 atmosphere containing 15 mol% of CO_2

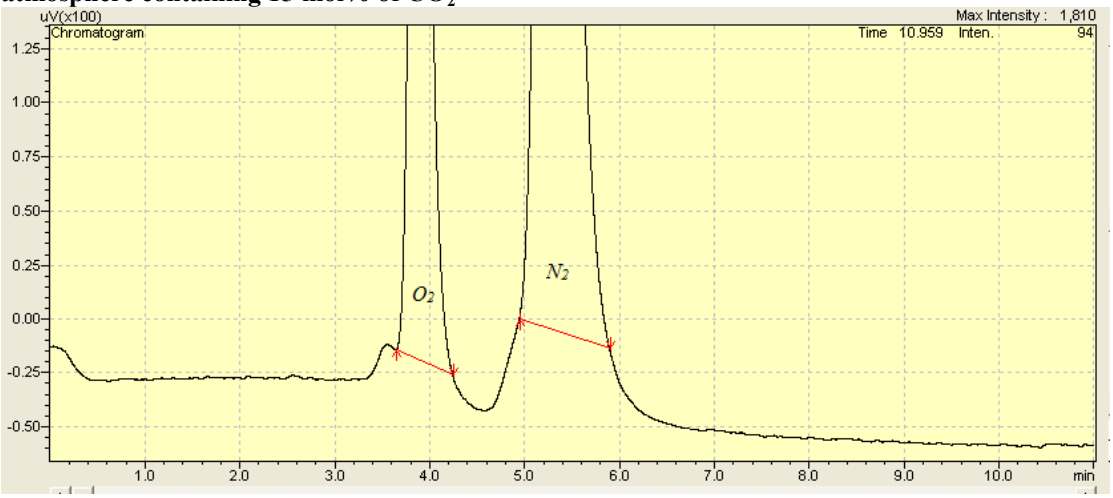

Figure 4.25. TCD chromatogram for gaseous products in sonolysis of pentane under an Ar/CO_2 atmosphere containing 15 mol% of CO_2

b) As no traces of expected products were detected in the previous experiments, the next step was to determine the influence of CO_2 in the atmospheric gas during C_5H_{12} sonication. So, the sonolysis of C_5H_{12} under a pure Ar atmosphere was carried out. The hydrostatic pressure of the liquid medium and the range of experimental temperatures were set at 0.2 MPa and 284.15±1 K, respectively. The ultrasound intensity was set at 35 W/cm^2 (240 W/l). The GC analysis is performed after 1 hour of ultrasound irradiation and no products of C_5H_{12} sonodegradation were found.

c) It was then decided to conduct a series of experiments at higher ultrasound power in order to study the effect of ultrasound intensity on the rate of CO_2 sonolysis in C_5H_{12}. For this C_5H_{12} was pressurized to 0.2 MPa with an Ar/CO_2 atmosphere containing 0.1 molar fraction of CO_2 and 60 W/cm^2 (410 W/l) ultrasound irradiation (the maximum achievable value of ultrasound intensity for the used equipment at selected experimental conditions) was applied to the sonicating system for 60 minutes. The temperature of the test was maintained at 284.15±1 K. The GC analysis, conducted after the sonication, did not reveal any chemical transformations of CO_2 and C_5H_{12}.

d) Finally, the effect of the test duration was investigated. Sonolysis of C_5H_{12} under an Ar/CO_2 atmosphere was performed over 240 minutes. Other experimental conditions were maintained similar to those in the previous series of experiments (4.4.3.1c). After the experiment was performed, the GC analysis was conducted and the GC analysis showed no products of either CO_2 sonolysis or C_5H_{12} decomposition. After carrying out the above experiments, it was concluded that C_5H_{12} cannot be considered as a suitable sonicating medium for the CO_2 utilization as long as no CO2 reduction occurred during this experimental work and any further investigation on using C_5H_{12} as a sonicating medium was terminated.

4.4.3.2. Sonochemical Reduction of Carbon Dioxide in Heptane Medium

The next hydrocarbon medium selected for the investigation of sonochemical reduction of CO_2 was heptane (C_7H_{16}). C_7H_{16} has a vapour pressure 10 times lower value than pentane (C_5H_{12}). So it was suggested that using C_7H_{16} as a liquid medium for sonication will offer more extreme conditions during the cavitation bubble collapse in comparison to C_5H_{12}. The experiment was planned as follows:

a) Firstly, sonolysis of C_7H_{16} under a pure Ar atmosphere was conducted. The hydrostatic pressure of the liquid medium was adjusted to 0.2 MPa with Ar and

ultrasonic irradiation of 35 W/cm^2 (240 W/l) was applied for one hour. The temperature of the experiment was kept at 284.15 K. The gaseous samples analysed by the GC did not reveal any products of C_7H_{16} degradation at these experimental conditions.

b) Secondly, the sonolysis of CO_2 in C_7H_{16} was investigated. The hydrocarbon medium was pressurized to 0.2 MPa with an Ar/CO_2 atmosphere containing 10 mol% of CO_2. Sonication was carried out for 60 minutes at ultrasound power of 35 W/cm^2 (240 W/l). The experimental temperature was maintained at 284.15 K during the whole experiment. However, no product of CO_2 sonolysis or C_7H_{16} decomposition was detected by the GC analysis.

c) As no products of sonolysis were obtained in the second experiment, it was decided to increase the ultrasound intensity and test duration in the next experiment. So, the mixture of atmospheric gases containing 10 mol% of CO_2 and 90 mol% of Ar was prepared. The hydrostatic pressure of the medium was set to 0.2 MPa. Sonolysis of CO_2 in heptane was conducted over 300 minutes at an ultrasound power of 60 W/cm^2 (410 W/l). GC analysis of a gas sample detected 3.92 µmol/l of CO as a product of CO_2 sonolysis as shown in Figure 4.26.

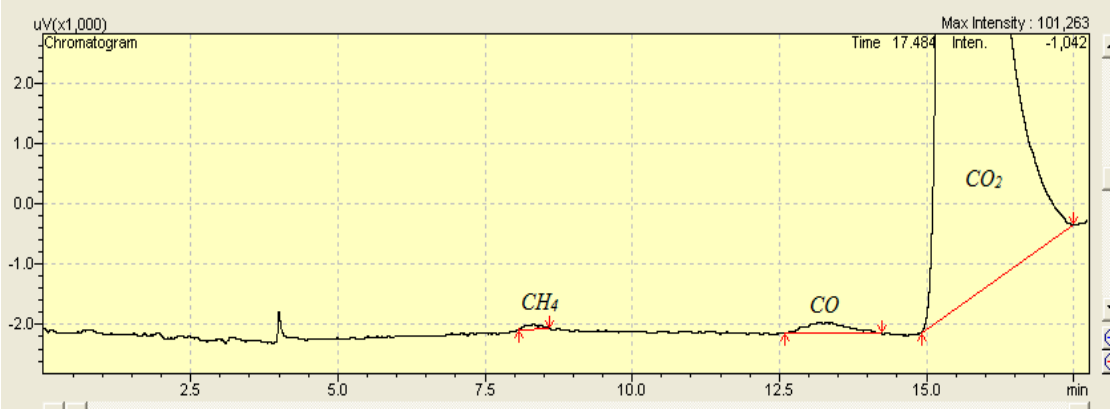

Figure 4.26. FID chromatogram for CO formation in sonolysis of heptane under an Ar/CO_2 atmosphere containing 10 mol% of CO_2

However, the process of sonodegradation of C_7H_{16} was observed to occur as 0.48 µmol/ of CH_4 and 0.36 µmol/l of H_2 (Figure 4.27) in the experiment. No other detectable products of C_7H_{16} sonodegradation were observed by the GC.

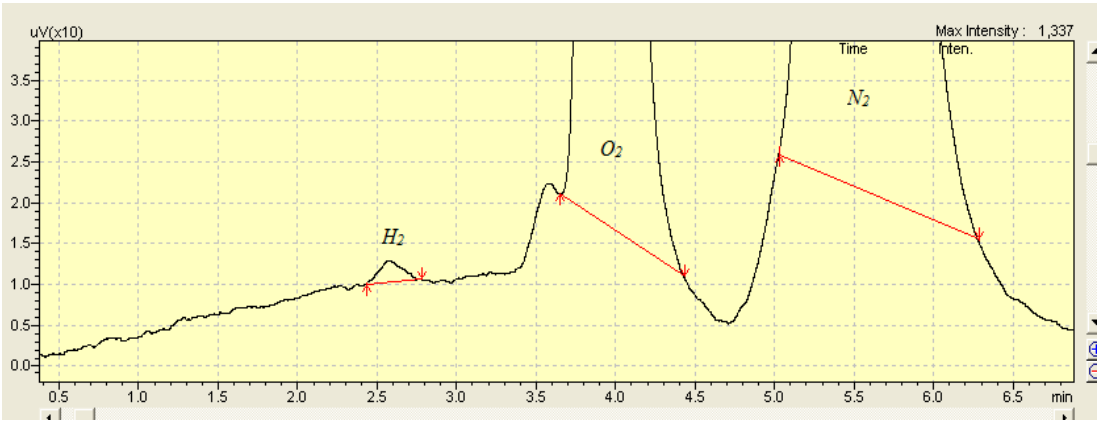

Figure 4.27. TCD chromatogram for H_2 formation in sonolysis of heptane under an Ar/CO_2 atmosphere containing 10 mol% of CO_2

The above experiment has led to the conclusion that the cavitation collapse in a water media provides better conditions for the sonochemical reactions to occur than the collapse of cavities in a heptane or a pentane media. This conclusion is directly linked to the physical properties of both sonicating media. These results suggest that due to unfavorable properties of a hydrocarbon medium in terms of its vapour pressure, ratio of specific heats, the conditions, which are generated during the cavitation bubble collapse in C_7H_{16} and C_5H_{12} media, are not as suitable as the conditions obtained when water is used as a sonicating medium.

4.4.3.3. Sonochemical Reduction of Carbon Dioxide in Heptane-Water Medium under an Ar/CO_2 Atmosphere

In view of the above results, it was then decided to investigate the sonochemical reduction of CO_2 in an emulsion of water and C_7H_{16}. The main idea behind the proposed test was an attempt to generate H_2 (or $H^{\cdot}$ radicals) during C_7H_{16} degradation to react with and reduce CO_2. Generally, it is known that water and C_7H_{16} are two immiscible liquids. However, the available literature suggests that C_7H_{16} is soluble in water but its molar solubility is just $9.5 \cdot 10^{-5}$ mol/litre at room temperature (Chiou 2002). It was proposed that the addition of a small amount of C_7H_{16} into a water media for sonication will guarantee the presence of heptane molecules in the cavitation bubble during sonolysis. Moreover, as long as the concentration of heptane in cavities is very low, it will not greatly affect the temperature and pressure of the collapse of a cavitation bubble. Thus, the degradation of heptane was more likely to occur under such conditions.

For this experiment, an emulsion containing heptanes and water in the ratio of 10 and 540 cm^3, respectively, was prepared and transferred into the reactor. The liquid medium was pressurised to 0.2 MPa with the Ar/CO_2 atmospheric gas. The concentration of CO_2 in the atmosphere was 10 mol%. Sonochemical reduction of CO_2 in the heptane-water media is conducted for 60 minutes at ultrasound power of approximately 60 W/cm^2 (410 W/l). The experimental temperature was at 289.15±1 K by using the external heat-exchanging system. The GC analysis performed after the test detected products of C_7H_{16} degradation along with CO, see Figure 4.28.

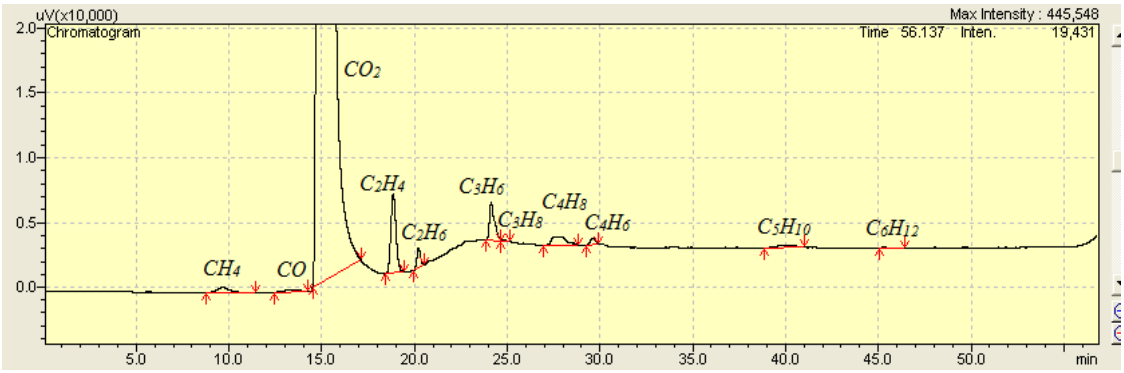

Figure 4.28. FID chromatogram for the products in sonolysis of heptane-water emulsion under an Ar/CO_2 atmosphere containing 10 mol% of CO_2

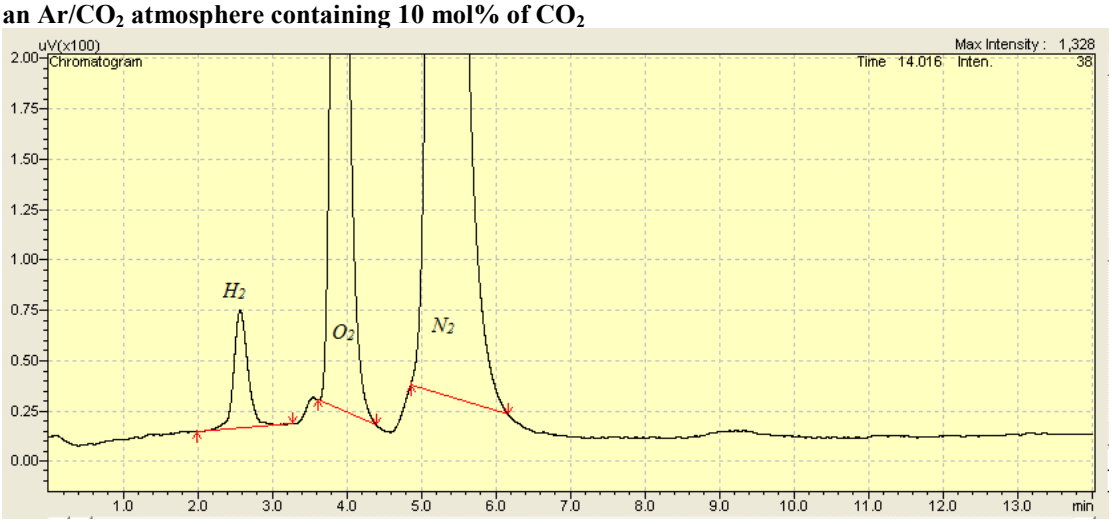

Figure 4.29. TCD chromatogram for H_2 formation in sonolysis of heptane-water emulsion under an Ar/CO_2 atmosphere containing 10 mol% of CO_2

The products of C_7H_{16} sonodegradation were found to be H_2 (Figure 4.29), CH_4, C_2H_4, C_3H_6, C_3H_8, C_4H_8, C_4H_6, C_5H_{10} and C_6H_{12}. Also, 3.59 µmol/l of CO was detected by the GC. It can be seen that although the amount of produced CO is lower, it is not significantly from that generated during sonoreduction of CO_2 in a pure water medium under similar experimental conditions (see Section 4.4.1.1e). Therefore, it was concluded that due to the presence of small amount of C_7H_{16} in the

reaction system in comparison to the experiment at similar experimental conditions when pure water is used as a sonicating medium (see Section 4.4.1.1e) the rate of CO_2 reduction during sonolysis reduced. Also, it should be taken into account that some amount of detected H_2 (approximately 10%, according to the experimental results obtained in Sections 4.4.1.1e) could be generated during the water sonolysis (see Table 4.6). The amounts of the products of C_7H_{16} degradation obtained from sonolysis of the heptane-water emulsion are estimated and listed in Table 4.7.

Table 4.6. Rates of products formation in sonolysis of water medium under an Ar/CO2 atmosphere (see Section 4.4.1.1e)

Products of sonolysis, μmol/l	
H_2	5.13
CO	0.78

Table 4.7. Rates of products formation in sonolysis of water-heptane medium under an Ar/CO_2 atmosphere

Products of sonolysis, μmol/l										
H_2	CH_4	C_2H_4	C_2H_6	C_3H_6	C_3H_8	C_4H_8	C_4H_6	C_5H_{10}	C_6H_{12}	CO
11.15	8.41	21.88	3.24	8.89	0.23	3.16	0.67	0.69	0.16	3.59

It can be seen from Tables 4.6 and 4.7, that more than tenthfolw amount of H_2 was generated due to the sonodecomposition of C_7H_{16} than in the pure water sonicating medium. Moreover, it is worth noticing that the products of sonochemical decomposition of C_7H_{16} did not contain any traces of acetylene (C_2H_2). The amounts of the generated products observed in the experiment were results compared with those found in other experiments on sonochemical degradation of hydrocarbons. It was found by Suslick et al. (1983) and Mizukoshi et al. (1999) in their studies that products of decane ($C_{10}H_{22}$) sonolysis are quite similar to those produced during high-temperature pyrolysis of hydrocarbons (Lifshitz and Frenklach 1975; Friedmann, Bovee, and Miller 1970) and C_2H_2 is one of the main products of the decane degradation under ultrasound irradiation. However, in our investigation no C_2H_2 is found in the products of the C_7H_{16} sonolysis. One of possible reasons of such discrepancy can be casused by difference in values of temeratures and pressures generated during cavitation collapse. It can be seen from Table 4.8 that the obtained results of sonolysis of C_7H_{16} comply well with the data on low temperature pyrolysis of C_7H_{16} found in the literature.

Table 4.8. Comparison of products obtained by sonochemical degradation of C_7H_{16} with the products of low temperature pyrolysis of C_7H_{16}

Products yields, mol %	Source of results			
	Rice-Kossiakoff theory (1942)	Bajus and Vesely (1979)	Aribike and Sisu (1988)	This Research
H_2	-	17.07	16.50	17.49
CH_4	18.42	18.90	5.48	14.66
C_2H_4	39.48	38.94	42.50	38.14
C_2H_6	15.79	2.83	1.06	5.65
C_3H_6	10.52	10.81	16.83	15.50
C_3H_8	0	0.42	0	0.40
C_4H_8	5.26	5.72	7.60	5.51
C_4H_6	0	0.73	5.73	1.17
C_4H_{10}	0	0.11	0	0
C_5H_{10}	5.26	2.85	3.06	1.20
C_5H_{12}	0	0.06	0	0
C_6H_{12}	5.26	1.56	1.25	0.28

It can be seen that the quality of products of the sonochemical decomposition of C_7H_{16} in our work agrees satisfactorily with those products of C_7H_{16} pyrolysis obtained by other authors.

A more detailed discussion on the proposed mechanism of C_7H_{16} sonodegradation is presented in Chapter 5.

4.4.4. Sonochemical Reduction of Carbon Dioxide in Methanol medium

4.4.4.1. Sonolysis of Methanol under an Ar/CO_2 Atmosphere

This section presents the experimental work carried out on the sonochemical reduction of carbon dioxide in a methanol medium. Methanol, which is a solvent in this process, is assumed to be both a medium for direct CO_2 sonolysis and an H_2 provider (see Section 4.3.4.1). Further, the experience gained from the previous experiments described in above sections (see Sections 4.4.1-4.4.3) had helped in planning the experimental conditions for this experiment. At least two parallel tests were carried out for every investigation at different experimental conditions. The difference in results between two tests at similar conditions did exceeded 10%. Average result for each experimental point was used.

Methanol of 500 cm^3 in volume was used as a sonicating medium in this experiment. The liquid medium was transferred to the experimental reactor and subjected to a pressure of 0.2 MPa Ar/CO_2 mixture of atmospheric gases containing 12 mol% of CO_2. Sonolysis was conducted over 60 minutes at maximum possible ultrasound intensity of approximately 70 W/cm^2 (530 W/l) at suitable experimental conditions of medium, temperature and hydrostatic pressure. The experimental temperature was maintained at 288.15 K by employing the cooling system. The gaseous sample was analysed with the GC after the test was completed, which revealed the presence of 0.86 µmol/l of CH_4, 0.79 µmol/l of CO (Figure 4.30) and 11.17 µmol/l of H_2 is detected (Figure 4.31). However, no detectable amounts of CH_2O due to CH_3OH sonolysis were found.

It can be noted from the obtained results that the formation of CO takes place when methanol was used as a sonicating medium, but it is not as much as when water was used as a sonicating medium. However, the generated CO can be also formed from methanol ultrasonic degradation (see Reactions 4.50-4.60). The formation of CH_4 in this experiment can be explained by the formation of $CH_3^{\cdot}$ radicals from the primary reaction of methanol sonodegradation (Reaction 4.50) which then react with bulk CH_3OH (Reaction 4.52). So it was though that CH_4 formation from the reaction of CO_2 reduction by H_2 at such small amount of evaluated H_2 cannot be considered as a mechanism according to the results obtained in Section 4.4.2.4.

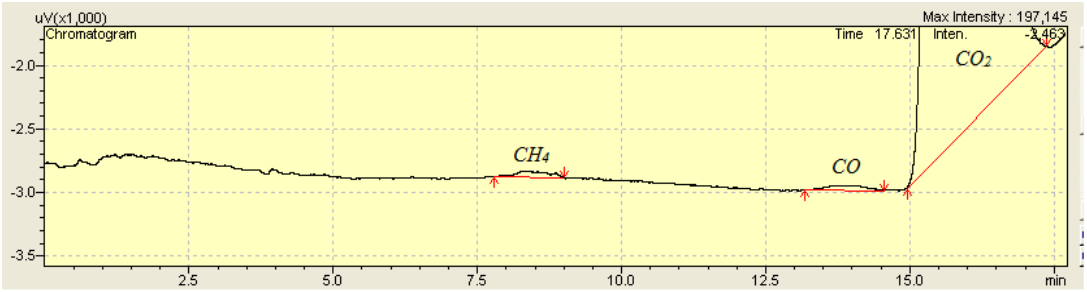

Figure 4.30. FID chromatogram for CH_4 and CO formation in sonolysis of methanol under an Ar/CO_2 atmosphere at 288.15 K

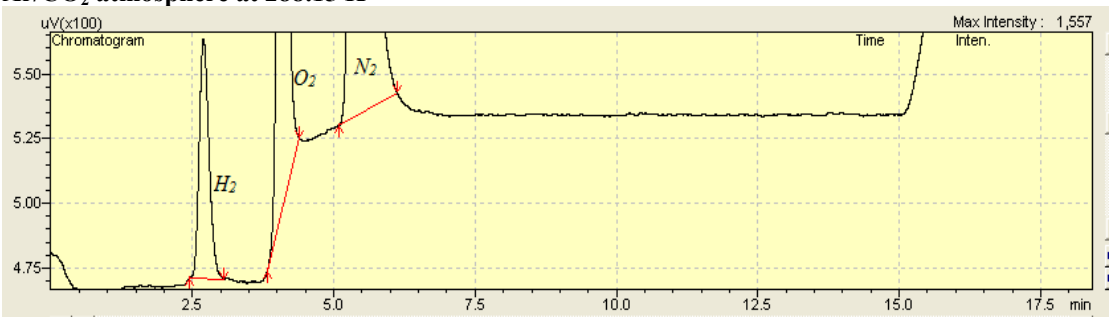

Figure 4.31. TCD chromatogram for H_2 formation in sonolysis of methanol under an Ar/CO_2 atmosphere at 288.15 K

Furthermore, as is known, a part of electrical energy is converted to heat during sonolysis, so that the tip of ultrasonic transducer, which serves a transmitter of ultrasonic energy into a liquid medium, reaches a high temperature (see Sections 4.4.2.2 and 4.4.2.3; Saunders, Clift, and Duck 2004; Duck et al. 1989). Therefore, more investigations on the sonochemical reduction of CO_2 in CH_3OH medium needs to be conducted in order to prove that the contact of CH_3OH medium with the hot surface of the ultrasonic sonotrode‟s tip does not add to the pyrolytic decomposition of CH_3OH and, hence, it is not responsible for the formation of the products obtained. This was carried out as described below.

4.4.4.2. Sonolysis of Methanol under an Ar/CO_2 Atmosphere at High Temperature Conditions using Raney Ni Catalyst

The experiment was carried out to study the effect of temperature on the sonochemical reduction of CO_2 in CH_3OH medium. In this experiment, it was decided to increase the experimental temperature in sonolysis of methanol under an Ar/CO_2 atmosphere. Thus, methanol of 500 cm^3 was preheated in the drying oven to a temperature of 323 K and then it was introduced into the reactor. The reactor was pressurized to 0.2 MPa by an Ar/CO_2 atmospheric gases mixture with CO_2 concentration of 12 mol%. Also, 2 grams of Raney Ni catalyst was added into the reaction mixture for the H_2 generation and to enhance the formation of CH_4 during the probable pyrolysis of CH_3OH (Reaction 4.75). The cooling system was disabled in order to reach the required temperature for sonolysis. Ultrasound of 70 W/cm^2 (530 W/l) was applied to the system and the sonolysis was carried out for one hour after the experimental temperature had reached approximately 340.15 K. The average hydrostatic pressure throughout the test was kept at around 0.27-0.28 MPa (due to the high temperature of the test). Moreover, despite the experimental temperature, CH_3OH is still a liquid due to the slightly elevated pressure in this experiment. According to the HYSYS computer software calculations, the boiling point of CH_3OH at 340 K are about 354 K and 370 K at 0.2 MPa and 0.3 MPa, respectively. At the conclusion of the experiment a gaseous sample is collected and analysed by the GC which showed the presence of 3.37 μmol/l of CH_4 and 821.15 μmol/l of H_2. However, no CO was detected as a product (Figures 4.32 and 4.33). This can be attributed to the high temperature of the process because the sonochemical reactions of CO_2 reduction are not favoured at high temperatures. So

the formation of CH_4 due to CO_2 reduction by H_2 evolved from the surface of Raney Ni catalyst cannot be considered as the route. Thus, it can be concluded that the formation of CH_4 occurs through the process of CH_3OH degradation (Reaction 4.50) by ultrasound. However, there was no production of CO from CO_2 reduction at the selected experimental conditions (high temperature) which do not favour the reduction process. Moreover, the fact that an amount of CH_4 produced in this test was larger than that in sonolysis of CH_3OH under an Ar/CO_2 atmosphere at 288.15 K, which fact, however, does not agree the principles of sonolysis in liquid media.

$$CH_3^{\cdot} + H_2 \rightarrow CH_4 + H^{\cdot} \qquad \text{[R. 4.75]}$$

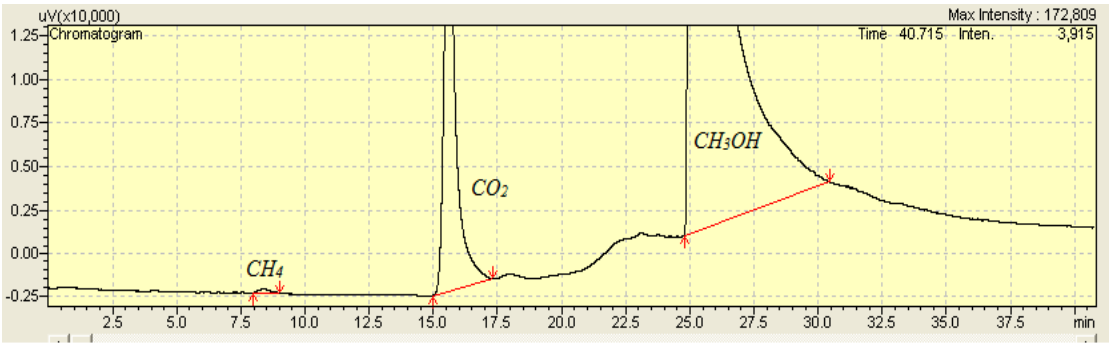

Figure 4.32. FID chromatogram for CH_4 formation in sonolysis of methanol under an Ar/CO_2 atmosphere at 340.15 K

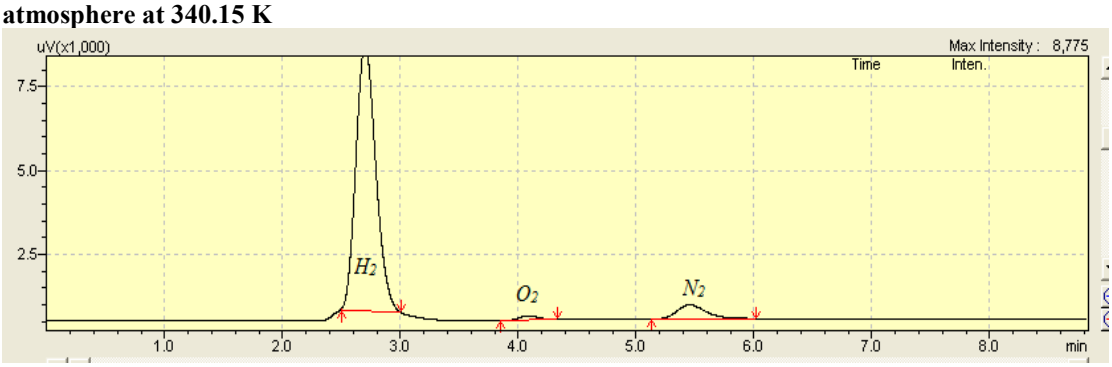

Figure 4.33. TCD chromatogram for H_2 formation in sonolysis of methanol under an Ar/CO_2 atmosphere at 340.15 K

Thus, on the one hand it is suggested that the pyrolytic degradation of CH_3OH occurs due to the contact of the sonicating medium with the surface of the ultrasonic transducer‟s tip leading to the subsequent generation of CH_4 according to Reaction 4.75. However, on the other hand, it is also considered that CH_4 is produced because of the presence of Raney Ni catalyst. In this case, it is expected that molecules of CH_3OH absorbed on the catalyst‟s surface which significantly reduces the activation energy barrier for the C-O bond decomposition according to Reaction 4.50. Then, formed $CH_3^{\cdot}$ radicals react with H_2 from the surface of Raney Ni catalyst and form

CH_4 (Reaction 4.75). In order to investigate the nature of the production of CH_4 an additional investigation was carried out as described in the next section.

4.4.4.3. Sonolysis of Methanol under an Ar/CO_2 Atmosphere at High Temperature Conditions

Sonolysis of CH_3OH was carried out under the similar conditions as in the previous investigation (Section 4.4.4.2), was carried out without the presence of Raney Ni catalyst in the reaction mixture. After sonolysis, samples of gaseous mixtures were analysed by the GC which did not revealed the presence of any traces of methane (Figure 4.34). This experiment confirmed that the formation of CH_4 in the previous test was due to the Raney Ni catalyst which lowers significantly the energy barrier for CH_3OH degradation. Thus according to Reaction 4.50, the thermal energy generated is sufficient to cause the C-O bond cleavage.

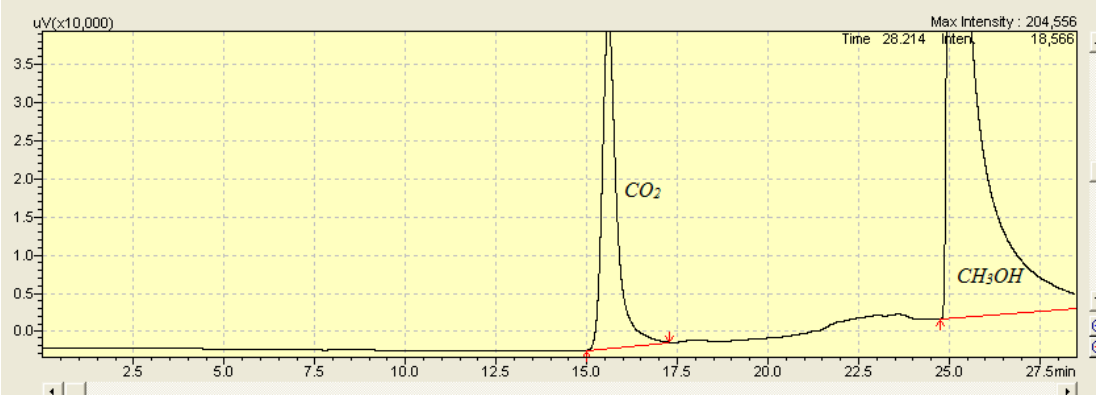

Figure 4.34. FID chromatogram of gaseous products in sonolysis of methanol under an Ar/CO_2 atmosphere containing 15 mol% of CO_2

Taking into account the low rates of the CO formation during the sonochemical reduction of CO_2 in CH_3OH medium, it was decided not to carry out any other experiment to try to achieve larger rates of CO_2 chemical fixation.

4.4.4.4. Ultrasound-Assisted Synthesis of Dimethyl Carbonate from Methanol and Carbon Dioxide at 288 K

In this experimental work the ultrasonic energy was applied for dimethyl carbonate (DMC) synthesis from CH_3OH and CO_2. According to Fang and Fujimoto (1996), Hou et al. (2002) and Wang et al. (2005), KOH and K_2CO_3 can be selected as basic catalysts for this experiment. Iodomethane (CH_3I) is also an essential component of the synthesis and serves as a provider of CH_3 radicals in the synthesis (Chun, He, and

Zhu 2001; Fujita et al. 2001). The mixture of CH_3OH, CH_3I, K_2CO_3 and KOH in the ratio of 85:4.3:0.5:0.5, respectively, was prepared and placed into the reactor. Then, the reacting mixture was pressurized with Ar up to 0.4 MPa and left for 15 minutes. After that, the gas is carefully vented and the reactor was subjected to a vacuum in order to remove any dissolved gases. Next, Ar/CO_2 at 0.2 MPa containing approximately 10 mol% of CO_2 ws introduced into the reactor. The sonolysis was conducted for 2 hours at the average experimental temperature of 288.15 K, which was maintained throughout the test by circulating iced water through the cooling system. The intensity of the ultrasound was kept at about 70 W/cm^2 (530 W/l) throughout the test. A small increase in the hydrostatic pressure was observed at the end of the experiment which can be attributed to the formation of gaseous products.

After the experiment was carried out, gaseous and liquid samples were collected for analysis by the GC which did not detect any DMC in the samples. However, 2.28 µmol/l of CO, 33.63 µmol/l of CH_4 (much larger amount than in sonolysis of methanol under an Ar/CO_2 atmosphere), C_2H_5I (Figure 4.35) and CH_2I_2 (Figure 4.36) were found as products. Also, small amount of C_2H_6 (0.42 µmol/l) was detected by the GC. Moreover, H_2 of 10.48 µmol/l was also produced during the test (Figure 4.37). The results of this experiment concluded that the sonochemical degradation of CH_3I was responsible for the formation of these products.

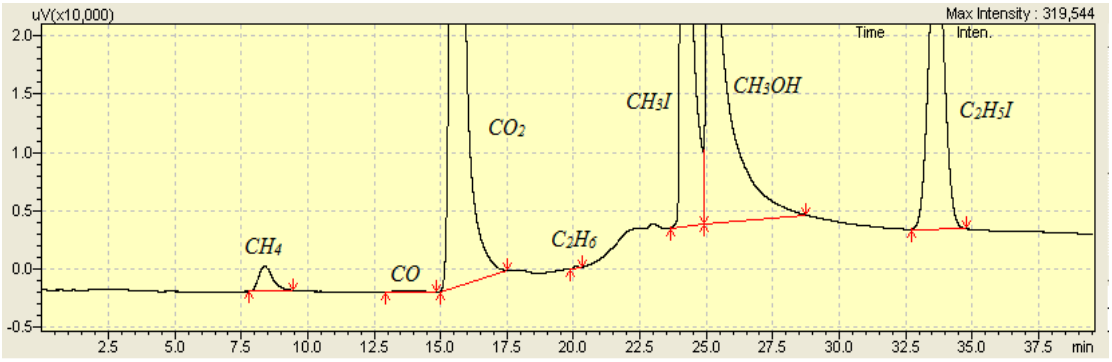

Figure 4.35. FID chromatogram of products of CH_3I sono-degradation at 288.15 K (gaseous phase)

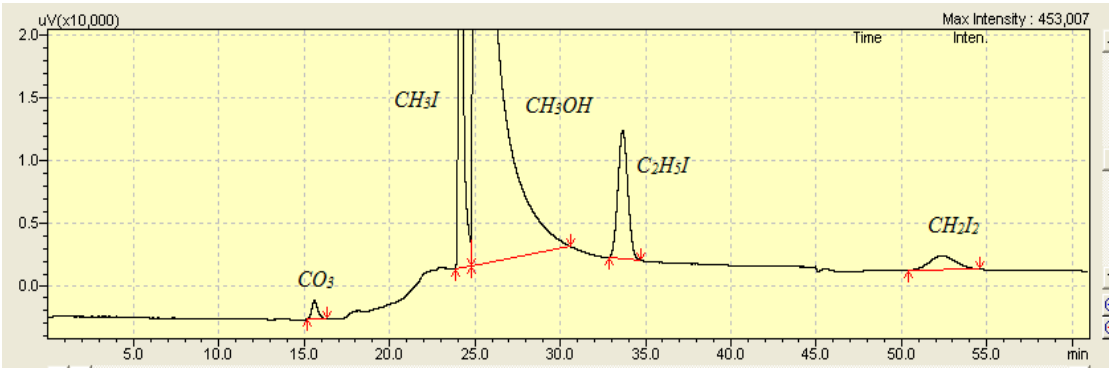

Figure 4.36. FID chromatogram of products of CH_3I sono-degradation at 288.15 K (liquid phase)

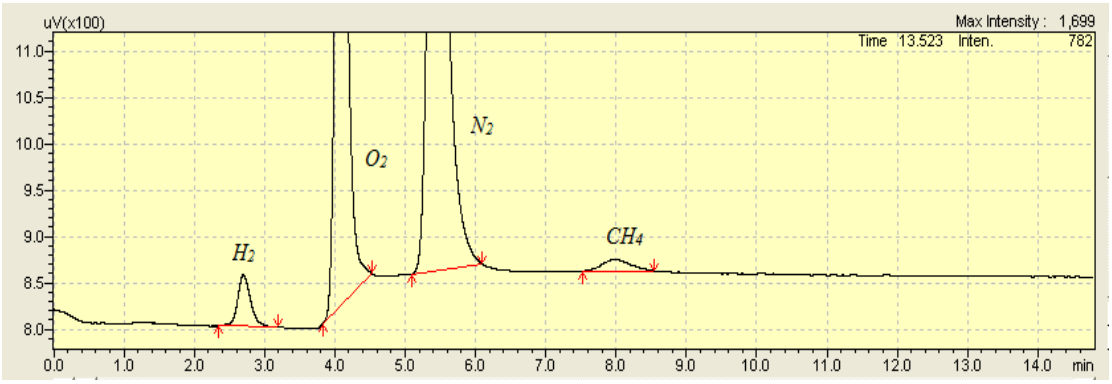

Figure 4.37. TCD chromatogram of H2 formation in the process of CH_3I sono-degradation at 288.15 K

Furthermore, in this experiment the synthesis of DMC through ultrasound energy was not successful. Based on the results obtained during this investigation, the mechanism of ultrasonic-assisted degradation of CH_3I in methanol can be proposed. The mechanism of CH_3I degradation at 20 kHz ultrasound will be discussed in detail in Chapter 5.

4.5. Conclusion

In conclusion, various experiments for sonochemical reduction of carbon dioxide dissolved in different liquid sonicating media in a low hydrostatic pressure condition are described in this Chapter. Three types of sonicating media such as water, liquid hydrocarbons (pentane and heptane) and methanol have been used. These liquids act as media for cavitation and provide hydrogen during the sonolysis.

The experiment on sonochemical reduction of CO_2 to CO in a water medium has confirmed the previous results that CO_2 can be reduced to CO. Also, it is shown that a mole fraction of CO_2 in atmospheric gas and intensity of ultrasound are very significant factors in determining the rate of sonolysis for CO_2. It is also shown that

trace amount of CH_4 can be formed from CO_2 reduction by H_2 only if a significant amount of H_2 is introduced into the reaction system.

The possibility of CO_2 reduction in a hydrocarbon medium is proposed this thesis and experimentally demonstrated for the first time. Furthermore, it has been demostrated that the physical properties of liquid hydrocarbons have major effect on CO_2 reduction. Also, the rates of heptane sonolysis in an aqueous medium were found to be significantly larger than those in a pure heptane medium.

It has also been concluded that methanol is a poor sonicating medium for the CO_2 sonochemical reduction process as it undergoes degradation during the sonolytic process and the total amount of CO evolved (from CO_2 reduction and CH_3OH decomposition) is significantly lower than that during the sonochemical reduction of CO_2 in an aqueous medium. Moreover, DMC is not found as product in ultrasound-assisted synthesis from CH_3OH and CO_2; however, the sonolytic decomposition of CH_3I is observed during this process. More detailed discussion of CO_2 reduction during its sonolysis in various sonication media at low hydrostatic pressure is presented in Chapter 5.

Chapter 5. Discussion of Experimental Results of Sonochemical Reduction of Carbon Dioxide in Various Media under Low Hydrostatic Pressure

5.1. Introduction

This chapter is devoted to discussion of the results obtained from experiments carried out on sonochemical reduction of CO_2 in various sonicating media under different experimental conditions presented in Chapter 4. The experimental work has revealed that CO_2 can chemically be utilized by sonication in liquid medium. Experimental conditions of sonolysis (for example, a composition of an atmospheric gas, temperature, intensity of ultrasound) as well as the physical properties of sonicating media play a significant role in determinating the rates of CO_2 reduction. It has also been observed that the sonochemical reduction of CO_2 is always accompanied by the formation of other products due to the sonolytic decomposition of sonicating media.

5.2. Sonochemical Reduction of Carbon Dioxide in Aqueous medium

5.2.1. Effect of Carbon Dioxide Concentration in an Atmospheric Gas on the Rates of Carbon Dioxide Reduction

The experiments carried out on the sonochemical reduction of CO_2 reveal that among the sonicating media studied, water sonicating medium gives the best rates of CO_2 sonoreduction. CO was one of products of sonochemical reduction of CO_2 according to the reaction (Reaction 5.1). The presence of formic acid (CH_3O) was not detected and, hence, its presence was not further analysed due to its very low ratio in comparison to the CO formation ratio (Henglein 1985).

$$CO_2 \xrightarrow{Ultrasound} CO + O^{\cdot} \qquad [R.\ 5.1]$$

Different responses between the concentrations of generated CO and experimental conditions are found. For instance, the effect of the CO_2 concentration in the atmospheric gases mixture on the rate of CO formation was observed (Chapter 4, Section 4.4.1.1). It was also observed that the CO_2 percentage in the gaseous atmosphere is affected the rate of water sonolysis. Figures 5.1 and 5.2 depict the effect of CO_2 concentration in the atmospheric gas on rates of formation of CO and H_2 during sonolysis. The yields of CO and H_2 are measured as μmol per litre

(µmol/l) of a gaseous sample. According to Henglein (1985) it can be assumed that the CO formation depends on the rate of CO_2 reduction during sonolysis, whereas the H_2 yield depends on the rate of water decomposition. It can be seen from Figures 5.1 and 5.2 that yields of both CO and H_2 decrease with increasing amount of CO_2 presence in the atmospheric gas. The sonolysis of CO_2 does not occur when the concentration of CO_2 exceeds over 50 mol%, but traces of H_2 are still found when the atmospheric gas contains 75 mol% fraction of CO_2.

Another product of CO_2 sonochemical fixation is CH_4; however, as it is described in Chapter 4, its formation crucially depends on the amount of H_2 in the reaction system. The formation of CH_4 is proposed to proceed according to the following reactions:

$$CO_2 + 4H_2 \rightarrow CH_4 + 2H_2O \qquad \text{[R. 5.2]}$$

$$CO_2 + 6H^{\cdot} \rightarrow CH_4 + 2\,OH^{\cdot} \qquad \text{[R. 5.3]}$$

Raney Ni and Raney Ni- Ru/C catalytic systems are applied in order to initiate CO_2 sonochemical reduction into CH_4. These catalytic systems are introduced to enhance H_2 formation which is an essential compound for the CH_4 formation. The investigation shows that neither the chosen catalysts nor generation of additional amount of H_2 during sonolysis lead to the formation of CH_4.

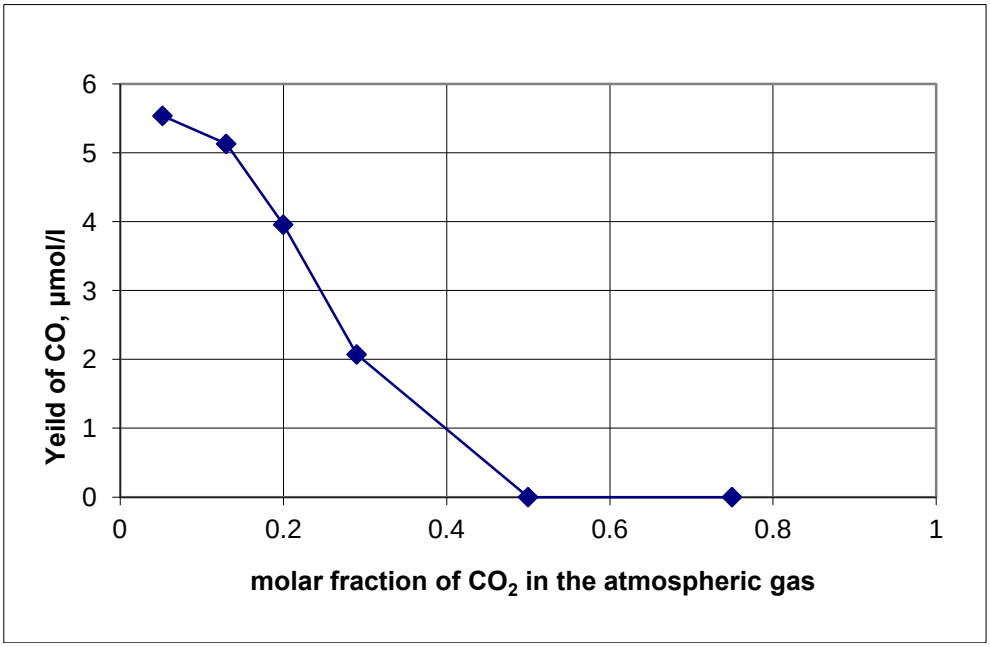

Figure 5.1. Rates of CO formation in sonolysis of water under various Ar/CO_2 atmospheres at 287.15 K and 0.2 MPa

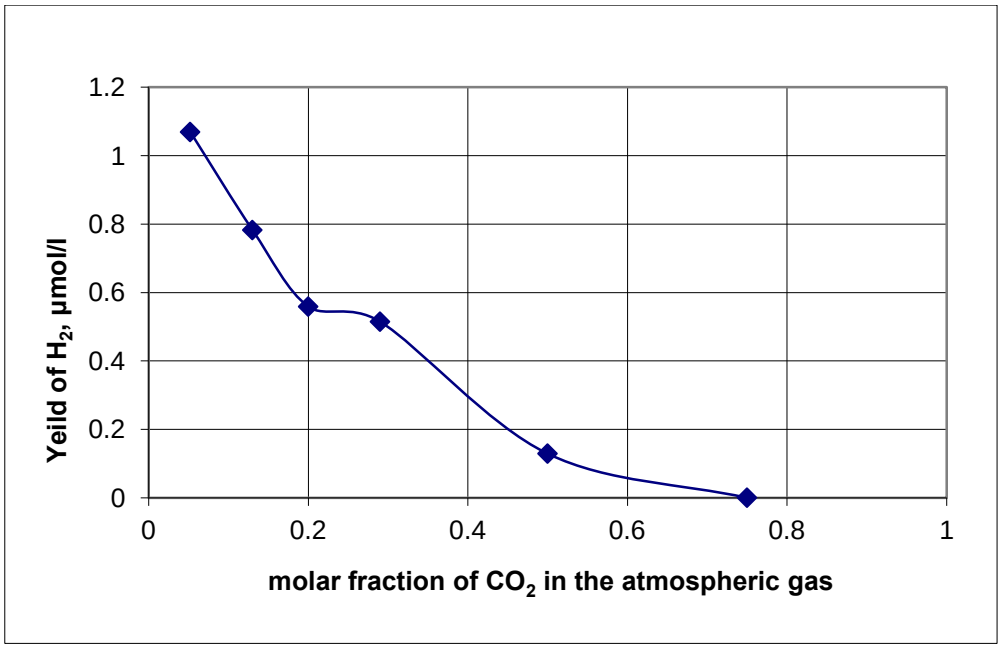

Figure 5.2. Rates of H_2 formation in sonolysis of water under various Ar/CO_2 atmospheres at 287.15 K and 0.2 MPa

However, the rates of CO produced during the catalytic sonochemical reduction of CO_2 are not significantly different from the rates of CO formation during usual sonolysis of CO_2 in an aqueous medium. It has been observed that the introduction of a significant amount of H_2 (7 mol%) into atmospheric gas lead to the formation of trace amounts of CH_4 (Chapter 4, Section 4.4.2.4). Also, it is worth noticing that the amount of CO formed in sonolysis under an Ar/CO_2/H_2 atmosphere (Chapter 4, Section 4.4.2.4) is lower than that in sonolysis under an Ar/CO_2 atmosphere at similar experimental conditions (Chapter 4, Section 4.4.1.1).

5.2.2. Effect of Ultrasonic Intensity on the Rates of Carbon Dioxide Reduction

The effect of ultrasonic intensity on efficiency of sonochemical reduction of CO_2 is also investigated (Chapter 4, Section 4.4.1.2). Sonolysis of water under Ar/CO_2 atmospheres containing 29-30% of CO_2 is investigated at ultrasound intensity of approximately 40, 60 and 95 W/cm^2 (275, 410 and 650 W/l) and at constant hydrostatic pressure of 0.2 MPa. The highest ultrasonic intensity corresponds to maximal intensity of ultrasound which could be produced by our ultrasonic equipment. It is worth noticing that it is generally known that higher numbers of cavitation bubbles are generated at higher ultrasonic intensities, so larger yields of products during sonolysis should be expected (Margulis 1984). However, such a relation is only true up to some point of intensity increase depending on many factors

such as characteristics of liquid medium, atmospheric gases and ultrasonic equipment. So a rise in ultrasonic intensity can also lead to opposite effects, that is, to a reduction in rates of sonolytic products. It is known that an increase in intensity of ultrasound leads to larger acoustic pressure amplitude (Mason and Lorimer 2002). Consequently, at some point of ultrasound intensity increase, the cavitation bubble may grow so large from its initial size during a rarefaction cycle that the time which is left for collapse is not enough. Other authors suggest that the high density of cavitation bubbles near the irradiating surface formed at intensity rise could prevent ultrasonic waves from transmission further into a liquid medium (Suslick 1988). Figure 5.3 presents the dependence of the rates of CO and H_2 formation on the ultrasound intensity. It can be seen from Figure 5.3 that when sonolysis is carried out at intensity of 40 W/cm^2 (240 W/l) there are no products detected except for traces of H_2. However, H_2 and CO are found in gaseous atmospheres after sonolysis is performed at higher ultrasound intensities (60 and 95 W/cm^2 (410 and 650 W/l)) at the other similar experimental condition. Moreover, the rates of products rise with increasing intensity of applied ultrasound. Thus, it can be concluded that no negative effects of ultrasonic intensity increase is demonstrated in this work. Furthermore, the absence of CO in experiments carried out at 40 W/cm^2 could be explained by insufficiently high amplitude of applied ultrasound and, consequently, suppression of cavity formation at such experimental conditions.

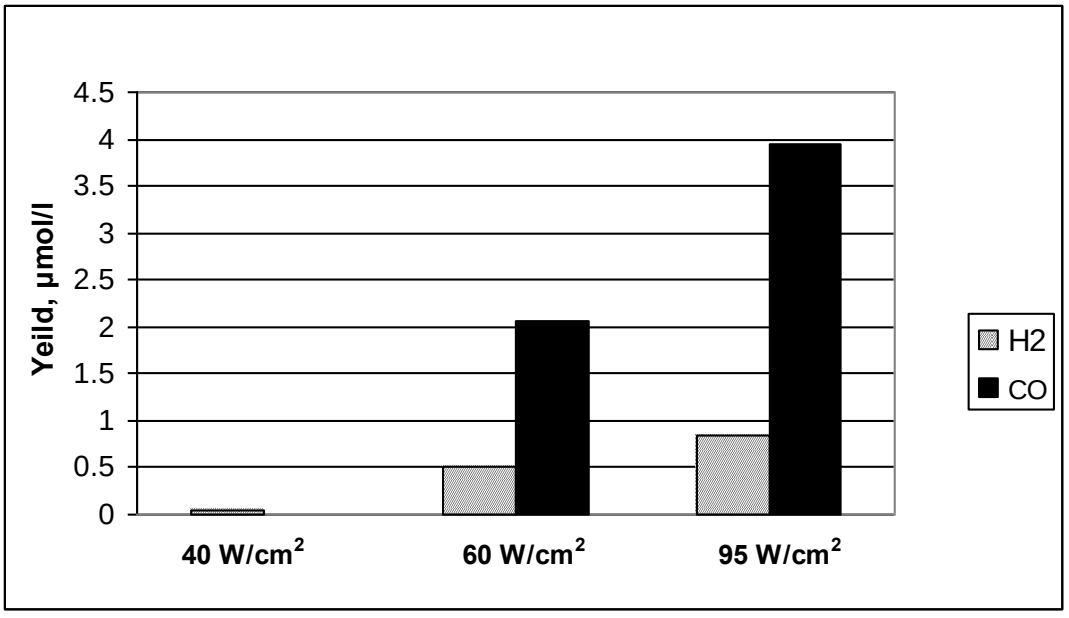

Figure 5.3. Rates of CO and H_2 formation in sonolysis of water under Ar/CO_2 atmospheres containing 0.29-0.3 mole fraction of CO_2 at various ultrasound intensities

In order to estimate the influence of ultrasonic intensity increase on the rate of CO_2 sonolysis, the yields of products (H_2 and CO_2) of CO_2 sonochemical reduction in a water medium at 60 and 95 W/cm^2 (410 and 650 W/l) was studied. So approximately 0.23 kilowatt of energy an hour was used in order to carry out the test on the sonochemical reduction of CO_2 at 60 W/cm^2 (410 W/l). On the other hand, 0.36 kilowatt of energy an hour was utilized for the CO_2 sonolysis at 95 W/cm^2 (650 W/l). Due to the low rates of CO_2 reduction in both experiments, it can be stated that changes in CO_2 concentration in the atmospheric are insignificant in time. Thus it can be assumed that 10.97 μmol/l ($\frac{1}{0.36} * 3.95$) of CO is produced when 1 kWh of electrical energy used at the intensity of 95 W/cm^2 (650 W/l), whereas the amount of CO in case of the intensity value of 60 W/cm^2 (410 W/l) is approximately 9 μmol/l ($\frac{1}{0.23} * 2.07$). From this estimation, it is seen that the approximate increase of 58% in the intensity of ultrasound led to the rise of approximately 22% in the amount of produced CO when the same amount of electrical energy is consumed during sonication. Thus, the higher rate of the produced CO can be explained by the larger amount of cavitational bubbles (reaction sites) generated during sonolysis at the higher intensity. However, the larger amount of the generated cavitational bubbles at high ultrasonic intensities leads to the so-called “cushioning” effect of the bubble collapse. Moreover, due to the higher intensity of ultrasound, a larger amount of electrical energy is converted to heat during the process, and therefore additional power is required in order to maintain the experimental temperature in a desired range (more powerful cooling system).

Assuming the same conditions as for CO formation, it was found that 2.33 μmol/l ($\frac{1}{0.36} * 0.84$) and 2.43 μmol/l ($\frac{1}{0.23} * 0.56$) of H_2 are produced per 1 kWh of electrical energy at the intensities of 95 and 60 W/cm^2 (410 and 650 W/l), correspondingly. So the increase of the H_2 formation is not observed with an increase of the ultrasonic intensity.

Furthermore, it was also demonstrated experimentally that a high temperature of sonolysis in unfavourable for the CO_2 reduction (see Chapter 4, section 4.4.2.2.). This can be explained by the following changes in the physics of cavitational collapse. The high value of the vapour pressure due to the elevated temperature of the process implies the presence of a large amount of water vapour (γ = 1.334) in the cavitational bubble resulting in decreases in temperatures and pressures formed

during the cavitational collapse, so the generated conditions are not great enough for a cleavage of the strong C=O bond (average energy for the C=O bond is 799 kJ/mol (Reger, Goode, and Ball 2010)). Also, the significant decrease in the sonochemical yield in the sonolysis of CO_2 at high temperature can be preconditioned as a result of the bubble collapse "cushioning" effect due to the much larger amount of generated cavities, as long as the formation of cavities are favourable due to lower values of viscosity, surface tension at the elevated experimental temperature.

5.3. Sonochemical Reduction of Carbon Dioxide in Hydrocarbon Medium

During this research, it was shown that the rates of CO_2 reduction in heptane (C_7H_{16}) are lower than the rates when a water medium is used. Taking into account the fact that the concentration of CO_2 in the atmospheric gas changed insignificantly during the experiment (see Chapter 4, section 4.4.3.2c), it can be assumed the rate of CO generation during sonolysis is approximately 0.78 μmol/l per hour when ultrasound of 60 W/cm^2 (410 W/l) intensity is applied. Then, this value is in approximately 7 times lower than the rate of CO generation during the CO_2 sonolysis in an aqueous medium at almost the same experimental conditions (see Figure 5.1). During the investigation, it is shown that the sonolysis of CO_2 in C_5H_{12} is not possible at studied conditions and available equipment (see Section 5.4). Also, it is found that the sonolytic decomposition of C_5H_{12} does not occur in the range of investigated conditions.

On the other hand, it was found that decomposition rates of liquid hydrocarbons are much higher when small amounts of hydrocarbons are present in the reacting system during sonolysis (Chapter 4, Section 4.4.3.3). Such obtained data coincide with results on sonolysis of light hydrocarbons (C_1-C_2) found in the literature (Hart, Fischer, and Henglein 1990). These authors found that water sonolysis using pure hydrocarbon atmospheric gases gave much lower rates of products formation.

Here a conclusion can be made that the presence of large concentrations of hydrocarbons, not only in the atmospheric gas, but as a sonicating medium in the reacting system lowers temperatures and pressures which are generated during the collapse and, consequently the rates of degradation.

Also, based on the obtained results in the sonolysis of C_7H_{16} (Chapter 4, Section 4.4.3.3) the mechanism of C_7H_{16} decomposition by means of ultrasound is

thoroughly discussed in this section. Moreover, in view of the absence of information about earlier works devoted to the sonolysis of C_7H_{16}, the products of the sonolysis of C_7H_{16} obtained in this study are compared to those which are produced during the pyrolysis of the hydrocarbon (Table 5.1).

It can be seen from the data in Table 5.1 that qualitative and quantitative characteristics of the products obtained from the sonolysis of C_7H_{16} during this research are in good agreement with the products of pyrolysis of C_7H_{16} found in the literature. Moreover, the theoretical distribution of products for C_7H_{16} pyrolysis according to the Rice-Kossiakoff radical mechanism is acceptable when compared with the distribution of the products obtained during our research. Based on these facts, it can be proposed that the Rice-Kossiakoff theory, along with results on the selectivity products from various studies devoted to the C_7H_{16} pyrolysis and the information on sonolysis of alkanes different from C_7H_{16}, can be used in an attempt to describe the mechanism of the sonolysis of C_7H_{16}.

The mechanism of C_7H_{16} sonolysis starts from the formation of high-reactivity particles (radicals) by means of ultrasound energy. As is postulated by Suslick et al. (1983), the primary step of sonolysis of alkanes is random cleavage of a C-C bond and formation of radicals. So, in the case of C_7H_{16} the reaction of the first step of sonolysis would be (Reactions 5.4-5.6):

$$CH_3CH_2CH_2CH_2CH_2CH_2CH_3 \rightarrow CH_3^{\cdot} + CH_3CH_2CH_2CH_2CH_2CH_2^{\cdot} \quad \text{[R. 5.4]}$$

$$CH_3CH_2CH_2CH_2CH_2CH_2CH_3 \rightarrow CH_3CH_2^{\cdot} + CH_3CH_2CH_2CH_2CH_2^{\cdot} \quad \text{[R. 5.5]}$$

$$CH_3CH_2CH_2CH_2CH_2CH_2CH_3 \rightarrow CH_3CH_2CH_2^{\cdot} + CH_3CH_2CH_2CH_2^{\cdot} \quad \text{[R. 5.6]}$$

However, according to Rice and Kossiakoff, radicals larger than ethyl ($C_2H_5^{\cdot}$) are very unstable and are likely to decompose before interacting with another molecule (Billaud and Freund 1986) (Reactions 5.7-5.10). Furthermore, the high amount of produced C_2H_4 can be explained by a $C_2H_5^{\cdot}$ radical"s break-up which is also responsible for the formation of $H^{\cdot}$ radicals (Reaction 7.11).

$$CH_3CH_2CH_2CH_2CH_2CH_2^{\cdot} \rightarrow 2\,C_2H_4 + C_2H_5^{\cdot} \quad \text{[R. 5.7]}$$

$$CH_3CH_2CH_2CH_2CH_2^{\cdot} \rightarrow 2\,C_2H_4 + CH_3^{\cdot} \quad \text{[R. 5.8]}$$

$$CH_3CH_2CH_2CH_2^{\cdot} \rightarrow C_2H_4 + C_2H_5^{\cdot} \quad \text{[R. 5.9]}$$

$$CH_3CH_2CH_2^{\cdot} \rightarrow C_2H_4 + CH_3^{\cdot} \quad \text{[R. 5.10]}$$

$$C_2H_5^{\cdot} \rightarrow C_2H_4 + H^{\cdot} \quad \text{[R. 5.11]}$$

Table 5.1. Comparison of the selectivity of products obtained in sonochemical degradation of heptane with the selectivity of the products from pyrolysis of heptane taken from different studies

source of data		Rice-Kossiakoff theory (1942)	Bujus and Vesely (1979)	Aribike and Susu (1988)	Chakraborty and Kunzru (2009)	Chakraborty and Kunzru (2009)	Chakraborty and Kunzru (2009)	Pant and Kunzru (1996)	This research
experimental conditions	Temp., K	-	973.15	973.15	903.15	833.15	793.15	973.15	-
	Pressure, MPa	-	0.1	0.1	0.1	0.79	2.93	0.1	-
Products yields, %	H_2	0	17.07	16.50	6.47	1.86	1.27	*n/m**	17.49
	CH_4	18.42	18.90	5.48	15.33	14.87	11.46	9.61	14.66
	C_2H_4	39.48	38.94	42.50	32.03	24.16	15.71	48.37	38.14
	C_2H_6	15.79	2.83	1.06	9.54	16.91	17.41	3.09	5.65
	C_3H_6	10.52	10.81	16.83	17.72	17.84	18.68	26.24	15.50
	C_3H_8	0	0.42	0	0.85	2.60	7.64	0.51	0.40
	C_4H_8	5.26	5.72	7.60	8.86	11.15	13.59	6.86	5.51
	C_4H_6	0	0.73	5.73	2.73	1.86	0.85	2.40	1.17
	C_4H_{10}	0	0.11	0	1.02	2.23	6.16	0	0
	C_5H_{10}	5.26	2.85	3.06	4.09	4.83	5.10	2.23	1.20
	C_5H_{12}	0	0.06	0	0	0	0	0	0
	C_6H_{12}	5.26	1.56	1.25	1.36	1.67	2.12	0.69	0.28

**n/m – not measured*

Then, based on Rice-Kossiakoff theory, the first reaction of the radical mechanism for C_7H_{16} is a random removal of a primary or secondary hydrogen atom from an alkane by a radical, generated in the primary step of sonolysis, and a formation of new radicals. The first chain reaction for C_7H_{16} would be (Reactions 5.12-5.15):

$$C_7H_{16} + R^{\cdot} \rightarrow CH_3CH_2CH_2CH_2CH_2CH_2CH_2^{\cdot} + RH \quad \text{[R. 5.12]}$$

$$C_7H_{16} + R^{\cdot} \rightarrow CH_3CH_2CH_2CH_2CH_2CH^{\cdot}CH_3 + RH \quad \text{[R. 5.13]}$$

$$C_7H_{16} + R^{\cdot} \rightarrow CH_3CH_2CH_2CH_2CH^{\cdot}CH_2CH_3 + RH \quad \text{[R. 5.14]}$$

$$C_7H_{16} + R^{\cdot} \rightarrow CH_3CH_2CH_2CH^{\cdot}CH_2CH_2CH_3 + RH \quad \text{[R. 5.15]}$$

where R is $CH_3^{\cdot}$, $C_2H_5^{\cdot}$ or $H^{\cdot}$; RH is CH_4, C_2H_6 or H_2

According to the radical mechanism, the products of cracking $C_7H_{15}^{\cdot}$ radicals depend on whether a primary or secondary H atom is removed from C_7H_{16}. In the case where it is the primary H atom, the $C_7H_{15}^{\cdot}$ radical will decompose into C_2H_4 and a $CH_3^{\cdot}$ radical (Reaction 5.16), whereas if the removed H atom is a secondary, the $C_7H_{15}^{\cdot}$ radical will degrade mainly to 1-alkene, C_2H_4 and the corresponding radical ($CH_3^{\cdot}$ or $C_2H_5^{\cdot}$) (Reactions 5.17-5.19). Both reactions 5.18a and 5.18b are predicted to occur, but it is shown that the decomposition via the propyl radical ($C_3H_7^{\cdot}$) goes four times faster than the decomposition to 1-hexane and a $CH_3^{\cdot}$ radical (Bajus et al. 1979).

$$CH_3(CH_2)_5CH_2^{\cdot} \rightarrow 3\,C_2H_4 + CH_3^{\cdot} \quad \text{[R. 5.16]}$$

$$CH_3(CH_2)4CH^{\cdot}CH_3 \rightarrow C_3H_6 + C_2H_4 + C_2H_5^{\cdot} \quad \text{[R. 5.17]}$$

$$CH_3(CH_2)3CH^{\cdot}CH_2CH_3 \rightarrow C_6H_{12} + CH_3^{\cdot} \quad \text{[R. 5.18a]}$$

$$\rightarrow C_3H_7^{\cdot}(CH_3^{\cdot} + C_2H_4) + C_4H_8 \quad \text{[R. 5.18b]}$$

$$CH_3(CH_2)_2CH^{\cdot}(CH_2)2CH_3 \rightarrow C_5H_{10} + C_2H_5^{\cdot} \quad \text{[R. 5.19]}$$

The presence of C_2H_6 in products can be explained by the reactions (Reactions 5.20 and 5.21) of $C_2H_5^{\cdot}$ radicals with H_2 or C_7H_{16} (Bajus et al. 1979).

$$C_7H_{16} + C_2H_5^{\cdot} \rightarrow C_2H_6 + C_7H_{15}^{\cdot} \quad \text{[R. 5.20]}$$

$$C_2H_5^{\cdot} + H_2 \rightarrow C_2H_6 + H^{\cdot} \quad \text{[R. 5.21]}$$

As long as higher alkenes are less stable, the decomposition of 1-C_6H_{12} through an allylic radical can explain the formation of 1,3-butadiene (1,3-C_4H_6) (Reactions 5.22 and 5.23).

$$C_6H_{12} + R^{\cdot} \rightarrow CH_2 = CHCH^{\cdot}CH_2CH_2CH_3^{\cdot} + RH \quad \text{[R. 5.22]}$$

$$CH_2 = CHCH^{\cdot}CH_2CH_2CH_3^{\cdot} \rightarrow CH_2 = CHCH = CH_2 + C_2H_5^{\cdot} \quad \text{[R. 5.23]}$$

where R is $CH_3^{\cdot}$, $C_2H_5^{\cdot}$ *or* $H^{\cdot}$; *RH is* CH_4, C_2H_6 *or* H_2

Furthermore, high concentrations of C_2H_4 and C_3H_6 can be caused not only by primary cracking of C_7H_{16} but also by the further cracking of formed 1-alkenes such as 1-butene, 1-pentene and 1-hexene (Kossiakoff and Rice 1943).

As long as there are no articles on sono-decomposition of C_7H_{16} found from the literature, the products of C_7H_{16} sonolysis obtained in this work will be analysed in terms of the products of sonolysis of other alkanes such as decane ($C_{10}H_{22}$) data on which is found from literature (Suslick et al. 1983; Mizukoshi et al. 1999). So as the selectivity of C_1-C_6 products of $C_{10}H_{22}$ sonolysis is 97.5 % from experimental work performed by Suslick et al. (1983) and 98.6 % from the investigation made by Mizukoshi et al. (1999), it is decided to use this data on $C_{10}H_{22}$ sonolysis in order to compare the distribution of products obtained in this work (Table 5.2).

It can be noticed from Table 5.2 that the absence of acetylene (C_2H_2) in the products of C_7H_{16} sonolysis is the main difference between this work's results and the results on the sonolysis of $C_{10}H_{22}$. An explanation of this fact can be the experimental conditions such as temperature and pressure generated during the cavitation collapse of micro-bubbles. As it is shown in some studies on pyrolysis of hydrocarbons (Murphy, Carroll and Klonowski 1997; Lifshitz and Frenklach 1975; Friedmann, Bovee and Miller 1970), the formation of C_2H_2 as a result of further C_2H_4 decomposition (Reaction 5.24) starts at temperatures about 1300 K, whereas no C_2H_2 can be formed at temperatures lower than 1200 K.

$$C_2H_4 \rightarrow C_2H_2 + H_2 \quad \text{[R. 5.24]}$$

So it can be suggested that the absence of C_2H_2 in products obtained in our research indicates that the temperature generated inside the cavitational bubble during the collapse in the C_7H_{16} sonolysis did not exceed 1300 K.

Table 5.2. Analysis of products of hydrocarbons sonolysis

Source of data		Suslick et al. 1983 ($C_{10}H_{22}$)	Mizukoshi et al. 1999 ($C_{10}H_{22}$)	This work (C_7H_{16})
Selectivity of products, %	H_2	44.92	29.92	17.49
	CH_4	9.77	5.50	14.66
	C_2H_2	7.25	12.51	0
	C_2H_4	9.63	37.97	38.14
	C_2H_6	1.28	2.69	5.65
	C_3H_4	0.61	0	0
	C_3H_6	8.29	3.95	15.50
	C_3H_8	0.89	0.86	0.40
	C_4H_8	5.25	1.18	5.51
	C_4H_{10}	1.31	0.75	0
	C_4H_6	0	0	1.17
	C_5H_{10}	3.77	1.51	1.20
	C_5H_{12}	0.59	0.38	0
	C_6H_{12}	1.90	0.77	0.28
	C_6H_{14}	0.78	0.28	0
	C_7H_{14}	1.23	0.38	0
	C_7H_{16}	0.45	0.23	0
	C_8H_{16}	1.17	0.58	0
	C_8H_{18}	0.25	0.17	0
	C_9H_{18}	0.59	0.28	0
	C_9H_{20}	0.08	0.09	0

It is worth noting that selectivities of products of the $C_{10}H_{22}$ sonolysis from two different studies differ (Table 5.2) significantly from each other. So a conclusion can be made that the conditions of experimental work (temperatures and pressures) along with such parameters as the design of the experimental setup (distribution of ultrasound), ultrasonic equipment and composition of reagents have a great influence, not only on rates of sonochemical reactions, but also on the selectivity of products generated during sonolysis. That is why it is so difficult to reproduce the results of sonochemical experiments knowing only the temperature and pressure conditions of a test.

5.4. Sonochemical Conversion of Carbon Dioxide into Usable Compounds in Methanol Medium

5.4.1. Sonochemical Reduction of Carbon Dioxide in Methanol Medium

Sonolysis of CO_2 in a methanol medium was performed (Chapter 4, Section 4.4.4.1-4.4.4.3). However, it is shown that the rates of CO formation are lower than those when the sonolysis of CO_2 in a water medium is investigated. Furthermore, it is also assumed that a part of CO can be formed during sonolysis of methanol (Reactions 5.25 and 5.26) generated during CH_3OH sonolysis. Moreover, (H_2) obtained during experimental work proves that sonolysis of CH_3OH takes place (Chapter 4, Section 4.4.4.1).

$$CH_2O + M \rightarrow H^{\cdot} + HCO^{\cdot} + M \quad \text{[R. 5.25]}$$

$$HCO^{\cdot} + M \rightarrow CO + H^{\cdot} + M \quad \text{[R. 5.26]}$$

Also, during the CO_2 sonolysis in methanol, CH_4 is one of the detected components. According to information found from literature (Buttner, Gutierrez, and Henglein 1991) it was assumed that the generated CH_4 was the product of CH_3OH decomposition under ultrasonic waves by the sequence of chemical reactions (Reactions 5.27 and 5.28):

$$CH_3OH \rightarrow CH_3^{\cdot} + {}^{\cdot}OH \quad \text{[R. 5.27]}$$

$$CH_3^{\cdot} + CH_3OH \rightarrow CH_4 + CH_2OH^{\cdot} \quad \text{[R. 5.28]}$$

Also, it is thought that CH_4 formation from the reaction of CO_2 reduction by H_2 at such small amount of evaluated H_2 (Chapter 4, Section 4.4.4.1) cannot be considered as a mechanism (see Section 5.1.1).

Furthermore, it was found that neither CO nor CH_4 are formed at high temperature sonolysis of methanol under an Ar/CO_2 atmosphere (Chapter 4, Section 4.4.4.3). It can be explained by the fact that large amounts of CO_2 and methanol vapour are trapped into cavitation bubbles due to the high temperature of sonolysis. Thus, temperatures and pressure which are generated during the collapse of cavitation bubbles appears to be not as great as those at low temperature sonolysis, so the sonochemical reactions of CO_2 reduction are unlikely to occur. Moreover, the absence of CH_4 as well as H_2 in products proves that sonolysis of CH_3OH is also impossible at such experimental conditions. However, it was shown that the addition

of the Raney Ni catalyst to the reaction mixture at high temperature sonolysis in CH_3OH leads to the formation of CH_4 due to the decomposition of CH_3OH adsorbed on the surface of the catalyst (Chapter 4, Section 4.4.4.2).

5.4.2. Mechanism of Methyl Iodide Degradation in Ultrasound-Assisted Synthesis of Dimethyl Carbonate

Experimental investigation of ultrasound-assisted synthesis of dimethyl carbonate (DMC) from CH_3OH and CO_2 was carried out at 288 K. Methyl iodide was used as $CH_3^{\cdot}$ radicals" provider in the synthesis. DMC is not found to be produced by the proposed method. However, it is shown from experimental work (Chapter 4, Section 4.4.4.4) that the process of CH_3I degradation is responsible for the formation of such products as CH_4, C_2H_6, C_2H_5I and C_2H_2I during ultrasonic-assisted synthesis of DMC from CH_3OH and CO_2. Moreover, according to the experiments on sonolysis of CO_2 in CH_3OH medium, it is thought that small amounts of the produced CH_4 are formed due to CH_3OH decomposition; however, it is found that CH_3OH decomposition is not responsible for the formation of C_2H_6 under proposed experimental conditions (Chapter 4, Sections 4.4.4.1).

It is known that CH_3I is a very unstable compound undergoing decomposition when subjected to the light and possess the relatively low value of C-I bond energy (53.8 kcal/mol; Carson, Carter, and Pedley, 1961). Thus, the experimental conditions of the test (Chapter 4, Section 4.4.4.4) provide sufficient energy for the fission of the C-I bond which is the primary step of the CH_3I degradation.

Next, the mechanism of decomposition of CH_3I in a methanol medium during ultrasound-assisted synthesis of DMC is discussed in detail.

Literature on pyrolysis (Butler and Polanyi 1943; Saito et al. 1980; Kumaran et al. 1996) and flash photolysis (Meyer 1968; Perry et al. 2007) of CH_3I are taken into account while describing the mechanism of decomposition of CH_3I.

Initially, the reaction of C – I bond fission (Reaction 5.29), when primary radicals ($CH_3^{\cdot}$ and $I^{\cdot}$) are formed, takes place during the cavitational collapse. Also, the formation of $CH_3^{\cdot}$ radicals is enhanced due to the primary reaction of sonolysis of methanol (Reaction 5.27) which was used as sonicating medium in the experiment. Moreover, C_2H_5I and C_2H_2I generated in the process can also undergo a primary decomposition (Reactions 5.30 and 5.31).

$$CH_3I + Ar \rightarrow CH_3^{\cdot} + I^{\cdot} + Ar \qquad \text{[R. 5.29]}$$

$$C_2H_5I + Ar \rightarrow C_2H_5^{\cdot} + I^{\cdot} + Ar \quad \text{[R. 5.30]}$$

$$CH_2I_2 + Ar \rightarrow CH_2I^{\cdot} + I^{\cdot} + Ar \quad \text{[R. 5.31]}$$

In the next stage of the CH_3I degradation mechanism, various products are formed due to reactions of radicals‟ propagation along with radicals‟ termination reactions. It is assumed that molecular iodine (I_2) is mainly formed through the reaction of the recombination of $I^{\cdot}$ radicals (Reactions 5.32 and 5.33) (Souffie, Williams Jr., and Hamill 1956; Davidson and Carrington 1952). No specific analysis in order to detect molecular iodine was performed. However, it is worth noticing that the liquid medium after the experiment does not possess a specific colour, which is indicative of an iodine solution. It can be explained by the low concentration of I_2 in the liquid medium (not sufficiently high to produce a visible prove of the presence of I_2) (Reaction 5.53). It is also assumed that the reverse formation of CH_3I could occur when $CH_3^{\cdot}$ radicals interact with formed I_2 or $I^{\cdot}$ radicals (Reactions 5.34 and 7.35).

$$I^{\cdot} + M \rightarrow IM^{\cdot} \quad \text{[R. 5.32]}$$

$$IM^{\cdot} + I^{\cdot} \rightarrow I_2 + M \quad \text{[R. 5.33]}$$

where M – is a collision partner

$$CH_3^{\cdot} + I_2 \rightarrow CH_3I + I^{\cdot} \quad \text{[R. 5.34]}$$

$$CH_3^{\cdot} + I^{\cdot} \rightarrow CH_3I \quad \text{[R. 5.35]}$$

The generation of $CH_2I^{\cdot}$ radical, which is a very important link in this mechanism of CH_3I degradation, is assumed to occurs due to the reaction of $CH_3^{\cdot}$ radicals with CH_3I (Reaction 5.36). As can be seen, this reaction is one of the routes of CH_4 formation. CH_4 also can be formed principally from the interaction between $CH_3^{\cdot}$ and H_2 or $H^{\cdot}$ radicals (Reactions 5.37 and 5.38) (Perry et al. 2007). Moreover, the formation of CH_4 is accelerated by Reaction 5.28 where generated $CH_3^{\cdot}$ radicals form CH_4 by reacting with CH_3OH. Furthermore, the formation of C_2H_6 is another possible way of recombination of $CH_3^{\cdot}$ radicals and CH_3I (Reactions 5.39 and 5.40).

$$CH_3^{\cdot} + CH_3I \rightarrow CH_4 + CH_2I^{\cdot} \quad \text{[R. 5.36]}$$

$$CH_3^{\cdot} + H_2 \rightarrow CH_4 + H^{\cdot} \quad \text{[R. 5.37]}$$

$$CH_3^{\cdot} + H^{\cdot} \rightarrow CH_4 \quad \text{[R. 5.38]}$$

$$CH_3^{\cdot} + CH_3I \rightarrow C_2H_6 + I^{\cdot} \quad \text{[R. 5.39]}$$

$$CH_3^{\cdot} + CH_3^{\cdot} \rightarrow C_2H_6 \quad \text{[R. 5.40]}$$

The formation of C_2H_5I (Reactions 5.41 and 5.42) and CH_2I_2 (Reactions 5.43 and 5.44) lies primarily through the $CH_2I^{\cdot}$ radical which, as it is already mentioned above, are the essential link in the mechanism of degradation of CH_3I.

$$CH_2I^{\cdot} + CH_3^{\cdot} \rightarrow C_2H_5I \quad \text{[R. 5.41]}$$

$$CH_3I + CH_2I^{\cdot} \rightarrow C_2H_5I + I^{\cdot} \quad \text{[R. 5.42]}$$

$$CH_2I^{\cdot} + I_2 \rightarrow CH_2I_2 + I^{\cdot} \quad \text{[R. 5.43]}$$

$$CH_2I^{\cdot} + I^{\cdot} \rightarrow CH_2I_2 \quad \text{[R. 5.44]}$$

Also, C_2H_5I generation can go through the recombination of $C_2H_5^{\cdot}$ radicals with I_2 or $I^{\cdot}$ radicals (Reactions 5.45 and 5.46).

$$C_2H_5^{\cdot} + I_2 \rightarrow C_2H_5I + I^{\cdot} \quad \text{[R. 5.45]}$$

$$C_2H_5^{\cdot} + I^{\cdot} \rightarrow C_2H_5I \quad \text{[R. 5.46]}$$

The presence of H_2 and $I^{\cdot}$ radicals in the reacting system can lead to the formation of HI (Reaction 5.47).

$$H_2 + I_2 \rightarrow 2\,HI \quad \text{[R. 5.47]}$$

On the other hand, KOH used as a catalyst in the process also reacts with HI producing potassium iodide (KI) which is soluble in CH_3OH (Reaction 5.48).

$$HI + KOH \rightarrow KI + H_2O \quad \text{[R. 5.48]}$$

The presence of KOH and CH_3OH in the system tends to explain the absence of the brownish colour, which is specific for the iodine methanol solution. So in the presence of a strong base such as potassium hydroxide (KOH), the reaction between I_2 and KOH occurs (Reaction 5.49). Eventually the solution does not contain the sufficient concentration of I_2 in order to indicate the presence of molecular iodine by eye.

$$3\,I_2 + 6\,KOH \rightarrow 3\,H_2O + 5\,KI + KIO_3 \quad \text{[R. 5.49]}$$

It can be seen from Reaction 5.49 that I_2 is converted into potassium iodide (KI) and potassium iodate (KIO_3). However, no precipitation of these salts of potassium is observed in the final reaction mixture, as long as KI is fairly soluble in methanol (about 1 gram in 8 cm^3) and KIO_3 is soluble in a KI solution.

Overall, it can be concluded that the products of CH_3I degradation obtained in ultrasound-assisted synthesis of DMC is quite similar to those at photolysis or electron-stimulated decomposition of CH_3I. The formation of H_2 during CH_3I degradation, which is the main distinctive feature, is explained by the sonolytic decomposition of a liquid medium (CH_3OH).

5.5. Analysis of Relation between the Physical Properties of Sonicating Media and Rates of CO_2 Reduction.

From the results obtained on sonochemical utilization of CO_2, it is shown that the best rates of CO_2 reduction are obtained when water is used as a sonicating medium. Moreover, lower CO_2 concentrations in the atmospheric gas and, consequently, in a liquid phase during the sonication process lead to higher ratios of sonochemical reactions.

In order to understand the difference in the results on sonochemical reduction of CO_2 in different sonicating media, the physical parameters of reagents used in the study have to be considered. The first physical parameter is to be considered is solubility of CO_2 in the liquid media. Table 5.3 presents data on the maximal solubility of CO_2 in CH_3OH, H_2O, C_5H_{12} and C_7H_{16} calculated by means of the HYSYS computer software. It can be seen from the tables that CO_2 is less soluble in H_2O than in other solvents.

Moreover, the physical properties of liquid solvents such as the vapour pressure and ratio of specific heats are also presented in Table 5.3. It can be noticed that H_2O and C_7H_{16} media have relatively low vapour pressures in comparison to the other liquids, so these liquid vapour pressures provide the lowest effect among all solvents on the decrease of the temperatures and pressure generated during the cavitation collapse.

Table 5.3 contains the data on the ratios of specific heats of atmospheric gases employed in the experimental work as well as the values of the ratio of specific heats for the sonicating media‟s vapour. It is known that atmospheric gases with high ratios of specific heats provide the greatest temperatures and pressures during the cavitation bubble collapse. From the experimental results, it can be seen the same relation is true for the liquid media‟ vapour trapped in the cavitational bubble during collapse. Thus, the liquids with low values of vapour pressure and high ratios of specific heats allow generating greater conditions during the cavitational collapse.

Table 5.3. Physical properties of liquid mediums and atmospheric gases used in sonochemical reduction of CO_2 (based on the HYSYS computer software calculations)

Compound	Physical parameter				
	P_{vapour}, kPa @ 293 K	Solubility of CO_2 @ 293 K and 0.2 MPa, gCO_2/1kg of medium	γ, @ 293 K	Surface tension, mN/m @ 293 K	Viscosity, centipoise @ 293 K
H_2O	2.4	2.61	1.334[1] (vapour)	72.75[3]	1.002
CH_3OH	12.8	24.5	1.256[1] (vapour)	22.70[4]	0.5851
C_5H_{12}	56.8	12.47	1.075[2] (vapour)	16.11[3]	0.2302
C_7H_{16}	5.3	12.6	1.054[2] (vapour)	20.53[3]	0.4134
Ar (gas)	n/a	-	1.674	-	n/a
CO_2 (gas)	n/a	-	1.292	-	n/a
H_2 (gas)	n/a	-	1.38	-	n/a

[1] - Tables of Physical & Chemical Constants, n.d.
[2]- Pohanish (2004)
[3] - Mohsen-Nia, Rasa, and Naghibi (2010)
[4] - Surface tension values of some common test liquids for surface energy analysis http://www.surface-tension.de/

It is known (Chapter 2, Section 2.3.6) that the lower values of the surface tension and viscosity of the liquid, the higher amount of cavities is generated. However, the large amount of formed cavities can lead to the so-called „cushioning effect".

In conclusion, the experimental results show that the best rates of CO_2 sonolysis are obtained when H_2O is used as a sonicating medium. Taking into account the physical parameters of H_2O it can be noted that H_2O has the lowest value of the vapour pressure and the solubility of CO_2 in it, and the largest values of the surface tension, viscosity and ratio of specific heats for its vapour among the considered solvents.

Chapter 6. Sonochemical Reduction of Dense-Phase Carbon Dioxide

6.1. Introduction

Over the years, the sonochemical effects on reaction rates, selectivity, formation of radicals have been studied in various liquids at pressure conditions close to atmospheric (see Chapter 4). This is because the formation of cavities is hindered at elevated pressures and the further increase in the pressure leads to the conditions when cavitation does not occur at all (Berlan and Mason 1992). Recently, the possibility of generating cavitation in dense-phase fluids (which are gases at ambient conditions) was experimentally demonstrated (Kuijpers et al. 2002). Kuijpers and colleagues experimentally showed the occurrence of cavitation in pressurized CO_2. Since then several authors studied the phenomenon of cavitation in dense-phase CO_2. However, most of those studies were not devoted to the CO_2 chemical reduction. Instead they studied the use of supercritical CO_2 as a solvent, extracting agent and medium for sonication. For example, Kemmere et al. (2004) demonstrated the mass-transfer enhancement during ultrasound-induced polymerization and formation of larger yields of high-molecular-weight polymers. Whereas, Balachandran (2006) investigated the influence of ultrasound on the extraction of essences from ginger using supercritical CO_2 both as an extracting agent and medium for sonication. Moreover, it is worth noticing that today the majority of ultrasonic studies using sc-CO_2 are based on the investigation of supercritical fluid extraction (Riera et al., 2004; Enokida et al., 2002; Hu et al., 2007).

The main purpose of the actual experimental work presented in this chapter is to investigate the possibility of performing the sonochemical reduction of liquid CO_2. Sonication of CO_2 in a supercritical state is also studied.

6.2. Theoretical Approach to Experimental Work

As discussed in Chapter 2, Section 2.3.5 an increase in the hydrostatic pressure of a sonicating medium leads theoretically to the more violent collapse of cavities (Chapter 2, Equations 2.12 and 2.13). However, the formation of cavities is suppressed when liquid media are subjected to elevated pressures and in this case higher acoustic pressures are needed to generate cavitation. Moreover, at some point of the hydrostatic pressure increase no cavitation can be formed at all, because the negative pressure (P_a) produced by ultrasonic waves is not large enough to

counteract hydrostatic pressure (P_h) and the surface tension forces in order to initiate the cavitation process (Equation 6.1):

$$P_v + P_g < P_h + 2\,\frac{\sigma}{R_0} - P_a \qquad \text{[Eqn. 6.1]}$$

However, unlike ordinary liquid media, liquefied gases (or dense-phase fluids) allow cavitation to occur at elevated pressures. The formation of cavitation in liquefied CO_2 is experimentally shown by Kuijpers et al. (2002). The cavitation phenomenon becomes possible due to vapour pressure of dense-phase fluids. In other words, liquefied gases possess higher values of the vapour pressure in comparison to ordinary liquids. So this high value of the vapour pressure overcome the high value of the Blake's threshold pressure caused by the high hydrostatic pressure, and cavitation bubbles can be generated at such conditions (Chapter 2, Equation 2.18):

$$P_v + P_g > P_h + 2\,\frac{\sigma}{R_0} - P_a \qquad \text{[Ch. 2; Eqn. 2.18]}$$

The Blake's threshold pressure symbolizes the value of pressure which must be overcome by an acoustic pressure in order to make a liquid medium cavitate. This pressure threshold can be determined by Equation 6.2 (Kuijpers et al. 2002):

$$P_B = P_h - P_v + \frac{4}{3}\sigma\sqrt{\frac{2}{3}\frac{\sigma}{\left(P_h - 2\frac{\sigma}{R_0} - P_v\right)R_0^3}} \qquad \text{[Eqn. 6.2],}$$

where

P_B – Blake's threshold pressure, Pa

P_h – Hydrostatic pressure, Pa

P_v – Vapour pressure, Pa

R_0 – Equilibrium radius of a cavitation bubble, m

σ – Surface tension of a medium, N/m

It can be noted that in the case of ordinary liquid mediums the vapour pressure variable in Equation 6.2 can be neglected because of its small contribution in comparison with the hydrostatic pressure variable. So in this case the Blake's threshold pressure is too high at elevated hydrostatic pressure, the applied acoustic pressure is not sufficient to initiate the growth of cavities (Equation 6.3).

$$P_B - P_a > 0 \qquad \text{[Eqn. 6.3]}$$

In the case of dense-phase fluids, the vapour pressure has a great effect. Kuijpers estimated (using Equation. 6.2) that the cavitation threshold for CO_2 at 293 K and 5.82 MPa equals that of water at 0.1 MPa and 293 K (Figure 6.1).

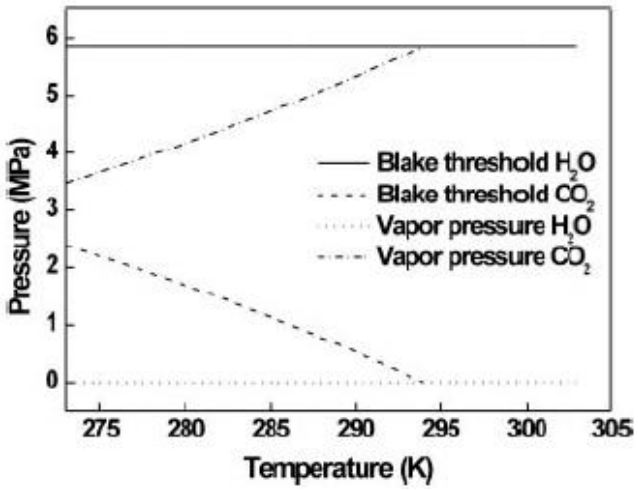

Figure 6.1. Blake's threshold pressure and vapour pressure for water and CO_2 at 5.82 MPa

It can be seen from Figure 6.1 that ultrasound of the same intensity, which is used to generate cavitation in water at ambient conditions, can be applied to liquid CO_2 pressurized at 5.82 MPa in order to overcome the Blake's threshold pressure.

6.3. Experimental Work

6.3.1. Sonolysis of Dense-Phase Mixture of Argon and Carbon Dioxide

A pressure test of the high pressure experimental apparatus was performed before experimental work was started in order to eliminate all possible leaks in the system (see Appendix B).

6.3.1.1. Reaction Mixture Preparation

The possibility of sonolysis of liquid CO_2 was investigated. Five 500 ml stainless steel cylinders were used according to a calculation made by Aspen HYSYS computer software in order to prepare the desired amount of Ar/CO_2 gas mixture containing approximately 95 mol% of CO_2. Then, the mixture of gases was loaded into the high-pressure reactor according to the methodology which is described in Chapter 3 (see Section 3.3.3). Table 6.1 presents the composition of gases for each cylinder, the amount of gaseous mixture loaded into the reactor (n_l) and the amount of gas which remains after loading in the cylinders (n_{cyl}).

Table 6.1. Composition and amount of Ar-CO_2 mixture loaded/remaining for each cylinder

	Cylinder #				
	1	2	3	4	5
mol% CO_2	94.02	94.84	94.97	94.88	95.4
mol% Ar	5.98	5.16	5.03	5.12	4.6
n_l, mol	1.2417	1.2231	1.2690	1.2243	1.2418
n_{cyl}, mol	0.0318	0.0323	0.0342	0.0345	0.0570

6.3.1.2. Estimation of Actual Amount of Reaction Mixture Loaded to the Reactor

Next, the amount of gaseous mixture which is trapped in different parts of the tubing connections during the loading procedure must be estimated in order to find the actual amount of Ar/CO_2 mixture in the reactor. Thus, the amount of mixture remaining in the pump and the pump-reactor tubing connection ($n_{p/p-r}$ in mol) and the amount of mixture remaining in the cylinders-pump tubing connection (n_{cyl-p} in mol) are estimated by using Equation 6.4. Properties of the gas mixtures are calculated using the HYSYS computer software and are presented in Table 6.2.

$$n = PV/ZRT \qquad \text{[Eqn. 6.4]}$$

where

n – Amount of substance, mol

R – Universal gas constant, m^3 Pa K^{-1} mol^{-1}

Z – Compressibility factor

T – Temperature, K

V – Volume, m^3

P – Pressure, Pa.

Table 6.2. Properties of Ar-CO_2 gas mixture trapped in different parts of the experimental apparatus after the loading procedure

	V, m^3	P, Pa	Z	T, K
Pump/pump-reactor tubing	0.000536	3170000	0.7826	289.15
Cylinders-pump tubing	0.000031	7349000	0.4212	294.35

$n_{p/p-r} = PV/ZRT = (3170000 * 0.000536)/(0.7826 * 8.314 * 288.15)$

$\boldsymbol{n_{p/p-r} = 0.906\ mol}$

$n_{c-p} = PV/ZRT = (7349000 * 0.000031)/(0.4212 * 8.314 * 294.35)$

$\boldsymbol{n_{c-p} = 0.221\ mol}$

So, the actual amount of gaseous mixture loaded into the reactor can be evaluated as following (Equation 6.5):

$$n_r = n_l - n_{p/p-r} - n_{c-p} \quad \text{[Eqn. 6.5]}$$

$n_r = (1.2417 + 1.2231 + 1.2690 + 1.2243 + 1.2418) - 0.906 - 0.221$

$\boldsymbol{n_r = 5.073\ mol}$

In the next stage, the actual molar percent of Ar and CO_2 in the reactor is calculated. As long as all five cylinders with the feed mixture contained slightly different concentrations of both compounds, the actual concentrations of Ar and CO_2 must be estimated as average values (Equation 6.6):

$$mol\%(A)_{av} = \left(\frac{n_1\ mol\%_1(A) + n_2\ mol\%_2(A) + \cdots + n_i\ mol\%_i(A)}{n_t}\right) \quad \text{[Eqn. 6.6]},$$

where

$mol\%(A)_{av}$ – Average molar percent of compound A, %

n – Amount of a gas mixture in a cylinder, in mol

mol%(A) - Molar percent of compound A in a cylinder, %

n_t – Total amount of the gas mixture in all cylinders, mol

$$mol\%(CO_2) = \left(\frac{1.2417 * 94.02 + 1.2231 * 94.84 + 1.2690 * 94.97 + 1.2243 * 94.88 + 1.2418 * 95.4}{6.2}\right)$$

$\boldsymbol{mol\%(CO_2) = 94.82\%}$

$$mol\%(Ar) = \left(\frac{1.2417 * 5.98 + 1.2231 * 5.16 + 1.2690 * 5.03 + 1.2243 * 5.12 + 1.2418 * 4.6}{6.2}\right)$$

$\boldsymbol{mol\%(Ar) = 5.18\%}$

After loading the gaseous mixture, the reactor is left overnight (approximately 15 hours). The temperature and pressure before the sonication experiment are 290.15 K and 6600000 Pa, respectively.

At the next point, the HYSYS computer software is used to estimate characteristics of the gas mixture in the reactor at specified conditions (Table 6.3).

Table 6.3. Properties of Ar-CO_2 reaction mixture containing 5.18 mol% of Ar and 94.82 mol% of CO_2 at specified conditions

Liquid fraction percentage, %	Liquid fraction density (ρ), kg/dm^3	Compressibility coefficient (Z)	Average molecular weight (M_{av}), g/mol	Temperature inside the reactor (T), K	Pressure inside the reactor (P), Pa
91.18	721.2	0.167	43.82	290.15	6600000

Based on data presented in Table 6.2, the volume of the liquid phase can be found using Equation 6.4 or Equation 6.7:

$$V = \frac{Z\ n\ R\ T}{P}$$

$$V = \frac{0.167 * (5.073 * 0.9118) * 8.314 * 290.15}{6600000}$$

$$\boldsymbol{V = 0.000282\ m^3\ or\ 282\ cm^3}$$

$$V = \frac{m}{\rho} = \frac{n\ M_{av}}{\rho} \qquad \text{[Eqn. 6.7]}$$

$$V = \frac{(5.073 * 0.9118) * 43.82}{721.2}$$

$$\boldsymbol{V = 0.28\ dm^3\ or\ 281\ cm^3}$$

So it can be seen that there is a sufficient amount of liquefied gases in the reactor to perform sonolysis.

6.3.1.3. Sonication Test

After all experimental preparations are finished, the sonication test is performed. Table 6.4 contains the experimental conditions which are monitored throughout the test.

Table 6.4. Sonolysis of liquefied mixture of Ar and CO_2 gases

T_r, K	P_r, Pa	*t*, min	*Power*, Watt	*Amplitude*, %
290.65	6600000	0	0	0
290.95	6632000	1	124	40
291.05	6658000	1.5	83	40
291.45	6698000	5	99	50
291.85	6748000	8	115	50
292.05	6786000	10	117	50
292.75	6872000	15	121	50
293.45	6991000	20	130	50

A sample of the mixture of gases after the sonication experiment was taken for chromatographic analysis. The GC analysis of the sample was conducted at CoreLab Australia. As a result, CO as products of CO_2 sonolysis at the liquid state was not detected.

6.3.2. Sonolysis of Dense-Phase Mixture of Methane and Carbon Dioxide. Test 1

6.3.2.1. Reaction Mixture Preparation

Sonolysis of a gas mixture containing CH_4 and CO_2 at the liquid state was studied. The idea behind the investigation was to utilize sonochemical energy in order to initiate the process of CO_2 reforming of CH_4. It is suggested that CH_4 will undergo degradation due to applied ultrasound energy producing $H^{\cdot}$ radicals. Those radical are supposed to react with CO_2 reducing it.

According to preliminary calculations made by the HYSYS computer software, six 500 ml stainless cylinders were used to prepare a mixture of CO_2 and CH_4 gases. The characteristics of the gas compositions are shown in Table 6.5. Also, Table 6.5 presents the amount of gaseous mixture loaded and the amount of the composition left in each cylinder after loading into the reactor.

Table 6.5. Compositions and amount of CH_4-CO_2 mixture loaded/remaining for each cylinder

	Cylinder #					
	1	2	3	4	5	6
mol% CO_2	91.2	91.54	91.26	91.2	92.0	91.43
mol% CH_4	8.8	8.46	8.74	8.8	8.0	8.57
n_l, mol	1.141	1.184	1.153	1.135	1.252	1.12
n_{cyl}, mol	0.058	0.064	0.063	0.08	0.081	0.12

6.3.2.2. Estimation of Actual Amount of Reaction Mixture Loaded to the Reactor

The amount of mixture trapped in the pump and pump-reactor tubing connection ($n_{p/p-r}$) and the amount of mixture remained in the booster-pump tubing connection (n_{cyl-p}) during the loading procedure are calculated using Equation 6.4. Properties of the gas compositions lost in different parts of the experimental setup are estimated by the HYSYS computer software (Table 6.6).

Table 6.6. Properties of CH_4-CO_2 gas mixture trapped in different parts of the experimental setup after the loading procedure

	V, m^3	P, Pa	Z	T, K
Pump/pump-reactor tubing	0.000536	3558000	0.7776	290.15
Cylinders-pump tubing	0.000031	5566000	0.5921	289.15

$n_{p/p-r} = PV/ZRT = (3558000 * 0.000536)/(0.7776 * 8.314 * 290.15)$

$\boldsymbol{n_{p/p-r} = 1.017\ mol}$

$n_{c-p} = PV/ZRT = (5566000 * 0.000031)/(0.5921 * 8.314 * 289.15)$

$$\boldsymbol{n_{c-p} = 0.121\ mol}$$

The actual amount of gaseous mixture loaded into the reactor can be found by using Equation 6.5:

$$n_r = (1.141 + 1.184 + 1.153 + 1.135 + 1.252 + 1.12) - 1.017 - 0.121$$
$$\boldsymbol{n_r = 5.85\ mol}$$

Then, the real molar percentages of CH_4/CO_2 mixture loaded to the reactor were calculated (Equation 6.6) as an average of all composition of the feed mixtures (see Table 6.5).

$$mol\%(CO_2) = \left(\frac{1.141 * 91.2 + 1.184 * 91.54 + 1.153 * 91.26 + 1.135 * 91.2 + 1.252 * 92.0 + 1.12 * 91.43}{6.985}\right)$$
$$\boldsymbol{mol\%(CO_2) = 94.82\%}$$
$$mol\%(Ar) = \left(\frac{1.141 * 8.8 + 1.184 * 8.46 + 1.153 * 8.74 + 1.135 * 8.8 + 1.252 * 8.0 + 1.12 * 8.57}{6.985}\right)$$
$$\boldsymbol{mol\%(Ar) = 8.56\%}$$

After loading the gaseous mixture, the reactor was left overnight. The temperature and pressure were 291.55 K and 7230000 Pa, respectively. Then, physical properties of the composition of gases at the conditions presented above (see Table 6.7) were estimated by the HYSYS computer software.

Table 6.7. Properties of CH_4-CO_2 reaction mixture containing 8.56 mol% of CH_4 and 91.44 mol% of CO_2 at specified conditions

Liquid fraction percentage, %	Liquid fraction density (ρ), kg/dm^3	Compressibility coefficient (Z)	Average molecular weight (M_{av}), g/mol	Temperature inside the reactor (T), K	Pressure inside the reactor (P), Pa
88.5	600.0	0.2076	41.81	291.55	7230000

Based on data presented in Table 6.7, the volume of the liquid phase can be calculated using Equation 6.4 or Equation 6.7:

$$V = \frac{0.2076 * (5.85 * 0.885) * 8.314 * 291.55}{7230000}$$
$$\boldsymbol{V = 0.00036\ m^3\ or\ 360\ cm^3}$$

$$V = \frac{(5.85 * 0.885) * 41.81}{600}$$
$$\boldsymbol{V = 0.361\ dm^3\ or\ 361\ cm^3}$$

6.3.2.3. Sonication Test

CO_2 reforming of CH_4 by using ultrasound energy in order to initiate the chemical transformations was studied after the reaction mixture of gases was loaded into the reactor. It can be shown by calculation that a sufficient amount of the feed (over 80%) is liquefied at the selected conditions.

Table 6.8 presents the experimental conditions which were monitored throughout the test.

Table 6.8. Sonolysis of liquefied mixture of CH_4 and CO_2 gases

T_r, K	P_r, Pa	t, min	*Power,* Watt	*Amplitude,* %
291.55	7230000	0	50	0
291.65	7195000	0.5	89	40
291.85	7220000	2	91	45
292.75	7292000	5	94	55
293.45	7396000	10	103	55
294.85	7484000	15	115	60
296.35	7570000	20	114	60

A probe of the composition is taken for a chromatographic analysis after the experiment was conducted. The GC analysis of the sample made by CoreLab Australia. As a result, no expected products of CO_2 reforming of CH_4 were obtained in the sample. So it can be concluded that the energy produced by the ultrasound waves is not sufficient to overcome the activation barrier for the reaction between CH_4 and CO_2 as well as for radicalization these compounds.

6.3.3. Sonolysis of Dense-Phase Mixture of Methane and Carbon Dioxide. Test 2

For the next experiment it was decided to reduce the temperature of the sonolysis by approximately 10 K in comparison with the previous test, while the concentration of CH_4 in composition was increased by 5 mol%.

6.3.3.1. Reaction Mixture Preparation

Based on calculations made by the HYSYS computer software, seven 500 cm^3 stainless steel cylinders were used for preparing a composition consisting of CH_4 and CO_2 gases. The characteristics of the compositions are shown in Table 6.9. This table presents the loaded amount of gaseous mixture and the amount of the composition left after loading into the reactor for each cylinder.

Table 6.9. Compositions and amount of CH_4-CO_2 mixture loaded/remaining for each cylinder

	Cylinder #						
	1	2	3	4	5	6	7
mol% CO_2	82.92	84.93	83.79	83.28	83.88	84.76	84.33
mol% CH_4	17.08	15.07	16.21	16.72	16.12	15.24	15.67
n_l, mol	1.074	1.106	1.094	1.129	1.135	1.138	1.146
n_{cyl}, mol	0.057	0.059	0.059	0.06	0.106	0.101	0.058

6.3.3.2. Estimation Actual Amount of Reaction Mixture Loaded to the Reactor

The amount of mixture trapped in the pump and pump-reactor tubing connection ($n_{p/p-r}$) and the amount of mixture remaining in the booster-pump tubing connection (n_{cyl-p}) during the loading procedure were calculated using Equation 6.4. Properties of the gas compositions lost in different parts of the experimental setup were estimated by the HYSYS computer software (Table 6.10).

Table 6.10. Properties of CH_4-CO_2 gas mixture trapped in different parts of the experimental setup after the loading procedure

	V, m^3	P, Pa	Z	T, K
Pump/pump-reactor tubing	0.000536	3093000	0.8348	294.15
Cylinders-pump tubing	0.000031	5986000	0.6330	293.15

$$n_{p/p-r} = PV/ZRT = (3093000 * 0.000536)/(0.8348 * 8.314 * 294.15)$$

$$\boldsymbol{n_{p/p-r} = 0.812\ mol}$$

$$n_{c-p} = PV/ZRT = (5986000 * 0.000031)/(0.6330 * 8.314 * 293.15)$$

$$\boldsymbol{n_{c-p} = 0.12\ mol}$$

The actual amount of gaseous mixture loaded into the reactor can be found by using Equation 6.5:

$$n_r = (1.074 + 1.106 + 1.094 + 1.129 + 1.135 + 1.138 + 1.146) - 0.812 - 0.12$$

$$\boldsymbol{n_r = 6.89\ mol}$$

After that, the actual molar percentages of CH_4/CO_2 mixture loaded to the reactor were calculated (Eqn. 6.6) as an average of all composition of the feed mixtures (see Table 6.9).

$$mol\%(CO_2) = \left(\frac{1.074 * 82.92 + 1.106 * 84.93 + 1.094 * 83.79 + 1.129 * 83.28 + 1.135 * 83.88 + 1.138 * 84.76 + 1.146 * 84.33}{7.822}\right)$$

$$\boldsymbol{mol\%(CO_2) = 83.99\%}$$

$$mol\%(Ar) = \left(\frac{1.074 * 17.08 + 1.106 * 15.07 + 1.094 * 16.21 + 1.129 * 16.72 + 1.135 * 16.12 + 1.138 * 15.24 + 1.146 * 15.67}{7.822}\right)$$

$$\boldsymbol{mol\%(Ar) = 16.01\%}$$

After loading the gaseous mixture, the reactor was placed into the cooling chamber (see Chapter 3, Figure 3.17) in order to reduce the temperature of the composition (Table 6.11).

Table 6.11. Procedure of cooling the CH_4-CO_2 reaction mixture to the required temperature

P, Pa	*T*, K	*t*, min
8754000	291.65	0
8360000	289.85	30
7970000	287.45	60
7853000	286.45	90
7694000	285.15	120
7578000	284.15	150
7447000	283.35	180

At the end of the cooling, the temperature and pressure of composition were noted as 283.35 K and 7447000 Pa, respectively. The physical properties of the composition of gases at the conditions presented above were estimated by the HYSYS computer software (Table 6.12).

Table 6.12. Properties of CH_4-CO_2 reaction mixture containing 16.01 mol% of CH_4 and 83.99 mol% of CO_2 at specified conditions

Liquid fraction percentage, %	Liquid fraction density (ρ), kg/dm^3	Compressibility coefficient (Z)	Average molecular weight (M_{av}), g/mol	Temperature inside the reactor (T), K	Pressure inside the reactor (P), Pa
79.46	416	250233	22516	283.35	7447000

Based on data from Table 6.12, the volume of the liquid phase can be calculated using Equation 6.4 or Equation 6.7:

$$V = \frac{0.2055 * (6.89 * 0.7946) * 8.314 * 283.35}{7447000}$$

$$\boldsymbol{V = 0.000356\ m^3\ or\ 356\ cm^3}$$

$$V = \frac{(6.89 * 0.7946) * 40.18}{618}$$

$$\boldsymbol{V = 0.356\ dm^3\ or\ 356\ cm^3}$$

6.3.3.3. Sonication Test

CO_2 reforming of CH_4 by using ultrasound energy in order to initiate the chemical transformations was studied after the reaction mixture of gases was loaded into the reactor. It is shown by calculation that a sufficient amount of the feed is liquefied at the selected conditions. Table 6.13 presents the experimental conditions which are monitored during the sonolysis.

Table 6.13. Sonolysis of liquefied mixture of CH_4 and CO_2 gases

T_r, K	P_r, Pa	t, min	*Power*, Watt	*Amplitude,* %
283.35	7447000	0	53.2	0
283.85	7515000	2	158	50
284.15	7576000	4	156	50
284.75	7644000	6	153	50
285.45	7719000	8	161	50
285.85	7850000	12	163	50
286.65	8002000	16	175	50
287.35	8152000	20	180	50

A sample of the mixture of gases was collected for a chromatographic analysis. The GC analysis of the sample was performed at CoreLab Australia. However, no products of CO_2 and CH_4 sonolysis or their recombination were obtained.

6.3.4. Sonolysis of Dense-Phase Mixture of Hydrogen and Carbon Dioxide

Sonochemical reduction of CO_2 by H_2 at the liquid state was studied. After a failure in the attempt to perform CO_2 reforming of CH_4, it was decided to use H_2 as a reducing agent. The formation of CH_4 in the process of sonochemical reduction of CO_2 by H_2 in aqueous medium is experimentally proven to occur in Chapter 4 (Section 4.4.2.4).

6.3.4.1. Reaction Mixture Preparation

Compositions of CO_2 and H_2 gases were prepared using eight 500 cm^3 stainless steel cylinders, according to preliminary calculations on the required amount of the gas feed and taking into account the amount which will be lost during the loading procedure. Due to the amount of cylinders needed, the loading procedure was performed into three stages according to the methodology described in Chapter 3. Table 6.14 presents the composition of gases for each cylinder, the amount of gaseous mixture loaded into the reactor and the amount of gas which remains in the cylinders after loading.

Table 6.14. Composition and amount of H_2-CO_2 mixture loaded/remaining for each cylinder

	Cylinder #							
	1	2	3	4	5	6	7	8
mol% CO_2	92.76	93.22	92.49	92.64	92.8	93.75	92.06	92.01
mol% H_2	7.24	6.78	7.51	7.36	7.2	6.25	7.94	7.99
n_l, mol	1.053	1.055	1.031	1.038	1.063	1.004	1.113	1.105
n_{cyl}, mol	0.052	0.052	0.051	0.118	0.112	0.117	0.084	0.083

6.3.4.2. Estimation of Real Amount of Reaction Mixture Loaded to the Reactor

During the loading procedure some gas mixture can be lost, or trapped in the different parts of the experimental setup. So the amount of mixture trapped in the pump and pump-reactor tubing connection ($n_{p/p-r}$) and the amount of mixture remained in the booster-pump tubing connection (n_{cyl-p}) are estimated using Equation 6.4. The properties of the mixtures trapped in different sections of the equipment are calculated by the HYSYS computer software (Table 6.15).

Table 6.15. Properties of H_2-CO_2 gas mixture trapped in different parts of the experimental setup after the loading procedure

	V, m^3	P, Pa	Z	T, K
Pump/pump-reactor tubing	0.000536	3837000	0.7819	292.15
Cylinders-pump tubing	0.000031	7508000	0.5865	292.15

$$n_{p/p-r} = P\,V/\,Z\,R\,T = (3837000 * 0.000536)/(0.7819 * 8.314 * 292.15)$$

$$\boldsymbol{n_{p/p-r} = 1.083\ mol}$$

$$n_{c-p} = P\,V/\,Z\,R\,T = (7508000 * 0.000031)/(0.5865 * 8.314 * 292.15)$$

$$\boldsymbol{n_{c-p} = 0.163\ mol}$$

The actual amount of gaseous mixture loaded into the reactor is found as follows:

$$n_r = (1.053 + 1.055 + 1.031 + 1.038 + 1.063 + 1.004 + 1.113 + 1.105) - 1.08 - 0.163$$

$$\boldsymbol{n_r = 7.216\ mol}$$

Next point, the actual molar percentages of loaded CO_2/H_2 composition is calculated using Equation 6.6 as an average of all feed compositions (see Table 6.13).

$$mol\%(CO_2) = \left(\frac{1.053 * 92.76 + 1.055 * 93.22 + 1.031 * 92.49 + 1.038 * 92.64 + 1.063 * 92.8 + 1.004 * 93.75 + 1.113 * 92.06 + 1.105 * 92.01}{8.462}\right)$$

$$\boldsymbol{mol\%(CO_2) = 92.7\%}$$

$$mol\%(H_2) = \left(\frac{1.053 * 7.24 + 1.055 * 6.78 + 1.031 * 7.51 + 1.038 * 7.36 + 1.063 * 7.2 + 1.004 * 6.25 + 1.113 * 7.94 + 1.105 * 7.99}{8.462}\right)$$

$$\boldsymbol{mol\%(H_2) = 7.3\%}$$

After loading the gaseous mixture, the reactor is left overnight. The temperature and pressure are 290.65 K and 8925000 Pa, respectively.

The physical properties of the composition of gases at the conditions presented above are estimated by the HYSYS computer software (Table 6.16).

Table 6.16. Properties of H_2-CO_2 reaction mixture containing 7.3 mol% of H_2 and 92.7 mol% of CO_2 at specified conditions

Liquid fraction percentage, %	Liquid fraction density (ρ), kg/dm^3	Compressibility coefficient (Z)	Average molecular weight (M_{av}), g/mol	Temperature inside the reactor (T), K	Pressure inside the reactor (P), Pa
82.92	51254	250157	20515	072543	6703222

Based on data presented in Table 6.16, the volume of the liquid phase can be calculated using Equation 6.4 or Equation 6.7:

$$V = \frac{0.2179 * (7.216 * 0.8292) * 8.314 * 290.65}{8925000}$$

$$\boldsymbol{V = 0.000353\ m^3\ or\ 353\ cm^3}$$

$$V = \frac{(7.216 * 0.8292) * 42.17}{714.6}$$

$$\boldsymbol{V = 0.353.1\ dm^3\ or\ 353.1\ cm^3}$$

6.3.4.3. Sonication Test

Sonochemical reduction of CO_2 by H_2 at the liquid state is conducted. The temperature and pressure of the mixture at the beginning of the experiment are 290.65 K and 8925000 Pa, respectively. Table 6.17 contains data on the experimental conditions which were monitored during the test.

Table 6.17. Sonolysis of liquefied mixture of H_2 and CO_2 gases

P_r, Pa	T_r, C	t, min	*Power*, Watt	*Amplitude*, %
8937000	290.75	0	0	0
9056000	291.65	5	104.5	50
9165000	292.25	10	106.5	50
9280000	292.95	15	107.5	50
9401000	293.75	20	119	55
9515000	294.45	25	119	55

A sample of the mixture after sonication was taken to CoreLab Australia for a chromatographic analysis. The GC analysis of the sample did not detect any product of CO_2 reduction.

6.3.5. Sonolysis of Supercritical Mixture of Methane and Carbon Dioxide

The attempt of sonolysis of a CO_2/CH_4 mixture at the supercritical state is performed. Balachandran et al. (2006) in their work on ginger extraction in supercritical CO_2 assumed that the formation of sub-critical cavitational bubbles of gas in the supercritical fluid could be a possible cause of cellular damage.

6.3.5.1. Reaction Mixture Preparation

Seven 500 cm^3 stainless steel cylinders with the desired molar percentages of CO_2 and CH_4 gases were used in order to prepare the required amount of the composition. This required amount is estimated by the HYSYS computer software. The composition of gases is loaded into the high pressure reactor strictly in accordance with the methodology described in Chapter 3. Table 6.18 shows the composition of gases, the amount of gaseous mixture loaded into the reactor and the amount of gas which remains after loading for each cylinder.

Table 6.18. Composition and amount of CH_4-CO_2 mixture loaded/remaining for each cylinder

	Cylinder #						
	1	2	3	4	5	6	7
mol% CO_2	83.84	84.24	84.15	83.25	83.74	84.07	83.6
mol% CH_4	16.16	15.76	15.85	16.75	16.26	15.93	16.4
n_l, mol	1.023	1.081	1.083	1.032	1.042	1.037	1.013
n_{cyl}, mol	0.098	0.07	0.068	0.065	0.077	0.097	0.092

6.3.5.2. Estimation of Real Amount of Reaction Mixture Loaded to the Reactor

Next stage, the amount of the mixture lost in the sections of the experimental setup such as the pump and pump-reactor tubing connection section ($n_{p/p-r}$) and the cylinders-pump tubing connection section (n_{cyl-p}) during the loading procedure are calculated using Equation 6.4. Characteristics of the mixtures trapped in different sections of setup were calculated by the HYSYS computer software (Table 6.19).

Table 6.19. Properties of CH_4-CO_2 gas mixtures trapped in different parts of the experimental setup after the loading procedure

	V, m^3	P, Pa	Z	T, K
Pump/pump-reactor tubing	0.000536	3438000	0.7997	288.15
Cylinders-pump tubing	0.000031	7854000	0.4162	292.15

$$n_{p/p-r} = P\,V / Z\,R\,T = (3438000 * 0.000536)/(0.7997 * 8.314 * 288.15)$$

$$\boldsymbol{n_{p/p-r} = 0.962\ mol}$$

$$n_{c-p} = PV/ZRT = (7854000 * 0.000031)/(0.4162 * 8.314 * 292.15)$$

$$\boldsymbol{n_{c-p} = 0.241\ mol}$$

The actual amount of gaseous mixture loaded into the reactor is found as follows:

$$n_r = (1.023 + 1.081 + 1.083 + 1.032 + 1.042 + 1.037 + 1.013) - 0.962 - 0.241$$

$$\boldsymbol{n_r = 6.108\ mol}$$

Next, the actual molar percentages of the loaded CO_2/CH_4 composition are calculated using Equation 6.6 as an average of all feed compositions (see Table 6.18).

$$mol\%(CO_2) = \left(\frac{1.023 * 83.84 + 1.081 * 84.24 + 1.083 * 84.15 + 1.032 * 83.25 + 1.042 * 83.74 + 1.037 * 84.07 + 1.013 * 83.6}{7.311}\right)$$

$$\boldsymbol{mol\%(CO_2) = 83.85\%}$$

$$mol\%(CH_2) = \left(\frac{1.023 * 16.16 + 1.081 * 15.76 + 1.083 * 15.85 + 1.032 * 16.75 + 1.042 * 16.26 + 1.037 * 15.93 + 1.013 * 16.4}{8.462}\right)$$

$$\boldsymbol{mol\%(CH_2) = 16.15\%}$$

After loading the gaseous mixture, the reactor is left overnight. The temperature and pressure are 288.5 K and 8111000 Pa, respectively.

The physical properties of the composition of gases at the conditions presented above are estimated by the HYSYS computer software (Table 6.20).

Table 6.20. Properties of CH_4-CO_2 reaction mixture containing 16.15 mol% of CH_4 and 83.85 mol% of CO_2 at specified conditions

Liquid fraction percentage, %	Liquid fraction density (ρ), kg/dm^3	Compressibility coefficient (Z)	Average molecular weight (M_{av}), g/mol	Temperature inside the reactor (T), K	Pressure inside the reactor (P), Pa
85.33	32556	250424	17551	06653	6111222

According to data presented in Table 6.20, the volume of liquid phase can be calculated using Equation 6.4 or Equation 6.7:

$$V = \frac{0.2646 * (6.108 * 0.8533) * 8.314 * 288.5}{8111000}$$

$$\boldsymbol{V = 0.000408\ m^3\ or\ 408\ cm^3}$$

$$V = \frac{(6.108 * 0.8533) * 39.71}{507.8}$$

$$\boldsymbol{V = 0.4075\ dm^3\ or\ 407.5\ cm^3}$$

6.3.5.3. Sonication Test

The reactor was placed into the dry oven (see Chapter 3, Figure 3.16) in order to obtain supercritical conditions for the prepared composition of gases. The mixture of gases is driven to the supercritical conditions by heating. Table 6.21 contains temperatures and pressures of the composition of gases monitored during the heating procedure.

Table 6.21. Reaching the supercritical conditions for CH_4-CO_2 reaction mixture containing 16.15 mol% of CH_4 and 83.85 mol% of CO_2

P, Pa	*T*, K	*t*, min	Point on diagram (see Figure 6.2)
8111000	288.35	0	1
8775000	294.95	30	2
9630000	298.95	60	3
10025000	300.95	90	4
12110000	308.05	140	5

Figure 6.2 depicts a PT diagram for the composition showing the process of heating the mixture of gases to the supercritical region. So, when the desired experimental conditions are achieved, the sonication experiment is performed. The results of the test are presented in Table 6.22.

Table 6.22. Sonolysis of CH_4-CO_2 reaction mixture at supercritical conditions

T_r, C	P_r, Pa	*t*, min	*Power*, Watt	*Amplitude*, %
308.15	12110000	0	0	0
307.55	12331000	8	133.5	50
308.05	12470000	16	142.5	55
308.15	12604000	24	137	60
-	-	60 overload at 24th min		

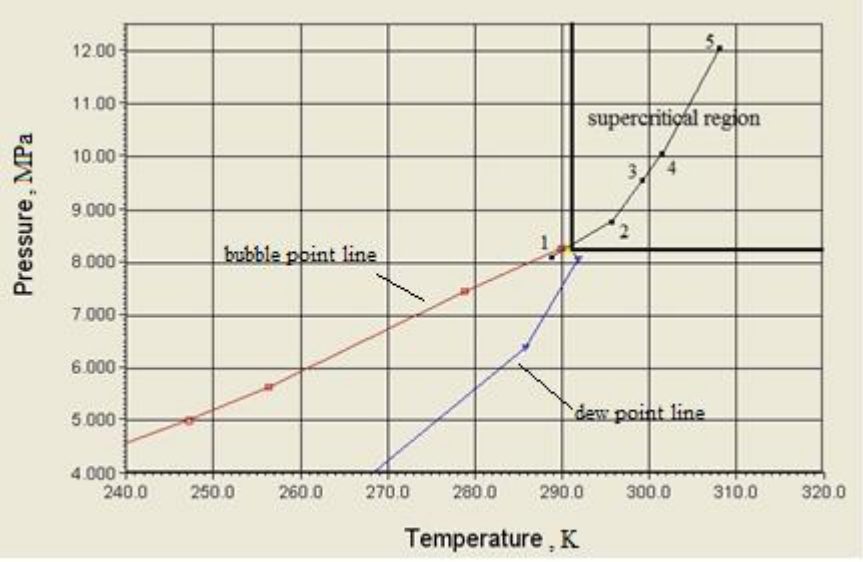

Figure 6.2. PT diagram for a gas mixture containing 16.15 mol% of CH_4 and 83.85 mol% of CO_2

The sample of the final composition was taken to CoreLab Australia for the chromatographic analysis after conducting the sonolysis. The analysis showed that reduction of CO_2 or formation of any expected products did not occur.

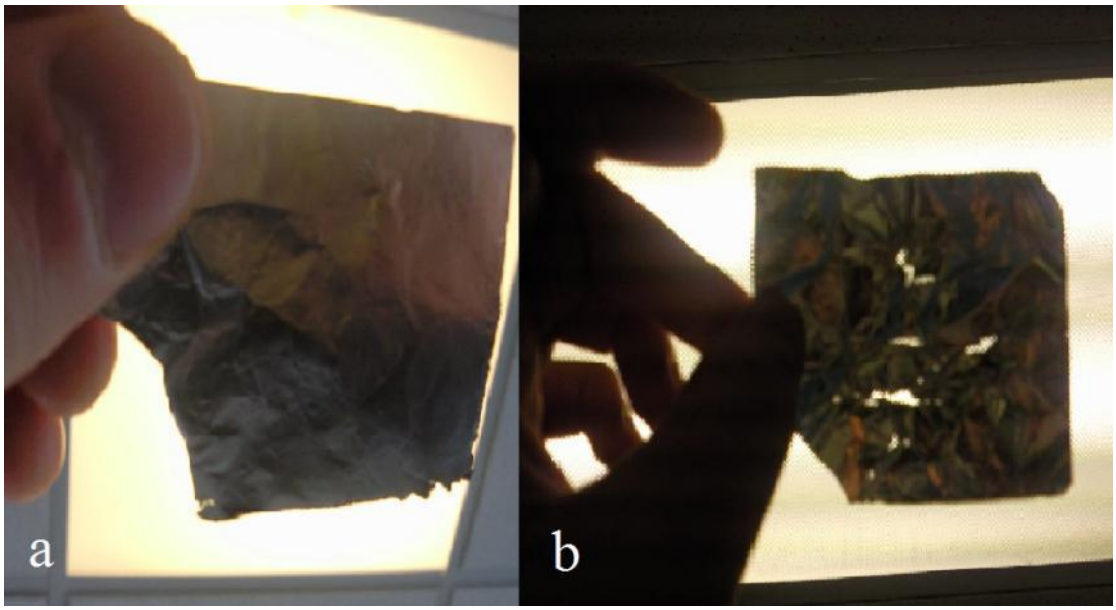

Figure 6.3. Aluminum foil after: a) Sonolysis of CO_2-CH_4 under supercritical conditions (section 6.3.5); b) Sonolysis of CO_2-CH_4 at the liquid state (section 6.3.3)

Moreover, the presence of cavitation is not detected in the sonolysis at supercritical conditions by the physical method using a piece of aluminum foil. Figure 6.3 (a) is a photo of the aluminum foil which is placed into the reactor before the sonolysis of a supercritical mixture of CO_2/CH_4. It can be seen that there are no holes (or perforations) in the foil in comparison with the other piece of aluminum foil (Figure 6.3 (b)) which is used as an indicator of cavitation phenomena in the sonolysis of CO_2/CH_4 at the liquid state (Section 6.3.3).

Thus, conclusion can be reached that no transient cavities grow and explode when a supercritical mixture of gases is subjected to ultrasound.

6.4. Conclusion

Sonolysis of liquefied gas mixtures (CO_2/Ar, CH_4/CO_2 and CO_2/H_2) was carried out. The idea behind the research consisted in radicalization of compounds of the reaction mixture during cavitational collapse accompanied by the formation of new products. It is shown that even though transient cavitation occurred at liquefied dense-phase fluids (Figure 6.3a) there were no sonochemical reactions initiated. So, it can be assumed that the collapse of the formed cavities is very weak and the generated hot

spots are unable to provide the conditions in order to induce the sonochemical reactions.

Sonolytic products are not detected in the experiment of the CO_2/CH_4 mixture sonolysis at supercritical state. The undamaged aluminum foil in this experiment (Figure 6.3b) shows that cavitational bubbles are not generated in supercritical CO_2. Thus, it can be stated that the absence of cavitation in supercritical mixture of gases is determined by the non-existence of boundaries between the liquid and gas phases at such conditions.

Chapter 7. Ultrasound-Assisted Oxidative Desulphurization of Sulphur-Containing Compounds by Potassium Permanganate

7.1. Introduction

In our research, the main purpose was to reduce CO_2 into valuable compounds, so any oxidation processes occurring would be unwanted. Therefore, it is important to understand the effects of ultrasound on oxidation, as well as the chemical and physical processes responsible for it.

In order to investigate the role of ultrasound in oxidation, oxidative processes where ultrasound is applied to increase reaction rates have to be examined. One such oxidative technology which has been known for a long time and extensively studied since the 1970s, is called oxidative desulphurization (ODS) (H. Mei, B. W. Mei, and Yen 2003; Collins, Lucy, and Sharp 1997; Tam, Kittrell, and Eldridge 1990; Harkness and Murray 1970)

Recently (in the 1990ʻs), the possibility of applying ultrasound in order to enhance reaction rates in ODS of sulphur containing compounds (such as thiols (mercaptanes) and disulphides) contained in oils or condensates has been investigated (Shiraishi and Hirai 2004; Dai, Zhao, and Zhang 2008; Dai, Zhao, and Qi 2010 (in press)). It was shown that ultrasound supports an oxidation process when certain reagents/catalysts are employed in ODS. This new technology is used to replace the conventional process of sulphur removal – hydrodesulfurization (HDS). In this process desulfurization of sulphur containing compounds takes place at elevated temperatures of 590 – 690 K and pressures of 4 – 20 MPa (Hearn, Gildert, and Putman, 1996; Kabe, Ishihara, and Tajima 1992). Moreover, a metallic catalyst such as Ni-Mo or Co-Mo is required. However, new regulations on sulphur content in fuels (no more than 10 μg/g) have been introduced recently in the European Union (McGeehan 2004). This implies that HDS in order to fulfil the new rules, has to be operated under more severe conditions (higher temperature, higher hydrogen pressure, a more active catalyst and longer residential time) and requires even more energy consumption (Nocca, Dorbon, and Padamsey 2003; Palmer, Ripperger, and Migliavacca 2001).

This chapter reports on the experimental investigation on ultrasound-assisted oxidative desulfurization of thiols and disulphides by $KMnO_4$, performed in order to

compare results with those where different oxidation systems are used. Moreover, based on the results obtained, a mechanism by which ultrasound enhances oxidation rates is discussed.

7.2. Theoretical Approach

As is generally known, the polarity of sulphides, disulphides, mercaptans and their corresponding hydrocarbons doesn"t differ a lot (Wu and Ondruschka 2010) so that it is impossible to perform extraction of these sulphur containing compounds from oil without chemical transformations. However, the polarity of oxidized derivatives such as sulphonic acids, sulphoxides and sulphones is significantly higher than that of sulphides, disulphides, mercaptans. Thus, the main aim of OSD is to convert all sulphur containing compounds present in oils into sulfonic acids, sulphoxides or sulphones followed by an extraction of these components by polar solvents (e.g. water, alcohols).

A large number of articles on ultrasound-assisted oxidative desulphurization (UAODS) can be found in the literature (Shiraishi and Hirai 2004; Dai, Zhao, and Zhang 2008; Wu and Ondruschka 2010). There have been various reaction systems under diverse experimental conditions investigated. The methodology of all experiments on UAODS found in the literature is very similar: oxidation of sulphur containing compounds supported with ultrasound is followed by extraction of products (sulphur compounds) with polar solvents. Also, it is interesting to note that all oxidative systems in the experimental work devoted to UAODS contained hydrogen peroxide (H_2O_2) as an oxidizing agent. The choice of H_2O_2 is easy to explain: H_2O_2 is quite a strong oxidizer; it is a stronger oxidizing agent than oxygen and chlorine. H_2O_2 oxidation potential equals +1.77 V which is a bit less than that of ozone (+2.07 V). Moreover, H_2O_2 is a liquid at standard conditions unlike such oxidizers as oxygen and chlorine, so this fact facilitates H_2O_2 handling and reaction apparatus design.

For our investigation of ultrasound effect on the oxidative process, $KMnO_4$ was selected as an oxidizing agent. This choice was made based on the facts that, first, no article on ultrasound-assisted ODS by $KMnO_4$ were found in the literature, and, second, it would be interesting to compare obtained results with ones provided in the articles where H_2O_2 is used as an oxidizer. Moreover, the oxidation potential of $KMnO_4$ is +1.67 V, which makes $KMnO_4$ a strong enough oxidizing agent.

7.3. Experimental Work

7.3.1. Preparation of Oxidative Mixture

Condensate with initial sulphur content of 0.5645% w/w was used for experimental work. The oxidative system containing 0.4 M water solution of $KMnO_4$ was prepared taking into account the sulphur content in the condensate feed, so that $KMnO_4$/sulphur = 2.5/1.

7.3.2. Experimental Procedure

Oxidation of sulphur containing compounds was carried out in a 150 cm^3 glass beaker. The mixture of 30 cm^3 of condensate as well as 30 cm^3 of 0.4 M water solution of $KMnO_4$, preheated to 323 K, was used for every performed test. During the first experiment the mixture was stirred by a magnetic stirrer with heating plate (C-MAG HS 7) at 500 rpm. The temperature of 323 K was maintained due to the heating function of the magnetic stirrer. During the other tests, the magnetic stirrer was not employed as ultrasound was used for stirring purposes. The reaction time for every test was set to 20 minutes. After the oxidation, the precipitated MnO_2 was separated from the liquid phase by means of filter paper following which the aqueous phase was separated from the organic phase in a 500 cm^3 separatory funnel. After that, the aqueous phase was discarded. Distilled water and methanol (≥ 99 % obtained from Sigma-Chemicals, Australia) were used for the extraction of oxidized sulphur compounds from the condensate. The extraction of oxidized sulphur compounds was performed two times for each sample with a condensate/solvent ratio of 1/2.

Table 7.1. Ultrasonic-assisted ODS of sulphur containing compounds by $KMnO_4$ (General experimental conditions: 323 K, 0.1 MPa, 30 ml of condensate (0.5645 %w/w of S), 30 ml of ~ 0.4 M water solution of $KMnO_4$, the reaction time of 20 min, two extraction steps)

Test, #	Method	Extractant	Final sulphur content, w/w%	Sulphur removal, %
1	Stirring at 500 rpm	H_2O	0.2322	58.9
2	Ultrasound at 100 W	H_2O	0.2635	53.3
3	Ultrasound at 250 W	H_2O	0.2506	55.6
4	Ultrasound at 100 W	CH_3OH	0.2695	52.2

7.3.3. Sample Analysis

All samples were collected and sent to GeoTech Services (Australia) for the sulphur content (% w/w) determination. The results of the analysis performed by GeoTech Services (Australia) are presented in Table 7.1. According to the results, it can be noted that the sulphur removal is almost 59 % when mechanical stirring of the reaction mixture is used. Moreover, it is very important to notice that the rate of oxidation is not improved when ultrasound is applied. Furthermore, usage of different extractants does not give significant changes between the final sulphur content in the samples. The detailed analysis of the oxidation mechanism by $KMnO_4$, the ultrasound effect of the oxidation rate and the comparison of the results obtained to oxidation of sulphur compounds by different oxidizing systems are presented in the next section (Section 7.4.)

7.4. Results and Discussion

As it is found from the conducted experimental work, the ultrasound assistance does not improve the oxidation rate of sulphur containing compounds while $KMnO_4$ was used as an oxidizing agent. However, ultrasound accelerates the rates of oxidation of sulphur compounds in experimental work devoted to UAODS by oxidizing systems containing H_2O_2. It should also be pointed that an increase in power of the applied ultrasound led to an increase in oxidation rates. So, in order to understand the effect of ultrasound on rates of oxidation of sulphur compounds, the mechanisms of oxidation for different oxidizing system, such as H_2O_2 (Deshpande, Bassi, and Prakash 2005), Fenton reagent (Dai et al. 2008), H_2O_2-acetic or formic acids/sulphuric or phosphoric acids (Mello et al. 2009; Otsuki et al. 2000) and the investigated in this work $KMnO_4$, are discussed.

7.4.1. Hydrogen Peroxide-Ultrasound Oxidizing System

The first oxidizing system considered is H_2O_2-ultrasoud. Normally, H_2O_2 decomposes into water and oxygen (O_2) spontaneously (Reaction 7.1).

$$2\,H_2O_2 \rightarrow 2\,H_2O + O_2 \qquad \text{[R. 7.1]}$$

This reaction is extothermic and thermodynamically favourable at standard conditions. H_2O_2 reduces to water while oxidizing sulphur compounds (e.g. oxidation of dialkyl sulphides (Reaction 7.2) and thiols (Reaction 7.3)).

$$RSR + H_2O_2 \rightarrow R_2SO + 3\,H_2O \quad \text{[R. 7.2]}$$

$$2\,RSH + H_2O_2 \rightarrow RSSH + 2\,H_2O \quad \text{[R. 7.3]}$$

where R is $CH_3^{\cdot}$, $C_2H_5^{\cdot}$ *and so on.*

Also, it should be noted that the decomposition of H_2O_2 in an alkali medium occurs more rapidly (Reaction 7.1), so acidic media are often applied for H_2O_2 in order to stabilize it or initiate the activation of H_2O_2 through $OH^{\cdot}$ radicals (see Sections 7.4.2 and 7.4.3). Dai, Qi, and Zhao (2009) showed experimentally that oxidation rates for H_2O_2-ultrasoud systems are higher than for H_2O_2 alone. This can be explained by the fact that when ultrasound is applied to the reaction system, H_2O_2 molecules can be broken into hydroxyl radicals ($OH^{\cdot}$) (Adewyui 2005; Shu and Chang 2005; Chitra, Paramasivan, and Sinha 2004) which are much stronger oxidizers than H_2O_2. The oxidative potential of $OH^{\cdot}$ radicals equals approximately + 2.8 V.

$$H_2O_2 \xleftrightarrow{Ultrasound} 2\,OH^{\cdot} \quad \text{[R. 7.4]}$$

So it seems like the rates of oxidation are accelerated due to the formation of $OH^{\cdot}$ radicals during the cavitation phenomenon caused by ultrasonic waves.

7.4.2. Hydrogen Peroxide-Carboxylic Acids-Ultrasound Oxidizing System

It has been experimentally explored that carboxylic acids such as formic (HCOOH) and acetic (CH_3COOH) in a mixture with H_2O_2 make fair oxidizing systems. The activation process of an H_2O_2-carboxylic acid oxidation system goes through the formation of peroxyacids (such as performic acid (HCOOOH) and peracetic acid (CH_3COOOH (Reaction 7.5)). Peroxyacids are very strong oxidizing agents due to $OH^{\cdot}$ radicals. Thus, such systems have stronger oxidative potential that H_2O_2 alone. Also, application of ultrasound increases the oxidative potential of an H_2O_2-carboxylic acid oxidizing system, apparently due to the formation of a greater number of $OH^{\cdot}$ radicals from H_2O_2.

$$CH_3COOH + H_2O_2 \leftrightarrow CH_3COOOH + H_2O \quad \text{[R. 7.5]}$$

7.4.3. Hydrogen Peroxide-Fenton Reagent-Ultrasound Oxidizing System

Another oxidizing system which is used in UAODS and which provides high oxidation rates of sulphur compounds is the Fenton reagent. The Fenton reagent is a

solution of H_2O_2 and an iron catalyst where iron has an oxidation number of +2 (e.g. $FeSO_4$). The iron (II) is used in this system as an activator of H_2O_2. At the first step of interaction between the components of the Fenton reagent, H_2O_2 oxidizes iron (II) to iron with oxidation number of +3, forming hydroxyl radicals and anions (De Visscher and van Langenhove 1998) (Reaction 7.6). In turn, the reaction between OH^- anions and $OH^\cdot$ radicals can also take place (Adewyui 2005) (Reaction 7.7). Then, iron (III) is reduced by the same amount of H_2O_2 to iron (II), peroxide radical and proton (Reaction 7.8) The Fenton oxidizing agents are usually utilized at acidic medium conditions in order to prevent H_2O_2 from decomposition process (Reaction 7.1).

$$Fe^{2+} + H_2O_2 \rightarrow Fe^{3+} + OH^\cdot + OH^- \quad \text{[R. 7.6]}$$

$$OH^- + OH^\cdot \leftrightarrow O^- + H_2O \quad \text{[R. 7.7]}$$

$$Fe^{3+} + H_2O_2 \rightarrow Fe^{2+} + OOH^\cdot + H^+ \quad \text{[R. 7.8]}$$

Thus, the oxidation of sulphur compounds in case of using the Fenton reagent mainly goes through the generation of a large number of $OH^\cdot$ radicals. Ultrasound, on the one hand, provides help to generate $OH^\cdot$ radicals through the H_2O_2 sonolysis. It was suggested (Dai 2008) that ultrasonic waves increase the effectiveness of Fe^{2+} dissociation by providing more $OH^\cdot$ radical through Reaction 7.4. Thus, as long as $OH^\cdot$ radicals are stronger oxidizers than H_2O_2 itself, the Fenton reagent is a better oxidizing system. Moreover, the possible cost-effective recoverability of the iron after the oxidation makes Fenton reagent economically attractive (Cao et al. 2009).

7.4.4. Potassium Permanganate-Ultrasound Oxidizing System

In this investigation, $KMnO_4$ is used as an oxidizing agent. The activation mechanism of $KMnO_4$ at neutral medium conditions involves the liberation of oxygen (O_2) (see Reaction 7.9).

$$2MnO_4^{2-} + H_2O = 2OH^- + 2MnO_2(s) + \frac{3}{2}O_2 \quad \text{[R. 7.9]}$$

It can be seen from the equation that no formation of $OH^\cdot$ radicals or OH^+ cations occurs during the activation of the $KMnO_4$ oxidizing system and the oxidation of sulphur compounds take place due to the generated molecular oxygen. So, the main reason why the oxidation process using $KMnO_4$ cannot be catalysed by ultrasound is

that it is not possible to produce $OH^{\cdot}$ radicals during $KMnO_4$ activation unlike in the case of using H_2O_2 as the oxidizer. Thus, it can be concluded that applying ultrasound for oxidation of sulphur containing compounds by $KMnO_4$ does not accelerate the rate of oxidation. However, it should be noticed that the formation of $OH^{\cdot}$ radicals can proceed through the sonolysis of water in the oxidizing system (Reaction 7.10) (Yanagida et al. 1999). Nevertheless, formation of $OH^{\cdot}$ radicals through the water sonolysis is negligible in comparison with the rate of O_2 generation by Reaction 7.9, so the effect of these radicals on an increase of the oxidation rate cannot be seen.

$$H_2 \xrightarrow{Ultrasound} OH^{\cdot} + H^{\cdot} \qquad \text{[R. 7.10]}$$

Overall, from the experimental investigation, conclusions on the possibility of using ultrasound to accelerate the oxidation process can be made. It can be deduced that ultrasound has its effect on oxidation rates through increasing rates of formation of radicals (e.g. $OH^{\cdot}$ radicals) which directly take place in oxidation processes. So, in order to apply ultrasound for improving oxidation rates, the right oxidation system must be chosen.

7.5. Conclusions

The results of the performed sulphur reduction are quite impressive taking into account the reaction time. During the investigation, the mechanism by which ultrasound accelerates oxidation rates is deduced. Also, it is shown that ultrasound does not improve rates of oxidation of sulphur compounds when $KMnO_4$ is used as oxidizing agent. It was shown that ultrasound accelerates the oxidation processes due to the enhanced formation of $OH^{\cdot}$ radicals when appropriate oxidizing systems are used. Moreover, it should be pointed out that during the oxidation of sulphur compounds by $KMnO_4$, the precipitation of MnO_2 occurs and requires an additional separation stage, complicating the process. Furthermore, the precipitated MnO_2 is assumed to reduce the contact area between oil and water phases during the process of oxidation. Thus, it can be concluded that ultrasound does not speed up the oxidation process itself but increase the oxidation ability of an oxidizer.

Chapter 8. Efficiency of Sonochemical Reduction of Carbon Dioxide as Technology for Carbon Dioxide Utilization

8.1. Introduction

The efficiency of ultrasound for CO_2 utilization is discussed in this chapter. All reactions occurring under ultrasonic irradiation can be divided into two groups. The first group of reactions are ones is which rates or/and products selectivity change due to the application of ultrasound. However, those reactions can be carried out without sonication (Margulis 2002). The application of ultrasound for such types of reaction is more likely to be operated on an industrial scale. For example, the pilot plant for indirect oxidation of cyclohexanol to cyclohexanone was funded by Electricite de France. Germany‟s Clausthal Technical University uses a sonochemical reactor which produces up to 4 metric tons of Grignard reagent per year. Ultrasound is found to reduce significantly the induction period in the synthesis of Grignard reagent (from 24 hours to 50 minutes) and to increase the conversion by a factor of 5 (Adewuyi 2001).

The other group consists of reactions which do not proceed at ambient conditions without ultrasound or some other energy (such as heat, UV radiation) being applied. The reactions of this group can be subdivided into six classes (Margulis 2004):

- REDOX reactions in a water medium occurring between solutes and the products of water dissociation under ultrasonic waves (Adewuyi 2001).
- Reactions which occur inside a cavitation bubble filled with dissolved gas or/and vapour of a liquid medium (see Chapter 4; Henglein 1985; Mead, Sutherland, and Verrall 1976).
- Chain reactions in solution initiated by radicals produced from dissociation of a component in the cavitation bubble (not by radicals produced from the sonolytic decomposition of water) (see Chapter 5, Section 5.2; Troia et al. 2006).
- Reactions resulting in polymerization or degradation of polymers (Donaldson, Farrington, and Kruus 1979; Kruus 1983; Cataldo 2000; Wang and Cheung 2005).
- Initiation of an explosion by ultrasound (Margulis 2004).

- Reactions in organic systems (not involving radicals produced from water decomposition) (Mizukoshi et al. 1999; Hart, Fischer, and Henglein 1990a; Suclick et al. 1983).

For such reactions, the efficiency of any process is judged by the relation of costs of produced products and used energy.

8.2. Efficiency of Sonochemical Process

In order to estimate the efficiency of a sonochemical process, a value called the sonochemical yield (SY) can be introduced (Berlan and Mason 1992). In general, SY is defined as the ratio of the chemical effect (the amount of generated products in mole or gram) to the power input (such as Watt, Joules) per unit of time. The energy conversion in a sonochemical process has to be considered in detail in order to understand the concept of SY (Figure 8.1).

The ultrasonic equipment transforms electrical power into vibrational (ultrasonic) energy that is mechanical energy (Berlan and Mason 1992). However, output power produced by the ultrasonic system is lower than input power due to electrical and heating losses occurring in the transducer. Then, one part of mechanical energy transmitted into the sonicating medium produces cavitation as another part of mechanical energy is wasted due to heat, attenuation, reflection and coupling losses. Nevertheless, not all of the cavitational energy produces the chemical effect. Some of the cavitational energy dissipates due to reflection and attenuation, whereas some energy is spent due to heating losses. So only the remaining cavitational energy produces the desired chemical effects.

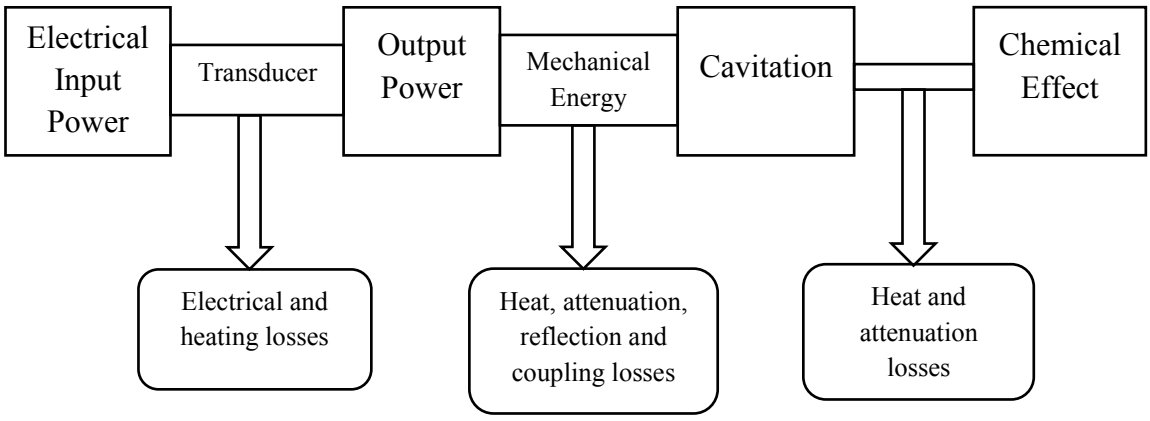

Figure 8.1. Energy conversion in a sonochemical process

So it can be seen that the energy efficiency of the sonochemical process is the main concern determining usage of an ultrasonic application on a large scale.

In view of information presented above, the efficiency of sonochemical reduction of CO_2 is studied. As is pointed out above, the estimation of any sonochemical process can be considered as a ratio of produced products to the amount of used energy. An ultrasonic technique of CO_2 reduction using low intensity and high-power ultrasound is a very energy-intensive process. Thus, the cost of electrical energy can be considered as the main barrier which restricts the creation of technology in the commercial scale. In the case of CO_2 utilization, the estimation of the efficiency of sonochemical reduction of CO_2 can be examined through the ratio of utilized and produced CO_2 during the process ($E_{CO2Utilization}$). In other words, the technique of sonochemical reduction of CO_2 in order to be considered "efficient" must obey a simple rule, according to which the amount of utilized CO_2 must exceed the amount of CO_2 produced by the technology per unit of time (Equation 8.1):

$$E_{CO_2Utilization} = \frac{CO_{2(utilized)}}{CO_{2(produced)}} > 1 \qquad \text{[Eqn. 8.1]}$$

8.3. CO_2 Emissions in the Energy Generation Sector

In order to estimate the effectiveness of the process of sonochemical reduction of CO_2 some additional information on the CO_2 global situation must be taken into account. The process of generating electricity is the largest source of CO_2 emissions and, in general, it is responsible for about 25 – 30% of all CO_2 released in the atmosphere by human activity (on average for USA and China which are responsible for more than 50 % of CO_2 emissions produced because of electricity generation).

Figures 8.2 and 8.3 present the percentage of electrical energy generated by different methods for China and USA during 2009. It can be clearly seen that 82 % of electricity in China is produced by the conventional thermal sources. This explains why China emits 42% more CO_2 per unit of electricity than USA[2].

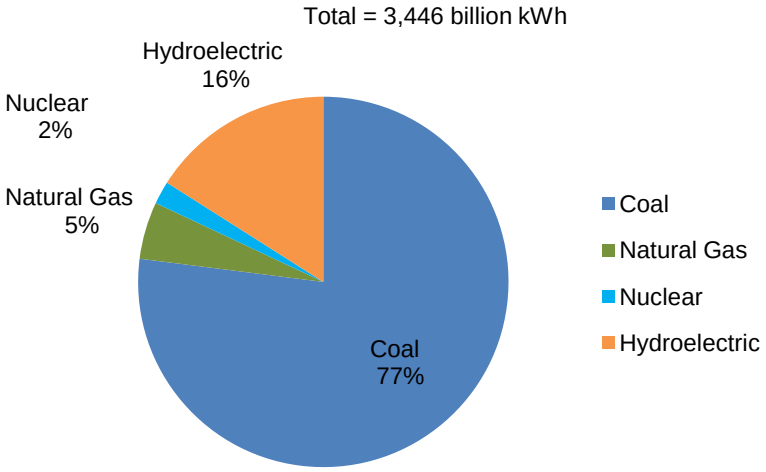

Figure 8.2. China electric power industry net generation, 2009

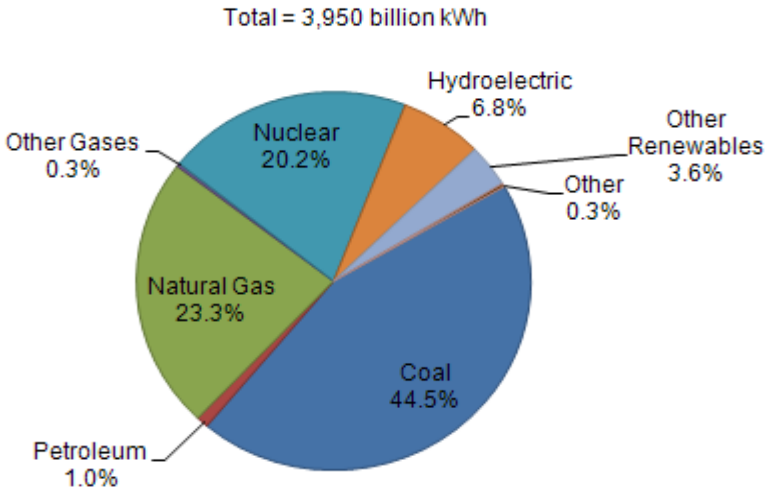

Figure 8.3. US electric power industry net generation, 2009

The amount of emitted CO_2 depends directly on methods of energy generation. Table 8.1 reveals the quantity of released CO_2 for one kilowatt-hour of electricity produced by major power generation methods.

Table 8.1. The amount of released CO_2 in gram per 1 kilowatt-hour by major power generation methods

Source of information	Method of power generation						
	Coal power plant	Gas-fired power plant	Nuclear power plant	Hydroelectric power plant	Oil power plant	Wind power plant	Solar power plant/ PV cells
Hertwich et al. (2008)	1150	885	13	3	810	48	105
ADEME Carbon Inventory (A tool for companies and office activities 2004)	900	430	6	4	-	12.5	105
Krewitt et al. (1997)	815	362	20	-	935	7	53
UK SDC (The role of nuclear power in a low carbon economy 2006)	891	356	16	-	-	-	-
Meier (2002)	974	469	15	-	-	14	39
CRIEPE (Energy Technology Life Cycle Analysis that Takes CO_2 Emission Reduction Into Consideration. 1995)	990	653	21	18	733	37	59
Paul Scherrer Institute (Dones, Heck, and Hirschberg 2003)	949	485	8	3	519	14	79
UK Energy Review (The Energy Challenge 2006)	755	385	11-22	-	-	11-37	-
Vattenfall AB (Vattenfall"s Life Cycle Studies of Electricity 1999)	980	450	6	3	820	6	50
Average	**934**	**497**	**13-14**	**6**	**763**	**20**	**70**

Using the data presented above (Figures 8.2, 8.3 and Table 8.1) it can be easily calculated that in order to produce one kilowatt-hour of energy on average from 546

to 745 grams of CO_2 is released. However, according to the best results on sonochemical reduction obtained during this research approximately 5.54 μmol/l of CO_2 can be utilized using 60 W of electrical energy (according to Chapter 5, Figure 5.1, assuming that CO_2 was reduced into CO only). Consequently, 1 kWh of energy will be enough to reduce approximately 92.35 μmol/l of CO2. In other words, applying one kWh of electrical energy it was possible to chemically utilize approximately 0.00406 grams of CO_2 at experimental conditions investigated and ultrasonic equipment used. Nevertheless, it can be seen that the amount of CO_2 reduced is completely negligible to the amount of assumedly produced CO_2 during the utilization process (due to consumption of 1 kWh of electricity). Moreover, during this research and according to other results of CO_2 sonolysis (Chapter 4) it is shown that low experimental temperature is required in order to provide higher rates of CO_2 reduction. Therefore, additional energy is needed to be spent in order to maintain the required experimental temperature of the process.

8.4. Conclusion

It is shown that the employment of sonochemical reduction of CO_2 as a technique for chemical utilization of CO_2 is extremely inefficient from an economical and practical point of view. This process is very energy inefficient and requires a strict control of experimental conditions. Moreover, even though it was experimentally obtained that the sonochemical reduction of CO_2 takes place in different sonicating medium, the rates of the CO_2 sonolysis are negligibly low for considering it as a technology.

Chapter 9. Conclusions

This thesis presents research devoted to the estimation of the efficiency of using ultrasonic energy for the chemical utilization of CO_2. The process of sonochemical reduction of CO_2 is studied under various experimental conditions. Different sonicating media and reagents are investigated in order to find the best rates of the CO_2 chemical conversion.

The main conclusion of this work was that chemical utilization of CO_2 by irradiation of ultrasonic waves may be possible, but may not be practically reasonable because of strict reaction conditions and huge energy expenses. However, the sonochemical technique has surplus values. For example, H_2 was also obtained along with CO from sonolysis of CO_2 and it is known that CO and H_2 are syngas and that they react to CH_3OH, a typical C_1 compound.

9.1. Sonochemical Reduction of CO_2 at Low Hydrostatic Pressure Conditions

At the first part of the research, a novel pilot-plant sonochemical reactor had been developed under this study in order to examine the ways of chemical utilization of CO_2 using ultrasonic irradiation. A low-frequency, high-intensity ultrasonic probe system served as a source of ultrasound. In this case, an importance of the design of the reactor system, which implied a circulation of a sonicating medium during the process of sonication along with the comprehensive cooling system, comes out. Such construction provided an excellent temperature control of a reaction mixture and enabled to practically illuminate the main disadvantage of the probe systems such as the poor temperature control. So this provided the opportunity of the uninterrupted use of ultrasound during sonolysis.

In Chapter 4, we demonstrated the potential of the low-frequency, high-power, pilot-plant sonochemical reactor for the CO_2 chemical utilization. The reduction of CO_2 was proven to be possible in aqueous and organic systems as traces of CO were detected in a number of tests at specified experimental conditions. CO_2 conversion rates were found to be dependant not only on the concentration of CO_2 in an atmospheric gas and ultrasonic power density but also on physical properties of sonicating mediums. On the other hand, the degradation of such compounds as n-

pentane, n-heptane, methanol and methyl iodide as by-processes occurring during the CO_2 reduction was investigated.

During the course of these experiments we have extensively investigated the possibility of sonochemical reduction of CO_2 in different sonicating media under low hydrostatic pressure conditions (0.2-0.3 MPa). In contrast to many research papers the pragmatic research work looked at all aspects of the importance of considering several physical, chemical and macroscopic aspects for the application of ultrasound to chemical processes. This work confirmed some of the previous results that CO_2 dissolved in water can be reduced to CO and CH_4 by sonolysis and that the lower concentration of CO_2 in an atmospheric gas provides higher rates of CO_2 reduction.

For the first time, it was experimentally demonstrated that liquid hydrocarbons can be also considered as sonicating medium for CO_2 sonolysis. Sonochemical reduction of CO_2 in a heptane medium is achieved at specified experimental conditions, however, the rates of reduction is not as large as when sonolysis performed in aqueous medium. On the other hand, reduction of CO_2 was not demonstrated when n-pentane was considered as a sonicating medium. Thus, it was stated that physical parameters of liquid hydrocarbons used as sonicating media are extremely important at the process of the CO_2 sonochemical reduction. Also, it was demonstrated that the rate of sonolysis of pure hydrocarbons is much lower than that in sonolysis of hydrocarbons in aqueous medium. Moreover, sonolysis of heptane was successfully conducted and the absence of C_2H_2 in products was the main difference from some results on sonolysis of hydrocarbons found in the literature.

Sonochemical reduction of CO_2 in CH_3OH medium was studied. According to the results obtained, CH_3OH was found to be an inefficient medium for CO_2 chemical fixation. Also, the idea of CO_2 fixation in the synthesis of dimethyl carbonate from CH_3OH and CO_2 using ultrasonic irradiation as an energy source was not successful as no traces of dimethyl carbonate were detected. Moreover, it was shown that methyl iodide, used as methyl radicals‟ promoter, undergoes a thermal rather than sonolytic decomposition with formation of products similar to ones obtained from the methyl iodide pyrolysis.

9.2. Sonochemical Reduction of Dense-Phase and Supercritical CO_2

At the second part of the research, a high-pressure sonochemical cell was developed in order to examine the possibility of sonochemical reduction of CO_2 at both liquefied and supercritical states. The system of a high-pressure pump – gas booster was employed in order to transfer the required amount of gases into liquid state. The method based on the Peng-Robinson EOS using the Aspen HYSYS computer software in order to estimate the required amount gas mixtures at specified experimental conditions was exploited.

In Chapter 6, the attempts to perform the chemical utilization of liquefied CO_2/Ar, CO_2/H_2 and CO_2/CH_4 mixtures were demonstrated. Although, the cavitation phenomenon appears to occur at such conditions, no sonochemical reactions were initiated. Furthermore, investigation on sonolysis of supercritical mixture of CO_2/CH_4 did not reveal the possibility of the sonochemical reactions to occur at such condition due to the absence of transient cavitation at all.

9.3. Ultrasound-Assisted Oxidation of Sulphur Containing Compounds by Potassium Permanganate

The last part of the research was devoted to investigation of the effect of ultrasound irradiation on the process of oxidation of sulphur containing compounds by potassium permanganate.

Chapter 6 presents experimental work UAODS of thiols and disulfides contained in condensate by $KMnO_4$. The results of investigation did not show an enhancement of the rate of desulfurization when ultrasound was applied to accelerate the rate of oxidation. Moreover, it was shown that the effect of ultrasound in oxidation consists in increasing the oxidating ability of an oxidizer (in case if the last chosen correctly).

Reference List

Adewuyi, Y. G., (2001), „Sonochemistry: environmental science and engineering applications", *Industrial & Engineering Chemistry Research,* 40, 4681-4715.

Adewyui, Y. G., (2005), „Sonochemistry in environmental remediation. 2. Heterogeneous sonophotocatalytic oxidation processes for the treatment of pollutants in water", *Environmental Science & Technology,* 39, 8557- 8570.

Anbar, M., and I. Pecht, (1964), „On the sonochemical formation of hydrogen peroxide in water", *Journal of Physical Chemistry,* 68, 352-355.

Apfel, R. E., (1972), „The tensile strength of liquids", *Scientific American,* 227 (6), 58-71.

Aresta, M., ed., (2003), „*Carbon dioxide recovery and utilization*", Norwell: Kluwer Academic Publishers

Aribike, D. S., and A. A. Susu, (1988), „Kinetics and mechanism of the thermal cracking of n-heptane", *Thermocimica Acta,* 127, 247-258.

Aronowitz, D., D. W. Naegeli, and I. Glassman, (1977), „Kinetics of the pyrolysis of methanol", *The Journal of Physical Chemistry,* 81 (25), 2555-2559

Bajus, M., V. Vesely, P. A. Leclercq, and J. A. Rijks, (1979), „Stream cracking of hydrocarbons. 1. Pyrolysis of heptane", *Industrial & Engineering Chemistry Product Research and Development,* 18 (1), 30-37.

Balanchandran, S., S. E. Kentish, R. Mawson, and M. Ashokkumar, (2006), „Ultrasonic enhancement of the supercritical extraction from ginger", *Ultrasonics Sonochemistry,* 13, 471-479.

Beckman, E. J., (2004), „Supercritical and near-critical CO2 in green chemical synthesis and processing", *Journal of Supercritical Fluids,* 28, 121-191.

Behrend, O., and H. Schubert, (2001), „Influence of hydrostatic pressure and gas content on continuous ultrasound emulsification", *Ultrasonics Sonochemistry,* 8, 271-276.

Berlan, J., F. Trabelsi, H. Delmas, A. M. Wilhelm, and J. F. Petrignani, (1994), „Oxidative degradation of phenol in aqueous media using ultrasound", *Ultrasonics Sonochemistry,* 1 (2), S97-S102.

Berlan, J., and T. J. Mason, (1992), „Sonochemistry: from research laboratories to industrial plants", *Ultrasonics,* 30 (4), 203-212.

Billaud, F., and E. Freud, (1986), „n-Decane pyrolysis at high temperature in a flow reactor", *Industrial and Engineering Chemistry Fundamentals,* 25 (3), 433-443.

Brohult, S., (1937), „Splitting of the haemocyanin molecule by ultrasonic waves", *Nature,* 140 (3549), 805.

Butler, E. T., and M. Polanyi, (1943), „Rates of pyrolysis and bond energies of substituted organic iodides (Part 1)", *Transactions of the Faraday Society,* 39, 19-36.

Buttner, J., M. Gutierrez, and A. Henglein, (1991), „Sonolysis of water-methanol mixtures", *Journal of Physical Chemistry,* 95, 1528-1530.

Calatayud, M., J. Andres, A. Beltran, (1999), „A theoretical analysis of adsorption and dissociation of CH_3OH on the stoichiometric $SnO_2(110)$ surface", *Surface Science,* 430, 213-222.

Cao, G. M., M. Sheng, W. F. Niu, Y. L. Fei, and D. Li, (2009), „Regeneration and reuse of iron catalyst for Fenton-like reactions", *Journal of Hazard Materials,* 172 (2-3), 1446-1449.

CARMA, n.d. http://carma.org/dig/show/world+country (accessed January 27, 2011)

Carson, A. S., W. Carter, and J. B. Pedley, (1961), „The thermochemistry of reductions caused by lithium aluminium hydride. I. The C-I bond dissociation energy in CH_3I", *Proceedings of the Royal Society of London, Series A, Mathematical and Physical Sciences,* 260 (1303), 550-557.

Cataldo, F., (2000), „Ultrasound-induced cracking and pyrolysis of some aromatic and naphthenic hydrocarbons", *Ultrasonics Sonochemistry,* 7, 35-43.

Chakraborty, J. P., and D. Kunzru. 2009. High pressure pyrolysis of n-heptane. *Journal of Analytical and Applied Pyrolysis* 86: 44-52.

China. Electricity. 2009. U.S. Energy information administration http://www.eia.doe.gov/cabs/China/Electricity.html

Chiou, C. T., (2002), *Partition and adsorption of organic compounds in environmental systems*, Hoboken, NJ: Wiley-Interscience

Chirta, S., K. Paramasivan, P. K. Sinha, and K. B. Lal, (2004), „Ultrasonic treatment of liquid waste containing EDTA", *Journal of Cleaner Production,* 12, 429-435.

Chun, Y., Y. G. He, and J. H. Zhu, (2001), „Microwave-assisted synthesis of dimethyl carbonate", *Reaction Kinetics and Catalysis Letters,* 74 (1), 23-27.

Cnossen, I., M. J. Harris, N. F. Arnold, and E. Yigit, (2009), „Modelled effect of changes in the CO_2 concentration on the middle and upper atmosphere: Sensitivity to gravity wave parameterization", *Journal of Atmospheric and Solar-Terrestrial Physics,* 71, 1484-1496.

Collins, F. M., A. R. Lucy, and C. Sharp, (1997), „Oxidative desulfurization of oils via hydrogen peroxide and heteropolyanion catalyst", *Journal of Molecular Catalysis A: Chemical,* 117, 397-403.

Dahnke, S. W., and F. J. Keil, (1999), „Modeling of linear pressure fields in sonochemical reactors considering an inhomogeneous density distribution of cavitation bubbles", *Chemical Engineering Science,* 54 (13-14), 2865-2872.

Dai, W. L., S. L. Luo, S. F. Yin, and C. T. Au, (2009), „The direct transformation of carbon dioxide to organic carbonates over heterogeneous catalysts", *Applied Catalysis A: General,* 366, 2-12.

Dai, Y., D. Zhao, and Y. Qi, (2010), „Sono-desulfurization oxidation reactivities of FCC diesel fuel in metal ion/H_2O_2 system", *Ultrasonics Sonochemistry* (in press).

Dai, Y., Y. Qi, and D. Zhao, and H. Zhang, (2008), „An oxidative desulfurization method using ultrasound/Fenton‟s reagent for obtaining low and/or ultra-low sulphur diesel fuel", *Fuel Processing Technology,* 89, 927-932.

Dai, Y., Y. Qi, and D. Zhao, (2009), „Effect of various sono-oxidation parameters on the desulfurization of diesel oil", *Petroleum Chemistry,* 49 (5), 436-441.

David, B., and P. Boldo, (2008), „A statistical thermodynamic approach to sonochemical reactions", *Ultrasonics Sonochemistry,* 15, 78-88.

Davidson, N., and T. Carrington, (1952), „Iodine inhibition in the flash photolysis of methyl iodide", *Journal of the American Chemical Society,* 74, 6277-6279.

De P. R. Silva, V., J. H. B. C. Campos, M. T. Silva, and P. V. Azevedo, (2010), „Impact of global warming on cowpea bean cultivation in northeastern Brazil", *Agricultural Water Management,* 97 (11), 1760-1768.

De Visscher, A., and H. van Langenhove, (1998), „Sonochemistry of organic compounds in homogeneous aqueous oxidising systems", *Ultrasonics Sonochemistry,* 5, 87-92.

Degrois, M., and P. Baldo, (1974), „A new electrical hypothesis explaining sonoluminescence, chemical actions and other effects produced in gaseous cavitation", *Ultrasonics,* 12, 25-28.

Deshpande, A., A. Bassi, and A. Prakash, (2005), „Ultrasound-assisted, base-catalyzed oxidation of 4, 6 – dimethyldibenzothiophene in a biphasic diesel-acetonitrile system", *Energy Fuels,* 19 (1), 28-34.

Donaldson, D. J., M. D. Farrington, and P. Kruus, (1979), „Cavitation-induced polymerization of nitrobenzene", *Journal of Physical Chemistry,* 83 (24), 3130-3135.

Dones, R., T. Heck, and S. Hirschberg, (2003), „Greenhouse Gas Emissions From Energy Systems: Comparison and Overview", *Paul Scherrer Institut Annual Report 2003 Annex IV* (Table 2, page 38), Villigen, Switzerland.
http://gabe.web.psi.ch/pdfs/Annex_IV_Dones_et_al_2003.pdf

Duck, F. A., H. C. Starritt, G. R. ter Haar, M. J. Lunt, (1989), „Surface heating of diagnostic ultrasound transducers", *The British Journal of Radiology,* 62, 1005-1013.

'Electric power industry 2009: Year in review', (2009), U.S. Energy information administration. http://www.eia.doe.gov/cneaf/electricity/epa/epa_sum.html

'Energy Technology Life Cycle Analysis that Takes CO_2 Emission Reduction Into Consideration', (1995), Central Research Institute of Electric Power Industry, Japan, Annual Research Report. http://www.webcitation.org/query?url=http://criepi.denken.or.jp/en/e_publication/a1995/seika95kankyo23E.html&date=2008-11-01

Entezari, M. H., P. Kruus, and R. Otson, (1997), „The effect of frequency on sonochemical reactions. III: Dissociation of carbon disulphide", *Ultrasonics Sonochemistry*, 4, 49-54.

Entezari, M. H., and P. Kruus, (1994), „Effect of frequency on sonochemical reactions. I: Oxidation of iodide", *Ultrasonics Sonochemistry,* 1 (2), S75-S79.

Entezari, M. H., and P. Kruus, (1996), „Effect of frequency on sonochemical reactions II. Temperature and intensity effects", *Ultrasonics Sonochemistry,* 3, 19-24.

Fang, S., and K. Fujimoto, (1996), „Direct synthesis of dimethyl carbonate from carbon dioxide and methanol catalyzed by base", *Applied Catalysis A: General,* 142, L1-L3.

Fitzgerald, M. E., V. Griffing, and J. Sullivan, (1956), „Chemical effects of ultrasonics "Hot spot" chemistry", *Journal of Chemical Physics,* 25 (5), 926-933.

Flannigan, D. J., and K. S. Suslick, (2005), „Plasma formation and temperature measurement during single-bubble cavitation", *Nature,* 434, 52-55.

Flint, E. B., and K. S. Suslick, (1991), „The temperature of cavitation", *Science,* 253, 1397-1399.

Flynn, H. G, (1964), „Physics of acoustic cavitation in liquids", In: W. P. Mason, ed., *Part B of Physical Acoustics*, 57-172, New York: Academy Press.

Fouilloux, P., (1983), „The nature of Raney nickel, its adsorbed hydrogen and its catalytic activity for hydrogenation reactions (review)", *Applied Catalysis,* 8 (1), 1-42.

Frenkel, Ya. I., (1940), „Electrical phenomena connected with cavitation caused by ultrasonic oscillations in a liquid", *Russian Journal of Physical Chemistry,* 14, 305-308.

Friedmann, N., H. H. Bovee, and S. L. Miller, (1970), „High temperature pyrolysis of C_1 to C_4 hydrocarbons", *Journal of Organic Chemistry,* 35 (10), 3230-3232.

Fujita, S., B. M. Bhanage, Y. Ikushima, and M. Arai, (2001), „Synthesis of dimethyl carbonate from carbon dioxide and methanol in the presence of methyl iodide and base catalyst under mild conditions: effect of reaction conditions and reaction mechanism", *Green Chemistry,* 3, 87-91.

Gasc, F., S. Thiebaud-Roux, and Z. Mouloungui, (2009), „Methods for synthesis diethyl carbonate from ethanol and supercritical carbon dioxide by one-pot or two-step reactions in the presence of potassium carbonate", *The Journal of Supercritical Fluids,* 50, 46-53.

Gogate, P. R., and A. B. Pandit, (2007), „Design of cavitational reactors", *Modeling of Process Intensification*, ed. F. J. Keil, 226-277, Weinheim: Wiley VCH Publisher.

Greenspan, M., and C. E. Tschiegg, (1967), *Journal of Research of the National Bureau of Standards, Section C,* 71, 229

Griffing, V., (1952), „The chemical effects of ultrasonics", *Journal of Chemical Physics,* 20 (6), 939-942.

Guo, X. C., Z. F. Qin, G. F. Wang, and J. G. Wang, (2008), „Critical temperatures and pressures of reacting mixture in synthesis of dimethyl carbonate with methanol and carbon dioxide", *Chinese Chemical Letters,* 19, 249-252.

Harada, H., (1998), „Sonochemical reduction of carbon dioxide", *Ultrasonics Sonochemistry,* 5 (2), 73-77.

Harada, H., C. Hosoki, and M. Ishikani., (2003), „Sonophotocatalysis of water in a CO_2-Ar atmosphere", *Journal of Photochemistry and Photobiology A: Chemistry,* 160, 11-17.

Harkness, A. C., and F. E. Murray, (1970), „Oxidation of methyl mercaptan with molecular oxygen in aqueous solution", *Atmospheric Environment,* 4, 417-424, New York: Pergamon Press Inc.

Hart, E. J., C.-H. Fischer, and A. Henglein, (1990a), „Pyrolysis of acetylene in sonolytic cavitation bubbles in aqueous solution", *Journal of Physical Chemistry,* 94, 284-290.

Hart, E. J., C.-H. Fischer, and A. Henglein, (1990b), „Sonolysis of hydrocarbons in aqueous solution", *Radiation Physics and Chemistry,* 36 (4), 511-516.

Harvey, E. N., (1939), „Sonoluminescence and sonic chemiluminescence", *Journal of the American Chemical Society,* 61 (9), 2392-2398.

Hearn, D., G. R. Gildert, and H. M. Putman, (1996 Jun, 20), „Process for the removal of mercapntans and hydrogen sulphide from hydrocarbon stream", World Intellectual Property Organization, WO/1996/018704.

Henglein, A., (1985), „Sonolysis of carbon dioxide, nitrous oxide and methane in aqueous solution", *Z. Naturforsch,* 40B, 100-107.

Henglein, A, (1987), „Sonochemistry: historical developments and modern aspects", *Ultrasonics,* 25, 6-16.

Hertwich, E. G., M. Aaberg, B. Singh, and A. H. Stromman, (2008), „Life-cycle assessment of carbon dioxide capture for enhanced oil recovery", *Chinese Journal of Chemical Engineering,* 16 (3), 343-353.

Hilgenfeldt, S., M. P. Brenner, S. Grossman, and D. Lohse, (1998), „Analysis of Rayleigh-Plesset dynamics for sonoluminescing bubbles", *Journal of Fluid Mechanics,* 365, 171-204.

Hochard-Poncet, F., P. Delichere, B. Moraweck, and H. Jobic, (1995), „Surface composition, structural and chemisorptive properties of Raney nickel catalysts", *Journal of the Chemical Society, Faraday Transactions,* 91, 2891-2897.

Hoffmann, M. R., I. Hua, and H. Hochemer, (1995), „Sonolytic hydrolysis of p-Nitrophenyl acetate: the role of supercritical water", *Journal* of Physical Chemistry, 99, 2335-2342.

Hou, Z., B. Han, Z. Liu, T. Jiang, and G. Yang, (2002), „Synthesis of dimethyl carbonate using CO_2 and methanol: enhancing the conversion by controlling the phase behaviour", *Green Chemistry,* 4, 467-471.

'Human-Related Sources and Sinks of Carbon Dioxide', (2010), U.S. Environmental agency. http://www.epa.gov/climatechange/emissions/co2_human.html

Hunicke, R. L., (1990), „Industrial applications of high power ultrasound for chemical reactions", *Ultrasonics,* 28, 291-294.

Ibisi, M., and B. Brown, (1967), „Variation of the relative intensity of cavitation with temperature", *Journal of the Acoustic Society of America,* 41 (3), 568-572.

'International energy outlook', (2007), US Department of Energy, Washington, DC, USA

IPCC Fourth assessment report, (2007), „*Climate change 2007: Mitigation of climate change',* Cambridge University Press, Cambridge, United Kingdom and New York, NY, USA

IPCC Second assessment report, (1996), „*Climate change 1995. The science of climate change',* Cambridge University Press, Cambridge, GB

Kabe, T., A. Ishihara, and H. Tajima, (1992), „Hydrodesulfurization of sulphur-containing polyaromatic compounds in light oil", *Industrial & Engineering Chemistry Research,* 31, 1577-1580.

Khoroshev, G. A., (1963), „Collapse of vapour-air cavitation bubbles", *Soviet Physics-Acoustics,* 9 (3), 275-279.

Kirpalani, D. M., and K. J. McQuinn. 2006. Experimental quantification of cavitataion yield revisited: focus on high frequency ultrasound reactors. *Ultrasonics Sonochemistry* 13: 1-5.

Kossiakoff, A., and F. O. Rice, (1943), „Thermal decomposition of hydrocarbons, resonance stabilization and isomerization of free radicals", *Journal of the American Chemical Society,* 65, 590-595.

Krewitt, W., P. Mayerhofer, R. Friedrich, A. Trukenmuller, T. Heck, A. Crebmann, F. Raptis, F. Kaspar, J. Sachau, K. Rennings, J. Diekmann, and B. Praetorius, (1997), *Externalities of Energy European Commission Research Project*, ExternE National Implementation Germany http://web.archive.org/web/20061007113502/externe.jrc.es/ger.pdf

Kruus, P., (1983), „Polymerization resulting from ultrasonic cavitation", *Ultrasonics,* 21 (5), 201-204.

Kudo, K., and K. Komatsu, (1999), „Selective formation of methane in reduction of CO_2 with water by Raney alloy catalyst", *Journal of Molecular Catalysis A: Chemical,* 145, 257-264.

Kujipers, M. W. A., D. van Eck, M. F. Kemmere, and J. T. F. Keurentjes, (2002), „Cavitation-induced reactions in high-pressure carbon dioxide", *Science,* 298, 1969-1971.

Kuijpers, M. W. A., M. F. Kemmere, and J. T. F. Keurentjes, (2004), *Encyclopedia of Polymer Science and Technology*, „Ultrasound-induced radical polymerization", New York: John Wiley & Sons.

Kumaran, S. S., M.-C. Su, K. P. Lim, and J. V. Michael, (1996), „The thermal decomposition of C_2H_5I", *Symposium (International) on Combustion,* 26 (1), 605-611.

Lee, G. D., M. J. Moon, J. H. Park, S. S. Park, and S. S. Hong, (2005), „Raney Ni catalysts derived from different alloy precursors part II. CO and CO_2 methanation activity", *Korean Journal of Chemical Engineering,* 22 (4), 541-546.

Lepoint, T., and F. Mullie, (1994), „What exactly is cavitation chemistry?“, *Ultrasonics Sonochemistry,* 1 (1), S13-S22.

Lepoint-Mullie, F., D. de Pauw and T. Lepoint, (1996), „Analysis of the „new electrical model“ of sonoluminescence“, *Ultrasonics Sonochemistry* 3, 73-76.

Li, H., and Y. Xu, (2001), „Liquid phase benzene hydrogenation to cyclohexane over modified Ni-P amorphous catalysts“, *Materials Letters,* 51, 101-107.

Lifshitz, A., and M. Frenklach, (1975), „Mechanism of the high temperature decomposition of propane“, *Journal of Physical Chemistry,* 79 (7), 686-692.

Lyman, J. L., and R. J. Jensen, (2001), „Chemical reactions occurring during direct solar reduction of CO_2“, *The Science of the Total Environment,* 277, 7-14.

Margulis, M. A., (1981), „Study of electrical phenomena related to cavitation I. Electrical theories of chemical and physicochemical action of ultrasound“, *Russian Journal of Physical Chemistry,* 55, 154-158

Margulis, M. A., (1984), „*Fundamentals of Acoustic Chemistry',* Moscow: Vysshaya Shkola (in Russian)

Margulis, M. A., (1985), *Russian Journal of Physical Chemistry,* 59, 1497 (In Russian)

Margulis, M. A., (1992), „Fundamental aspects of sonochemistry“, *Ultrasonics,* 30 (3), 152-155.

Margulis, M. A., (1994), „Fundamental problems of sonochemistry and cavitation“, *Ultrasonics Sonochemistry,* 1 (2), S87-S90.

Margulis, M. A., (2002), „Sonochemistry as a new promising area of high energy chemistry“, *High Energy Chemistry,* 38 (3), 135-142.

Margulis, M. A., and I. M. Margulis, (1999), „Theory of local electrification of cavitation bubbles: new approaches“, *Ultrasonics Sonochemistry,* 6, 15-20.

Mason, T. J., (1992), „Industrial sonochemistry: potential and practicality“, *Ultrasonics,* 30 (3), 192-196.

Mason, T. M., and J. P. Lorimer, (2002), „*Applied Sonochemistry: Uses of Power Ultrasound in Chemistry and Processing*“, Weinheim: Wiley-VCH Verlag GnvH.

Mc Geehan, J. A., (2004), „Diesel engine oils for a new era of low emission vehicles: status of oil category for 2007“, In: *14th International Colloquium Tribology and Lubrication Engineering,* 31–36, Stuttgart/Ostfildern, Germany

McNamara III, W. B., Y. T. Didenko, and K. S. Suslick, (1999), „Sonoluminescence temperatures during multi-bubble cavitation“, *Nature,* 401, 772-775.

Mead, E. L., R. G. Sutherland, and R. E. Verrall, (1976), „The effect of ultrasound on water in the presence of dissolved gases“, *Canadian Journal of Chemistry,* 54, 1114-1120.

Mei, H., B. W. Mei, and T. F. Yen, (2003), „A new method for obtaining ultra-low sulphur diesel fuel via ultrasound assisted oxidative desulfurization“, *Fuel,* 82, 405-414.

Meier, P. J., (2002), „Life-Cycle Assessment of Electricity Generation Systems and Applications for Climate Change Policy Analysis“, Ph.D. thesis, University of Wisconsin-Madison. http://fti.neep.wisc.edu/pdf/fdm1181.pdf

Mello, P. A., F. A. Duarte, M. A. G. Nunes, M. S. Alencar, E. M. Moriera, M. Korn, V. L. Dressler, and E. M. M. Flores, (2009), „Ultrasound-assisted oxidative process for sulphur removal from petroleum product feedstock“, *Ultrasonics Sonochemistry,* 16, 732-736.

Merouani, S., O. Hamdaoui, F. Saoudi, and M. Chiha, (2010), „Influence of experimental parameters on sonochemistry dosimetries: KI oxidation, Fricke reaction and H_2O_2 production“, *Journal of Hazardous Materials,* 178, 1007-1014.

Meyer, R. T., (1968), „Flash photolysis and time-resolved mass spectrometry. II. Decomposition of methyl iodide and reactivity of $I(^2P_{½})$ atoms“, *Journal of Physical Chemistry,* 72 (5), 1583-1591.

Mizukoshi, Y., H. Nakamura, H. Bandow, Y. Maeda, and Y. Nagata, (1999), „Sonolysis of organic liquid: effect of vapour pressure and evaporation rate", *Ultrasonics Sonochemistry,* 6, 203-209.

Mohsen-Nia, M., H. Rasa, and S. F. Naghibi., (2010), „Experimental and theoretical study of surface tension of n-pentane, n-heptane, and some of their mixtures at different temperatures", *Journal of Chemical Thermodynamics,* 42, 110-113.

Moulton, K. J., S. Koritala, and E. N. Frankel, (1983), „Ultrasonic hydrogenation of soybean oil", *Journal of the American Oil Chemists' Society,* 60 (7), 1257-1258.

Murphy, D. B., R. W. Carroll, and J. E. Klonowski, (1997), „Analysis of products of high-temperature pyrolysis of various hydrocarbons", *Carbon,* 35 (12), 1819-1823.

Neppiras, E. A., (1980), „Acoustic cavitation", *Physics Reports (Review Section of Physics Letters),* 61 (3), 159-251.

Neppiras, E. A., and B. E. Noltingk, (1951), „Cavitation Produced by Ultrasonics: Theoretical Conditions for the Onset of Cavitation", *Proceedings of the Physical Society B,* 64, 1032-1038.

Nocca, L. J., M. Dorbon, and R. Padamsey, (2003), „Ultra-Low Sulfur Diesel with the PRIME-D Technology Package", *National Petrochemical & Refiners Association*, Annual Meeting

Noltingk, B. E., and E. A. Neppiras, (1950), „Cavitation produced by ultrasound", *Proceedings of the Physical Society B,* 63, 674-685.

Ondrey, G., I. Kim, and G. Parkinson, (1996), „Reactors for the 21st century", *Chemical Engineering,* June, 39-45.

Otsuki, S., T. Nonaka, N. Takashima, W. Qian, A. Ishihara, T. Imai, and T. Kabe, (2000), „Oxidative desulfurization of light gas oil and vacuum gas oil by oxidation and solvent extraction", *Energy Fuels,* 14 (6), 1232-1239.

Palmer, R. E., G. Ripperger, and J. Migliavacca, (2001), „Revamp your Hydrotreater to Manufacture Ultralow Sulfur Diesel", *National Petrochemical & Refiners Association*, Annual Meeting

Pant, K. K., and D. Kunzru, (1996), „Pyrolysis of n-heptane: kinetics and modelling", *Journal of Analytical and Applied Pyrolysis,* 36, 103-120.

Peng, D.-Y., and D.B. Robinson, (1976), „A New Two Constant Equation of State", *Industrial & Engineering Chemistry Fundamentals,* 15 (1), 59-64.

Perry, C. C., N. S. Faradzhev, T. E. Madey, and D. H. Fairbrother, (2007), „Electron stimulated reactions of methyl iodide coadsorbed with amorphous solid water", *Journal of Chemical Physics,* 126, 1-14.

Plesset, M. S., (1949), „The dynamics of cavitation bubbles", *Transactions ASME Journal of Applied Mechanics,* 16, 228-231

Pohanish, R. P., (2005), „*HazMat Data: For First Response, Transportation, Storage, and Security',* 2nd ed. Hoboken**,** New Jersey**:** J. Wiley & Sons

Raso, J., P. Manas, R. Pagan, and F. J. Sala, (1999), „Influence of different factors on the output power transferred into medium by ultrasound", *Ultrasonics Sonochemistry,* 5 (4), 157-162.

Lord Rayleigh, J. W. S., (1917), „On the pressure developed in a liquid during the collapse of a spherical cavity", *Philosophical Magazine,* 34, 94-98.

Reger. D. L., S. R. Goode, and D. W. Ball, (2010), „*Chemistry principles and practice*", 3rd ed. US: Brooks/Cole Cengage Learning, 357-358.

Richards, W. T., and A. L. Loomis, (1927), „The chemical effects of high frequency sound waves. I. A preliminary study", *Journal of American Chemical Society,* 49, 3086-3100.

Riesz, P., and T. Kondo, (1992), „Free radical formation induced by ultrasound and its biological implications", *Free Radical Biology & Medicine,* 13, 247-270.

Riesz, P., T. Kondo, and C. M. Krishna, (1990), „Sonochemistry of volatile and non-volatile solutes in aqueous solutions: e. p. r. and spin trapping studies", *Ultrasonics,* 28 (5), 295-303.

'*The role of nuclear power in a low carbon economy*", (2006), UK Sustainable Development Commission.http://www.sd-commission.org.uk/publications/downloads/SDC-NuclearPosition-2006.pdf

Saito, K., H. Tahara, O. Kondo, T. Yokubo, T. Higashihara, and I. Murakami, (1980), „The thermal gas-phase decomposition of methyl iodide", *Bulletin of the Chemical Society of Japan,* 53, 1335-1339.

Sakakura, T., J. C. Choi, and H. Yasuda, (2007), „Transformation of carbon dioxide", *Chemical Reviews,* 107, 2365-2387.

Saunders, O., S. Clift, and F. Duck, (2004), „Ultrasound transducer self heating: development of 3-D finite-elements models", *Journal of Physics: Conference Series 1*, 72-77.

Segebarth, N., O. Eulaerts, Y. Kegelaers, J. Vandercammen, and J. Reisse, (2002), „About the Janus double-horn sonicator and its use in quantitative homogenous sonochemistry", *Ultrasonics Sonochemistry,* 9 (2), 113-119.

Shiraishi, Y., and T. Hirai, (2004), „Desulfurization of vacuum gas oil based on chemical oxidation followed by liquid-liquid extraction", *Energy & Fuel* 18, 37-40.

Shu, H. Y., and M. C. Chang, (2005), „Decolorization effects of six azo dyes by O_3, UV/O_3 and UV/H_2O_2 processes", *Dyes and Pigments,* 65, 25-31.

Song, C., A. F. Gaffney, and K. Fujimoto, (2002), „*CO_2 conversion and utilization*", Washington: American Chemical Society

Souffie, R. D., R. R. Williams Jr., and W. H. Hamill, (1956), „Hot radical reactions in the photolysis of methyl iodide vapour", *The Journal of the American Chemical Society,* 78, 917-920.

Suclick, K. S., S. J. Doktycz, and E. B. Flint, (1990), „On the origin of sonoluminescence and sonochemistry", *Ultrasonics,* 28, 280-290.

Suslick, K. S., ed., (1988), „*Homogenous sonochemistry in ultrasound: it's chemical, physical and biological effects'*, 123-164, New York: VCH

Suslick, K.S., J. J. Gawlenowski, P. F. Schubert, and H. H. Wang, (1983), „Alkane Sonochemistry", *Journal of Physical Chemistry,* 87, 2299-2301.

Suslick, K. S., J. J. Gawienowski, P. F. Schubert, and H. H. Wang, (1984), „Sonochemistry in non-aqueous liquids", *Ultrasonics,* 22 (1). 33-36.

'Surface tension values of some common test liquids for surface energy analysis', http://www.surface-tension.de/

'Tables of Physical & Chemical Constants', Kaye&Laby, National Physical Laboratory, n.d. (accessed on January 27, 2011) http://www.kayelaby.npl.co.uk/general_physics/2_3/2_3_6.html

Tam, P. S., J. R. Kittrell, and J. W. Eldridge, (1990) Desulfurization of fuel oil by oxidation and extraction. 2. Kinetic modelling of oxidation reaction", *Industrial & Engineering Chemistry Research,* 29, 329-333.

'The Energy Challenge. Electricity Generation', (2006), UK Government http://webarchive.nationalarchives.gov.uk/+/http://www.berr.gov.uk/files/file32007.pdf

Thompson, L. H., and L. K. Doraiswamy, (1999), „Sonochemistry: science and engineering", *Industrial and Engineering Chemical Research*, 38, 1215 – 1249.

Thornycroft, J. I., and S.W. Barnaby, (1895), „S. W. Torpedo-boat destroyers", *Minutes of the Proceedings Institution of Civil Engineers,* 122 (4), 51-69.

'A tool for companies and office activities: the 'Carbon Inventory' of ADEME', (2004) http://www.manicore.com/anglais/missions_a/carbon_inventory.html

Troia, A., D. M. Ripa, R. Spagnolo, and V. Maurino, (2006), „Single bubble sonochemistry: decomposition of alkyl bromide and the isomerization reaction of maleic acid", *Ultrasonics Sonochemistry,* 13, 429-432.

Van Iersel, M. M., J. Cornel, N. E. Benes, and T. F. Keurentjes, (2007), „Inhibition of nonlinear acoustic cavitation dynamics in liquid CO_2“, *Journal of Chemical Physics,* 126, 1-8.

‘Vattenfall“s Life Cycle Studies of Electricity“, (1999), Vattenfall AB. http://barsebackkraft.se/files/lifecycle_studies.pdf

Wang, H., B. Lu, Q. H. Cai, F. Wu, and Y. K. Shan, (2005), „Synthesis of dimethyl carbonate from methanol and carbon dioxide catalyzed by potassium hydroxide under mild conditions“, *Chinese Chemical Letters,* 16 (9), 1267-1270 (In English)

Wang, R., and H. M. Cheung, (2005), „Ultrasound assisted polymerization of MMA and styrene in near critical CO_2“, *The Journal of Supercritical Fluids,* 33, 269-274.

Weissler, A., (1953), „Sonochemistry: the production of chemical charges with sound waves“, *Journal of the Acoustic Society of America,* 25 (4), 651-657.

Weissler, A., (1959), „Formation of hydrogen peroxide by ultrasonic waves: free radicals“, *Journal of the American Chemical Society,* 81 (5), 1077-1081.

Weissler, A., I. Pecht, and M. Abnar, (1965), „Ultrasound chemical effects on pure organic liquids“, *Science,* 150, 1288-1289.

Whillock, G. O. H., and B. F. Harvey, (1997), „Ultrasonically enhanced corrosion of 304L stainless steel I: The effect of temperature and hydrostatic pressure“, *Ultrasonics Sonochemistry,* 4 (1), 23-31.

Wood, R. W., and A. L. Loomis, (1927), „The physical and biological effects of high frequency sound waves of great intensity“, *Philosophical Magazine Series, 7* 4 (22), 417-436.

Wu, Z., and B. Ondruschka, (2010), „Ultrasound-assisted oxidative desulfurization of liquid fuels and its industrial application“, *Ultrasonics Sonochemistry,* 17, 1027-1032.

Yanagida, H., Y. Masubichi, K. Minagawa, T. Ogata, J. Takimoto, and K. Koyama, (1999), „A reaction kinetics model of water sonolysis in the presence of a spin-trap", *Ultrasonics sonochemistry,* 5, 133-139.

Yasui, K., T. Tuziuti, J. Lee, T. Kozuka, A. Towata, and Y. Iida, (2010), „Numerical simulations of acoustic noise with the temporal fluctuation in the number of bubbles", *Ultrasonics Sonochemistry,* 17, 460-472.

Yasui, K., T. Tuziuti, M. Sivakumar, and Y. Iida, (2005), „Theoretical study of single-bubble sonochemistry",*Journal of Chemical Physics,* 122, 1-12.

Zhou, Y., S. Hu, X. Ma, S. Liang, T. Jiang, and B. Han, (2008), „Synthesis of cyclic carbonates from carbon dioxide and epoxides over betaine-based catalysts", *Journal of Molecular Catalysis A: Chemical,* 284 (1-2), 52-57.

Every reasonable effort has been made to acknowledge the owners of copyright material. I would be pleased to hear from any copyright owner who has been omitted or incorrectly acknowledged.

Appendix A. Selection of Hydrostatic Pressure

Sonolysis of CO_2 in various liquids under elevated hydrostatic pressures (over 1.5 MPa) was carried out in order to select pressure conditions for investigation devoted to the sonochemical reduction of carbon dioxide (Chapter 4). Liquids such as water, methanol, 20% methanol solution, ethylene glycol and glycerol were used as sonicating mediums. After every test was conducted, the gaseous phases were analyzed in order to detect the products of sonolysis (Table A.1). The presence of sonolytic products in the gaseous phases was not confirmed by the GC-analysis.
Aluminum foil was used for determination of cavitational intensity at elevated pressures.

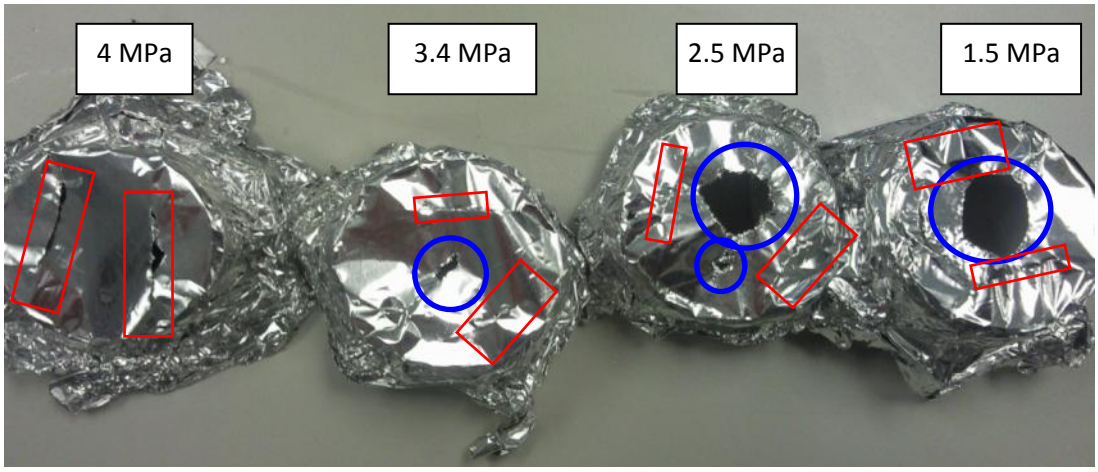

Figure A.1. Damaged aluminum foil from sonolysis of water under an Ar/CO_2 atmosphere at different hydrostatic pressure

Figure A.1 represents damaged aluminum foil pieces used for estimation of the cavitation phenomenon in water sonolysis under CO_2/Ar atmosphere (1, 2 and 3 experiment from Table A.1, the test at 4 MPa is not included in Table A.1 as no cavitation was detected). Aluminum foil was fixed inside the reactor on a distance of 10 mm from the tip of the ultrasonic horn. The breaks marked by red rectangles were made intentionally before experiments in order to avoid the rupture of foil during pressurization of the reaction vessel with the atmospheric gases. The holes marked by blue circles show the seriousness of inflicted damage caused by ultrasound. From these results it can be seen that the hydrostatic pressure of the test has a significant effect on cavitation. So, according to the results, it is clear that the higher hydrostatic pressure, the more suppressed the cavitational cloud. Thus, even though the

formation cavities and the cavitational collapse are possible at elevated pressure, the strength of the cavitational collapse is significantly lowered due to the “cushioning” effect. In other words, the weaker cavitational collapse provides the weaker conditions (temperatures and pressure during collapse) which are not sufficient for sonolytical transformations. Moreover, it was found that a high value of the viscosity of a sonicating medium leads to suppression of cavitational bubbles cloud.

Thus, according the obtained results, it was decided to use the low hydrostatic pressure conditions in investigation devoted to sonochemical reduction of CO_2 (Chapter 4).

Table A.1. Sonochemical reduction of carbon dioxide in various liquids at elevated pressures*

Experiment #	1	2	3	4	5	6	7	8	9	10	11
liquid medium	water	water	water	methanol	methanol	methanol	ethylene glycol	*20%*-methanol solution	*20%*-methanol solution	glycerol	glycerol
compound	mole percentage of compound in a gas sample, *%*										
CO_2	8.69	3.64	0.14	1.55	1.38	0.08	4.38	2.67	2.21	3.71	2.56
H_2	-	-	-	-	-	-	-	-	-	-	-
CO	-	-	-	-	-	-	-	-	-	-	-
O_2***	Little	Little	-	Little	-	-	-	Little	-	-	Little
N_2***	0.12	0.11	0.21	0.16	0.14	-	0.19	0.13	0.41	-	0.15
CH_4**	-	4.41**	-	-	2.89**	-	-	-	3.90**	-	6.82**
C_2H_4	-	-	-	-	-	-	-	-	-	-	-
C_2H_6	-	-	-	-	-	-	-	-	-	-	-
C_2H_2	-	-	-	-	-	-	-	-	-	-	-
Average experimental pressure, MPa	1,5	2,5	3,4	1,2	1,5	2,2	1,5	1,5	2,5	1,5	2,4

* - The experimental time of each run is set to one hour; the experimental pressure is maintained in a range of 287±1 K. The analyses of samples were performed at Curtin University, Department of Chemical Engineering under supervision of Dr. Gia Pham

** - CH_4 was used as a component of the atmospheric gas in experiments 2, 5, 9 and 11

*** - contaminations from atmospheric air during transportation of gas mixtures from the reactor to the sampling cylinders

Appendix B. Pressure Test of High Pressure Apparatus

A pressure test of the experimental equipment must be conducted before experimental work on sonochemical reduction of CO_2 at liquid and supercritical state is started. A thorough description of the experimental apparatus and all parts of the equipment and the methodology of the experimental work are presented in Chapter 3 (Section 3.3.3).

The pressure test is performed in order to detect all possible leaks in the system and eliminate them. Also, this test is used to check the maximum pressure declared in the reactor specification to which the reactor can be pressurized. The results of the high-pressure experimental setup are presented in Table B.1.

Table B.1. The pressure test for the high pressure apparatus

Start Pressure, MPa	Start Temp, K	Final Pressure, MPa	Final Temp, K	Time	Comments
2.880	298.25	2.817	297.45	20 min	A leak where the temperature sensor couples to the reactor base is detected and eliminated.
4.170	296.75	4.142	295.95	overnight (20 hours)	no leaks are detected
9.785	297.25	9.739	296.35	30 min	One small leak in the temperature sensor is detected (not in the same spot as before)
The reactor was depressurized by venting Ar into the atmosphere. The discovered leaks are eliminated and all other connections are checked one more time.					
9.939	296.95	9.921	296.75	90 min	No leaks are discovered at this stage.
13.412	299.65	13.391	299.25	90 min	Also no leaks are revealed at such conditions.

Argon (Ar) was used in order to perform the test because this gas is inert and naturally benign. The maximum working conditions for the reactor are declared by Parr Instrument Inc. (USA) are 15 MPa and 473.15 K. However, the maximum working pressure recommended by the manufacturer is 14 MPa for safety reasons.

The test is successfully completed and it is concluded that the experimental setup has passed the pressure test regarding the maximum working conditions declared in the specification provided by the manufacturer.